FAST AND SENSITIVE DETECTION OF GLYCOPROTEINS FROM RECOMBINANT HUMAN ERYTHROPOIETIN AND DARBEPOETIN IN EQUINE PLASMA BY LC-MSMS

Foo, Hsiao Ching

Awarding institution:
King's College London

University of London

FAST AND SENSITIVE DETECTION OF GLYCOPROTEINS FROM RECOMBINANT HUMAN ERYTHROPOIETIN AND DARBEPOETIN IN EQUINE PLASMA BY LC-MSMS

by

HSIAO CHING FOO

A thesis submitted in partial fulfilment

of the requirements for the degree

Doctor of Philosophy

November 2014

ABSTRACT

Recombinant human erythropoietin as well as the other synthetic analogs darbepoetin alpha and methoxy-polyethyleneglycol-epoetin-β, are protein-based drugs which have the ability to stimulate erythrocyte production that leads to their abuse as blood doping agents in both human and equine sports. These epoetins may produce anti-rhEPO antibodies that can cause severe inhibition of erythropoiesis, leading to anemia and even death. Thus, it is essential to develop an efficient screening method to detect these doping agents in equine plasma at low concentration.

A fast and sensitive method was explored in this project to differentiate and identify recombinant human erythropoietin and darbepoetin in equine plasma by LC- MSMS for doping control. Various approaches were investigated to improve the sensitivity, differentiating the unique peptide fragments of the synthetic analogs, and by creating more on-line techniques to reduce the sample handling time and avoid contamination.

Capillary flow and nano flow chromatography were study and compared with conventional high flow LC. Results of this study showed that capillary flow is capable of detecting immunoaffinity-extracted plasma at 0.2 ng. Nano flow has also been shown to give better sensitivity when compared with capillary flow. I had also explored the fabrication of an internal tapered capillary tip packed with commercial

C_{18} silica to use as a nano-electrospray tip. This application was shown to improve the sensitivity for detecting the peptides.

To differentiate the synthetic analogs, requires the identifying of the unique peptide fragments, which involves enzyme digestion and deamination. Immobilised enzyme reactors were fabricated to reduce the handling time, avoiding autolysis and sample contamination. The on-line enzyme reactors for both the trypsin digestion and deglycosylation were shown to be as effective as the off-line in-solution digestion. It also showed better sensitivity for some peptides.

A novel organo cross-linker was synthesised and polymerised with a polar zwitterionic monomer to form a HILIC monolith. The morphology of fabricating the HILIC monolith was studied. Different polymerisation times were studied, with a shorter polymerisation time resulting in a monolith that had a significant proportion of both mesopores and macropores and this allowed rapid and high resolution separation of large biomolecules.

Finally, with the configuring of the orthogonal set-up, solved the incompatibility of the loading buffer, which is highly aqueous, and the high organic buffer used for HILIC phase. This configuration enables an on-line concentration and desalting, which minimised the preparation steps, therefore achieving good sensitivity.

ACKNOWLEDGEMENT

The author acknowledges the following groups and individuals who have been giving her great support in her journey towards completing her PhD studies:

I would like to express my utmost gratitude to my sponsor, Singapore Turf Club for their genourous funding towards this project and her postgraduate research studies.

I would sincerely like to thank my supervisor, Dr. Norman Smith, Head of the Microsepration Lab in King's College London for co-ordinating this project. She is very grateful for his advice and in getting her project underway. During this period, he has dealt with her with great patience and given lots of advice in fabricating the monolithic columns and internal tapered tips.

I would like to extend my gratitude to Dr. Shawn Stanley, my co-supervisor from Singapore Turf Club, for designing this project, guiding her through the practical work, giving her lots of practical advice, especially on the nano mass spectrometry part and the preparation and handling of the proteins and peptides. She would also like to extend her appreciation to him for giving her lots of encouragement and patience during these 6 years of her studies.

Her beloved family and friends for giving her lots of encouragement and support all these years.

Table of Contents

LIST OF FIGURES

LIST OF TABLES

LIST OF ABBREVIATIONS

AA	Ammonium acetate
ACN	Acetonitrile
AIBN	α, α’ azoisobutyronitrile
APCI	Atmospheric pressure chemical ionisation
ASN	Asparagine
ASP	Aspartic acid
BVPE	1, 2-bis(*p*-vinylphenyl)ethane
CE	Collision energy
CE-MS	Capillary electrophoresis mass spectrometry
CERA	Continuous erythropoietin receptor activator
CID	Collision-induced dissociation
CPG	Controlled pore glass

CYS	Cysteine
DAM	Deaminated
DITC	Diisothiocyanate
DMBVBS	Dimethyl bis (*p*-vinylbenzy)silane
DP	Declustering potential
DPO	Darbepoetin
DTT	DL-dithiothreitol
EICC	Extracted ion current chromatogram
ELISA	Enzyme-linked immunosorbent assay
EPO	Erythropoietin
ESA	Erythropoiesis-stimulating agent
ESI	Electrospray ionisation
FA	Formic acid

HETP	Height equivalent theoretical plates
HILIC	Hydrophilic interaction liquid chromatography
HPLC	High performance liquid chromatography
IAP	Immunoaffinity purification
I.D.	Internal diameter
IEF-PAGE	Isoelectric focusing polyacrylamide gel electrophoresis
IMERs	Immobilised enzyme reactors
ISTD	Internal standard
LC-MS	Liquid chromatography mass spectrometry
MAIIA	Membrane-assisted isoform immunoassay
MDLC	Multi-dimensional Liquid Chromatography
MICERA	Methoxy polyethylene glycol-epoetin beta
mM	Millimole

MudPIT	Multidimensional protein identification technology
nM	Nanomole
NP	Normal-phase
PNGase F	Peptide-N-glycosidase F
PPT	Parts per trillion
PTMs	Post-translational modifications
PWHH	Peak width at half-height
RF	Radio frequency
rhEPO	Recombinant human erythropoietin
RP	Reversed-phase
RPM	Revolutions per minute
SDS-PAGE	Sodium dodecyl sulfate polyacrylamide gel electrophoresis
SEM	Scanning electron microscopy

SER	Serine
SPE	N-(3-sulfopropy)-N-(methacryloxyethyl)-N,N-dimethyl ammonium betaine
SRM	Selected reaction monitoring
THR	Threonine
TIS	Turbo ionspray
TOF	Time of flight
UPLC	Ultra performance liquid chromatography
WCX	Weak cation exchange
WGA	Wheat germ agglutinin
γ-MAPS	3-(trimethoxysilyl) propyl methacrylate

LIST OF PUBLICATIONS

1. Talanta 100 (2012) 344-348 ‘’Monolithic *poly* (SPE-*co*-BVPE) capillary columns as a novel hydrophilic interaction liquid chromatography stationary phase for the separation of polar analytes’’.

2. Talanta 135 (2015) 18-22 ‘’Fabrication of an on-line enzyme micro-reactor coupled to liquid chromatography-tandem mass spectrometry for the digestion of recombinant human erythropoietin’’.

Chapter 1

Introduction & Theory

1.1 Erythropoietin

Erythropoietin (EPO) is an endogenous glycoprotein hormone produced primarily in the kidney. EPO is a glycosylated protein hormone which maintains erythropoiesis homeostasis [1]. It is a key component in the formation of red blood cells and the consequent improvement of blood oxygen-carrying capacity [2]. Endogenous human EPO (hEPO) has a mass of about 30.4 kDa, and consists of 165 amino acids, aligned in a single polypeptide chain, with two intramolecular disulphide bonds (Cys-7 – Cys161 and Cys-29 – Cys33), three N-linked sites of glycosylation (at asparagines residues 24, 38 and 83) and one O-linked site of glycosylation (at serine residue 126) [3, 4]. The resulting carbohydrate content accounts for roughly 40 % of the total molecular mass of the glycoprotein; Figure 1.1 shows the model of the three dimensional structure of erythropoietin and Figure 1.2 shows the two-dimensional structure of erythropoietin.

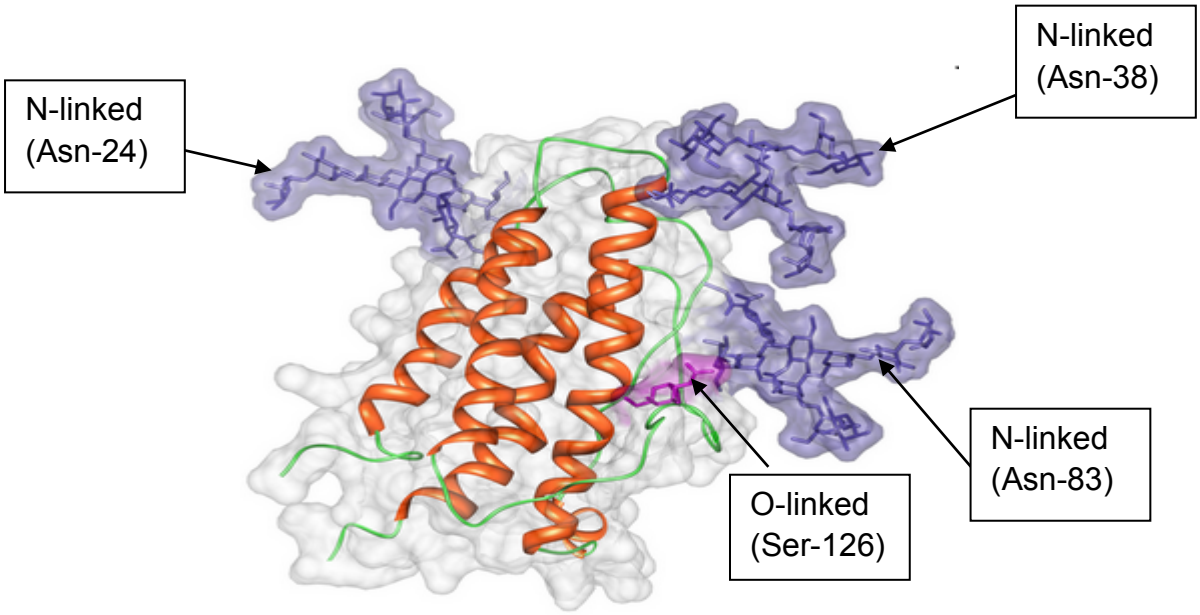

Figure 1.1 Model of the three dimensional structure of erythropoietin. The four α-helices are in orange, loops between helices are depicted in green. The 3 N- and 1 O- glycosylation sites are indicated in violet and pink respectively [5].

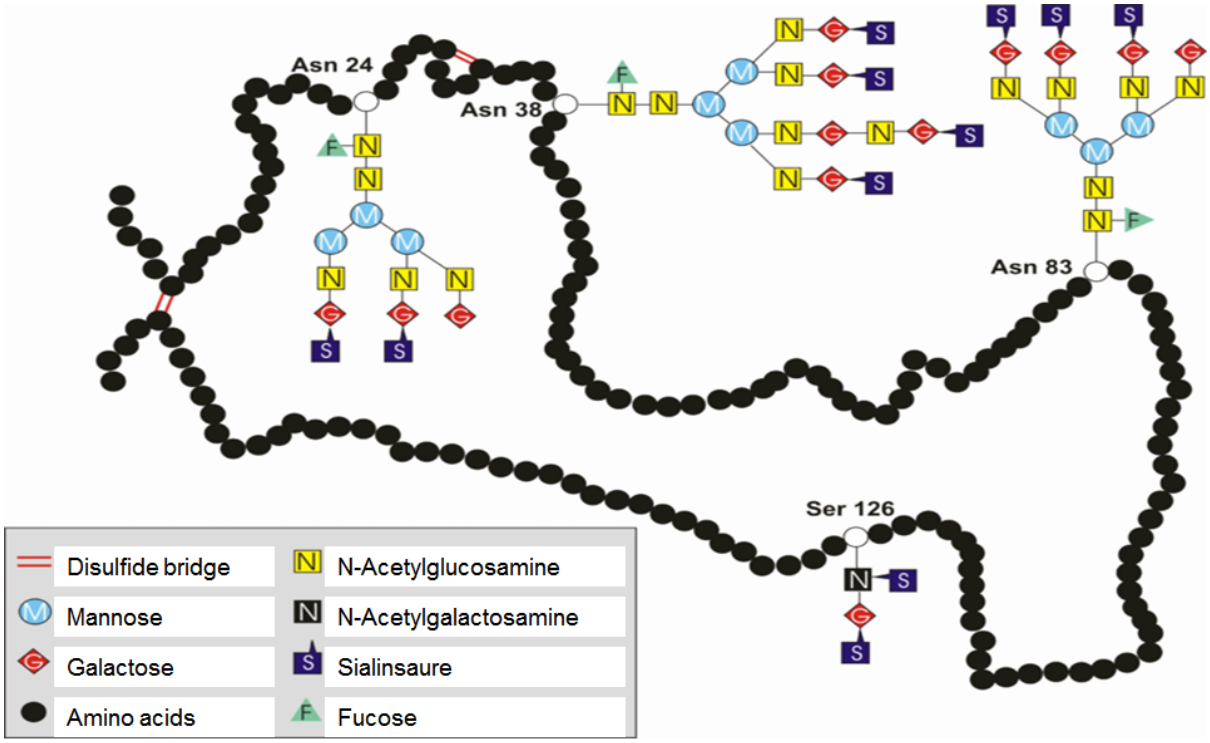

Figure 1.2 The two dimensional structure of erythropoietin [6]. Human EPO consists of 165 amino acids, aligned in a single polypeptide chain, with two intramolecular disulphide bonds and four independent polysaccharide chains bound to Asn^{24}, Asn^{38}, Asn^{83} and Ser^{126}.

Genetically engineered recombinant human EPO (rhEPO), darbepoetin alfa (DPO) and methoxy polyethylene glycol-epoetin beta (PEG-epoetin *β*, MICERA) or continuous erythropoietin receptor activator (CERA) are synthetic analogues of the endogenous hormone erythropoietin (EPO). These erythropoietin-stimulating agents have the ability to stimulate the production of red blood cells and are commercially available for the treatment of anaemia in humans [7]. These are erythropoiesis-stimulating agents which are prohibited in racehorses and humans because they are known to have performance-enhancing effects due to their stimulation of red blood cell production, thereby improving delivery of oxygen to the muscle tissues [8].

Recombinant human EPO (rhEPO) has the same polypeptide backbone as hEPO but differs in its glycosylation pattern. Darbepoietin α (DPO) (NESP or Aranesp) is a second-generation rhEPO, which has a similar polypeptide backbone as rhEPO but with five different amino acids. It has been intentionally modified to increase the duration of action while retaining the pharmacological effect of rhEPO [9]. It contains two additional sites of N-linked glycosylation (at Asn-30 and Asn-88) and five amino acid substitutions relative to rhEPO [9]. Consequently, DPO has an increased molecular mass (37.1 KDa) and an increased proportion of carbohydrates, 51 % as compared to the Epoetins 41 %. Due to the additional sialic acid content, DPO has a slower serum clearance and, therefore, a longer half-life than the epoetins [10]. The terminal half-life of intravenous (i.v.) administered Darbepoetin-alpha is three- to four fold longer than Epoetin-alpha and beta (24 h vs 8 h), thus affecting biochemical and biological properties of NESP. Figure 1.3 shows the comparison of the structure of rhEPO and darbepoetin alfa.

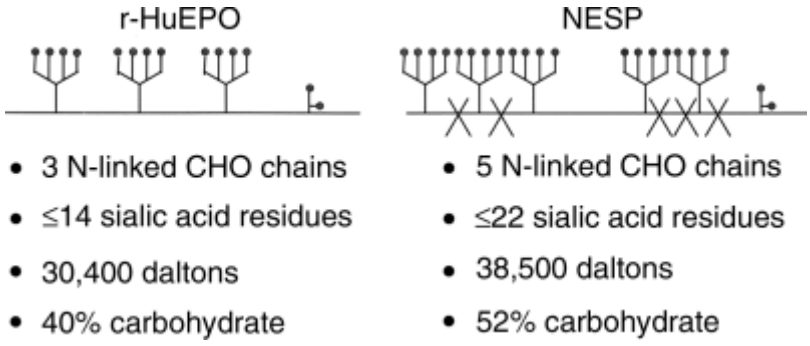

Figure 1.3 Comparison of the structure of rhEPO and darbepoetin alfa. The ''X''s in darbepoetin alfa represent the five amino acid exchange sites that were required to allow the attachment of two extra N-linked carbohydrate chains [11].

The amino acid compositions of endogenous horse EPO (eEPO), rhEPO or DPO are approximately 80-90 % similar (Figure 1.4).

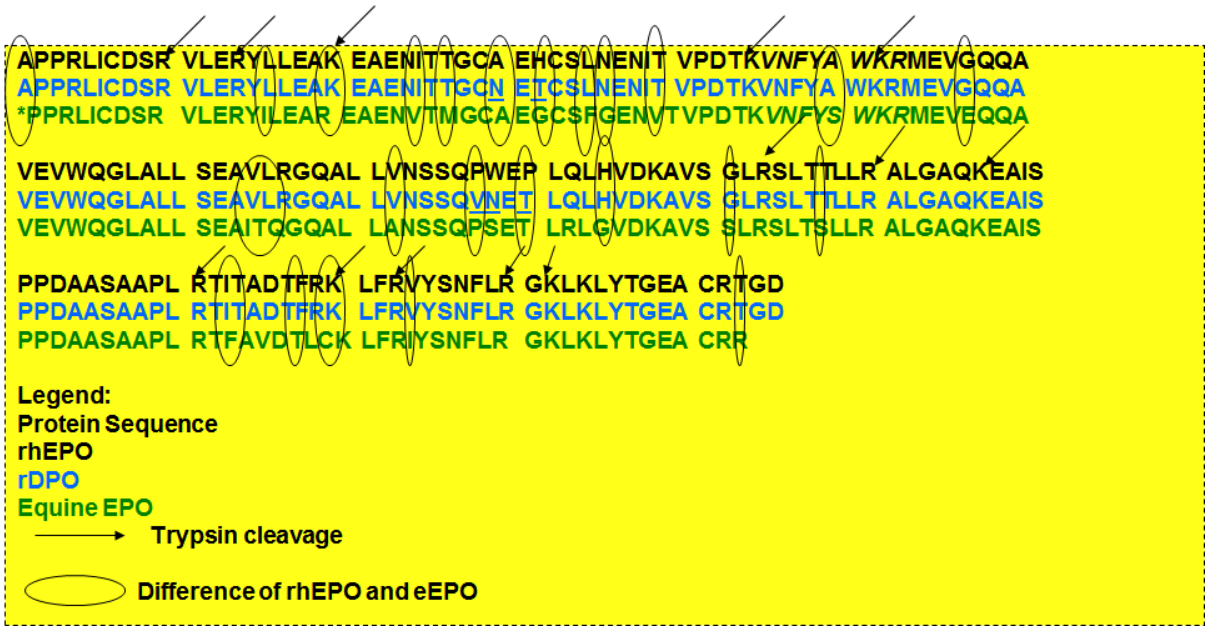

Figure 1.4 Sequence alignment of rhEPO, DPO and eEPO

In 2007, methoxy polyethylene glycol-epoetin beta (PEG-EPO) or CERA, better known as Mircera®, a third-generation erythropoiesis-stimulating agent (ESA) was released by Roche Pharma AG, Reinach, Switzerland. This is synthesised by pegylating rhEPO β. This increases its molecular weight by ~ 30 KDa, with the resulting molecular mass being about 60 KDa, twice the size of epoetin, which increases its half-life, and decreases its urinary excretion [12]. Figure 1.5 shows a comparison of epoetin and Micera structures. This is a long-acting erythropoietin derivative with methoxy polyethylene glycol butanoic acid linked to the N-terminal amino group or the ε-amino group of any lysine, predominantly Lys^{45} and Lys^{52}, in

the protein molecule. Micera has an even longer half-life than Epoetins and Darbepoetin-alpha in circulation, about 130 or 140 hours [13].

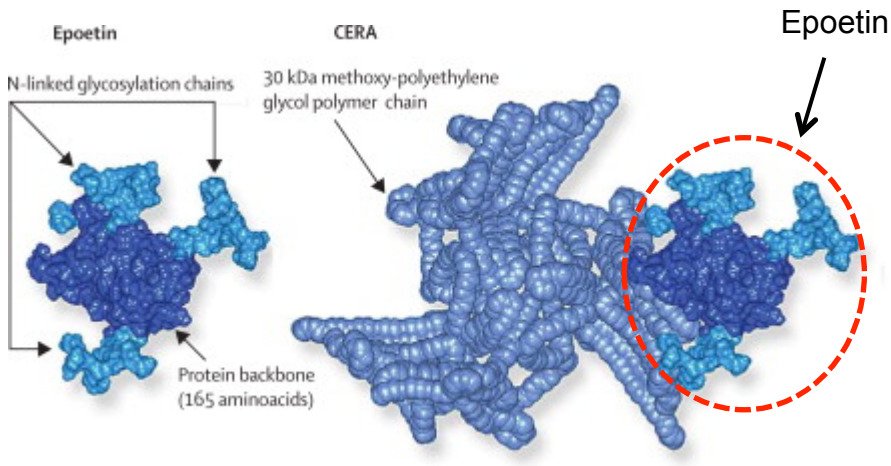

Figure 1.5 Comparison of epoetin (left) and Micera structures (right) From Macdougall, 2006 [11].

DPO, rhEPO, and PEG-EPO are genetically engineered substitutes for treatment of anaemia in patients with chronic renal failure or kidney diseases [14-15]. Since they can stimulate red blood cell production and lead to increased oxygen delivery to the muscle tissues, these protein-based drugs have become one of the most frequently used doping agents in endurance sport and horse racing. It has been demonstrated in humans that rhEPO provides a significant erythropoietic benefit in trained individuals as evidenced by increases in haemoglobin, haematocrit concentrations, maximal oxygen uptake, and exercise endurance time [16-19]. Deaths in endurance athletes were attributed to rhEPO-induced erythrocytosis [20]. The use of all rhEPO analogues is banned by the majority of human and animal sports regulatory authorities [21-24]. Like many other banned substances, the use of these protein-

based drugs in racehorses during competition violates the rule of fair competition. A second reason to ban the use of rhEPO and DPO is the potentially harmful effects on the health of the horse. Recombinant human EPO and DPO are foreign proteins and when injected into a horse, produce anti-rhEPO antibody that may cross-react with endogenous EPO causing inhibition of erythropoiesis and death of some horses [25-26]. Therefore, these drugs are banned in equine sports as implied in Article 6 of the International Agreement on Breeding, Racing and Wagering (Published by the International Federation of Horseracing Authorities (IFHA)) and as stated in the Equine Anti-Doping Rules published by the Federation Equestre Internationale.

Therefore, for ethical reasons and for the animal's safety, it is important to develop reliable analytical methods for direct detection of rhEPO and DPO in plasma. Since rhEPO became available in the market in the mid-1980s and DPO in the early 2000s, various methods using techniques such as enzyme-linked immunosorbent assay (ELISA), radioimmunoassay and isoelectric-focusing followed by double blotting were developed for the detection of these drugs [27-34]. However, a shortcoming of these methods is the lack of definitive mass spectral data to provide unambiguous proof for the presence of the prohibited substance in a sample. Liquid chromatography-mass spectrometry (LC-MS) has become more mature and widely employed in many analytical laboratories in the past decade and as a result, definitive confirmation of macromolecules, such as proteins and peptides, in complex biological samples has become a reality [35]. LC-MS is an effective method for analyses of both polypeptide chains and sugar chains in glycoproteins [36-37]. Glycoproteins are digested into peptides and glycopeptides bearing one sugar chain by proteases such as trypsin, endoproteinase Lys-C, Glu-C, and Asp-N, and the

digests are then subjected to LC-MS equipped with reversed-phase (RP) or hydrophilic interaction liquid chromatography (HILIC). Nevertheless, none of the reported LC-MS or CE-MS methods have been shown to be adequately sensitive for detection or confirmation of the presence of rhEPO or DPO in ‘’real world’’ racehorse samples [3]. The difficulty with LC-MS detection and confirmation of rhEPO and DPO in plasma samples arises from the fact that they are hormone protein-based drugs, and thus, their effective dose and plasma concentration are very low, *e.g*., ~1 ng/ml or 29 fmol/ml in plasma [38]. Unlike small molecule drugs, protein-based drugs such as rhEPO and DPO are difficult to separate from plasma due to the presence of abundant proteins. The extremely low concentration of rhEPO or DPO in plasma makes confirmation very difficult. However, plasma was still the preferred test sample because the concentration of rhEPO or DPO in plasma was higher than that in urine. Despite the inherent difficulties, the aim of the present study was to develop a sensitive and reliable LC-MSMS method for unequivocal confirmation of the presence of rhEPO and DPO at very low concentrations in equine plasma.

The detection of rhEPO and DPO using various mass spectrometric instruments has been reported since 2000 [3, 38-43]. Guan *et al*. (2007) [38] claimed that they were the first to develop a sensitive LC-MS method for confirmation of the presence of rhEPO and DPO in ‘’real-world’’ equine samples, resulting in the first confirmation reports for rhEPO/ DPO in the racehorse anywhere in the world. In their paper, they have confirmed the presence of rhEPO and DPO in equine plasma by electrospray mass spectrometry (linear Ion trap, LTQ) in combination with upstream liquid chromatography (LC) separation. Guan *et al*. has reported the confirmation of rhEPO and/ or DPO in equine plasma using immunoaffinity purification with polyclonal anti-

rhEPO antibodies immobilised on magnetic beads in order to isolate rhEPO/ DPO from equine plasma followed by buffer exchange and trypsin digestion to obtain the targeted peptides for LC-MSMS full scan analysis. Yu *et al*. has also reported a modified immunoaffinity extraction and trypsin digestion steps in combination with a multidimensional nano-LC system to further cleanup the sample extract by trap column loading and detection using nano-electrospray using selected reaction monitoring (SRM) mode. Both the groups are using buffers to link the anti-rhEPO antibody to the magnetic beads and subsequently followed by immunoaffinity purification of rhEPO and then tryptic digestion of the purification of the protein. Yu *et al*. reported only on EPO peptide T6, VNFYAWK from immunoaffinity purification (with anti-rhEPO antibodies) and trypsin digestion of rhEPO/DPO/PEG-EPO. Guan *et al*. showed that an immunoaffinity extraction procedure followed by trypsin digestion isolated a T6 peptide, VNFYAWK and a T17 peptide (VYSNFLR). The reported detection limits for rhEPO and DPO were 0.1 ng/ml [38], however Yu *et al*. [8] using a similar method, were not able to reproduce these detection levels. They have modified the immunoaffinity extraction and trypsin digestion steps in combination with a multi-dimensional nano-LC system to further cleanup the sample extract by trap column loading and detection using nano-electrospray in the selected reaction monitoring (SRM) mode. They could confirm rhEPO, DPO and PEG-EPO in equine plasma at 0.1, 0.2 and 1.0 ng/ml respectively.

As shown in Figure 1.4, eEPO and rhEPO have an 84 % identical amino acids composition which is extremely similar, consequently it provides the opportunity to use such substances for horse doping. There have been reports showing that the use of these erythropoiesis-stimulating agents on horses may not enhance

performance and have even caused serious health problems [29-30, 38, 41]. Covert administration of these drugs to horses does occur, which compromises not only horse welfare but also the integrity of equine sports.

In equine sports, screening for the rhEPO analogues in urine/ plasma is based on the use of commercially available rhEPO ELISAs [19, 41, and 44]. However, they are good only for detection, not for confirming the presence of rhEPO or DPO in a test sample, due to possible cross-reactivity with other proteins [38]. The International Olympic Committee (IOC) has adopted an electrophoretic method combining Western blotting for the detection of rhEPO and DPO in human urine. The same method was also used for the detection of rhEPO and DPO in equine urine samples. However, the method occasionally produced false positive results [45]. Its major drawback is the lack of mass spectral data or ‘’fingerprints’’ that are required for confirmation of a positive finding. The highly complex glycosylation pattern of rhEPO makes the application of more sophisticated analytical instrumentation necessary [35]. Liquid chromatography-mass spectrometry (LC-MS) methods were reported for the characterization of tryptic digests of rhEPO and DPO standards [3, 39-40] and the intact proteins [24].

1.2 Erythropoietin purification

Erythropoietin purification is required for two different reasons: the first one is that pure EPO is required for its characterisation. The second reason, and the most important one for this work, is that all direct methods explained before need a prior

immunopurification step for EPO analysis. Identification of post-translational modifications (PTMs) of proteins in biological samples often requires access to pre-analytical purification and concentration methods. In the purification step high or low molecular weight substances can be removed by size exclusion filters, and high abundant proteins can be removed, or low abundant proteins can be enriched, by specific capturing tools [46]. A proper pre-treatment and purification of biological samples, in order to isolate low-abundance proteins, prior to analytical techniques such as IEF-PAGE, SDS-PAGE, 2D-electrophoresis, capillary electrophoresis and LC-MSMS is essential in proteomics [47]. This interference can be reduced by using EPO affinity purification as sample pre-treatment instead of ultrafiltration. A column with anti-EPO bound to porous beads has been utilised for the purification of serum samples and ultrafiltration retention from urine samples [48]. For identification of human EPO in equine plasma samples, affinity purification with anti-hEPO bound to magnetic particles has been used in a lengthy procedure, as a pre-step for LC-MSMS doping control [38]. These magnetic beads are often re-used however potential carryover cannot be ignored. Traditional affinity columns, using anti-EPO immobilised on porous particles will be too expensive to be used as disposable items.

Immunoaffinity purification is a valuable and particularly powerful tool to improve the signal-to-noise ratio of immune-based methods [49]. It has the advantage of specifically purifying urine samples by isolating the various isoforms of EPO thanks to a specific antibody targeting both endogenous and exogenous forms of the hormone. This results in a lower background noise, and better resolution of the different isoforms. The immunoaffinity purification (IAP) strategies include immunoaffinity depletion that can be used to remove abundant proteins from

biological matrixes [50-51] and immunoaffinity capture that utilises a single antibody to isolate and enrich the target peptides or proteins from biological samples. Offline affinity purification using different carriers, such as macroporous polymeric beads, agarose or sepharose beads [52-53] and magnetic beads [54-56], *etc*., for immobilisation of a variety of enzyme and / or to capture antibodies, enables more flexibility in terms of selection of carriers, antibodies, assay formats, and experimental conditions as compared to the online approach.

Affinity chromatography separation using the lectin wheat germ agglutinin (WGA) has also been used to distinguish hEPO forms [57] by their varying content of polylactosamine structures [58]. An on-line combination of lectin affinity chromatography with lateral flow immunoassay (strip) for differentiation of recombinant and endogenous erythropoietin was developed by Lönnberg *et al*. [59-62]. The technology was named ‘’membrane-assisted isoform immunoassay’’ (MAIIA) [63]. The so-called ‘*’EPO WGA MAIIA*’’ test uses wheat germ agglutinin (WGA) in the ‘’separation zone’’ of the strip- a lectin with specificity for *N*-acetylglucosamine and *N*-acetylneruaminic acid-containing glycans and which was already known for its non-selectivity regarding the capture of EPO isoforms [64].

In the field of human doping control, a novel kit for rhEPO affinity purification has been tested for enrichment and purification of EPO from human urine and plasma samples. The kit can be used as a pre-step in the EPO doping control procedure, as an alternative to the commonly used ultrafiltration, for detecting aberrantly glycosylated isoforms. This kit showed a high recovery of rhEPO. The kit is useful for

applications in which it is essential to avoid carry-over effects, a problem commonly encountered with conventional particle-based affinity columns.

EPO detection using membrane-assisted isoform immunoassay (MAIIA) technology is a combination of two techniques, namely a membrane-based chromatographic technique for the separation of isoforms of a protein together with an immunoassay technique for the detection of the separated isoforms [65-68]. Both steps are performed on one single usage device. The sample preparation modifications of the kit reagents allow us to work with an anti-EPO monolith membrane contained in a disposable column (anti-EPO monolith column) in order to couple to a mass spectrometer. This was evaluated to extract efficiently recombinant human EPO (rhEPO) from horse plasma and urine samples. The sample preparation was improved to allow the detection of rhEPO target peptides by mass spectrometry. This technology is flexible, and several types of ligands can be applied to distinguish subpopulations through affinity chromatography interaction [63 and 65]. The detection sensitivity and specificity have been shown to be high [66-67]. It seems possible to adapt the technology to high-throughput testing [68].

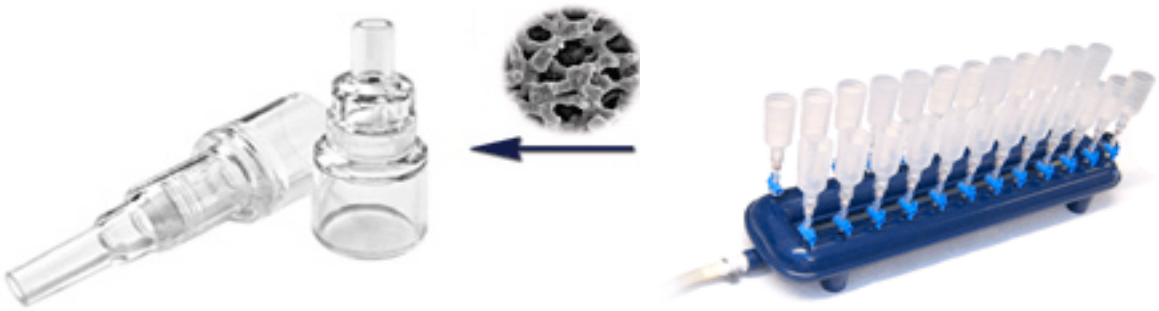

Figure 1.6 The EPO affinity purification set-up [46]

1.3 Tryptic digestion

Protein digestion is an indispensable step in contemporary proteomics, followed by liquid chromatography coupled to mass spectrometry (MS). Trypsin is the most popular enzyme to fragment proteins (tryptic digestion) for their identification/ characterization in proteomic studies due to its high cleavage specificity. Trypsin is a serine protease that specifically cleaves at the carboxylic side of lysine and arginine residues and typically provides peptides in a mass range suitable for high-resolution/ high sensitivity mass mapping through mass spectrometry (MS). Trypsin is thus well suited for protein identification through database searching [69]. Tryptic digestion can be performed in-solution. However, the traditional in-solution based protein digestion has several drawbacks, such as a long digestion time (up to 24 h), unavoidable enzyme autodigestion, limited enzyme-to-substrate ratio and off-line operation [70]. The use of too high concentrations of free trypsin in solution, relative to the substrate(s), leads to excessive amounts of autocatalytic tryptic fragments, which limits detection sensitivity and/ or sequence coverage and increases the occurrence of false-positive peaks in a mass spectrum. To circumvent long digestion times, the proteolytic enzyme can alternatively be immobilised on a solid support. As an attractive approach, recent attention has been drawn in developing immobilised enzyme reactors (IMERs), which not only have high digestion efficiency, with a higher density (concentration) of the enzyme molecules on such surfaces, but are also easily coupled with separation and detection systems in order to achieve automated and high-throughput protein analysis [71-73]. The use of enzyme reactors enables the application of much higher enzyme-to-substrate ratios (with its subsequent advantages of faster digestion times) and significant reduction in autolysis products (sometimes even complete absence). In addition, the stability of

trypsin toward chemical denaturants and organic solvents could be enhanced when immobilised on the solid supports [74]. Proteolytic enzyme immobilisation approaches include co-polymerisation with polyacrylamide gels [75-76], binding onto microbeads [77-78], silica-based substrates (*e.g.*, beads and monoliths) [79-81], synthetic polymers [82-83], coating of the inner walls of open capillaries or microchannels in microfluidics devices [84-85]. For IMERs, enzymes can be immobilised on different supports, however, a large range of favourable monolithic supports for enzyme immobilisation have attracted significant attention due to facile preparation, fast mass transfer and low backpressure [86-87]. Porous polymer monolithic supports have been recently introduced as novel materials, in which the diffusion resistance during mass transfer has been proved to be relatively small. In addition, this kind of material has the excellent ability to be applied under acid or basic conditions. The micrometer sized pores and large surface area of monoliths reduce the diffusion path length and also provide a low-pressure drop, thus leading to high digestion efficiency, which are advantageous for enzyme immobilisation [88]. Therefore, they are regarded as ideal supports for the immobilisation of enzymes and fast conversion of substrates [89-91]. The other main goal of enzyme immobilisation is to obtained rugged and efficient enzyme reactors. The sample that is digested may also be present in an acidic solution during multidimensional separations, for instance, after an immuno- affinity clean up or after sample fractionation using a cation-exchange column.

Due to the small volume of the resulting reactors, they are compatible with micro- and nano-HPLC and can be operated both in buffers and in aqueous solutions containing a modifier.

Enhanced flow-through and mass transfer properties are important physical features of the materials containing a high density of immobilised enzymes for yielding a rapid and efficient proteolysis, especially in proteomics where a large number of proteins are processed for protein identification/ characterisation by mass spectrometry. It is also important to have a stable and robust enzyme reactor that can withstand aqueous as well as partial organic buffers.

1.4 Protein Glycosylation

Glycosylation refers to the attachment of a carbohydrate moiety to a protein. Glycosylation of proteins has long been recognised as a common and highly important post-translational modification (PTM) in the modulation of their structures and functions [92]. Besides their intrinsic functions in aiding cellular architecture and modifying protein properties (*e.g*. solubility and stability), glycoproteins are also involved in mediating and modulating cell adhesion, signalling, and trafficking [93-95]. Glycosylation is also important in the production of therapeutic proteins, since it can significantly affect the potency of a biological drug. It is well known that the changes in glycosylation can affect the physicochemical, pharmacokinetic, and biological properties of therapeutic glycoproteins. The variable composition, linkage, branching points, configuration of constituent monosaccharides, and the diversity in the degree of glycosylation at different sites in glycoproteins are the main reasons resulting in the complexity of the current analytical approaches to their characterisation. Glycan mapping can be carried out with glycans released from the protein or with glycopeptides generated by enzymatic digestion. Carbohydrate moieties are typically linked to asparagine (N-linked) or serine/ threonine (O-linked) units within the

polypeptide backbone. The N-linked glycosylation at the carboxamide side-chain of a particular asparagine (Asn) residue or O-linked glycosylation at the alcohol side chain of a particular serine (Ser) or threonine (Thr) residue is only partly determined by the gene DNA sequence and corresponding protein amino acid sequence. Various glycosidases can be used to cleave the glycan moiety from the peptide backbone and/ or sequentially remove and identify monosaccharide units from the oligosaccharide non-reducing termini [96-97]. The analysis of deglycosylated peptides requires the removal of glycan attachments from glycopeptides. For N-linked glycopeptides, the N-glycosidic bond can be specifically cleaved using the enzyme Peptide-N-glycosidase F (PNGase F), providing deglycosylated peptides. The PNGase F catalysed deglycosylation results in the conversion of asparagine to aspartic acid in the glycopeptide sequence. This enzyme releases asparagines (Asn)-linked glycans from glycoproteins and glycopeptides by hydrolysing the amide bond at the Asn side chain [98]. The released oligosaccharides that can be of high mannose, hybrid or complex type, remain intact and therefore suitable for detailed analysis by mass spectrometry. Although the deglycosylation is usually performed in solution or in a gel using soluble PNGase F, immobilisation of this glycolytic enzyme can significantly improve the glycan release and identification of protein glycosylation [99].

To determine N-linked glycosylation sites by MS, an efficient deglycosylation process is essential. Peptide-N-glycosidase F (PNGase F) is one of the most widely used glycosidase for liberating N-linked glycans, leading to the deamination of asparagine residues to aspartic acid simultaneously as shown in Figure 1.7. PNGase F is able to remove most N-glycans, while the enzymes in the Protein Deglycosylation Mix

(PNGase F, O-Glycosidase (Endo-α-N-Acetylgalactosaminidase) and other enzymes) remove N-glycans, short O-glycans, and certain long chain O-glycan.

EPO is a protein-based drug used for the treatment of anaemia. It is the major glycoprotein regulator for erythropoiesis, the process that controls the production of red blood cells in mammals. Erythropoietin contains three *N*-glycans at Asn 24, 38, and 83, and one *O*-glycan at Ser-126. This glycoprotein has two disulphide bonds. There are various pathways for protein modification with sugars (glycans), the most common of which are the addition of glycans to an asparagine (*N*-linked) or to a serine or threonine (*O*-linked) in the secretory compartment. Therefore, due to the relatively large molecular weights of glycosylated peptides and the complex fragmentation that originates from both peptide and glycan cleavages, in order to overcome some of these issues in proteomic analysis, the labile sugar groups are often removed by deglycosylation prior to MS analysis.

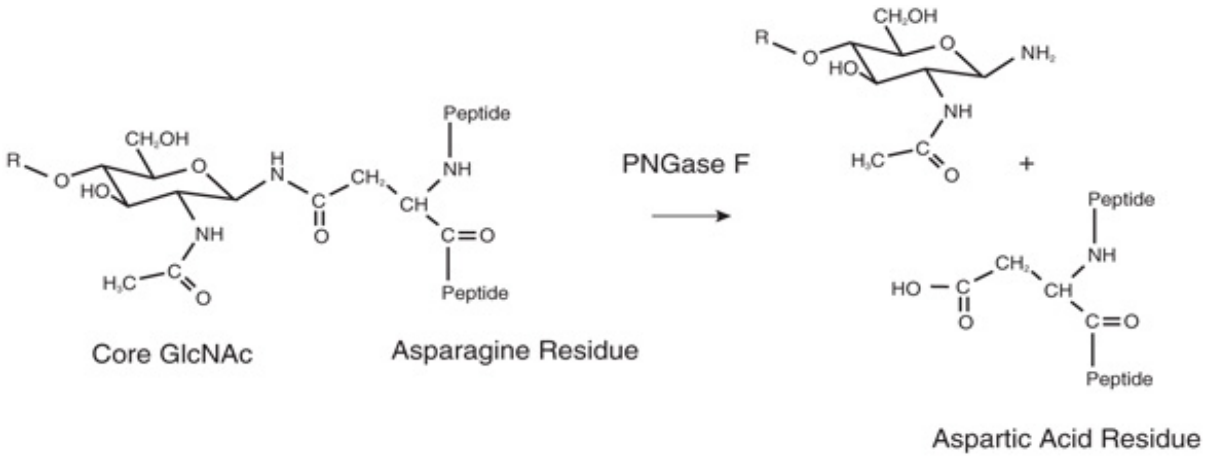

Figure 1.7 Schematic diagram shows cleavage products from PNGase F treatment of N-glycans [100]

The administration of these substances is prohibited under the rules governing Thoroughbred racing and to monitor compliance the doping control samples that we collect from racehorses are extracted and screened for the presence of the tryptic peptides common to these two epogens. However, when a positive result is obtained, it is necessary to differentiate rhEPO from DPO by targeting the analysis towards the peptides T5 (21-45) and T9 (77-97), as the amino acid sequence from this region is specific to each protein. Unfortunately, rhEPO and/or DPO T5 and T9 are glycopeptides with highly variable sialic acid containing glycan motifs and this severely hinders detection under ESI-MS conditions. This necessitates the inclusion of a deglycosylation step and for this study the glycosidase mixture (PNGase F, O-Glycosidase and Neuraminidase) that was used previously [3] was replaced by the Promega Deglycosylation Mix™ that also contains the β1-4-galactosidase and β-N-acetylglucosaminidase enzymes.

However, traditional deglycosylation protocol by PNGase F is usually performed in solution, which suffers from drawbacks, such as long incubation time, low deglycosylation yields, manual manipulation, and probably spontaneous nonenzymatic deamination of the asparagine residue, caused by high temperature and pH, which would significantly affect the accuracy of N-linked glycosylation site determination [101]. As a promising alternative, on-column deglycosylation with immobilised enzymatic reactors has drawn much attention. Novotny et al. [92] prepared a monolithic reactor with immobilized PNGase F to remove N-glycans from small and medium-sized glycoproteins. Svec *et al*. [99] fabricated another two kinds of monolith based PNGase F-immobilised enzymatic reactors (IMERs), enabling the effective deglycosylation of even large glycoproteins. Later, an on-chip silica

PNGase F-IMER was developed and integrated with other functional chips to perform glycoprotein deglycosylation, protein removal, glycan capture, and identification [102].

Immobilised enzyme reactors have recently gained in popularity, as they can be reusable and can be connected on-line to other analytical techniques, such as LC and MS, while such a process can also be automated. PNGase F enzymes are commercially available only in small quantities and at a relatively high cost. Such enzymes are more challenging to immobilise with high yield, since either the concentration and/ or volume can be a limiting factor for an efficient immobilised enzyme reactor. Through the approach shown herein, the volume is less of a limiting factor, while the concentration has to be relatively high for optimal enzyme incorporation. Enzyme reactors can thus increase the throughput of analytical assays and enhance productivity. In contrast to the free-solution use of glycosidases at comparable sample consumption, the enzyme microreactors are reusable in repetitive analyses. The immobilized PNGase F reactor rapidly releases N-linked glycans from glycoproteins and is suitable for their fast and robust analysis.

1.5 Identifying N-Terminal Aspartic Residues by Asp-N

Asp-N is an endoproteinase that hydrolyses peptide bonds on the N-terminal side of aspartic and cysteic acid residues: Asp and Cys. Asp-N activity is optimal in the pH range of 4-9. Endoproteinase Asp-N, a metalloprotease from a mutant strain of *Pseudomonas fragi*, has been reported to specifically cleave on the N-terminal side

of aspartyl and cysteic acid residues. A metalloprotease from *Pseudomonas fragi* was first purified in 1975 and demonstrated substrate specificity toward the N-terminal side of small or hydrophilic residues [103]. Enzymes with altered substrate specificities were later found in two mutant strains, including one enzyme, Protease V, which demonstrated specificity for cleavage on the N-terminal side of cysteic acid residues [104]. This enzyme was later found to recognise both cysteic acid and aspartic acid residues [105]. Asp-N efficiently cuts at the N-terminal side of Asp residues [106]. In these experiment, the Asp-N enzyme was utilised to differentiate the deamination of rhEPO and DPO, since after deglycosylation, both rhEPO and DPO which contained asparagine fragments, give a peptide fragment with aspartic acid each. Both the aspartic acid fragments give different peptide sequence, when cleaved at the Asp site. Hence, providing more sensitivity and confirmative result for the mass spectrometry screening to determine which erythropoietin analogues is being used for the doping.

1.6 HILIC monolith as a separation column

1.6.1 Monoliths

Monoliths have been identified as a suitable choice for the separation of complex biological samples, such as proteolytic digests in proteomics by providing better stability, resolution and sensitivity, compared to the regular separation medium. Monolithic columns have been extensively studied for use in micro-HPLC [107-109] since first introduced for capillary liquid chromatography in 1989 by Hjertén and Liao [110]. Monolithic capillary columns have been an attractive alternative high-performance separation medium because of their higher permeability at a similar

column efficiency and higher mechanical stability than particle-packed columns. It also offers a wide selection of monomers with different functional groups. Monolithic capillaries are used at micro- or nano-flow rates instead of normal flows and these small flow rates are ideal when coupling to a mass spectrometer (MS). With the small flow, there is an advantage of using less mobile phase. A smaller internal diameter (i.d.) can be used for monolithic capillaries, and as the column i.d. reduces, the sensitivity increases. The other great advantage for monoliths, due to their low backpressure, is that it allows the flow to be greatly increased even when using small i.d. column. By reducing the size (diameter) of the packing material particle size to make the pores as shallow as possible, these can minimise the band broadening effect. The effect of mass transfer is also lower at lower linear velocity of the mobile phase. The contribution of the mobile phase mass transfer for a monolith column is greater than that of a traditional particle-packed column. A greater flow allows a greater mass transfer. Monolithic columns have been successfully used with fast gradients and high flow rates [111-113].

The monolithic separation medium is made up of a continuous, rigid polymeric rod with a porous structure. The lack of intraparticular void volume improves mass transfer and separation efficiency, which allows for the very fast separation of biopolymers. The capability of coupling these columns to ESI-MS results in very fast and sensitive LC-MS analysis, making these columns ideally suited for high-throughput LC-MS proteomics [114]. The mass transfer process for monoliths is significantly higher than conventional particle-based stationary phases, as the van Deemter plots (as shown in Figure 1.13) of plate height versus mobile phase linear velocity are shown to be very shallow which means that fast separations can be

performed without compromising efficiency. Even at high velocities, the mass transfer contribution in monolithic materials is low. This is due to the lack of interparticular voids in the column which results in all of the mobile phase flowing through the separation medium rather than around it as in the case of particle packed capillaries. In addition, these monoliths also show high permeability, which allows them to be used at high flow rates [115]. Thus, monoliths can be described as the integrated continuous porous separation media without the interparticular voids and thus circumventing the preparation of end frits for microscale separation columns. Mobile phases are forced through the porous monolithic media, which results in convective flow and consequently enhances the mass transfer rate [116].

Monolithic supports can be described as a continuous rod of polymeric- organic or inorganic- material consisting of macro- and mesopores that are distributed uniformly across the entire structure [117–120]. Macropores (flow channels; flow through pores) enable mobile phase flow through the monolithic bed, whereas mesopores provide most of the surface area that is necessary for analyte retention. Since monoliths possess no interstitial void volume, all the mobile phase has to flow through the pore channels of the support. The generated convective flow enhances the mass transfer of analytes and accordingly has a positive effect towards chromatographic efficiency [121-122].

Since the pore dimensions control the specific surface area and the hydrodynamic properties of the stationary phase, optimising the pore size distribution represents one of the main challenges to obtaining high separation efficiency. It has been

shown that the type and amount of porogens, the amount of crosslinker and initiator as well as the polymerisation temperature are the key parameters to optimise the porous properties of monolithic stationary phases [123-124].

1.6.2 Conditions affecting monolith morphology

Monolithic columns are easy to produce, have a wide variety of chemistries and it does not require retaining frits. The polymerisation process is initiated either thermally or by photo induction of a mixture consisting of monomers and porogenic solvents. However, the compositions of the monomers and porogen have a profound effect on the overall morphology of the resulting monolith. The porous structures of these monoliths result from a phase separation of the solid polymer from the porogen mixture during polymerisation, and the pore characteristics depend heavily on the solvency of porogens and their content in the polymerisation mixture.

1.6.2.1 Porogens

Porogens create pores and flow through channels as the growing polymer becomes insoluble and precipitates out during phase separation. As the polymerisation progresses and the polymeric chains grow into a network of insoluble nuclei, two kinds of void volumes are formed. Those resulting from the repulsion between the insoluble polymeric macromolecules become the continuous flow through channels (macropores) while those produced from coalescence of smaller polymeric nuclei become the rough ridges or the meso or micropores. Solvents that have good solvency for the forming polymer will result in the formation of small pores whereas

macroporogenic solvents, which show poor solvency for the forming polymer, will result in the formation of macro-sized pores [114]. The porogenic solvents dominantly selected for the preparation of monolith-type media are usually poor solvents of the monomers utilized to form macro-through pores required for liquid flow. In the case of the porogenic poor solvents, the growing polymer chains tend to aggregate with each other because van der Waals attraction surmounts the steric hindrance mutually expelling the polymer chains [122]. In order to balance the effect favourably, both the good and poor solvents are employed by adjusting their ratio to give the best results. The poor porogens (macroporogens) are usually polar solvents *e.g*. alcohols such as 1-propanol, methanol or dodecanol. The good porogens (microporogens) are usually non-polar solvents *e.g*. tetrahydrofuran, and toluene.

1.6.2.2 Crosslinkers

The degree of crosslinking affects the rigidity and homogeneity of monolith. A change in percentage of crosslinkers in the monomer mixture affects both porous properties and the chemical composition of the monolith. An increase in the percentage of crosslinker leads to a decrease in the average pore size due to the formation of highly crosslinked microglobules [125]. Crosslinkers are bi-functional chemicals responsible for creating a network between the polymeric chains. The higher the amount of the crosslinker, the more rigid the three dimensional structure of the polymer becomes. This same rigidity limits the swelling propensity of the nuclei. High amount of crosslinking also triggers an earlier phase separation, as a function of the two reactive sites present in single crosslinking molecule.

1.6.2.3 Initiators and polymerisation temperature

In order to obtain reproducible and uniform porous structures for monoliths, the temperature of the polymerisation process has to be controlled carefully because of the significant effect of heating on the rate of growth of nuclei. At a higher temperature, both initiator decomposition and rate of propagation are faster, the number of growing nuclei becomes larger and therefore, the final pore size becomes smaller. A faster polymerisation may result in less uniform porous structure. As the polymer chains continue to grow, their sizes will reach a certain limit of insolubility in the solvent which, will result in phase separation when the insoluble polymeric nuclei are formed. The higher the temperature, the earlier is the onset of phase separation. This translates into an increased number of small diameter nuclei, and thus smaller pores. An increase in initiator content results in faster nucleation than growth, which leads to smaller size microglobule.

1.6.3 Hydrophilic monoliths

The separation of polar and hydrophilic compounds can be significant challenging when using reversed-phase HPLC, which is by far the most popular HPLC mode. In order to achieve adequate retention of polar analytes, highly aqueous mobile phases are often required, which can cause a number of issues such as stationary phase collapse [126] and decreased sensitivity in ESI-MS [127]. Normal-phase HPLC is a useful separation technique for providing effective retention for polar molecules, but the poor solubility of polar analytes in non-aqueous mobile phases, together with lower peak efficiency, reduced selection of stationary phases, and decreased reproducibility, has great limitations [128]. Hydrophilic interaction chromatography

(HILIC), which was first introduced in the 1970s by Alpert [129], is a useful alternative and rival technique to RPLC for separating polar compounds.

Hydrophilic interaction chromatography (HILIC) is a technique, where analyte retention is believed to be caused by partitioning of the analyte between a water-enriched layer of stagnant eluent on the surface of a hydrophilic stationary phase and a relatively hydrophobic bulk eluent as shown in Figure 1.8. HILIC separations are carried out using polar stationary phases and a high-organic, low-aqueous mobile phase in order to achieve retention of very polar compounds that are difficult to retain using reversed-phase methods. Such mobile phase properties largely solved the solubility problem of polar compounds when using normal-phase HPLC. Additionally, the organic-rich mobile phases used with HILIC can assist spray formation, improve ionisation efficiencies and thus enhance the detection sensitivity in detectors relying on vaporisation of the eluent. Therefore, HILIC is an excellent technique in combination with ESI-MS detectors [130-133].

The complexity of peptide mixtures that are analysed in proteomics necessitates fractionation by multidimensional separation approaches prior to mass spectrometric analysis. In this work, hydrophilic interaction liquid chromatography based strategies for the separation of complex peptide mixtures were introduced and evaluated. HILIC has one of the highest degrees of orthogonality to RPLC [134]. The retention time in HILIC increases with increasing polarity or hydrophilicity, opposite to the trend observed in RP, HILIC is not a variation of NPLC as the HILIC technique employs water-miscible solvents compatible with mass spectrometry, and the elution is

achieved by running an aqueous gradient [129, 135-137]. Samples are loaded at high organic solvent concentration and eluted by increasing the polarity of the mobile phase. Most importantly, HILIC has been found to allow enrichment and the targeted analysis of post-translational modifications (PTMs) such as glycosylation [136], N-acetylation [137] and phosphorylation [138] in proteomics applications. HILIC has been proposed as another means of enriching N-acetylated tryptic peptides [138]. When it contains a neutralised N-terminus, the hydrophilicity of an N-acetylated peptide is decreased. This reduction in polarity is even more pronounced at pH 3, where only basic peptide residues are charged and acidic residues are protonated. Boersema *et al*. has shown that this subgroup of trypsinized peptides that are N-terminally blocked, could be enriched due to their shorter retention compared with ‘’normal’’ trypsinized peptides.

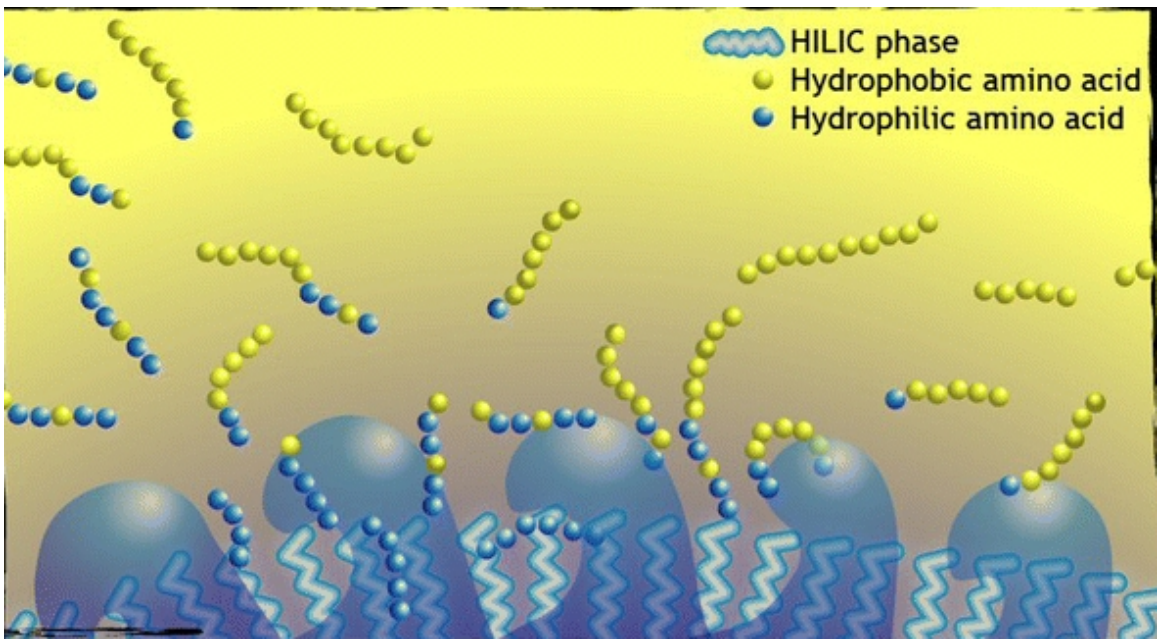

Figure 1.8 HILIC separation mechanisms [139]

The use of water as the strongly eluting solvent gives HILIC a number of advantages over conventional normal phase chromatography (NPLC). Interfacing with electrospray MS is often a problem with NP, since ionisation is not easily achieved in totally organic, non-polar eluents. Therefore, HILIC can be seen as a form of normal-phase (NP) chromatography. NP is typically performed with non-aqueous, non-water-miscible solvents, while HILIC is performed with water-miscible solvents and elution is achieved using an aqueous gradient [129, 134, 140-142]. Using a HILIC stationary phase, the higher the organic concentration of the mobile phase, the greater the retention of the more polar compounds [143].

The hydrophilic stationary phase entraps water from the mobile phase and thus generates an aqueous layer [129]. Elution is obtained through increasing the hydrophilicity of the mobile phase which is obtained by increasing the water content. The final separation mechanism of elution is most likely a combination of partitioning and electrostatic interactions or hydrogen bonding to the stationary phase [140]. The various types of interactions with a HILIC stationary phase are shown in Figure 1.9.

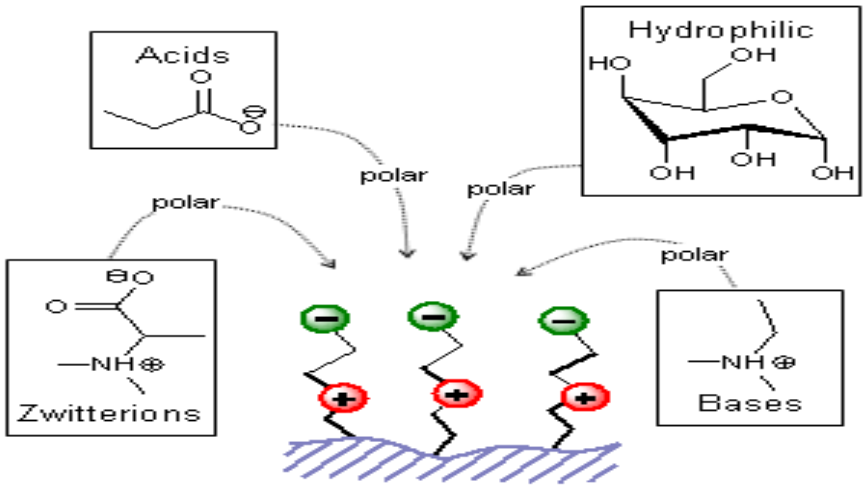

Figure 1.9 Various types of interactions with HILIC stationary phase [144]

The extent to which each mechanism dominates is dependent on the actual type of stationary phase used and the mobile phase conditions, including the level and type of organic content, the type and concentration of salts and the pH [145].

In reversed-phase separation, the digested peptides from EPO protein are eluted in order of increasing hydrophobicity, but with hydrophilic interaction chromatography the least hydrophobic peptides (hydrophilic) will be retained most strongly by the column. Thus, the elution order is reversed. The use of HILIC columns for the analysis of the peptides obtained from an enzymatic digest of a protein would therefore be expected to provide increased retention and resolution of the hydrophilic peptides, including glycopeptides, compared with RP columns. Hence, digested peptides can be identified by HILIC that may not have been retained and resolved by RP. In general, under RP conditions, the least hydrophobic peptides (hydrophilic) will elute early, making their quantitation by MS analysis more difficult. Moreover, some

very hydrophobic peptides are difficult to dissolve in aqueous conditions, which are usually used as solvents for RPLC-MS analysis. This also leads to lower sensitivity. Therefore, with high organic solvent mobile phase, and the sample mixed with a high percentage organic solvent, some highly hydrophobic peptides will be dissolved and separated better with the HILIC column. Another benefit of the HILIC separation mode is the enhanced signal in MS due to more efficient desolvation of highly organic mobile phases, as they have a lower density and surface tension than water, which results in more efficient desolvation [146].

1.7 An Orthogonal set-up of RP-WCX-HILIC

High-resolution separations prior to MS minimise ion suppression and under sampling challenges associated with the analysis of highly complex proteomes, which often span several orders of dynamic range in protein abundance. The complexity of a sample can be further reduced prior to mass spectrometric analysis by the addition of extra dimensions of separation. Thus, the developments and applications of multidimensional LC (MDLC) have facilitated advances in proteomics. Multidimensional protein identification technology (MudPIT) has become prominent with directly coupled-column MDLC for proteomic research [147]. In MudPIT, a sample fractionated in the first dimension *via* strong cation exchange chromatography is further separated in the second dimension using RPLC. This configuration is relatively simple, but the first dimension can only be run in a stepwise mode, which limits resolution. In addition, possible combinations of separation modes are restricted by the limited combinations of mobile phases that could be used for effective orthogonal separation. It is possible to utilize MudPIT-like

strategies with a continuous gradient through some additional considerations in methodology [148]. In column-switching MDLC, fractions from the first dimension are transferred online, or stored in a series of loops, for the second dimension where the separation is accomplished using two or more columns. This setup allows greater flexibility in terms of combinations of separation modes. Online hyphenation possesses certain advantages, such as minimal loss of sample, no vial contamination, and no sample dilution [133, 149].

Over the years, a number of alternative configurations have been developed. In recent years, HILIC was introduced as a dimension for 2D-LC-MS and was shown to remove some of the disadvantages of existing techniques [137-150]. RPLC cannot separate many of the post-translationally modified isoforms (*e.g*. methylated, acetylated, and phosphorylated) from the unmodified proteins and from each other [151]. Weak cation exchange-hydrophilic interaction LC (WCX-HILIC) has proven to be an excellent complementary orthogonal mode to RPLC and has been successfully used to separate acetylated isoforms of histone H4 [152], methylated isoforms of histone H4 [153], phosphylated isoforms of histone H1 [154], as well as sequence variants of histone H1 [155].

WCX-HILIC, a mixed-mode chromatography introduced by Alpert in 1990 [128], features the simultaneous presence of dominant hydrophilic interaction (due to the use of a higher percentage of organic solvent in the mobile phase than traditional WCX) and electrostatic interaction (due to an ionic stationary phase) [155] between the stationary phase and the analyte.

Weak cation exchangers possess charged functional groups over a limited pH range. While mobile phase pH has a negligible effect on the ionization of functional groups of strong cation exchangers, it affects the ionization of functional groups of weak cation exchangers significantly. Weak cation exchange (WCX) was used because of the high polarity of the carboxylic acid functionality. A gradient of decreasing pH protonates the functional groups of a weak cation exchange stationary phase, leading to elution of retained peptides. WCX was employed before HILIC due to its compatibility with the solvents. Both can accommodate high concentrations of organic solvent. WCX traps at a higher pH and releases analytes at a lower pH, while the HILIC phase is also running at a high organic content with the aqueous component at low pH. Hence, it has a compatibility of the orthogonality of WCX-HILIC. Reversed-phase chromatography (RPC) is the most commonly used general-purpose method for peptide HPLC. However, RPC fails in some cases, some peptides are not retained whilst others co-elute. A good alternative is cation exchange HPLC. At pH < 4, the carboxyl- groups on the peptides lose their (-) charge, and peptides have a net (+) charge. They are retained by a strong cation exchange (SCX) material and can be eluted by an increasing salt gradient, in order of increasing absolute number of basic residues. This is displacement chromatography; the ions of the salt out compete the peptides for the binding sites of the stationary phase. The capacity is approx. 4x greater than with RPC. However, the peptides were eluted with a gradient to 15 % acetic acid (HOAc). Acetic acid is a weak acid and is only 1 % dissociated in aqueous solution. This suggests that it could uncharge the stationary phase of a weak cation exchange material. The volatility of the solvent made this method appealing.

In this experiment, the EPO samples are prepared and digested in ammonium bicarbonate buffer, in the aqueous form. Hence it is not suitable to be directly injected onto the HILIC column, which requires high amounts of organic solvent. Thus a multi-dimensional LC set-up is designed in order to trap and enhance the detection of the digested glycosylated and non-glycosylated peptides on the HILIC column. A reversed-phase captrap was used to trap and de-salt the digested peptides. Samples were loaded with high aqueous content at pH 5.5, with a small amount of organic from the low flow pump onto the captrap. Samples were trapped and de-salted on the captrap. After a while, it was released at high organic content and with a small amount of aqueous at a pH of 5.5 onto the WCX. Peptides were released and trapped onto the WCX column at high organic and high pH. After sometime, the valve is switched, and another pump with high organic and a small amount of aqueous with a low pH of 2.7 will transfer the peptides from WCX to HILIC. The mobile phase is compatible, as HILIC has been conditioned at this mobile phase of high organic and aqueous at low pH. Thus, this multi-dimensional set-up will help to trap, de-salt and enhanced the peak resolution.

1.8 LC/MS Quantification

1.8.1 Brief History of Chromatography

The evolution of chromatography began in the early 1900s when Tswett produced a colourful separation of plant pigments through a column of calcium carbonate and alumina [156]. He had created an analytical separation of these compounds based on the differing strength of each compound's chemical attraction to the particles. Compounds that were attracted more strongly to the particles slowed down, while

the other compounds attracted more strongly to the solvent moved faster. This causes each compound to move at a different speed, thus creating a separation of the compounds. In Tswett's opinion, a scientist always must consider the whole sample and separate all the substances present [157].

Chromatography methods did not make much progress after Tswett's work until the mid-20th century research in new techniques emerged. Martin and Synge developed partition chromatography to separate chemicals [158]. There were some difficulties found in the initial partition chromatography due to the lack of reproducibility in the properties of the silica gel and not homogeneous in the packing of columns. Consequently, they then developed another method that was the paper chromatography. In 1949, Martin collaborated with Anthony T. James on developing gas chromatography. In 1952, Martin won the Nobel Prize in Chemistry and shared with Synge, for their earlier chromatographic work. Chromatography has since developed into an invaluable laboratory tool for separation and identification of compounds.

Chromatography is the process where analytes are separated due to their varying distribution between two phases, a stationary phase and a mobile phase. Compounds travel in the mobile phase interacts with stationary phase. Those that are strongly retained by the stationary phase move slowly, while those that interact only weakly move rapidly. Compounds that move rapidly are thereby separated from the compounds that move slowly.

Horváth's group [158-159] demonstrated a novel stationary phase based on the modification of an ion-exchange column for fast LC with a pressure-driven solvent delivery set-up to separate nucleosides, nucleotides and bases. Horváth named High Pressure Liquid Chromatography (HPLC) in his 1970 Pittcon paper, which originally indicated the fact that high pressure was used to generate the flow required for liquid chromatography in packed columns. Earlier, pumps only had a pressure capability of 500 psi (35 bar). This was called high-pressure liquid chromatography, or HPLC. Then later, these new HPLC instruments could accommodate up to 6000 psi (400 bar) of pressure, and incorporated improved injectors, detectors and columns. HPLC began to be more popular in the late 1970s, with the continuous advancement made in performance, the acronym HPLC remained, however, it was re-named as high performance liquid chromatography.

1.8.1.1 Overview of modern Liquid Chromatography

High performance liquid chromatography is now one of the most powerful tools in analytical chemistry. It has the ability to separate, identify, and quantitate the compounds that are present in any sample that can be dissolved in a liquid. In the modern HPLC, compounds in trace concentrations as low as parts per trillion (ppt) can be easily detected. In 2004, Ultra Performance Liquid Chromatography (UPLC)™ technology emerged, with further advances in instrumentation and column technology. These advances achieved very significant increases in resolution, speed, and sensitivity in liquid chromatography. Columns with smaller particles, 1.7 μm and instrumentation with specialised capabilities designed to deliver mobile phase at 15,000 psi (1,000 bar) were able to achieve a new level of performance. Importantly,

there was at least 10-fold decrease in analysis time with at least 2-fold increase in peak resolution and sensitivity [160]. Today, scientists are conducting research using columns containing particles even smaller than 1μm in diameter particles and instrumentation capable of performing at 100,000 psi (6,800 bar) [160].

HPLC has become an indispensible analytical tool for analytical scientist in the analysis of complex sample mixtures. It has gained the leadership for separation, purification, identification and quantification as a powerful analytical tool. Facing the challenge for faster and more robust analytical and separation, concurrently with the increasing number of complexity of sample types and stricter monitoring regulations, researchers continue to focus on the innovations for new column technologies and optimisations on instrumentation.

1.8.1.2 LC Theory

The components of a basic HPLC set-up are shown in a simple diagram in Figure 1.10. The mobile phase is delivered to the column by a high-pressure pump that is used to generate a specified flow rate of mobile phase. Sample is injected into the injector, where the mobile phase flow from the pump to the injector, carrying the sample to the column where separation of the sample takes place. The column contains the chromatographic packing material needed to effect the separation. This packing material is called the stationary phase. Analytes in the sample will exhibit competitive affinities towards the eluent and the stationary phase. The higher the affinity of the analyte towards the stationary phase, the longer is its retention in the

column. The analytes are eluted into the detector, where the detector is necessary to see the separated compound bands as they elute from the HPLC column. The detector produces signals, which these signal are transformed into interpretable data called chromatograms.

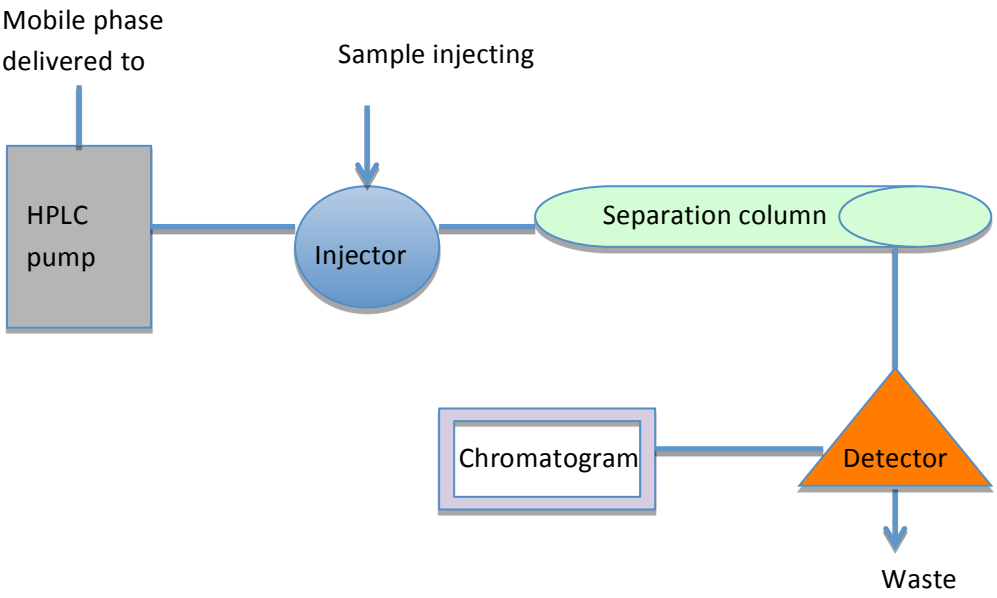

Figure 1.10 A schematic diagram of HPLC set-up

HPLC is an extremely versatile technique where analytes are separated through a column packed with micrometer-sized particles. There are various types of LC techniques: normal-phase, reversed-phase, ion exchange and size exclusion chromatography. Reversed-phase chromatography is the most commonly used separation technique. Reversed-phase has a broad application range that can handle compounds of diverse polarity and molecular mass. The retention of an analyte depends on its partition between the polar mobile phase and the non-polar

stationary phase. Reversed-phase columns consist of silica or polymeric carrier and a coating of long chain saturated hydrocarbons or other non-polar functional groups. The most popular packing material is octadecylsilane with an 18-carbon aliphatic chain. The partitioning of an analyte between the mobile and stationary phase depends upon hydrophobic interactions between the sample and the mobile phase. Small polar molecules elute more rapidly than large apolar ones [161-162]. In normal phase, the stationary phase is a polar silica material while the mobile phase is a non-polar organic solvent, typically involving high concentrations of hexane. Highly polar solutes therefore retain very strongly in normal phase. In recent years, HILIC has become the alternative technique of choice for the analysis of hydrophilic and ionic solutes. HILIC is considered a variation of normal phase because both techniques have polar stationary phases in common. The mobile phase differs for HILIC, like reversed-phase, it uses a water miscible organic solvent. A water-acetonitrile mixture with the addition of buffer salts is used, and elution takes place by the increasing of water content in the mobile phase. Therefore, for HILIC the initial condition is high organic solvent. The retention in HILIC is described as a mixed-mode mechanism, in which partitioning of the analyte between the organic-rich mobile phase and the water-enriched layer is regarded as the main retention mechanism.

1.8.1.3 Definition of chromatographic terms and relevant equations

Chromatography is the ability to separate molecules through partitioning characteristics of molecule to remain in a stationary phase versus a mobile phase. Chromatography is the process of separation, as shown in Figure 1.11.

A chromatogram is a graph that shows the response of a detector in the form of elution.

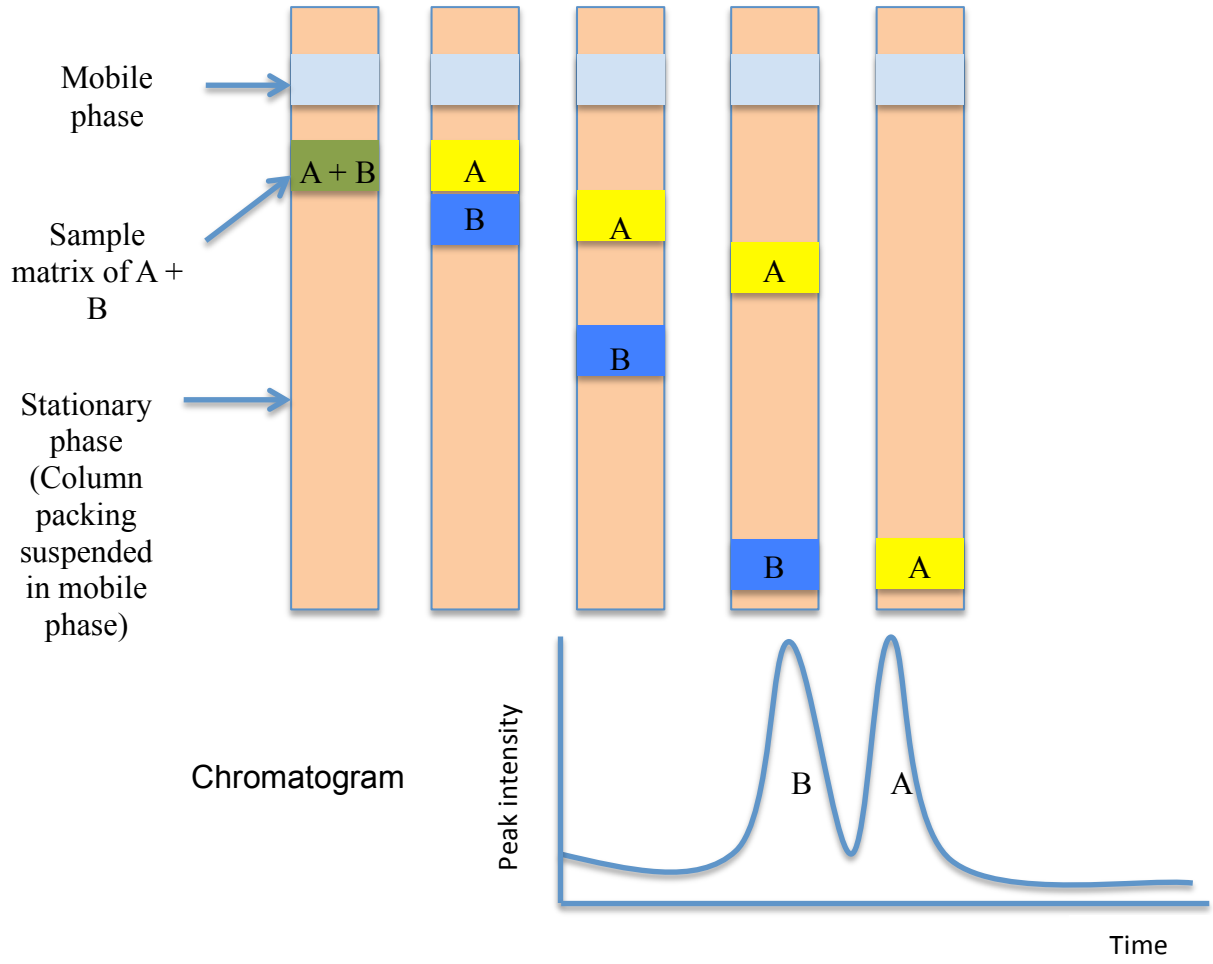

Figure 1.11 Schematic diagram showing the process of chromatographic separation

Retention time, t_R, is the time for each component takes to travel from the injector to the detector, with a fixed flow rate, a longer retention time indicates stronger interaction between the analyte and the stationary phase.

Void time, t_0, or dead time, is the time of migration of the unretained analytes or mobile phase travels through the column. In LC separations, the solvent used for the samples is also the mobile phase; hence void volume is sometimes represented as t_m.

Adjusted retention time, for a solute is the additional time required for solute to travel the length of the column beyond the time required by unretained solvent:

$$t_r' = t_r - t_m$$

Retention factor/ Capacity factor, k', describes the time spent by an individual analyte in each of the two phases, based on the ratio of time that an analyte spends on the column, relative to those unretained, at a given flow rate. It is defined as follows:

$$k' = \frac{t_r - t_0}{t_0}$$

$$k' = \frac{\text{time solute spends in stationary phase}}{\text{time solute spends in mobile phase}}$$

Selectivity factor, α, is an indication of how well the compounds separate. It is defined as the ratio between the k values of two compounds,

$$\alpha = \frac{k_B}{k_A}$$

Where k_B is the retention factor for the more strongly retained compound and k_A is the retention factor for the less strongly held compound. The selectivity factor is always greater than one.

Efficiency, N, is used to describe column performance based on the number of theoretical plates. The value N is related to the column length (L) and the size or height (H) of an individual plate by the following equation:

$$N = L/H$$

Chromatography columns with high numbers of theoretical plates produce very sharp narrow peak resulting in better peak separation. From the above equation, increasing the length of the column or decreasing the plate height can increase N. The higher the N value, the better is the column efficiency.

Height Equivalent to a Theoretical Plate (H), the shorter each theoretical plate, the more plates are ‘’contained’’ in any length of column, hence, this will have more plates per meter and higher column efficiency will be achieved.

The value of N is also related to the width of a peak by the following formula:

$$N = 5.54\ (t_r/\ W_{0.5})^2 \text{ or } N = 16\ (t_r/\ W)^2$$

Resolution, R_S, the separation or distance between two peaks is known as their resolution and is a function of the 3 factors discussed above: **retention** (time taken for analytes to elute, which relates to *k*), **selectivity** (the difference between the analytes from each other, which relates to α), and **efficiency** (how good the column is, which relates to N). Therefore, these factors formed the equation:

$$R_S = ¼\ ((\alpha - 1)/\alpha)\ (k/k+1)\ N^{1/2}$$

There is another equation that commonly used to calculate R_S, from actual measurements of peak retention times and measured peak widths. It is defined as:

$$R_S = 2\ (t_R\,B - t_R\,A)/\ (W_b\,A + W_b\,B)$$

Where A and B are the two peaks, t_R = retention time and W_b = peak width at the base of each peak (Figure 1.12).

Another equation similar can be used, when baseline is not established, peak width at half height can be used to calculate as follow:

$$R_S = 1.18\ (t_R B - t_R A)/\ (W_{0.5} A + W_{0.5} B)$$

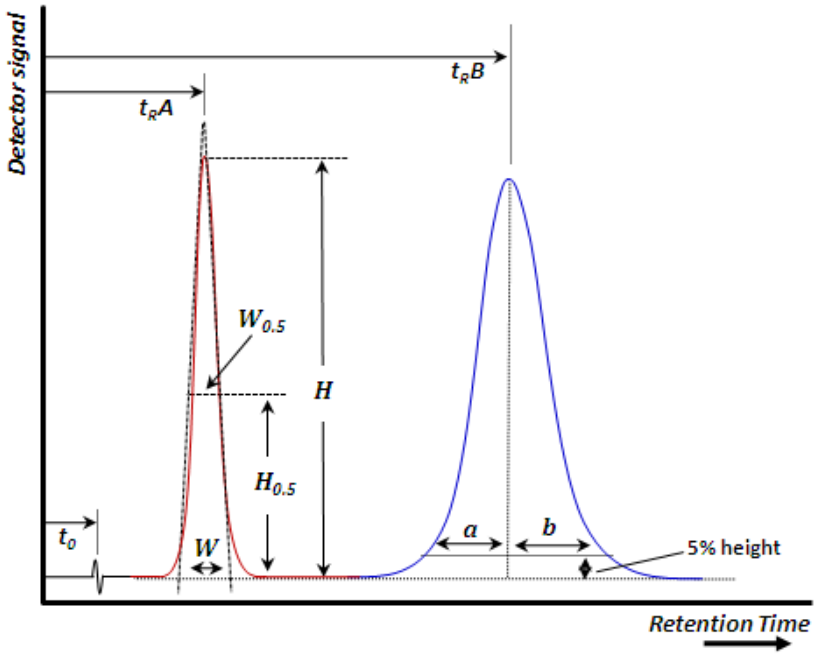

Figure 1.12 Chromatogram showing the resolution of the two peaks

1.8.1.4 Band broadening and Van Deemter plots

Band broadening is a phenomenon that reduces the efficiency of the separation and leading to poor resolution and chromatographic performance. To obtain optimal separations, sharp, symmetrical chromatographic peaks must be obtained. This means that band broadening must be limited. It is also beneficial to measure the efficiency of the column.

As previously stated, column efficiency is related to the ‘’number of theoretical plates’’ or N. Plate theory developed by Martin and Synge, view column as divided into a number (N) of adjacent imaginary segments called theoretical plates. Separate equilibrations of the sample between the stationary and mobile phase occur in these ‘’plates’’. The analyte moves down the column by transfer of equilibrated mobile phase from one plate to the next. The ‘’plates’’ serve as a way of measuring column efficiency, either by the number of theoretical plates in a column, N (the more plates the better), or by the Height Equivalent to a Theoretical Plate HETP, (the smaller the better).

$$N = L/ H \text{ or } HETP = L/ N$$

The rate theory of chromatography is a more realistic description of the processes at work inside a column that takes account of the time taken for the solute to equilibrate between the stationary and mobile phase. Unlike the plate model, which assumes that equilibration, is fast. The rate theory takes into account the mechanism of band broadening, the effect of rate of elution on band shape, the availability of different paths for different solute molecules to follow and the diffusion of solute along length.

In 1956, J.J. Van Deemter derived an equation that included the main factors contributing to column band broadening. He described the individual terms (A, B & C) and derived the Van Deemter equation and also shows a graphical representation of the contribution terms (figure 1.13).

$$\mathbf{HETP = A + B/\mu + C\mu}$$

Where **μ** = the average linear mobile phase velocity. **A** defines as eddy diffusion (multi-path effect); the mobile phase moves through the column which is packed with stationary phase, where solute molecules will take different paths through the stationary phase at random. Hence, these multiple paths arise due to inhomogeneities in column packing and small variations in the particle size of the packing material. This multiple path effect tends to make the band of analytes broader as it moves through the column. **B** defines as random molecular diffusion is a constant expressing the longitudinal diffusion coefficient in the mobile phase. The concentration of analyte is less at the edges of the band than at the center. Analyte diffuses out from the center to the edges. Hence this causes band broadening. However, if the velocity of the mobile phase is high then the analyte spends less time on the column, which decreases the effects of longitudinal diffusion. Therefore, using high linear velocity (high mobile phase flow with narrow columns), will reduce the effects of this broadening factor. **C** is the resistance to mass transfer within particle caused by mobile phase. The analyte takes a certain amount of time to equilibrate between the stationary and mobile phase. If the mobile phase flow rate is high, and the analyte has a strong affinity for the stationary phase, then the analyte in the mobile phase will move ahead of the analyte in the stationary phase. The band of analyte will be broadened. The higher the velocity of mobile phase, the worse the broadening will be.

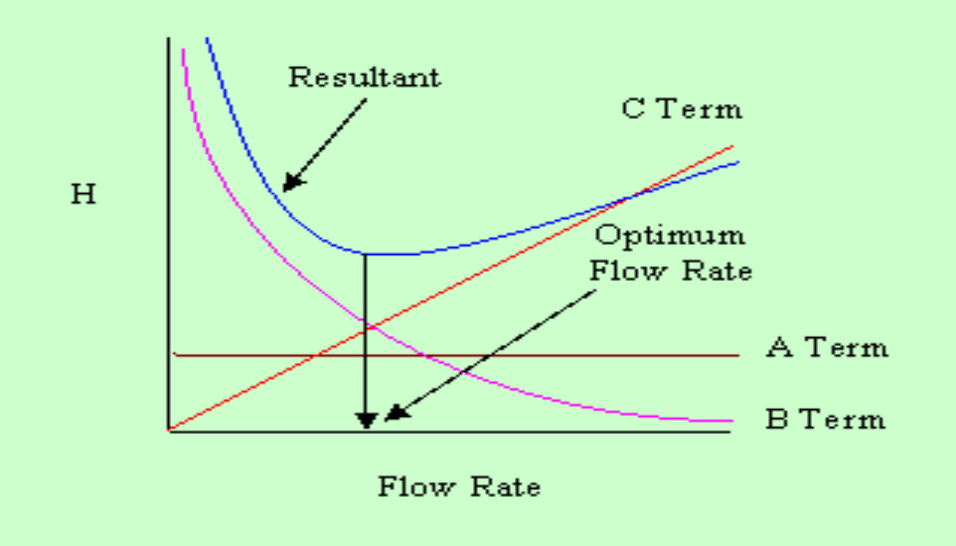

Figure 1.13 van Deemter curve [163]

1.8.2 Overview of Modern Mass Spectrometry

At the beginning of the 1990s mass spectrometry was introduced as a new sensitive detection technique for HPLC in the field of doping analysis [164]. Mass spectrometry has emerged as an invaluable technique with a wide array of applications ranging from clinical to biodefense. With the development of different ionisation techniques and mass analysers, more challenging samples can be analysed, thereby making mass spectrometry an important analytical tool in the field of biophysics. Mass spectrometry is the only technique that offers the combination of high sensitivity with structural information. The different ionisation techniques allow for the analysing of analytes from small metabolites to large macromolecules.

1.8.2.1 Principles of MS

Mass spectrometer generates multiple ions from the sample, it then separates them according to their specific mass-to-charge ratio (m/z). Therefore, mass spectrometry allows quantification of ions and provides structural information by the identification of a distinctive fragmentation patterns. Mass spectrometry also provides an alternative to ELISA and other antibody-based assay, by relying on the discriminating power of mass analysers to select a specific analyte and on ion current measurements to determine quantification.

There are three major components of a mass spectrometer: 1. An ion source generates gas-phase ions from the sample, 2. A mass analyser separates ions based upon their mass-to-charge ratio (m/z), and 3. A detector monitors the ion current and converts it to a signal that is stored by a data system, which is then displayed as mass spectrum. The basic components of a mass spectrometer are illustrated in Figure 1.14.

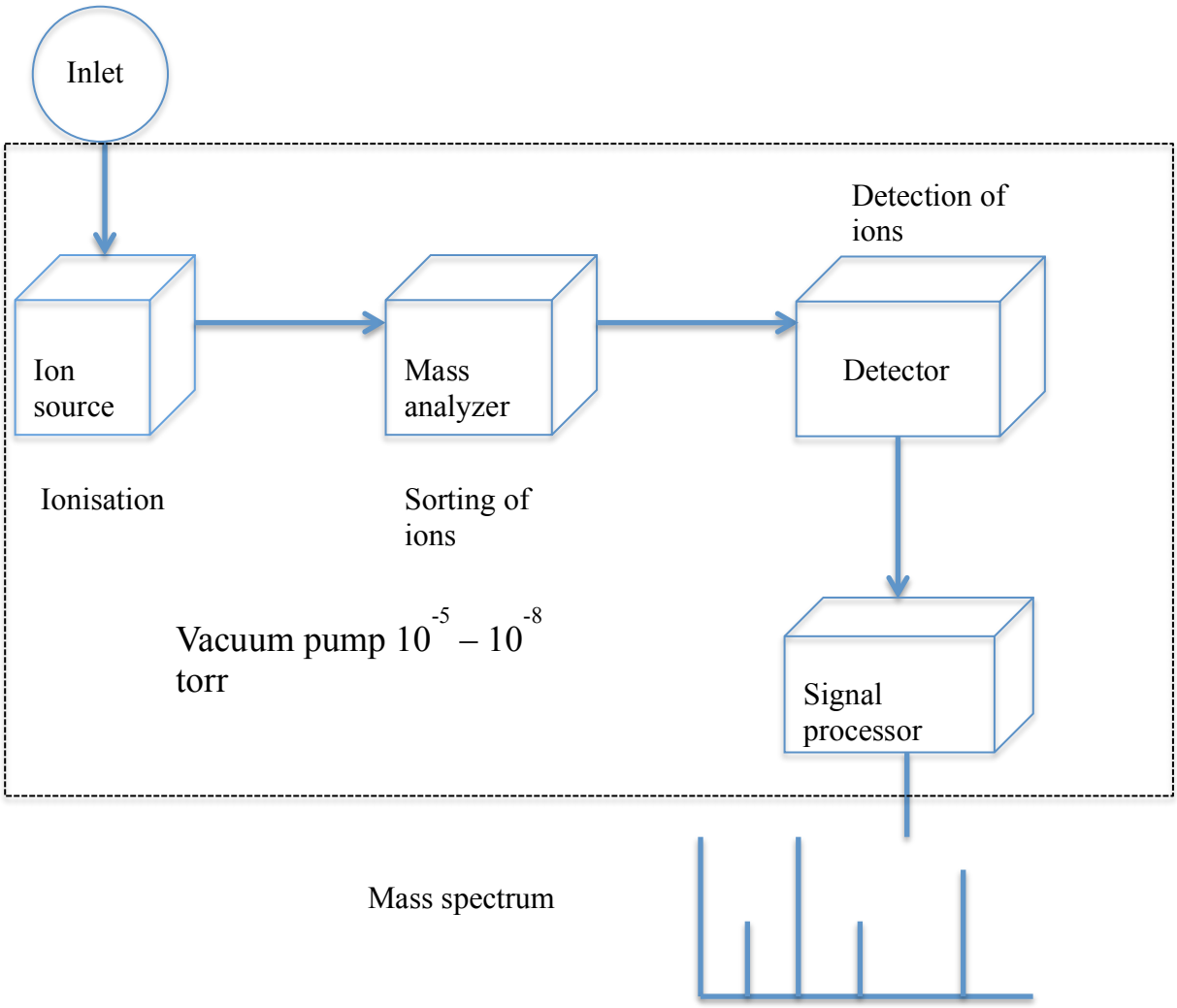

Figure 1.14 Basic components of a mass spectrometer

1.8.2.2 Ionisation modes

The key to using MS for solutions is the ability to transfer the analytes into the vacuum of the mass spectrometer as ionic species. There are a variety of ion sources used to generate ions for mass spectral analysis. For LC-MS, the commonly ionisation modes used are electrospray ionisation (ESI) and atmospheric pressure chemical ionisation (APCI). Electrospray ionisation (ESI) is an ionisation technique used to analyse polar compounds. In ESI gaseous ions are generated directly from a

liquid solution. In ESI, the analytes are often dissolved in a mixture of water and an organic solvent, such as acetonitrile or methanol. Normally, formic acid or acetic acid is added to the aqueous buffer to facilitate protonation of the analyte for the positive ion mode. Whereas, ammonia solution is added to facilitate deprotonation in the negative ion mode. Acidic molecules form negative ions $[M - H]^-$ in solutions with high pH, and basic molecules form positive ions $[M + H]^+$ at low pH. Positive ion electrospray: electrospray ion sources are soft ionisation sources, they produce mostly protonated molecular ions, MH^+. For small molecules, electrospray produces only one peak, the MH^+ peak at mass M+1.

For GC-MS, it is known as electron ionisation (EI), which is caused by a beam of 70 eV electrons in the source. EI provides enough energy to fragment the molecular ion, so that many fragment ions occur in the spectrum. EI spectra are often quite complicated. Electrospray spectra are much easier to interpret than EI spectra.

For ESI, ions in an electrospray source can be formed in the original solution. For example, quaternary amines, R_4N^+, are by their nature already are ions. Ions can be formed from basic compounds by protonation by added acids. The proton transfer can occur in the solution or in the droplets produced by the electrospray source. $M + H^+ \rightarrow MH^+$.

If the compound has several basic sites, like a small peptide with several amine side chains, multiply charged ions may also be formed: $M + 2H^+ \rightarrow MH_2^{2+}$ and $M + 3H^+ \rightarrow MH_3^{3+}$ *etc*. The MS determines the m/z value that is the mass divided by the charge.

Proteins can often produce very high charge states with z~ 40 or more. Small moleucles usually show only one predominant charge state. From this discusiion, it is easily seen that pH control for the sample solution can have a strong effect on the ionisation efficiency and the distribution of the charge states for the analyte ions. Consequently, sample soultions for electrospray MS usually are buffered or have added acids to enhance and control the formation of ions.

The spray tip of the ion source must carry the electrospray current, so it acts as the anode of an electrochemical cell. Therefore, if the molecule can't be easily protonated, ions may still be formed by electrochemical processes in the spray tip. Through direct protonation or electrochemical oxidation, most types of compounds can be analysed. Only nonreactive hydrocarbons are not detectable by electrospray ionisation.

Electrospray is a soft ionisation technique. EI produces fragment rich spectra. The fragment ions are useful to help determine the structure of the compound. On the other hand, in EI some classes of compounds don't produce intense parent peaks, so the molecular weight is difficult to determine. While the ease of molecular weight

determination is strength for electrospray, the lack of structural information from fragment ions can be a draw back. Hence, MSMS techniques can solve this problem.

In MSMS analysis, the MH^+ ions formed from the electrospray source are fragmented by adding extra collisional energy. MSMS is based on an ion trap analyser. In ion traps, ions can be held for long period of time, giving an easy opportunity to fragment the parent MH^+ ions. The trap is always filled with about 1 Torr of helium gas. A small radio frequency field can be applied to the trap to cause the ions to move faster. The parent ions collide with the helium background gas causing fragementation. After adding this collisional energy, the resultant ions are scanned in the normal way to determine their m/z. This process is called collision-induced dissociation, CID. CID MSMS spectra are very similar to EI spectra and can be interpreted similarly.

MSMS spectra can be acquired manually by selecting the mass of the parent ion to be fragmented and the amount of collisional energy. MSMS can also be done automatically. In Auto MSMS mode, the computer determines the mass of the most intense parent ions and subjects those ions to MSMS.

MSMS analysis is particularly useful for biopolymers. Proteins, peptides, and oligonucleotides can be sequenced using MSMS. The auto MSMS analysis of proteolytic digests of proteins is one of the two MS techniques that have spawned the new field of proteomics. The other MS technique is MALDI.

The major processes (shown in Figure 1.15) involved during ion formation in ESI are: 1) the solution containing the analyte, eluting from the analytical column, passes through a needle (the electrospray needle) that has a high potential applied to it (2 to 5 kV). This forces the spraying of charged droplets from the needle with a surface charge of the same polarity to the charge on the needle. 2) the droplets are repelled from the needle towards the MS sampling cone on the counter electrode, as the droplets traverse the space between the needle tip and the cone, solvent evaporation occurs and shrinkage of the charged droplets, and repeated droplet disintegration resulting in small highly charged droplets, and 3) this produce smaller droplets and the process of further reduction of droplet size is repeated and naked charged analyte molecules are generated. These charged analyte molecules can be single or multiple charged [165]. There are two major theories that explain the final production of gas-phase ions: the ion evaporation model (IEM) and the charge residue model (CRM). The IEM theory explained as the droplet reaches a certain radius the field strength at the surface of the droplet becomes large enough to assist the field desorption of solvated ions [166, 167]. The CRM theory explained that electrospray droplets undergo evaporation and fission cycles, eventually leading progeny droplets that contain on average one analyte ion or less [168]. The gas-phase ions form after the remaining solvent molecules evaporates, leaving the analyte with the charges that the droplet carried.

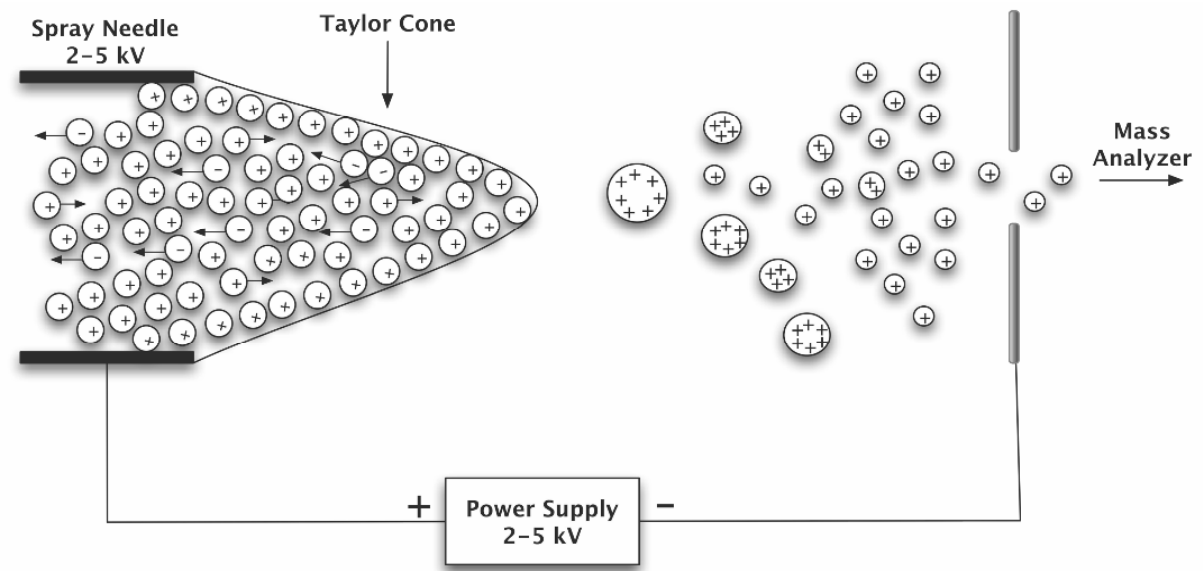

Figure 1.15 Schematic diagram of ESI ionisation process on Applied Biosystem, Thermo and Waters Mass spectrometer. [165]

Nebuliser settings: Flows of nitrogen gas are used to nebulise the analyte solution and dry the droplets. There are several gas flow rates that need to be set for proper operation of the source (shown in Figure 1.16). Nitrogen gas is used because it is relatively cheap and very pure. The nebuliser pressure determines the nebulisation efficiency. When the nebuliser is working properly, a fine and even mist will be seen at the tip of the spray needle. The spray cone should be stable and not showing fluctuations in size.

The dry gas has two purposes. This gas is heated to provide for efficient evaporation of the solvent. The dry gas also acts a barrier that helps keep the transfer capillary clean. If the dry gas flow is not sufficient, droplets and contaminants can clog or contaminate the transfer capillary. The vacuum system must be turned off to clean

the capillary. Therefore, the dry gas flow must be ensured 5-9 L/s before beginning the spray from ESI needle.

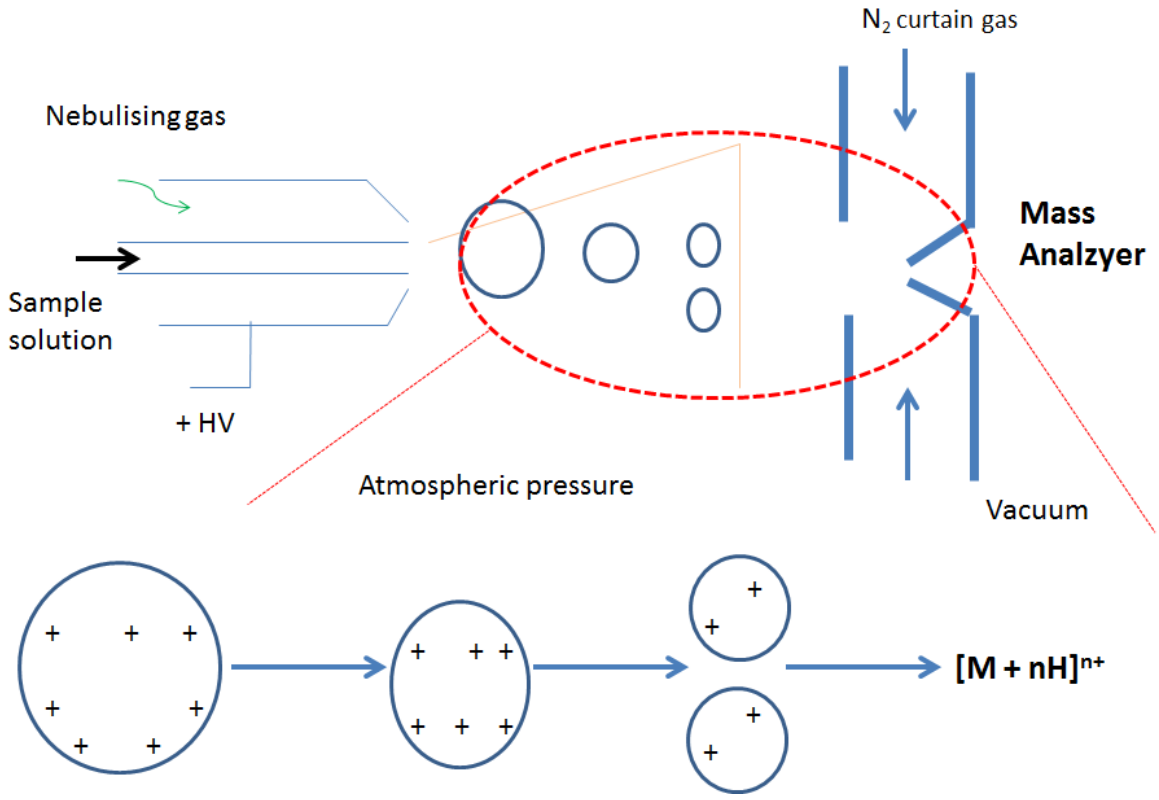

Figure 1.16 Electrospray Ionisation (ESI)

Nano-electrospray ionisation- The advent of nano-electrospray ionisation (nano-ESI) has considerably extended the usability of ESI in the analytical mass spectrometric laboratory. One of the remarkable features of nano-ESI is its extremely low sample consumption. Only a few microliters of analyte solution are sufficient for molecular weight determination and structural investigations by MS/MS. But nano-ESI is more than just a minimized-flow ESI; the low solvent flow rate also affects the mechanism of ion formation [169]. This can be attributed to the different initial droplet sizes which

are in the μm range for ionspray, while in nanospray they are about one order of magnitude smaller (as shown in Figure 1.17).

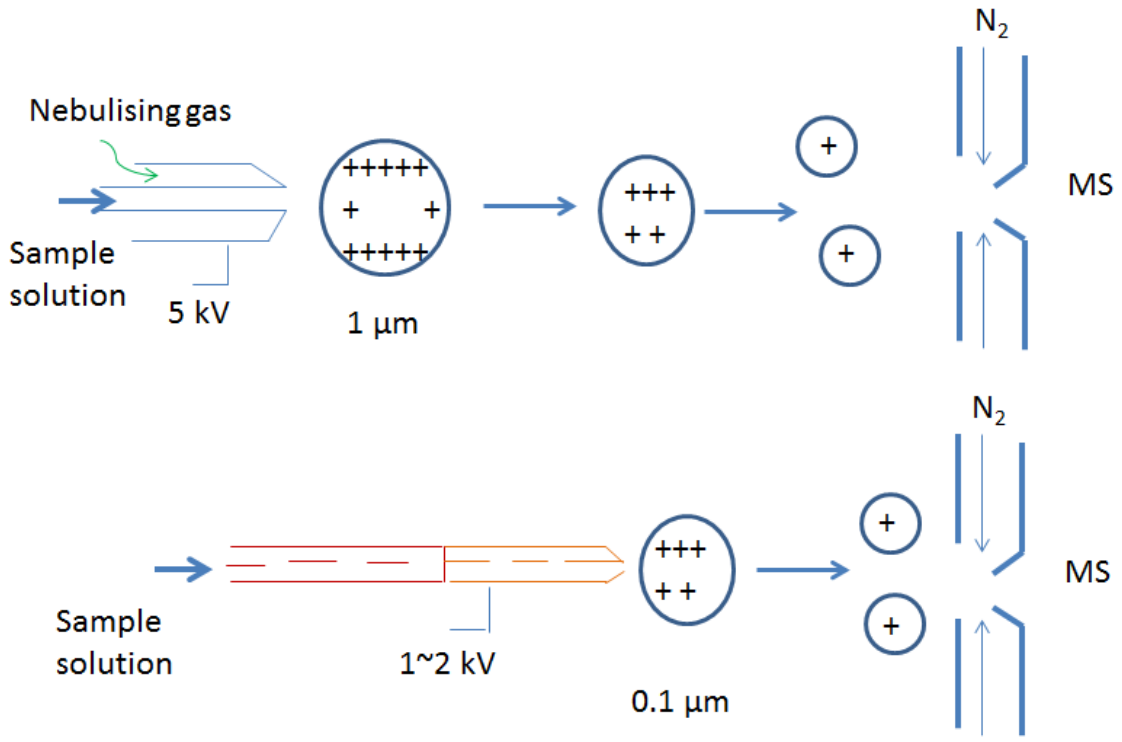

Figure 1.17 Comparison of ESI and Nano-ESI- ionisation efficiency

1.8.2.3 MS analyzers used in Bioanalysis

A mass analyser is the component of the mass spectrometer that takes ionised masses and separates them based on mass to charge ratios and outputs them to the detector where they are detected and converted to a digital output. There are several types of mass analysers used for the separation of ions; they are quadrupole, time of flight (TOF), magnetic sector, electrostatic sector, quadrupole ion trap and ion

cyclotron resonance mass analysers. Among these analysers, quadrupole and ion trap mass spectrometers are the most commonly used.

The quadrupole mass analyse is a ‘’mass filter’’, it consists of four parallel rods. Each opposing rod pair is connected together electrically, and a radio frequency (RF) voltage is applied between one pair of rods and the other. Combined DC and RF potentials on the quadrupole rods can be set to pass only a selected mass-to-charge ratio. Ions travel down the quadrupole between the rods. Only ions of a certain mass-to-charge ratio will reach the detector for a given ratio of voltages, other unstable ions will collide with the rods. Thus, this allows selection of an ion with a particular m/z or allows the analyst to scan for a range of m/z values by continuously varying the applied voltage [170].

Ion trap mass analyser employs similar principles as the quadrupole analyser mentioned above; it uses an electric field for the separation of the ions by mass to charge ratios. The analyser is made with a ring electrode of a specific voltage and grounded end cap electrodes. The ions enter the area between the electrodes through one of the end caps. After entry, the electric field in the cavity due to the electrodes causes the ions of certain m/z values to orbit in the space. As the radio frequency voltage increases, heavier mass ion orbits become more stabilised and the light mass ions become less stabilised, causing them to collidew with the wall, and eliminating the possibility of traveling to and being detected by the detector.

The quadrupole ion trap usually runs a mass selective ejection, where selectively it ejects the trapped ions in order of increasing mass by gradually increasing the applied radio frequency voltage.

Liquid chromatography-tandem mass spectrometry (LC-MSMS) is the preferred method used for bioanalysis as it is fast and sensitive.

Triple quadrupole mass spectrometers are ideal for quantitative work, as they allow for linear, highly sensitive, simultaneous multi-component analysis. A triple quadrupole mass spectrometer is a tandem mass spectrometer consisting of two quadrupole mass spectrometers in series, with a (non mass-resolving) radio frequency RF-only quadrupole between them to act as a cell for collision-induced dissociation (CID). The first analyser (Q1) selects the ions of interest, the ions are then fragmented in the collision cell (Q2), and the fragments are analysed in the third quadrupole (Q3), which act as a mass filter. This collision cell is an RF-only quadrupole (non-mass filtering) usually using Ar gas for collision induced dissociation of selected precursor ion from Q1. Subsequent fragments are passed through to Q3 where they may be filtered or fully scanned. This process is illustrated in Figure 1.18. In MS/MS operation, different scan modes can be used to get complementary, qualitative information.

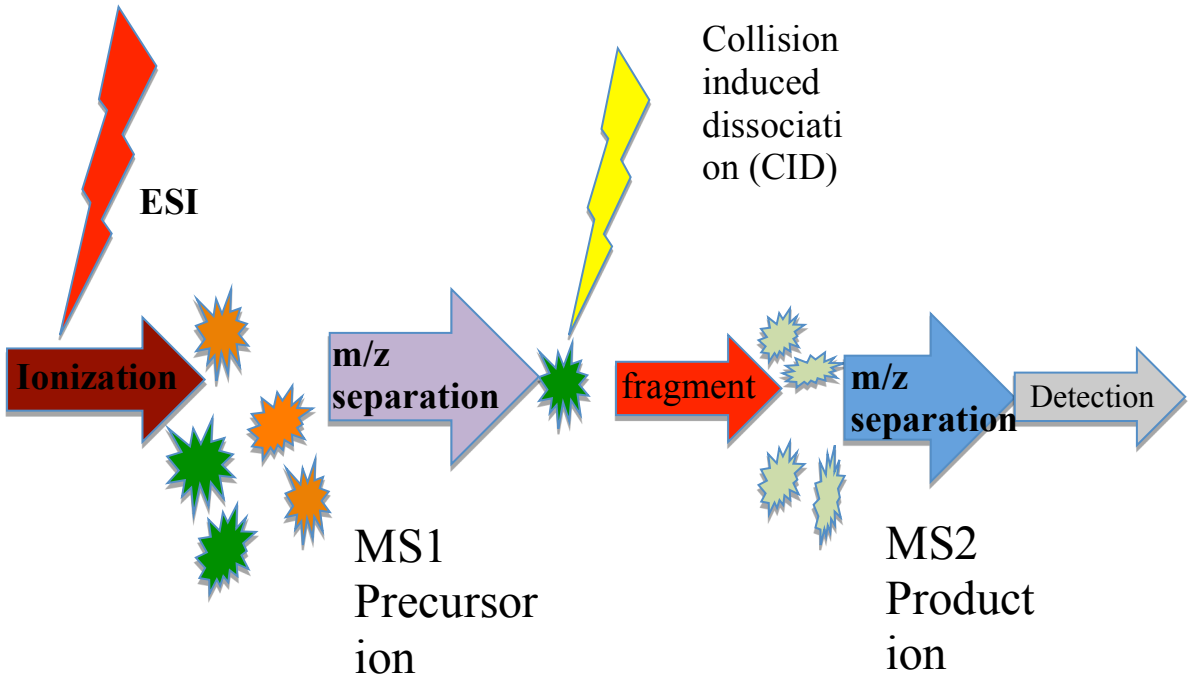

Figure 1.18 Schematic of tandem mass spectrometry

Selected reaction monitoring (SRM), also known as multiple reaction monitoring (MRM) is one of the scan method used in tandem mass spectrometry. SRM/ MRM is a highly sensitive and selective method for the targeted quantitation of protein/ peptide abundances in complex biological samples, allowing scientists to fine tune an instrument to specifically look for the peptides, or proteins fragments, of interest. SRM/ MRM allow scientists to select peptides of interest while all other peptides are filtered out. Peptides are detected by mass spectrometry analysis and the exact concentrations are determined as shown in Figure 1.19.

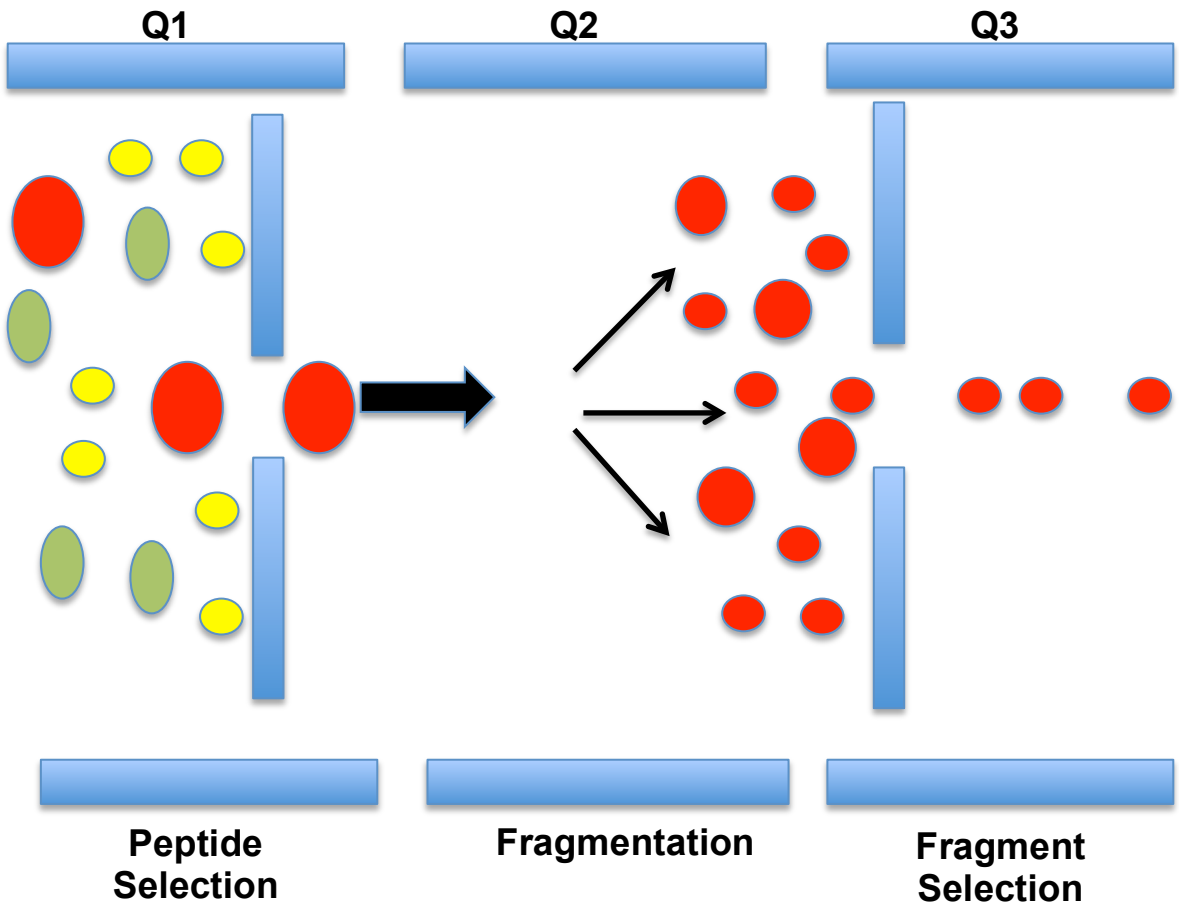

Figure 1.19 Schematic diagram of SRM/ MRM experiment

The first mass analyser (Q1) is set to only transmit the precursor m/z of a protein, the collision energy is optimised to produce a diagnostic charged fragment of a protein fragment (peptide) in the second mass analyser (Q2), and the third mass analyser (Q3) is set to transmit this diagnostic peptide fragment only. Therefore, only the exact m/z transition is detected.

In SRM experiment, a predefined precursor ion and one of its fragments are selected by the two mass filters of a triple quadrupole instrument and monitored over time for

precise quantification. A series of transitions (precursor/ fragment ion pairs) in combination with the retention time of the targeted peptide can constitute a definitive assay. Hence, this approach allows for greater specificity, sensitivity, speed and quantitation of an analyte of interest.

1.9 Research aims

The objectives of this research project are to have a fast and sensitive detection of glycoproteins from recombinant human erythropoietin and darbepoetin in equine plasma by LC-MSMS, and this will be achieved by the following various techniques:

1) To understand the art of fabricating monoliths with various factors affecting the morphology of monoliths, and demonstrating that fabricated HILIC monolith separation performance can be compared to commercially available columns

2) To learn the technique of immobilizing trypsin enzyme and deglycosylation on monolithic capillary to make an enzyme reactor

3) To learn the technique of immunoaffinity extraction

4) To set-up an on-line detection technique for rhEPO and DPO with a trypsin enzyme reactor and deglycosylation reactor coupled to MS as shown in Figure 1.20.

5) To set-up an on-line LCMS, orthogonal reversed-phase trap-WCX-HILIC to de-salt, trap and enhance peak resolution as shown in Figure 1.20.

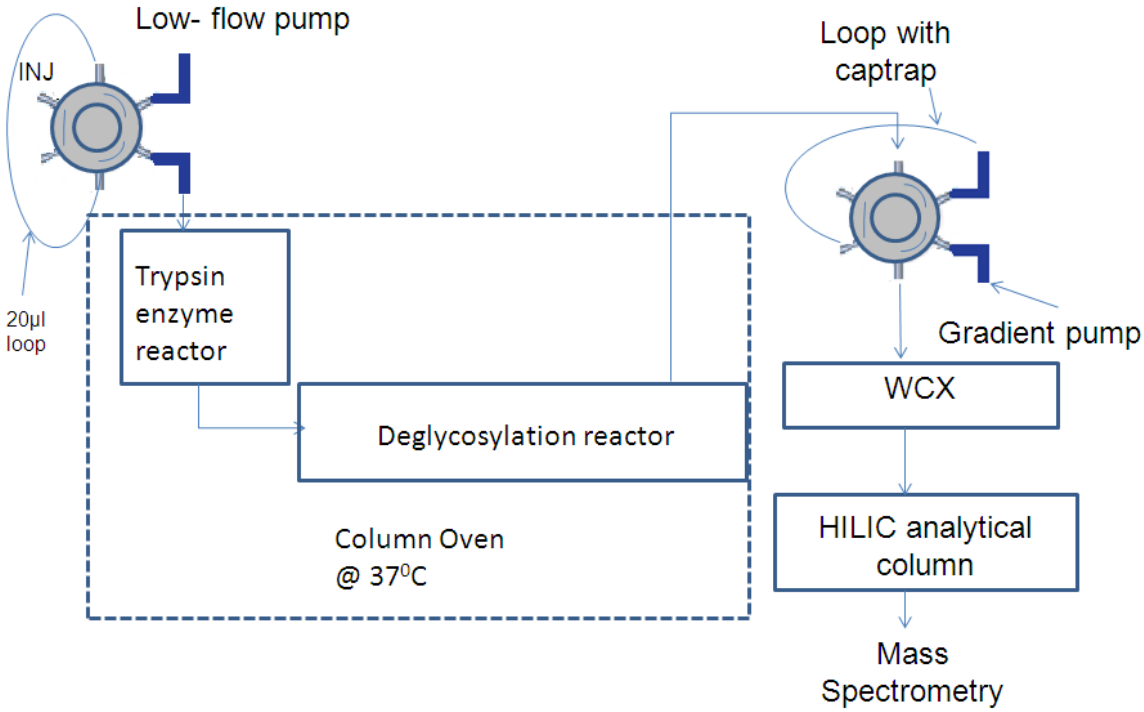

Figure 1.20 Schematic diagram of an on-line set-up for detection of rhEPO and DPO

Chapter 2 Fast and sensitive detection of rhEPO using capillary flow LC-MSMS Methodology and the fabrication of an internal-tapered capillary tip for nano-electrospray ESI-MS

2.1 Introduction

Recombinant human erythropoietin (rhEPO), as well as the synthetic analogs darbepoetin-α (DPO) and methoxy-polyethyleneglycol-epoetin-ß (CERA), are protein-based drugs used for the treatment of anemia by stimulating red blood cell production. Therefore, in a healthy mammal, this could also boost stamina and, not too surprisingly, it had been reported to be widely abused by both human and equine athletes [43,171]. Recombinant human EPO, DPO and CERA are foreign proteins in a horse and therefore horses treated with these epoetins may produce anti-rhEPO antibodies that can cause severe inhibition of erythropoieses, leading to anemia and occasionally even death [25-26, 38]. Thus, there is a need to create an efficient screening method to detect rhEPO, DPO & CERA in plasma at the low concentrations found after administration.

To deter the abuse of rhEPO, DPO & CERA in the racehorse, for both welfare and performance enhancement reasons, it is crucial to have an efficient screening method that can detect these epoetins in plasma at the very low concentrations (~0.1 to 1 ng per ml) that are present after administration [38]. Mass spectrometry is the technique of choice for specific identification of prohibited substances in equine doping control analyses [172] and, when used in combination with LC, this is also the preferred technique for identification of protein-based drugs such as rhEPO. Selected reaction monitoring (SRM) is well known for its sensitivity and generally methods using this approach are both reproducible and robust.

Early attempts at screening for these drugs [3, 39-40, 173] by LC-MS were hindered by a lack of sensitivity and, as a result, were unable to detect the protein in post-administration plasma obtained from racehorses. Then in 2008 Guan and his co-workers published a method [38, 44, 171] that could successfully detect low concentrations of rhEPO and DPO in equine plasma. However, their instrument configuration utilised a LC column with a diameter of 1 mm and my view was that even better sensitivity from this analysis could be achieved by using a smaller column diameter and a lower flow rate (down-sizing effect). Whilst nano LC could give the best response, it can be a challenge to set-up the system properly. For example, care must be taken to minimise any dead volume in the flow path or the anticipated gain in sensitivity can be destroyed by poor chromatography. Furthermore, the nano flow rate used generally equates to a longer analysis time for each sample and I was aiming for a solution which optimised both sensitivity and sample throughput. In order to address this need, I opted to use a capillary LC-MS utilising a 300 µm i.d. column with a 4 µl per minute flow rate. I have evaluated the performance of this capillary flow system and these results were compared with those obtained using the higher flow rate LC approach used in Guan's publication.

In this chapter, I describe a capillary flow LC system using an Eksigent Tempo® LC system coupled to a 4000 QTRAP® LC/MS/MS instrument. The rhEPO tryptic peptides were separated at a flow rate of 4 µl/min on a 300 µm i.d. column and the limit of detection was around 0.2 ng per ml of immunoaffinity extracted equine plasma when screening for the T17 peptide obtained from the digest of the EPO protein. Peak width at half-height (PWHH), calculated from the extracted ion

chromatograms from the SRM transitions for the target analytes, was less than 0.1 min in all cases and resolution was satisfactory when using a 30 min solvent gradient.

This methodology was successfully applied to the identification of the peptides obtained from digestion of the rhEPO protein and the shorter analysis time improved the efficiency of the operation resulting in a reduction in the amount of solvent consumed.

In this chapter, I also explored my experiment with using the nano-spray source. I had also reported on the fabrication of fused silica capillaries with internal tapered tips filled with reversed-phase silica packing to act as an analytical column and emitter to the nano-electrospray MS.

The tip was prepared by slowly heating the fused silica capillary end in the Oxy acetylene flame. The part of the coated capillary which was burnt was stripped off after heating, which left the glass exposed. This exposed part of the glass capillary end was heated at the hottest part of the flame, and was observed under the microscope, where we can see that the inner channel of the capillary was shrinking. The internal diameter of the heated end was reduced to approximately 7-10 μm. After the formation of this tapered tip in the internal capillary, I can also see molten silica form at the outside of the glass capillary which eventually sealed the capillary. Following this, it was required to attach the other end of the capillary to an HPLC pump using water as solvent. The capillary tip was then gently brushed from side to

side across some fine abrasive paper until there was a stream of solvent out from the tip, but not breaking the tip. The microscope can be used to investigate that the tip is still in good condition. If the flow is in droplet form, this could mean that the tip has broken. Hence, it requires a skill to make this internal tip successfully.

There are advantages in using internal tapered tips over the commercially available external tapered tip and that is that external tapered tips were fragile, have poor durability, and are easily broken. Hence, this is successfully overcome by using an internal tapered tip. One publication [174] showed a comparison between external versus internal tapered tips, with the latter showing enhanced electrospray stability, resulting in significantly lower short-term noise. In this work, I explored this novel procedure to fabricate an internal tapered capillary tip with the aim to enhance stability, sensitivity, and robustness for the nano-electrospray MS.

2.2 Materials and Instrumentation

2.2.1 Materials.

DL-dithiothreitol (DTT) and ammonium formate were all purchased from Sigma Aldrich (Singapore). HPLC-grade methanol and acetonitrile (ACN) were obtained from Fisher Scientific (Singapore). Ammonium bicarbonate and ammonium acetate were purchased from Merck (Singapore). Sequencing grade modified Trypsin (P/N No. V5111) was purchased from Promega (Singapore). The water used throughout all experiments was produced by a Milli-Q Gradient A10 from Millipore (Singapore). Epoetin alfa, Eprex® the recombinant human erythropoietin, 10,000 IU/ ml was

purchased from Jassen-Cilag AG, (Schaffhausen, Switzerland). Human EPO 1 mg/ ml protein was purchased from Genway Biotech, Inc. (San Diego, CA, USA). Nanosep 30 KDa OMEGA was obtained from PALL Corporation (USA). Polyclonal anti-rhEPO antibody (purified rabbit IgG) was purchased from R&D Systems (Minneapolis, MN). Magnetic beads, Dynabeads M-280 Tosylactivated, (concentration: 2 x 10^9 beads/ml, approximately 30 mg/ml) were purchased from Invitrogen (Singapore). Igepal CA-630 (molecular biology grade), polyethylene glycol 6000 was purchased from Sigma Singapore. Magnetic particle concentrator was purchased from Invitrogen. Ultrafree-CL centrifugal filter devices (2 ml capacity) with 0.22 µm membrane pore size and Centricon centrifugal filter devices (2 ml capacity) with molecular weight cut-off of 30 KDa were purchased from Millipore (Singapore). 5 ml plastic vial (Argos Technologies. Elgin, Illinois). 75 µm i.d. fused silica capillary was purchased from Polymicro (U.S.A). The 2.5 µm Kinetex silica packing was removed from a Phenomenex column packing material. ‘’The Little Torch’’ with Sapphires from Smith Equipment (U.S.A), attached to a tank of acetylene and a tank of oxygen, was used as the burner to make the internal tapered tips.

Buffers used for linking anti-rhEPO antibody to the magnetic beads and subsequent immunoaffinity separation of rhEPO were prepared according to Invitrogen’s manual; phosphate buffered saline (PBS, pH 7.4); borate buffer, 0.1 M, pH 9.5 (Buffer B); PBS (pH 7.4) plus 0.1 % (w/v) bovine serum albumin (BSA), 2 mM EDTA, and 0.02 % (w/v) sodium azide (Buffer C); Tris buffer (0.2 M, pH 8.5) plus 0.1 % (w/v) BSA (Buffer D); washing buffer, 1 % (w/v) Igepal CA-630 in PBS (pH 7.4); elution buffer, 0.1 % PEG 6000 in PBS (adjusted to pH 2.0 with concentrated HCl). All the buffers were stored at 4 ºC.

2.2.2 Instrumentation

2.2.2.1 Capillary Flow Set-up: A Tempo® nano MDLC by Eksigent was coupled to AB Sciex 4000 QTRAP® LC/MS/MS with Eksigent AS1 Autosampler. The analytical column used with this set-up was a 2.7 µm C18-HALO® column with a dimension of 0.3 x 150 mm. A trap column (Captrap® from Michrom) was installed on the 1/32'' 6-port VICI switching valve. Flow rate 4 µl/min. A custom-made turbo ion spray probe was fabricated by inserting a 15 µm i.d. fused silica capillary into the probe to reduce the dead volume when using a lower flow rate.

2.2.2.2 High Flow Set-up: An Agilent 1100® LC Binary pump was coupled to an AB Sciex 4000 QTRAP® LC-MSMS with Eksigent AS1 Autosampler. The analytical column used with this set-up was a 3.5 µm XTerra® C18 (1 mm i.d. x 50 mm). A trap column (Captrap® from Michrom) was installed on the 1/16'' 6-port VICI switching valve. Flow rate 100 µl/min.

The LC gradient for both capillary and high flow set-up: Mobile phase A- 0.15 % Formic Acid in water, Mobile phase B- 100 % ACN

TIME (MIN)	MOBILE PHASE A (%)	MOBILE PHASE B (%)
0	96	4
1	96	4
30	38	62
31	20	80
34	20	80
35	96	4
45	96	4

Table 2.1 LC gradient for both capillary and high flow

2.2.2.3 Nano-flow Set-up: The autosampler and LC pump set-up was similar to the capillary flow above, except instead of using a Turbo-ion source, a NanoSpray® III Source and Heated Interface was used. The fabricated internal tapered fused silica capillary tip was installed on the nano-spray mounting bracket and arm.

The mobile phase used in both CH 1 and CH 2 are Mobile phase A- 0.15 % FA in water, Mobile phase B- 100 % ACN. The CH 1 pump with a high flow rate of 20 µl/min was used as loading pump, loading the sample at 50 % A and 50 % B isocratic. The CH 2 pump with a low flow rate of 500 nl/min was used as gradient pump. The gradient starts at high aqueous, 95 % A and 5 % B for 2 min, then a 5 min gradient, reaches 100 % B at 7 min, which is then held for 3 min. At 11 min, it was returned to its initial condition and re-equilibrated till 25 min.

2.2.2.4 MS condition for turbo ionspray (TIS). The curtain gas flow was set at 10; the collision gas flow (CAD) was set high, with an Ionspray voltage set at 5500 V. The ion source gas, GS 1 was set at 20 psi, and GS 2 was set at 0 psi. The interface temperature was set at 0 ºC. The collision energy (CE) was set at 20 and the declustering potential was set at 100 V.

2.2.2.5. MS condition for nano-electrospray. The curtain gas flow was set at 25 psi; the collision gas flow (CAD) was set high, with an Ionspray voltage set at 3800 V. GS 1 was set at 14 psi, and GS 2 was set at 0 psi. The interface temperature was set at 150 ºC. The collision energy (CE) was set at 20 and the declustering potential was set at 100 V.

2.2.3 Preparation of samples

2.2.3.1 Procedure for linkage of anti-rhEPO antibody to magnetic beads.

A brief summary of the procedure for immunoaffinity separation of rhEPO from equine plasma and LC-MSMS confirmation is described in Figure 2.1. Linkage of the anti-rhEPO antibody to magnetic beads was carried out as previously reported [33, 38].

(a) The magnetic beads, Dynabeads M-280 tosylactivated in the original vial were re-suspended by brief shaking. 1 ml of the re-suspended beads was transferred into a 5 ml plastic vial.

(b) The vial was placed in the magnetic particle concentrator (MPC-S) for 2 min, and the supernatant was transferred to waste using a disposable plastic pipette.

(c) The vial was removed from the MPC-S, and 1 ml of borate buffer (0.1 M, pH 9.5) (Buffer B) was added to wash the beads. Steps (b) and (c) were repeated discarding the wash buffer and re-suspending the beads in 1 ml of the borate buffer.

(d) Polyclonal anti-rhEPO antibody (0.5 mg) was dissolved in 0.5 ml of the borate buffer, and added to the magnetic beads suspended in 1 ml of the borate buffer.

(e) The mixture from step (d) was incubated at 37 °C for 24 hr.

(f) Step (b) above was repeated to remove the supernatant.

(g) Coated magnetic beads were washed twice with 1 ml of PBS (pH 7.4) plus 0.1 % BSA, 2 mM EDTA and 0.02 % sodium azide (Buffer C) for 5 min each at ambient temperature.

(h) Coated magnetic beads were incubated with 1 ml of Tris buffer (0.2 M, pH 8.5) plus 0.1 % BSA (Buffer D) for 4 hr at 37 ºC, to block residual tosyl groups.

(i) Coated magnetic beads were washed with 1 ml of Buffer C for 5 min at ambient temperature, and re-supended in 1 ml of Buffer C. Magnetic beads coated with anti-rhEPO antibody were now ready for use.

2.2.3.2 Procedure for immunoaffinity separation of rhEPO and DPO from equine plasma.

RhEPO and DPO were extracted from equine plasma by anti-rhEPO antibody linked to magnetic beads, using the reported procedure [33, 38].

(a) An aliquot of 400 µl of magnetic beads coated with anti-rhEPO antibody was washed with 2 ml of Buffer C in a 5 ml plastic vial and then re-suspended in 400 µl of Buffer C.

(b) 2 ml of equine plasma spiked with rhEPO (0.2 ng in 5 µl of water) was added and mixed to the washed magnetic beads. The mixture was incubated in the oven at 37 °C for 24 h. During the entire incubation period, the mixture was gently shaken using the Stuart Rotator SB3; this is to prevent precipitation of magnetic beads.

(c) After the incubation, the vial was centrifuged at 100 x g rcf for 1 min at 20 °C, and then placed in the magnetic particle concentrator (MPC-S) for 2 min, after which the supernatant was discarded. The magnetic beads were washed with 2 ml of 1 % Igepal CA-630 in PBS (pH 7.4) in the vial that was continually rotated by the rotator for 5 min at ambient temperature. The vial was placed in the MPC-S for 2 min, and the supernatant was discarded. The beads were then washed three times.

(d) After the supernatant was discarded, 1 ml of 0.1 % PEG 6000 in PBS (pH 2) was added to the magnetic beads in order to elute rhEPO from the antibody. The magnetic beads and the elution buffer were incubated in the vial that was gently shaken as described in step (b) for 30 min at ambient temperature.

(e) After the incubation, the vial was centrifuged at 100 x g rcf for 1 min and then placed in the MPC-S for 2 min, and the supernatant containing rhEPO was collected into the 0.22 µm membrane pore size filter device with, using a disposable plastic pipette.

(f) The magnetic beads with anti-rhEPO antibody were washed with 2 ml of Buffer C for 5 min at ambient temperature, and then separated using the MPC-S, and the

supernatant was discarded. The magnetic beads with anti-rhEPO antibody were stored in Buffer C (2 ml) at 4 °C for future use.

2.2.3.3 Procedure for buffer exchange of rhEPO eluate in preparation for tryptic digestion.

The eluates from the immunoaffinity separation, containing phosphate buffer (pH 2) and PEG 6000, were not suitable for subsequent tryptic digestion of rhEPO, therefore this required buffer exchange to ammonium bicarbonate (50 mM, pH 7.8) which was suitable for tryptic digestion. This was achieved by using a Centricon centrifugal filter device with molecular weight cut-off of 30 KDa. The molecular weight of rhEPO is 30.4 KDa and thus, it can be retained by the filter.

(a) The eluate from the immunoaffinity separation of rhEPO from equine plasma was collected into an Ultrafree-CL centrifugal filter device with a 0.22 μm membrane pore size, and filtered by centrifugation at 2500 x g rcf for 5 min.

(b) The filtrate was transferred into the filter device with molecular weight cut-off of 30 KDa, and the latter was centrifuged at 3500 x g rcf for 35 min at 20 °C, resulting in 50 - 100 μl of the solution remaining on the filter membrane. The resulting filtrate was discarded.

(c) 400 μl of ammonium bicarbonate (50 mM, pH 7.8) was added to the filter membrane and centrifuged at 3500 x g rcf for 15 min at 20 °C, and the filtrate was discarded.

(d) The process in (c) was repeated for four times.

(e) The final bicarbonate buffer (50 - 100 µl) containing rhEPO on the filter membrane was recovered by inverting the filter device (with its cap on) and centrifuging at 500 x g rcf for 2 min. The bicarbonate buffer containing rhEPO was now in the tube, ready for trypsin digestion. The sample was reduced before trypsin digestion by adding 5 µl of 100 mM DTT to the sample for 10 min at room temperature. After the sample was reduced, it was ready for trypsin digestion.

2.2.3.4 Tryptic digestion of rhEPO.

10 µl of trypsin (20 µg in 100 µl ammonium bicarbonate) was added to each rhEPO extract in ammonium bicarbonate buffer (50 mM, pH 7.8). The mixture was vortexed and incubated in a water bath at 37 °C for 3 h. The digestion was terminated by adding 4 µl of 10 % formic acid in water. The digested protein was subsequently analysed by LC-MSMS.

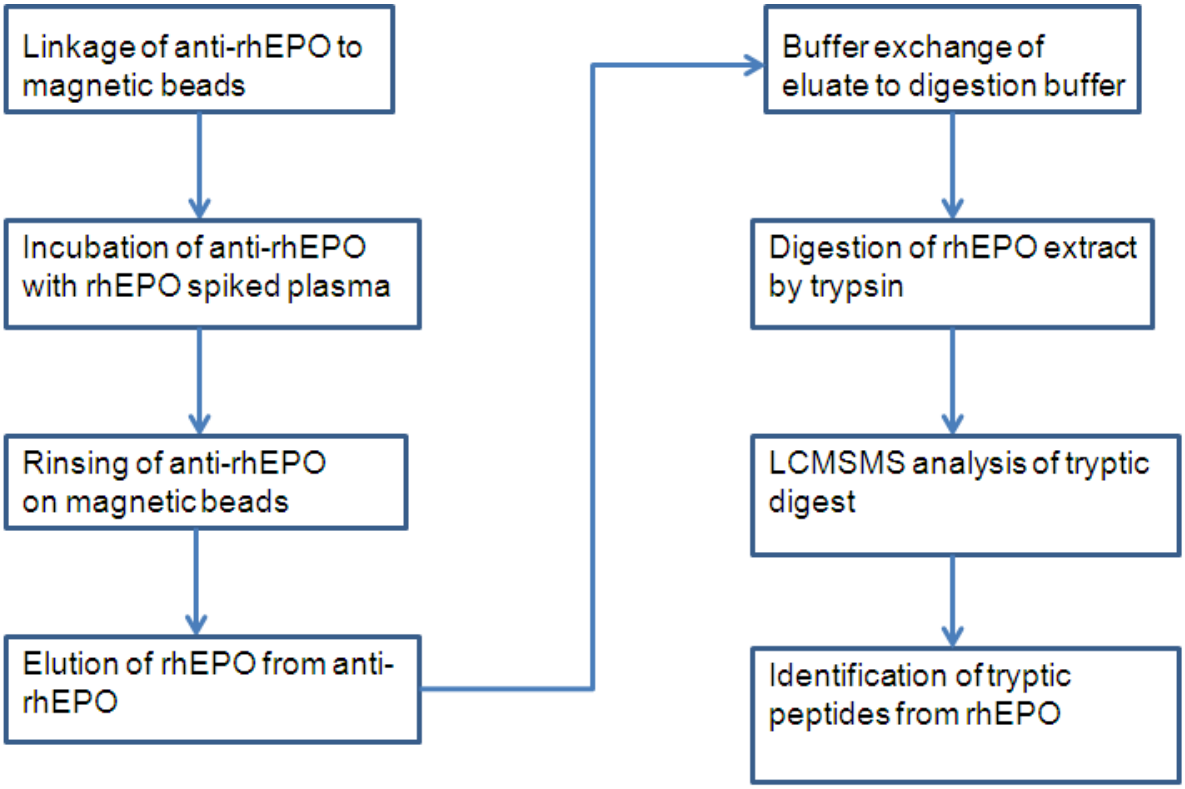

Figure 2.1 Flow chart showing the steps in immunoaffinity separation of rhEPO and DPO from equine plasma and LC-MSMS confirmation.

2.2.3.5 Fabricating internal tapered tip.

A 75 µm i.d. fused silica capillary was cut into a length of 10 cm. The front end about 0.5 cm was inserted into the torch with Oxy acetylene flame. For a couple of seconds, it could be seen that the capillary coating was being stripped off which left the plain glass surface exposed. The fused silica capillary was removed from the flame and cleaned with methanol. It was viewed using a microscope. From the microscope, I could see the front end is clear glass, and the inner diameter could be seen clearly from the microscope (Figure 2.2a). The fused silica capillary was placed into the middle part (blue) of the flame to further burn it until it could be seen from the microscope (Figures 2.2b & c) that the inner channel had shrunk to a diameter of

approximately 17 - 40 µm Figures 2.2d & 2.3 show the formation of a tapered tip in the inner layer, although sometimes, the internal and diameter was sealed. In this case, it was required to attach the other end of the capillary to a HPLC pump to set a gentle flow, while the glass end was brushed gently onto an abrasive paper, until a stream of flow was flushed out. If droplets were seen dripping from the glass end, the tips are most likely broken; hence this was examined under the microscope to see if the tip was broken.

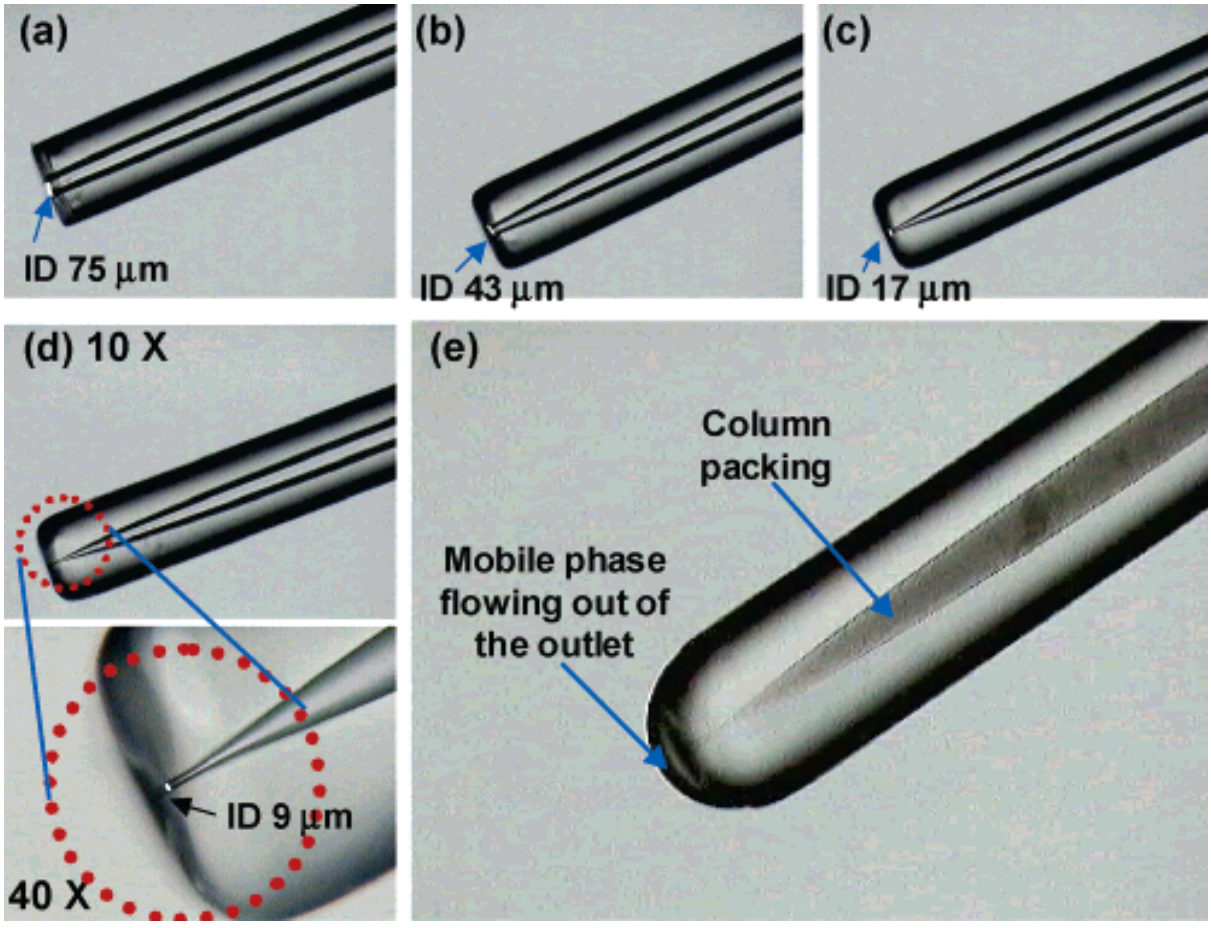

Figure 2.2 Various microscopic views of the steps of fabricating an internal tapered fused silica capillary column [174]

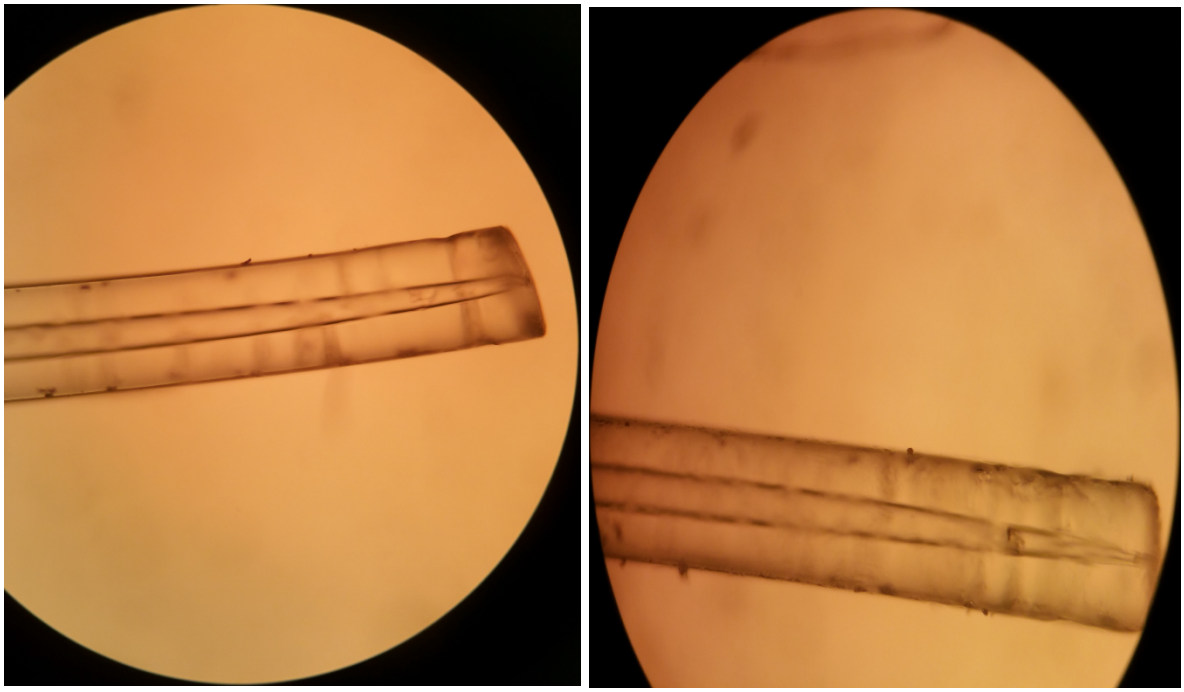

Figure 2.3 Microscopic view of a fabricated internal tapered fused silica capillary tip

2.2.3.6 Packing the fabricated internal tapered tip with silica.

A small piece of Teflon sleeve was inserted over the capillary with the internal taper end to protect the glass tip from breaking. The other end of the capillary was attached to the column packer, which was attached to a tank of argon gas. The column packer was placed on top of a magnetic stirrer plate. The column packer was filled with the 2.5 µm Kinetex silica (removed from a commercial Phenomenex Kinetex silica column) made into slurry with acetonitrile. A magnetic stirrer was placed inside to stir the slurry (Figure 2.4). When the argon tank was turned on, the homogeneous slurry was forced by the gas pressure, into the fused silica capillary, after which we could see solvent flowing out from the tapered tip. The packed silica tip was ready to use on the nano-electrospray source. A packed internal tapered fused silica capillary is shown in Figure 2.2e.

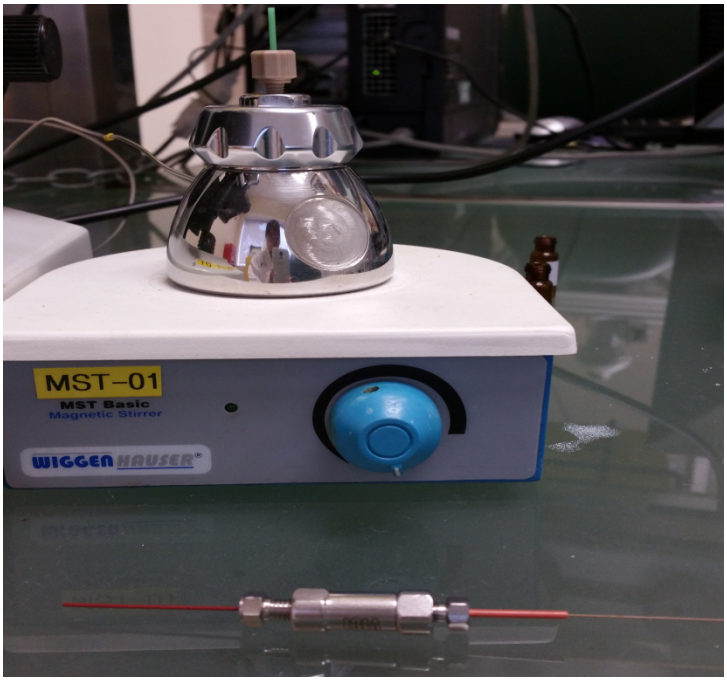

Figure 2.4 Column packer sitting on the magnetic stirrer plate, attached to an argon gas supply

2.3 Results and Discussion

The complexity of a plasma proteome presents a great challenge in the study of low abundance proteins. In equine plasma as in human and other species, there are many abundant proteins which make it extremely difficult to reproducibly recover low concentrations of rhEPO and DPO from these complex matrices. It is very common for abundant proteins such as albumin and immunoglobins to prevent proteins of interest, at a physiological concentration, from being recovered and studied. One of the approaches to overcome this challenge was by immunodepletion [56]. However, there is drawback for this approach, as it results in loss of low abundant target proteins or analytes [41]. According to Guan *et. al* [38], the use of polyclonal anti-

rhEPO antibodies can improve the recovery of rhEPO from plasma by 2-fold. The specificity of this method for detecting rhEPO and DPO in equine plasma resulted from the approaches taken in sample preparation and the subsequent analysis. Specifically, the anti-body-based immunoaffinity separation used in this study provides the highly selective separation of the analytes from plasma proteins. The 30 KDa filter membrane used for the buffer exchange also ensured that the analytes retained by the membrane is the intact rhEPO or DPO protein and not their peptide fragments.

Hence, for a start on extracting the rhEPO from equine plasma, I followed the Guan's publication method on immunoaffinity extraction for my study on the comparison of the capillary flow and high flow LC.

I had carried out two experiments, one on the high flow LC system and the other on the capillary flow LC system. Extracted ion current chromatograms (EICC) Figures 2.5a and b) show the analysis of synthetic peptide (20 ng on column) standards run on the high flow and capillary flow LC systems set-ups respectively. Comparing the two sets of data, we can see that there is an average increase of around 3 times in the peak intensity on the capillary flow set-up. In particular, the EICC representing the T17 fragment from the EPO protein, which gave the best response of any of the target peptides under ESI conditions, showed an increase of over 5 times in the intensity of the peak. The peak width at half height (PWHH) achieved for both the experiments were less than 0.1 min.

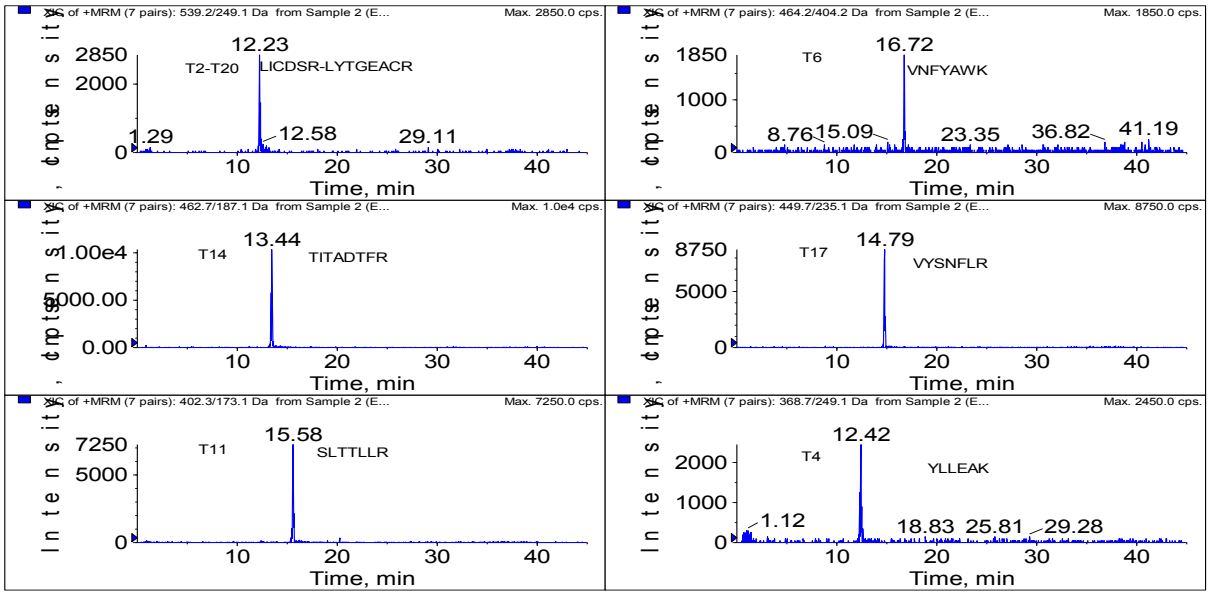

Figure 2.5a) 20 ng/ml Tryptic digest EPO protein standards run on high flow

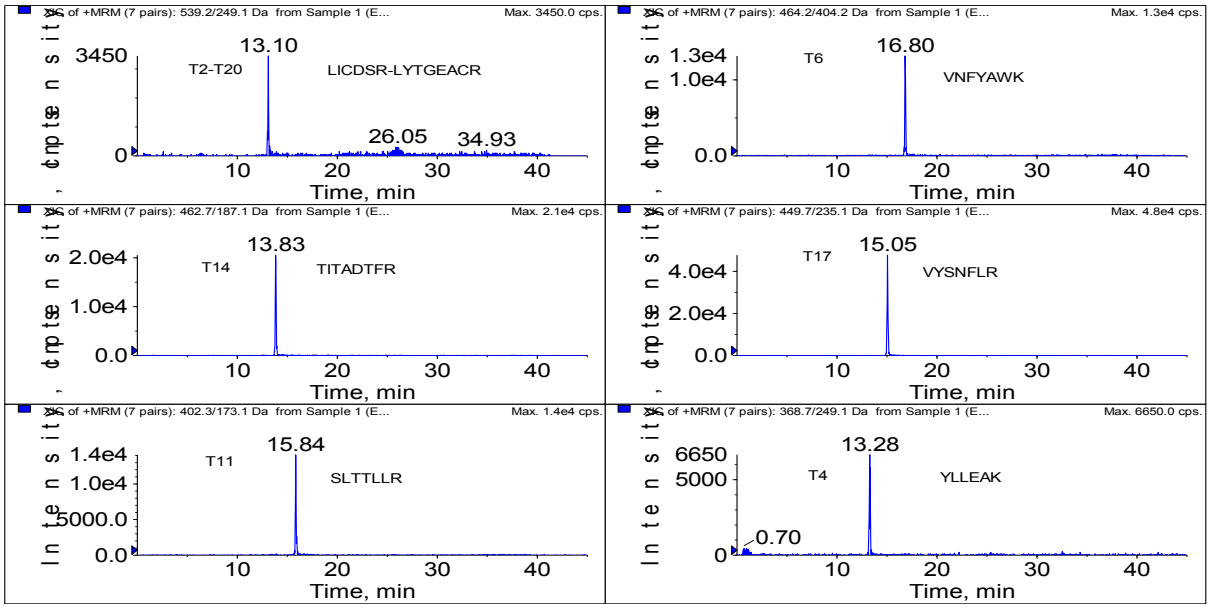

Figure 2.5b) 20 ng/ml Tryptic digest EPO protein standards run on capillary flow

A total of 20 ng of rhEPO, obtained from a solution of Eprex, was digested with trypsin (Promega) at 37 ºC for 2 hours using a 50 mM ammonium bicarbonate buffer.

Here again, it can be seen (Figures 2.6a and b) that there is an increase in the signal response obtained from the peptides screened on the capillary flow setup of 4 µl/min. For example, the peptide T4 fragment from rhEPO was not detectable when using the high flow rate 100 µl/min screening configuration, but is evident in the capillary flow analysis. The other peptides also have a better response of twice or even higher for peptide T17 upon running at low flow rate.

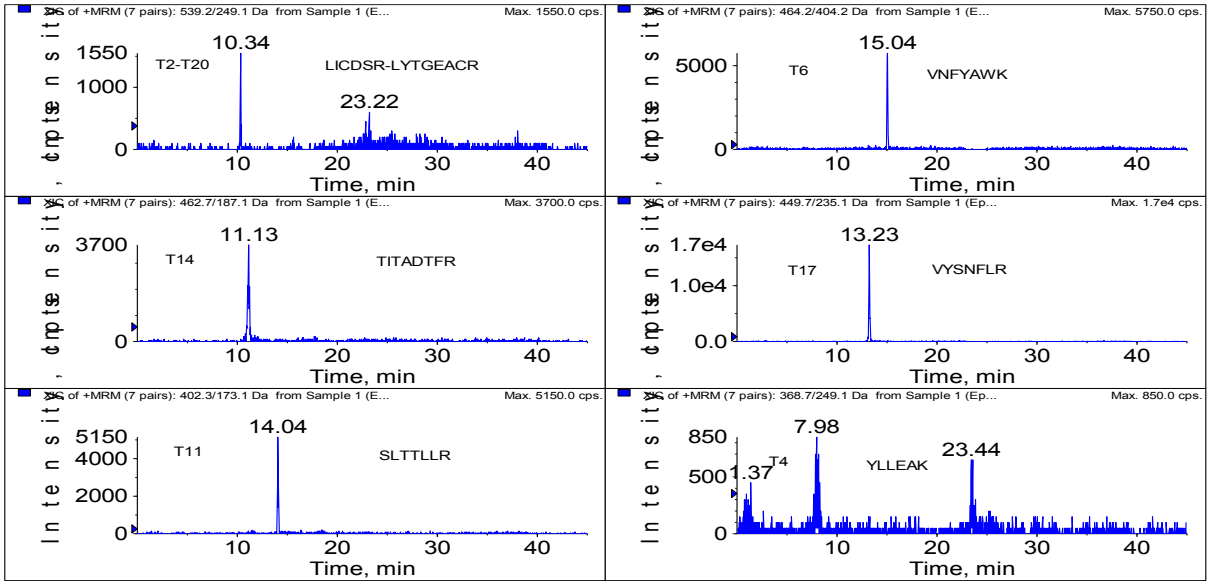

Figure 2.6a) Eprex 20 ng/ml run on high flow set-up

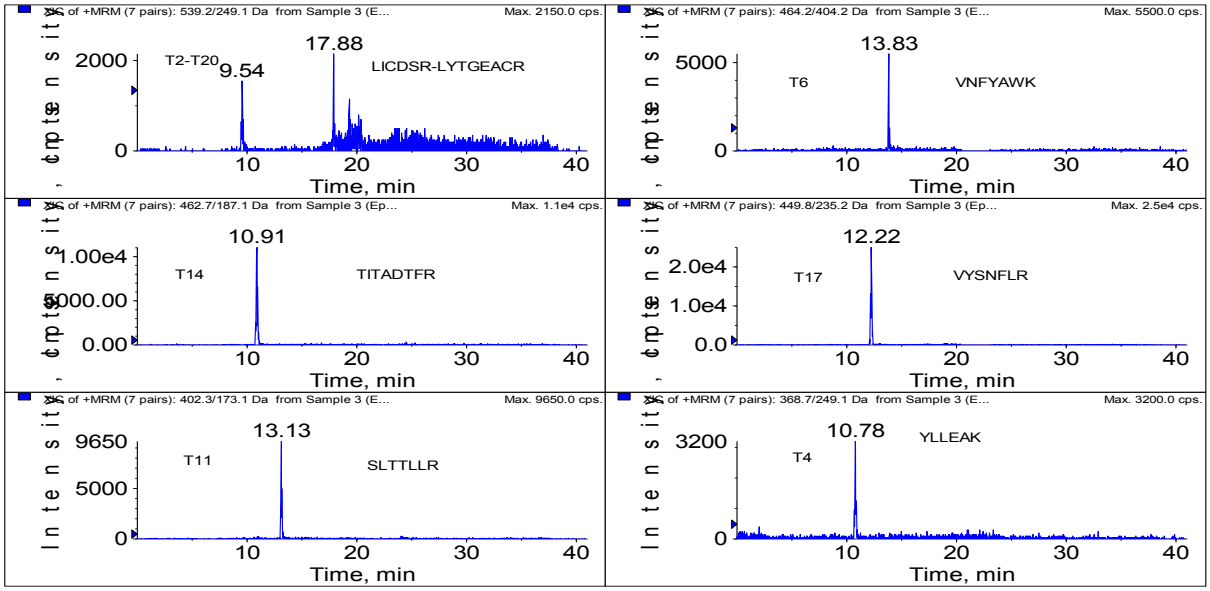

Figure 2.6b) Eprex 20 ng/ml run on capillary flow set-up

Equine plasma was spiked with rhEPO at a concentration of 0.2 ng/ml and 10 ng/ml. The extraction method involved analyte enrichment using immunoaffinity isolation of rhEPO from 1 ml of equine plasma with an anti-rhEPO antibody linked to magnetic beads. This was followed by buffer exchange of the extract in preparation for tryptic digestion of the proteins. Analyses were carried out on the high flow and capillary flow LC-MSMS. At 10 ng/ml the peptides were detectable using the high flow set-up, however, at the lower concentration (0.2 ng/ml of spiked plasma, data not shown) none of the peptides were detected. In contrast, using the capillary system, we were able to detect three of the tryptic peptides at 0.2 ng/ml of spiked equine plasma. This data, which is shown in Figure 2.7b), gives an intensity of 1E3 for the highest sensitivity peptide fragment, T17, which approaches that seen in the 10 ng/ml of spiked plasma (3E3) shown in Figure 2.7a, which was run on high flow.

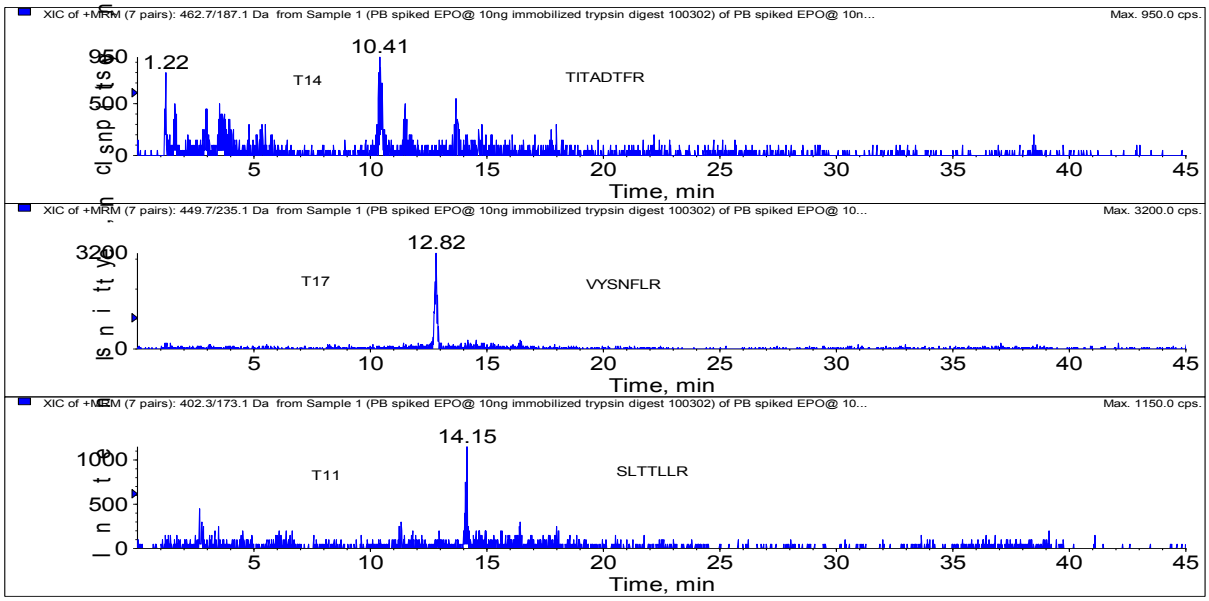

Figure 2.7a) Spiked 10 ng/ml Eprex in plasma run on high flow

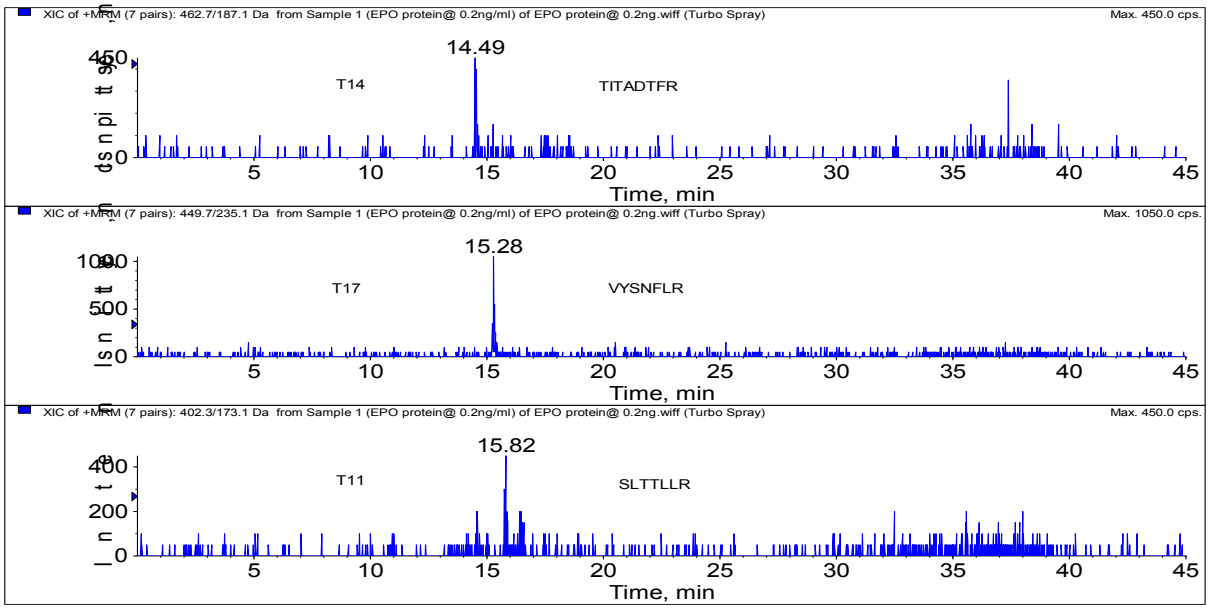

Figure 2.7b) Spiked 0.2 ng/ml Eprex in plasma on capillary flow

Hence, it can be seen that the low flow capillary set-up is more sensitive than the high flow system. The capillary flow is capable of detecting the immunoaffinity extracted EPO peptide T17 at 0.2 ng/ml in spiked equine plasma at the intensity of E3 level, whereas, the high flow is only capable of detecting the 10 ng/ml of immunoaffinity extracted EPO peptide from spiked equine plasma, which also gives an intensity of E3 level. This is due to the column particle size we are using for the low flow. A 2.7 µm particle size C18 HALO column was used for the low flow compared to the 3.5 µm XTerra® C18 particle size. Particle size and pore size of silica are very important parameters of a reversed phase column when selected for HPLC analysis. Small particle sizes of less than 3 µm including sub- 2 µm have been widely used for achieving high performance and fast separation.

The combination of mass spectrometry and nanoflow liquid chromatography (nano LC) techniques is a key element of proteomics research. The strength of using a nanoLC/MS is that it enables the analysis of limited amounts of biological sample with high sensitivity. However, the low solvent flow rates used in nanoLC make chromatographic optimisation more challenging than higher flow rate applications. It is therefore important that the nanoflow interface to the mass spectrometer be robust, easy to use, and flexible enough to provide optimum performance on a wide variety of applications. Using the commercially available emitter, which was an external tapered tip made of fused silica glass, was very fragile and easily broken. Another disadvantage is that the voltage cannot be set too high, as a voltage of more than 2000 V can cause the glass tip to break producing a poor spray. Hence, I have chosen to try out the novel fabrication of an internally tapered tip within the fused silica capillary. For this application, I had set the voltage to 3800 V and the tapered

tip, which act as an emitter was in the inner layer of the capillary, and was not therefore so fragile.

A typical nano-spray set-up is shown in the schematic diagram (Figure 2.8) below, and Figure 2.9 shows an electrospray was generated by applying voltage to an emitter *via* a tip. The spray tip or end of the emitter is a conical aggregate of moving fluid called the Taylor Cone. The Taylor Cone tapers into a fine fluid jet which ultimately radiates into a fan-shaped aerosol called a plume. Vacuum force from the mass spectrometer inlet then draws the plume into the MS for analysis.

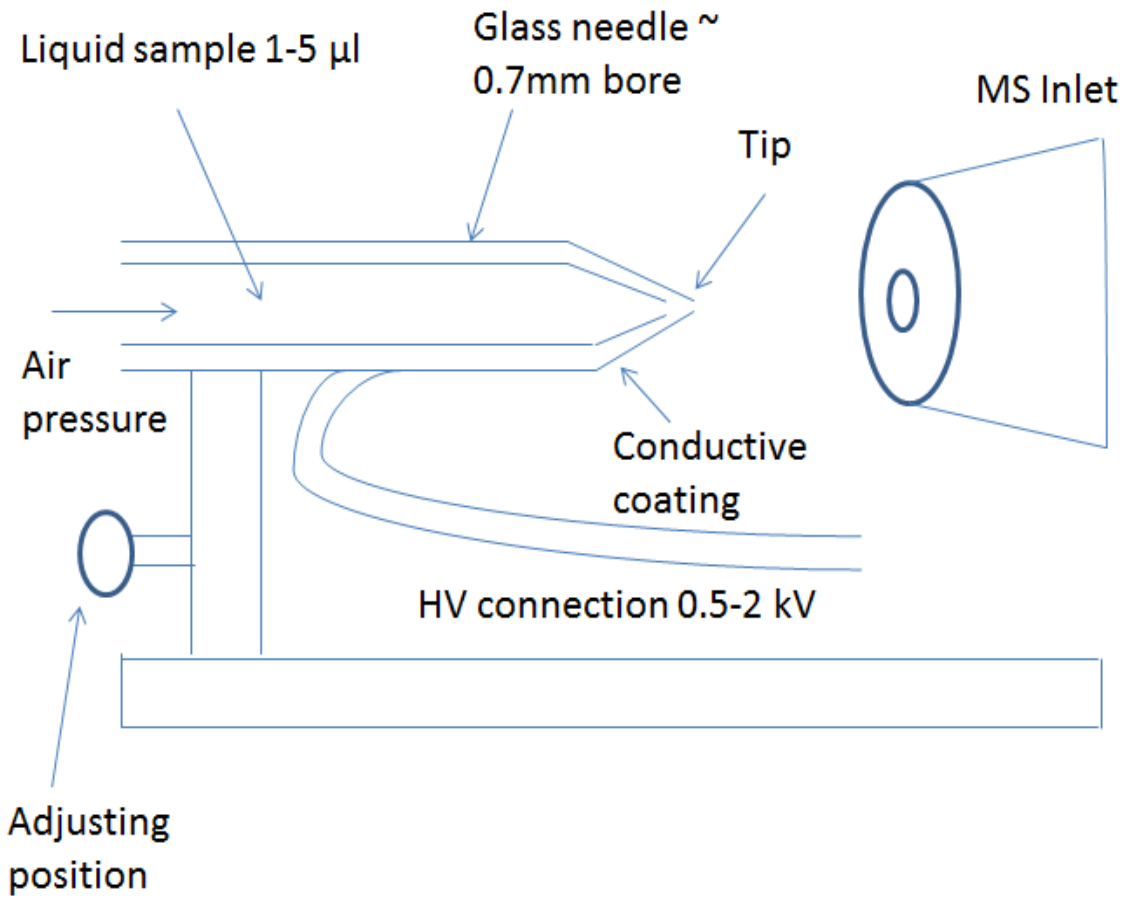

Figure 2.8 Schematic diagram of a nano-spray set-up [175]

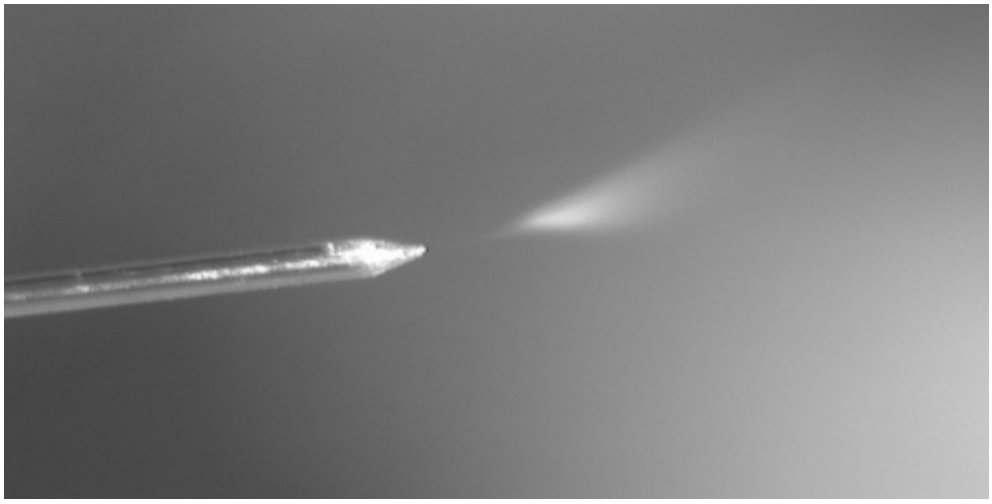

Figure 2.9 An emitter showing a fan-shaped aerosol called a plume.

The fused silica capillary fabricated with an internal tapered tip was packed with 2.5 µm Kinetex C18 reverse phase coated silica. It was installed on a nano-electrospray source to act as an emitter. I injected Eprex with concentrations of 2 ng and 0.2 ng on-column on the 2.5 µm Kinetex silica packed in the fused silica capillary with internal tapered tip. Figure 2.10 and 2.11 show 2 ng of Eprex trypsin digested on-line (trypsin enzyme reactor) and off-line respectively. Eprex digested on-line coupled to the fabricated internal tapered tip obtained a good sensitivity of E3 and E4 (Figure 2.10) for most of the peptides digested. EPO peptide T11, T14 and T17 had an intensity of E4 with a sharp peak shape and a PWHH of 0.1 min. Off-line digested Eprex injected directly into the internal tapered capillary packed with silica, had also shown to have a sensitivity of E3 and E4 level. Some peptides showed better sensitivity than the on-line digestion, however some peptides showed poorer sensitivity than the on-line digestion, for example, EPO peptide T2-T20 and T4 showed poorer sensitivity than the on-line digestion.

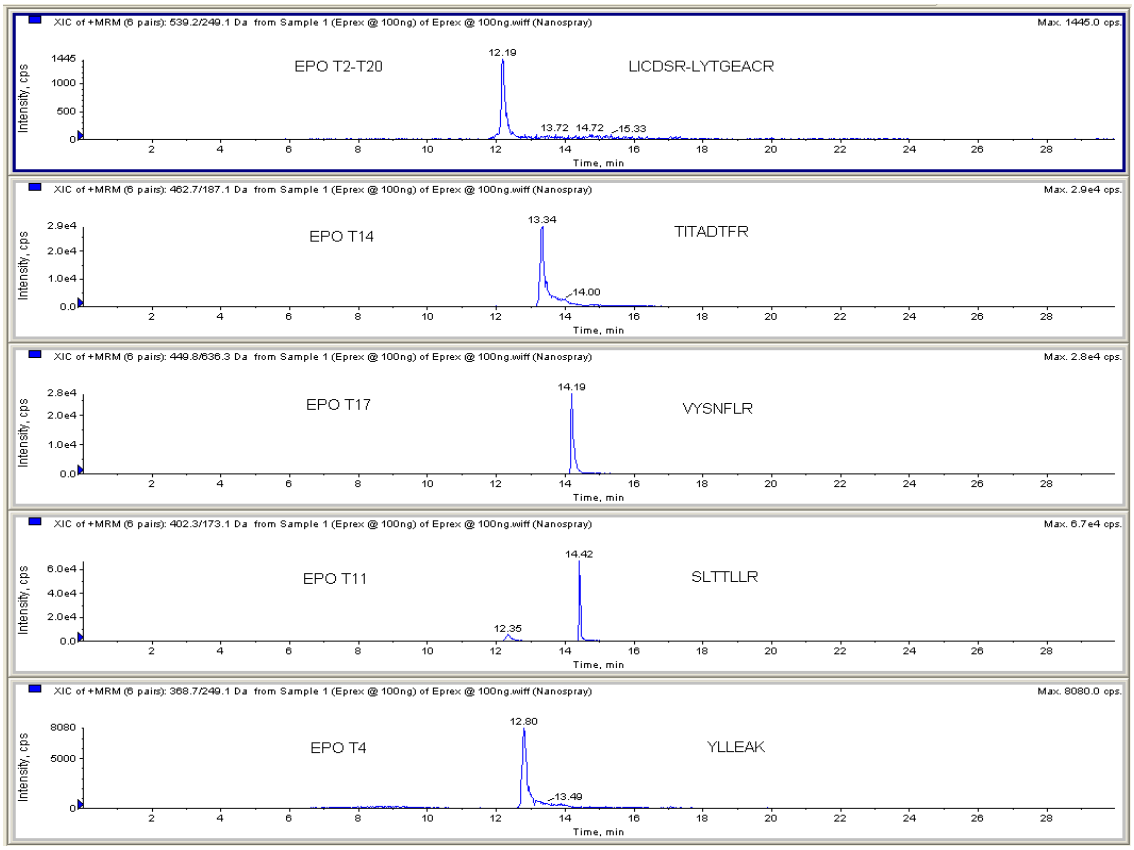

Figure 2.10 Extracted ion chromatogram showing 2 ng of Eprex injected onto trypsin reactor coupled to a fabricated 75 µm fused silica capillary with internal tapered tip, packed with 2.5 µm Kinetex silica.

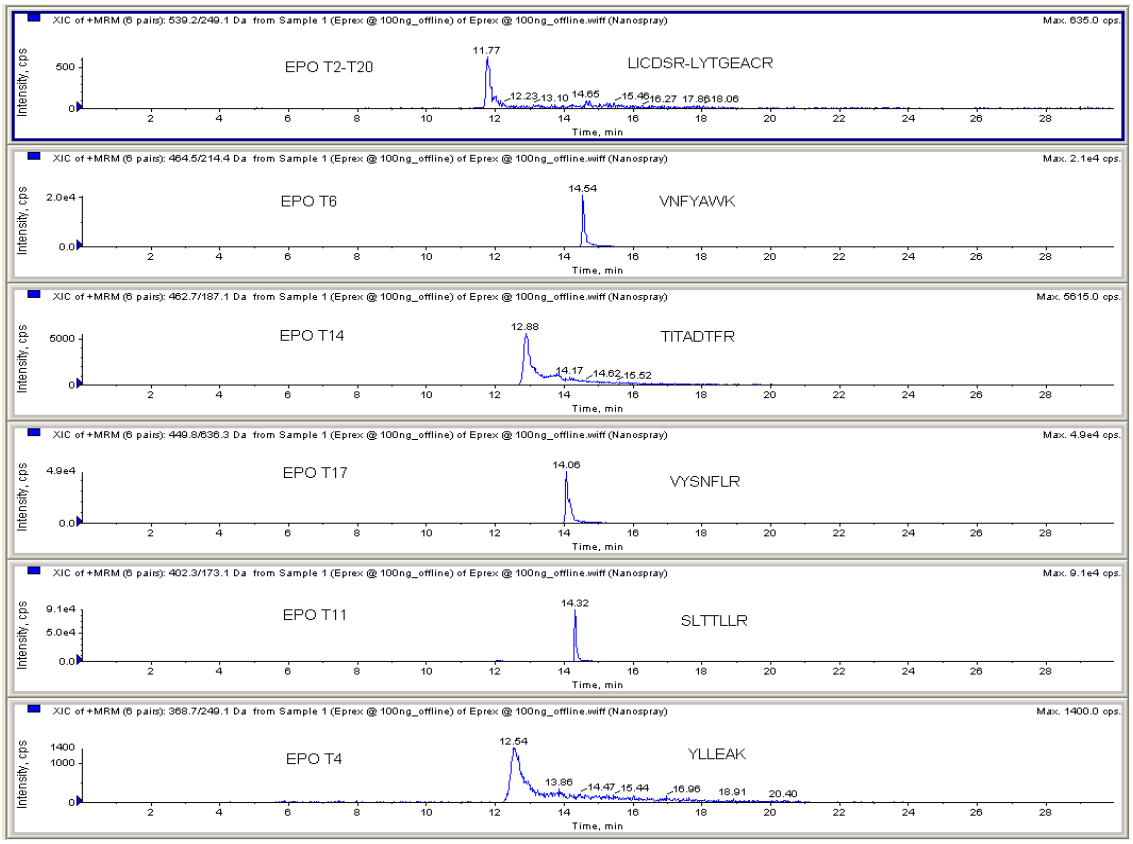

Figure 2.11 Extracted ion chromatogram showing 2 ng of off-line trypsin digested Eprex injected onto a fabricated 75 µm fused silica capillary with internal tapered tip, packed with 2.5 µm Kinetex silica.

Figures 2.12 and 2.13 below show 0.2 ng of Eprex trypsin digested on-line and off-line respectively. A better sensitivity was obtained for the nano flow compared to the capillary flow shown in the above experiment. EPO peptide T17 obtained an intensity of 1 E3 for the 0.2 ng injected on the capillary flow, whereas, the nano flow obtained an intensity of 4 E3 and 6 E3 for the 0.2 ng of trypsin digested Eprex on-line and off-line respectively. For the off-line digestion, it could be seen that the EPO peptide T6 appearing at 7 E2, whereas, in the capillary flow, it could not be seen this peptide at 0.2 ng digestion. Figure 2.13 showing 0.2 ng off-line trypsin digested Eprex injected

onto a fabricated 75 μm fused silica capillary with internal tapered tip packed with silica which is able to achieve an intensity of 1.5 E4 for EPO peptide T11, comparing to 0.2 ng Eprex digested run at capillary and high flow with only an intensity of E3 and E2.

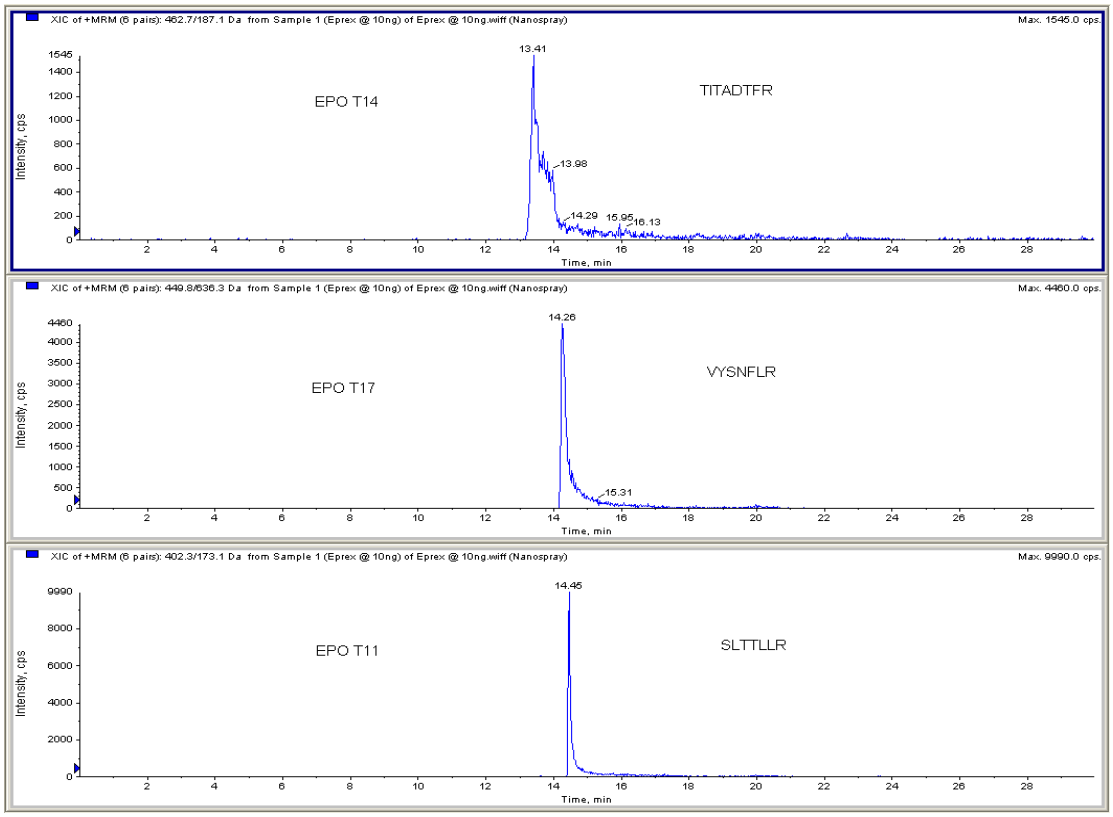

Figure 2.12 Extracted ion chromatogram showing 0.2 ng of Eprex injected onto trypsin reactor coupled to a fabricated 75 μm fused silica capillary with internal tapered tip, packed with 2.5 μm Kinetex silica.

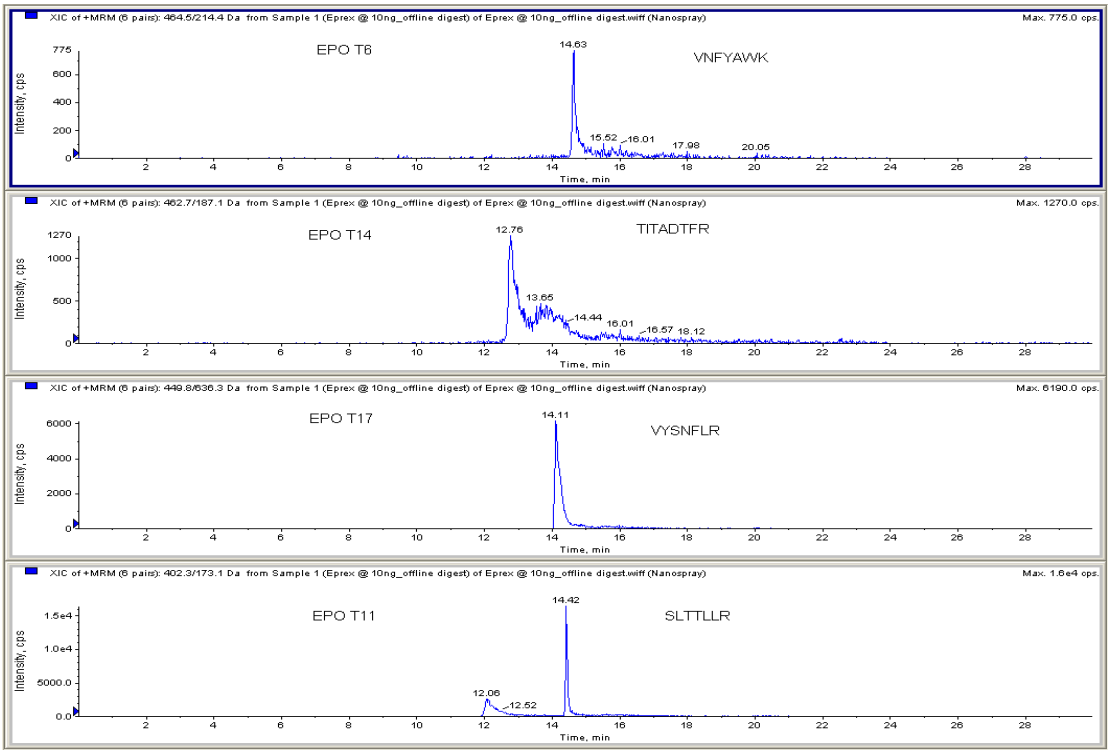

Figure 2.13 Extracted ion chromatogram showing 0.2 ng of off-line trypsin digested Eprex injected onto a fabricated 75 µm fused silica capillary with internal tapered tip, packed with 2.5 µm Kinetex silica.

Nano flow LC is much more sensitive than the higher flow LC, however, the disadvantage is more time is spent adjusting the nano spray in order to achieve a good sensitivity. Installing and coupling of the column should also be carried out carefully, or this will lead to increased dead-volume, which will result in peak tailing and poor peak shape. Thus, these disadvantages will result in not being able to achieve reproducible results.

2.4 Conclusion

A sensitive and selective LC-MSMS method was developed for screening for the presence or absence of rhEPO or DPO in equine plasma. The methods conducted using a capillary flow and nano flow LC system were evaluated as a screening tool for detecting tryptic peptides derived from epoetins isolated from equine plasma using immunoaffinity chromatography. Capillary and nano flow are capable of achieving a much lower detection limit than the higher flow rate configuration without either significantly decreasing resolution or broadening the peak widths. Sensitivity was also superior. Thus, this chromatographic system is well suited to achieve our goal of detecting these low concentration analytes using a relatively high throughput configuration. Nano flow is much more sensitive than the higher flow and capillary flow; however, to optimise nano flow requires skill and knowledge in setting up the nano-electrospray.

Chapter 3: Immunoaffinity extraction of rhEPO/ DPO and enhancing the sensitivity for detection of DPO unique peptide markers

3.1 Introduction

In order to isolate low abundance proteins, targeted pre-analytical purification and concentration of the analyte from the highly complex biological samples is required. This is time consuming and consequently the isolation of the EPO and DPO from biological matrices is a bottleneck towards achieving successful detection of the peptides. In plasma samples, it contains a large amount of albumin, which makes it difficult to prepare a sample free from other proteins for the analyses of low abundance proteins. In the purification step, high or low molecular weight substances can be removed by size exclusion filters, and highly abundant proteins can be removed by techniques such as immunodepletion, or low abundant proteins can be enriched by specific capturing tools, such as affinity extraction [46].

Hence, in order to avoid interference from other proteins, an immunological detection step can be included in the analytical step; however, insufficient specificity might still result in interference as found in some EPO doping control method [64, 176-177]. In 2000, World Anti-Doping Agency (WADA) accredited this control method which based on isoelectric focusing (IEF) followed by a double-blotting process, preceded by an ultrafiltration concentration of EPO from athletes' urine to identify rhEPO intake [64, 178-179]. However, non-specific interferences from abundant urine proteins is claimed to result in bands that are not related to EPO or its analogues [48]. Thus, in 2003, WADA reviewed the method and suggested some improvements, such as the use of an immunoaffinity method. The reason for this proposal was that EPO affinity purification, as sample pre-treatment, can reduce interference more significantly than ultrafiltration. Affinity chromatography separation, using the lectin wheat germ agglutinin (WGA), has also been used to distinguish hEPO forms [61]. In 2008, Guan

et al. identified rhEPO in equine plasma by using affinity purification with anti-hEPO antibody bound to magnetic particles, which is a lengthy procedure that is shown in Chapter 2, as a pre-analytical step for LC-MSMS detection. The magnetic particles were regenerated and re-used, however, this was not acceptable as it could result in carry-over from a positive sample and may cause a negative sample to be falsely reported as being positive. These different methods require skilled technicians, several hands-on steps, and expensive equipment and also take several days to complete the steps.

In 2010, Lönnberg *et al.* presented a 6 µl column with a length of only 0.15 mm, which can be used for purification and concentration of EPO from biological samples. The column is disposable and it also simplified the pre-analytical sample treatment and to avoid carry-over from a positive sample. This is known as MAIIA technology and provided an improved method of isoform identification for the glycoproteins hEPO, as the extraction gives a good recovery and the technique does not discriminate between the minor differences between subpopulations. The technology is also flexible; several types of ligands can be applied to distinguish subpopulations through affinity chromatography [59 and 65].

Detection limit challenges associated with measuring low-abundance protein can be addressed with hybrid immunoaffinity-mass spectrometric assays, such as antipeptide antibody capture followed by liquid chromatography/ tandem mass spectrometry. Due to the low levels that are anticipated to be present in the sample, EPO affinity purification is the preferred sample pre-treatment method to reduce interferences, as it is more effective than ultrafiltration.

In order to achieve confirmatory results from this glycoprotein, both sample preparation and LC-MSMS analysis need to be optimised. The method comprised analyte extraction and enrichment by immunoaffinity separation with anti-rhEPO antibodies, dual digestion by trypsin and followed by enzymatic released of N-linked glycans with peptide-N-glycosidase F (PNGase F) and analysis by LC-MSMS. The most important step in the sample preparation for proteomics is the conversion of proteins to peptides and in most cases trypsin is the preferred enzyme. Trypsin is a protease that specifically cleaves the proteins creating peptides both in the optimal mass range for MS sequencing and with a basic residue at the carboxyl terminus of the peptide, producing information-rich, easily peptide interpretable peptide fragmentation mass spectra.

Recombinant human erythropoietin (rhEPO) and darbepoetin (DPO) have a number of identical peptide fragments after enzymic digestion with trypsin. However, there are still some slight differences in their amino acid sequence. In order to identify which of these two epogens is responsible for the detection of these common peptides, it is necessary to differentiate between the proteins by targeting the analysis towards the peptides T5 (21-45) and T9 (77-97), as the amino acid sequence from this region is specific to each protein. The five variant amino acids in DPO are located in the two regions that relate to two tryptic peptides T5 and T9. The two unique deglycosylated tryptic peptides were identified as (T5) ^{21}EAENITTGCAEHCSLNENITVPDTK^{45} with a disulfide bond between ^{29}Cys and ^{33}Cys and (T9) ^{77}GQALLVNSSQVNETLQLHVDK^{97}.

Unfortunately, these are glycopeptides, with highly variable sialic acid containing glycan motifs, and this severely hinders detection under ESI/MS conditions. Thus, the glycopeptides with glycosylation poorly ionise under positive electrospray ionisation conditions, and cannot be detected at low concentrations level. To overcome this problem the glycans can be removed from the glycopeptides and removing the micro-heterogeneity improves the ionisation and increases sensitivity. A side effect of deglycosylation reaction is that the T5 and T9 are deaminated to aspartic acid residues by the PNGase F.

These deglycosylated peptides, which consist of 21 to 25 amino acids in each fragment, are much larger than other tryptic peptides, e.g. T17, T14 and T11 and this could have a negative effect on the sensitivity of detecting these peptide fragments, when compared to those peptide fragments that are only 7 – 8 amino acids in length. The longer the amino acids length, the bulky the peptides (have a greater molecular mass, which usually contained more than one charge), hence, the sensitivity are not as good compared to the shorter amino acids length, which is smaller in molecular mass and easier to detect.

According to Guan *et al.* publication [43], his group had differentiated and identified by using the two unique deglycosylated tryptic peptides. They had also investigated that T5 of DPO was not observed even after deglycosylation by PNGase F, this could be due to the disulfide bonds not reduced and alkylated. They had identified T9 from DPO and T5 from rhEPO.

I have investigated different enrichment methods and found combining trypsin with Asp-N enzyme digestion after deglycosylation is a suitable way of generating specific peptide fragments that also ionise well under +ve ESI conditions. The Asp-N enzyme is utilised to cleave the N-terminal side of Asp amino acid into smaller peptides Thus, in order to enhance the sensitivity of these glycopeptides, I have employed endoproteinase Asp-N enzyme which selectively cleaves the peptide bonds N-terminal to aspartic acid residues in the deglycosylated peptide fragments to smaller peptide fragments. The smaller peptide fragments could help in enhancing the sensitivity of detecting and differentiating the rhEPO and DPO. Hence, in this Chapter the use of the Asp-N enzyme will be demonstrated to identify the T9 deaminated peptide fragment as described in Table 3.1.

Thus, proteolytic enzyme digestion is an indispensable tool in proteomics; it helps to cleave the peptide bonds, producing information-rich and easily interpretable peptide fragmentation mass spectra. Mass spectrometry is a powerful analytical tool that is highly sensitive and enables identification of the modified position, hence; this is commonly used in combination with peptide mapping on reversed-phase or HILIC HPLC, after digestion by trypsin or other enzymes.

<table>
<tr><td>Epogens</td><td colspan="4">Peptides after tryptic digestion</td></tr>
<tr><td rowspan="3">rhEPO</td><td colspan="4">GQALLVNSSQPWEPLQLHVDK (EPO T9)
PNGase F Deamination</td></tr>
<tr><td colspan="4">GQALLV↑DSSQPWEPLQLHV↑DK (EPO T9DAM) (2360.2244)
Asp-N
Cleavage on the N-terminal side of aspartic acid</td></tr>
<tr><td>(T9A1)
GQALLV
(600.3715)</td><td colspan="2">(T9EPOA1)
DSSQPWEPLQLHV
(1535.7488)</td><td>(T9A2)
DK</td></tr>
<tr><td rowspan="3">DPO</td><td colspan="4">GQALLVNSSQVNETLQLHVDK (DPO T9)
PNGaseF Deamination</td></tr>
<tr><td colspan="4">GQALLV↑DSSQV↑DETLQLHV↑DK (DPO T9DAM) (2295.1826)
Asp-N
Cleavage on the N-terminal side of aspartic acid</td></tr>
<tr><td>(T9A1)
GQALLV
(600.3715)</td><td>(T9DPO)
DSSQV
(535.2358)</td><td>(T9DPOA1)
DETLQLHV
(954.4891)</td><td>(T9A2)
DK</td></tr>
</table>

Table 3.1 PNGase F and Asp-N digestion of T9 Tryptic fragments (77 – 97)

3.2 Materials and Instrumentation

3.2.1 Materials.

DL-dithiothreitol (DTT) was purchased from Sigma Aldrich (Singapore). Ammonium bicarbonate was purchased from Merck Singapore. HPLC-grade methanol and acetonitrile (ACN) were obtained from Fisher Scientific (Singapore). Sequencing grade modified Trypsin (P/N No. V5111), protein deglycosylation mix kit and sequencing grade Asp-N were purchased from Promega (Singapore). The water used throughout all experiments was obtained from a Milli-Q Gradient A10 from Millipore (Singapore). Epoetin alfa, Eprex® the recombinant human erythropoietin, 10,000 IU/ ml was purchased from Jassen-Cilag AG, (Schaffhausen, Switzerland). Darbepoetin alfa, Aranesp® 40 µg/ 0.4ml were obtained from Amgen Manufacturing Limited a subsidiary of Amgen Inc. (Thousand Oaks, CA, USA). Peptide DSSQPWEPLQLHV (human EPO peptide T9EPOA1), peptide GQALLV (human EPO peptide T9A1), peptide GQALLVNSSQPWEPLQLHVDK (human EPO peptide T9DAM) and peptide VYSNFFLR (human EPO peptide T17F) were synthesised by Auspep Pty. Ltd. (Tullamarine, Victoria, Australia). The vacuum manifold for processing 24 columns, QIAvac 24 Plus, and the connecting system (Qiagen, www.qiagen.com) was used together with a vacuum pump for passing the liquids through the columns. The EPO purification kit was obtained from MAIIA Diagnostics (Art. No. 0250, Uppsala, Sweden, www.maiiadiagnostics.com).

3.2.2 Instrumentation.

Experiments were undertaken on a Dionex Ultimate 3000 XRS UHPLC$^+$ focused pump, with a Dionex Ultimate 3000 XRS open autosampler coupled to an ESI source of the TSQ Quantiva MS operated by Xcalibur software, and were all from Thermo Scientific. The autosampler has a 6-port injection valve with a 20 µl injection loop. The C18 column was coupled directly between the injection port and the ESI source.

3.2.3 LC Conditions

3.2.3.1 The column used was a Kinetex C18 50 x 2.1 mm, 2.6 µm, and 100Å fused core.

3.2.3.2 The mobile phase used was (A) 0.1 % formic acid in water and (B) ACN at a flow rate 400 µl/ min;

3.2.3.3 The initial conditions were 95 % A and 5 % B followed by a linear gradient to 5 % A and 95 % B at 5 minutes. After holding at 5 : 95 for 5 min, the composition was returned to initial conditions over 60 seconds. The column was re-equilibrated in preparation for the next injection between 11 and 20 min.

3.2.4 MS Conditions

3.2.4.1 The positive ion source voltage was set at 3500 V, sheath gas at 20 arbitrary units, AUX gas at 2 arbitrary units, sweep gas at 0 arbitrary units, Ion transfer tube at 350℃, vaporizer temp at 0℃ and CID gas at 2 arbitrary units.

3.2.5 Preparation of standard mix.

EPO peptide standard mix, GQALLVNSSQPWEPLQLHVDK (EPO peptide T9DAM), GQALLV (EPO peptide T9A1), DSSQPWEPLQLHV (EPO peptide T9EPOA1) and VYSNFFLR (EPO peptide T17F) were prepared at a concentration of 10 ng/ml in their initial running mobile phase conditions (C18 reversed-phase- 5 % ACN, 95 % 0.1 % FA in water).

3.2.6 Preparation of calibrants.

10 µg/ml of each standard (EPO T9DAM, T9A1, T9EPOA1, DPOT9DAM, T9DPOA1 and T17F) was prepared individually as working stock solutions (WSS). 1 µM of each standard was then prepared from the 10 µg/ml of WSS and adjusted according to its purity. Two sets of calibrators were prepared. A contained EPO T9DAM, T9A1, T9EPOA1 and T17F and calibrator B contained DPO T9DAM, T9A1, T9DPOA1 and T17F. All calibrants prepared were diluted 10 x with buffer (95 % 0.1FA and 5 % ACN) before injection onto TSQ Quantiva LC-MSMS. Five calibration points were prepared at concentrations of 2, 4, 6, 8 and 10 nM.

3.2.7 Preparation of samples.

All samples were prepared at 0.1 µM based on the mass of each protein. 1 M of Eprex is 32,000 mg/ml. For 0.1 µM, 3.2 µg/ml was required. Therefore, 36 µl of 84 µg Eprex was put into an Eppendoff tube, with 100 µl of 1 µM internal standard (T16T17F), then topped up with 864 µl of 50 mM ammonium bicarbonate. 1 M of Aranesp is equal to 37,100 mg/ml. For 0.1 µM, 3.71 µg/ml was required. Therefore,

37 µl of 100 µg Aranesp was put into an Eppendorf tube, with 100 µl of 1 µM internal standard, and topped up with 863 µl of 50 mM ammonium bicarbonate. After preparing the samples at 0.1 µM, 100 µl of each sample was taken and placed in a vial, followed by 10 µl of 100 mM DTT and left at room temperature for 10 min. A 10 µl of Try/ Lys C enzyme was added into the vial and incubated in the oven at 37 ºC for 3 hr. The tryptic digestion was followed by deglycosylation steps, where 5 µl of 10x deglycosylation reaction buffer and 5 µl of protein deglycosylation mix were added respectively. This was then incubated overnight at 37 ºC. The following day, the sample was removed from the oven and 10 µl of 2 µg Asp-N enzyme was added to the sample and incubated at 37 ºC for 2 hr. The samples were diluted 10 x with buffer (95 % 0.1FA and 5 % ACN) before injection onto TSQ Quantiva LC-MSMS.

3.2.8 Preparation of sample by IAC using MAIIA.

Prepare the anti-EPO column using the EPO purification kit from MAIIA Diagnostics, by placing the 25 ml funnel on top of the vacuum manifold. 1 ml of a pH neutral buffer was added to the funnel with vacuum suction. 20 ml of spiked Eprex in plasma (20 ng/ml) was added to the funnel and vacuum was applied in order to filter the sample. 1 ml of washing buffer was added. After filtering, the anti-EPO column was placed on top of the Eppendorf tube and then centrifuged at 1500 rpm for 3 min. Another Eppendorf tube with 20 µl of 0.5 M ammonium bicarbonate and 2 µl of 10 ng/ ml of internal standard added was prepared and placed next to the anti-EPO column in the centrifuge. When 50 µl of desorption buffer was added on top of the anti-EPO column it was then moved across to placed it on the other prepared Eppendorf tube which contained the ammonium bicarbonate and internal standard;

EPO peptide VYSNFFLR, T16T17F. It was centrifuged again at 1500 rpm for 3 min. The sample is then ready for the reduction and digestion step.

3.2.9 Preparation of sample for reduction and digestion.

The samples were reduced by adding 10 µl of 100 mM DTT and then leaving at room temperature for 10 min. For post-spiked plasma, it was added 20 µl of 1 ng/µl into the extracted plasma blank. The samples were tryptic digested by adding 10 µl of 20 µg/ 100µl trypsin for incubation at 37 ºC for 3 hr. Deglycosylation was carried out by adding 5 µl of 10 x deglycosylation reaction buffers and 5 µl of protein deglycosylation mix from the Promega protein deglycosylation kit. Samples were then gently vortexed and centrifuged at 3000 rpm to allow the sample to collect at the bottom of the tube. Samples were then incubated in the oven at 37 ºC for 16 hr. After the deglycosylation step, 10 µl of Asp-N enzyme at 2 µg/ 50µl was added to the samples and incubated in the oven at 37 ºC for 2 hr. This digested sample was injected onto the RP column.

3.3 Results and Discussion

Plasma is a complex protein containing matrix and consequently the detection of the presence of rhEPO or DPO, which are protein-based drugs, requires extraction and enrichment by immunoaffinity separation with anti-rhEPO antibodies. An efficient pre-analytical purification and concentration step is very important, as it contributes to the sensitivity of the detection of the epogens in the mass spectrometer. In this Chapter, I have described the use of MAIIA as the immuonaffinity extraction. Post-spiking was carried out after the blank plasma samples went through the MAIIA

extraction procedure and Eprex was spiked together with the internal standard (IS), where the IS is added to demonstrate whether the enzyme is suitably active. When the non-glycosylated peptides, EPO T11 and EPO T17, in the pre- and post-extraction spiking are compared, (Figures 3.1 and 3.2) have an area of 1 E5 for pre-spiked and 8 E4 for post-spiked for EPO T11 and 8 E4 for pre-spiked and 6 E4 for post-spiked for EPO T17 respectively. Thus, this shows that there wasn't much loss in the extraction. As for glycosylated peptides, EPO T9DAM peptide showed a 10 x lower peak area than the post-spiked product (Figure 3.3 and 3.4). This might be due to the Asp-N enzyme which had converted the EPO T9DAM to the smaller peptide fragments T9A1and T9EPOA1, which resulted in a much higher area in the pre-spiked plasma (Figure 3.3), 4.7 E4 and 7.7 E3 respectively compared to the post-spiked plasma (Figure 3.4) 2.8 E4 and 3.8 E3 respectively. Hence, this has shown that spiked plasma gave a better intensity of the smaller T9 peptide fragments than the post-spiked plasma. Therefore, the overall results showed that using the MAIIA pre-purification and concentration steps it was possible to achieve a very good recovery for these epogens. The EPO T9 standard mix (Figure 3.5) was prepared, containing T9A1, T9EPOA1 and EPO T9DAM with T17F internal standard as a reference of retention time to the sample injected.

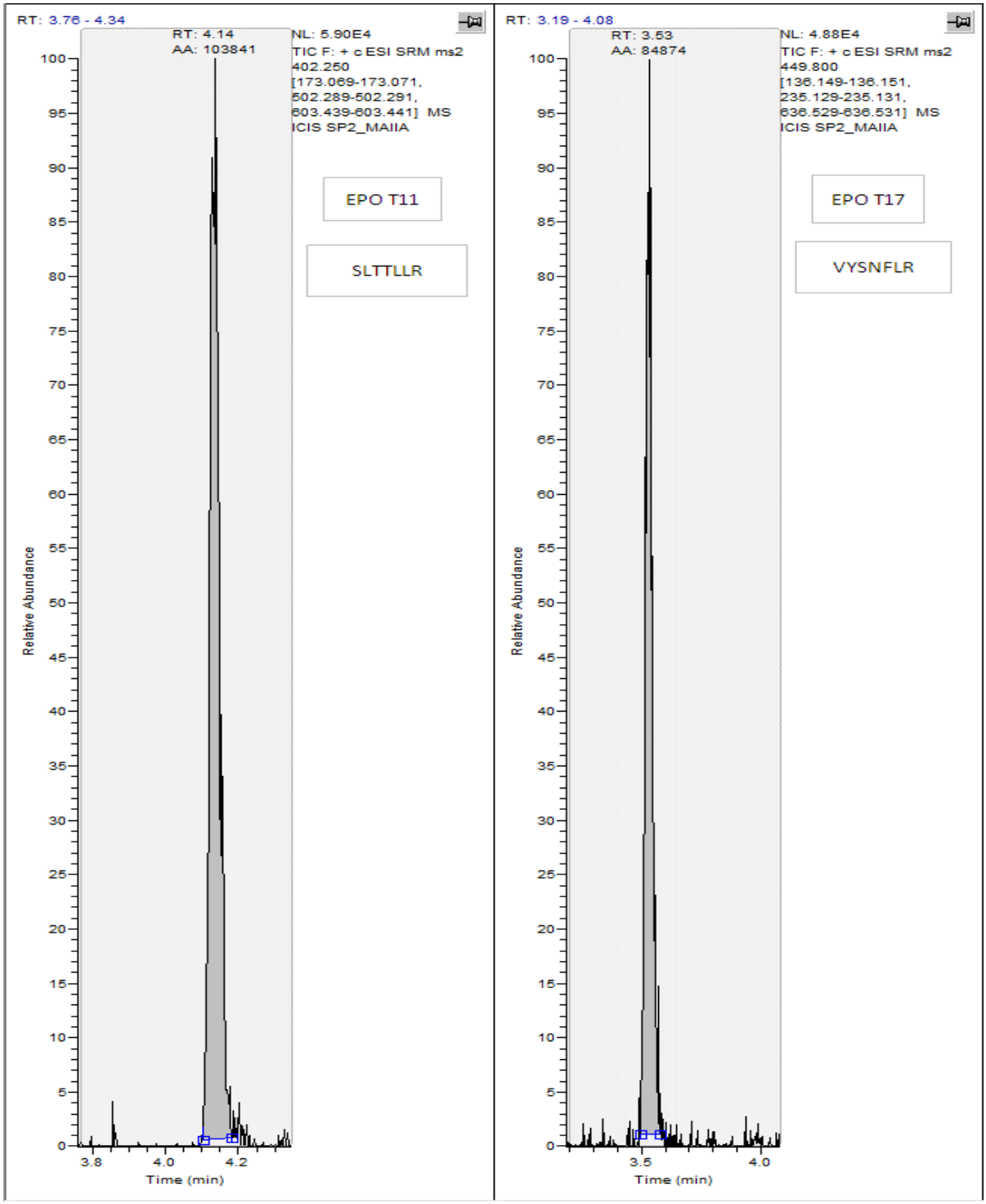

Figure 3.1 Pre- spiked plasma with Eprex- non-glycosylated peptides

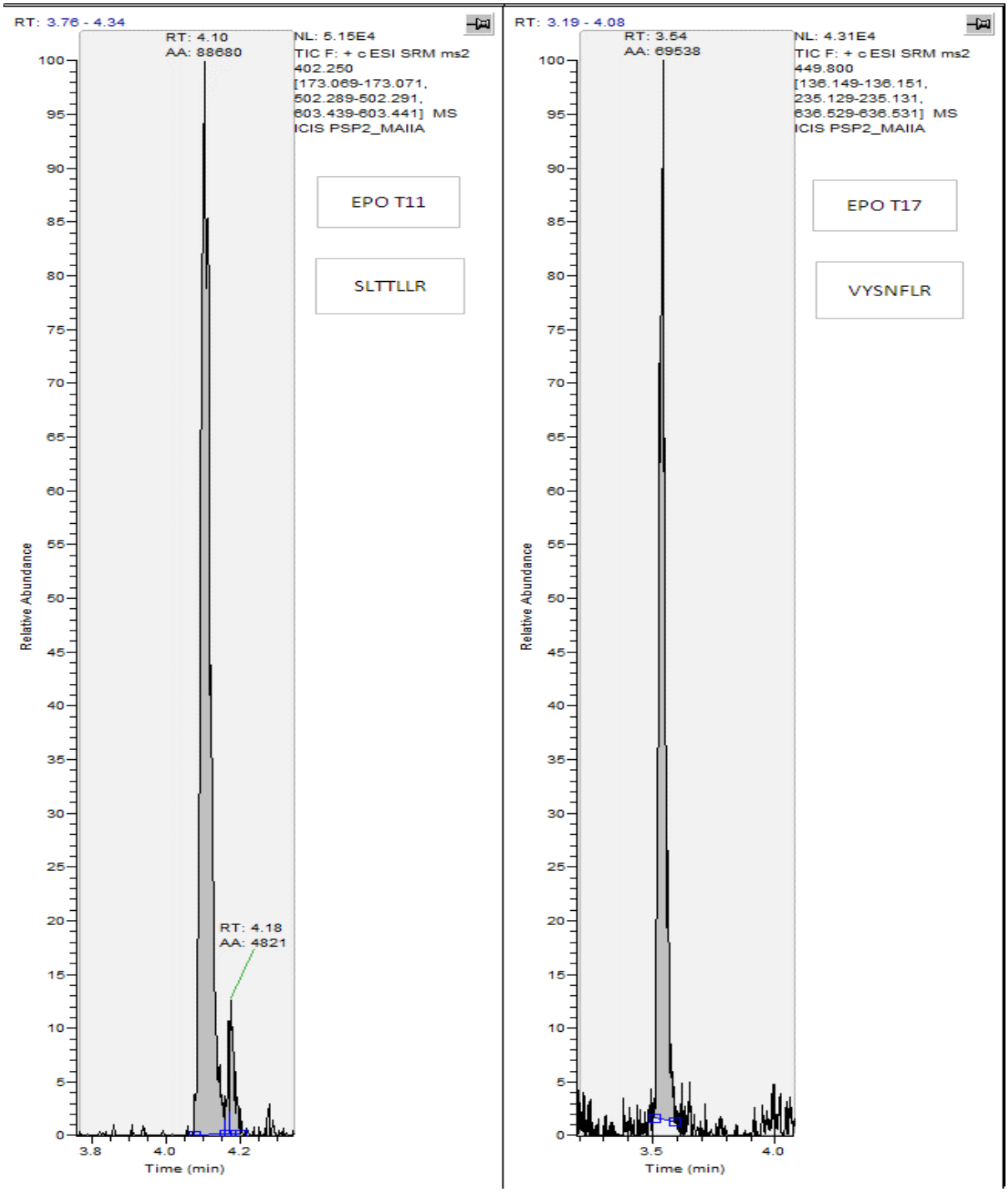

Figure 3.2 Post-spiked plasma with Eprex- non-glycosylated peptides

Figure 3.3 Pre-spiked plasma with Eprex- glycosylated peptides

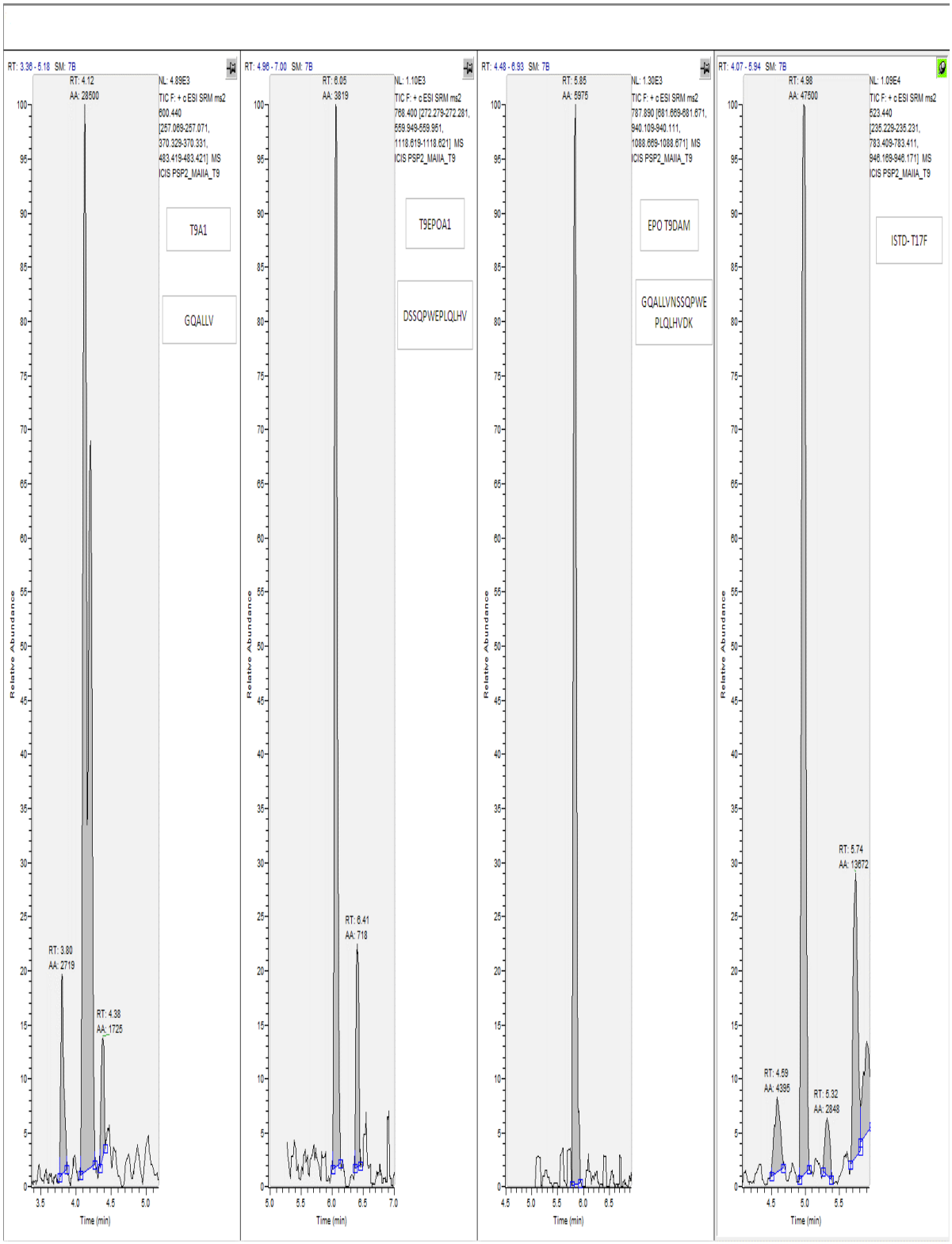

Figure 3.4 Post-spiked plasma with Eprex- glycosylated peptides

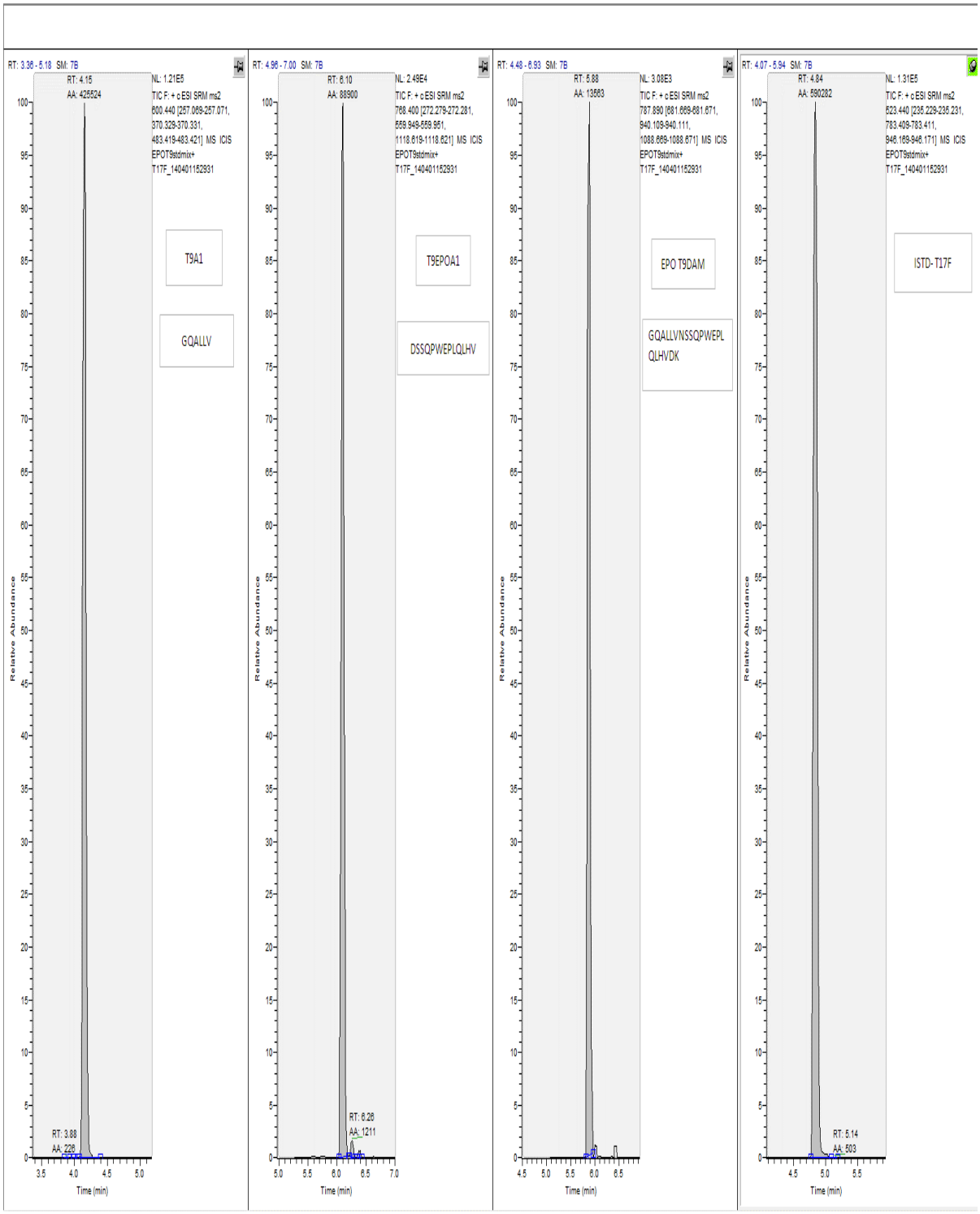

Figure 3.5 Extracted ion chromatogram of T9 stdmix and ISTD

Two sets of calibrants were prepared as described in section 3.2.6. For calibrant mixture A, only T9A1 calibration curves were plotted, because EPO T9DAM and T9EPOA1 were unable to be detected at all the calibration levels. For calibrant mixture B, T9A1 and T9DPOA1 calibration curves were plotted and, in this instance, only DPO T9DAM was unable to be detected at all the calibration levels. A linearity of > 0.99 was achieved for T9A1 in calibrant mixture A and T9A1 and T9DPOA1 in calibrant mixture B. The calibration curve A (Figure 3.6) was used to determine the concentration of T9A1 in the 10 nM Eprex sample, which shows a concentration of 4.725 nM. Calibration curve B (Figures 3.7 and 3.8) was used to determine the concentration of T9A1 and T9DPOA1 respectively in the Aranesp sample. The 10 nM Aranesp, was shown to contain 7.068 nM of T9A1 and 2.809 nM of T9DPOA1. Both the Eprex and Aranesp samples showed a higher intensity for peptide T9A1 for both the deaminated peptide EPO T9DAM and DPO T9DAM (Figures 3.9 and 3.10). However, peptide T9A1 is a common fragment for both the rhEPO and DPO. However, the T9EPOA1 and T9DPOA1 peptides could be used to differentiate between the two epogens. Figures 3.11 and 3.12 show that Eprex and Aranesp were tryptic digested and deglycosylated, this could be seen that the deaminated peptide T9 for both the rhEPO and DPO are low at 4.5 E4 and 2.1 E4 respectively. However, after the Asp-N digestion step, peptides T9A1, and T9EPOA1 could be seen as 7.4 E5 and 7.8 E4 respectively in rhEPO while T9A1 and T9DPOA1 could be seen as 1.7 E6 and 6.6 E6 respectively in DPO. Figure 3.9 shows that Asp-N digestion of the Eprex, for the uncommon peptide fragment T9EPOA1 still remains low at 7.8 E4, however the T9A1 peptide shows an area of 7.4 E5 but this is a common fragment which also contain in DPO. In this case, T9EPOA1 shows a similar area to EPO T9DAM, whereas for Aranesp, a significant difference could be seen in DPO T9DAM

and T9DPOA1. For rhEPO, it is not ideal to confirm by using the T9 peptide, as it gives a low sensitivity, even after the Asp-N digestion. This could be due to the T9EPOA1, which still contained a much longer peptide fragment compared to T9DPOA1. Hence, rhEPO could be confirmed by using the other glycopeptide EPO T5 which was further discussed in Chapter 5.

In Figure 3.12, it could be seen that after tryptic digestion and PNGase F digestion of Aranesp, the other tryptic peptides, T6, T11 and T17 could achieve an intensity of E6 – E7 level; however, T9 DAM could only achieve 1.5 E4. From Figure 3.10, we could see the Asp-N digestion fragments, where the T9DPOA1 achieved at 9 E5 and T9A1 achieved at 3 E6. However, T9A1 is a common fragment to rhEPO. Hence, we could differentiate which epogen was present by identifying the T9DPOA1 fragment which has given a much better sensitivity. Thus, this has greatly enriched the sensitivity with which the presence of amino acids, characteristic to each epogen, contained in the sequence from the deglycosylated fragment of T9 peptide can be detected. This provides a simpler and easier way of establishing whether rhEPO or DPO was the protein responsible for the common peptides (*e.g.* T17).

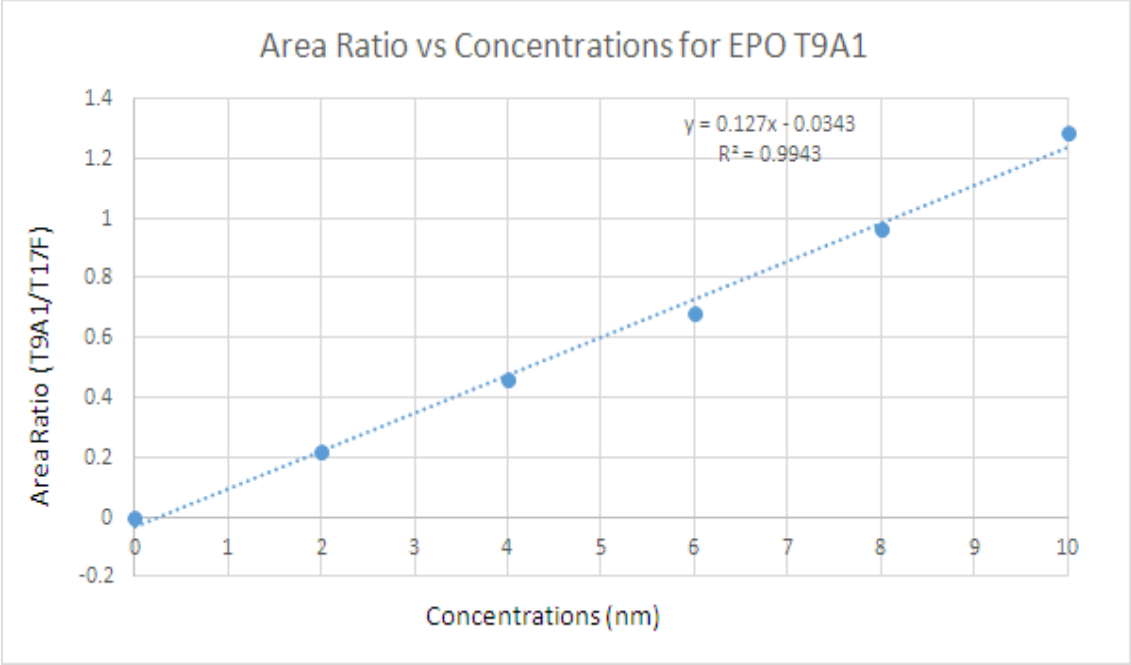

Figure 3.6 Calibration curve for calibrant A- T9A1

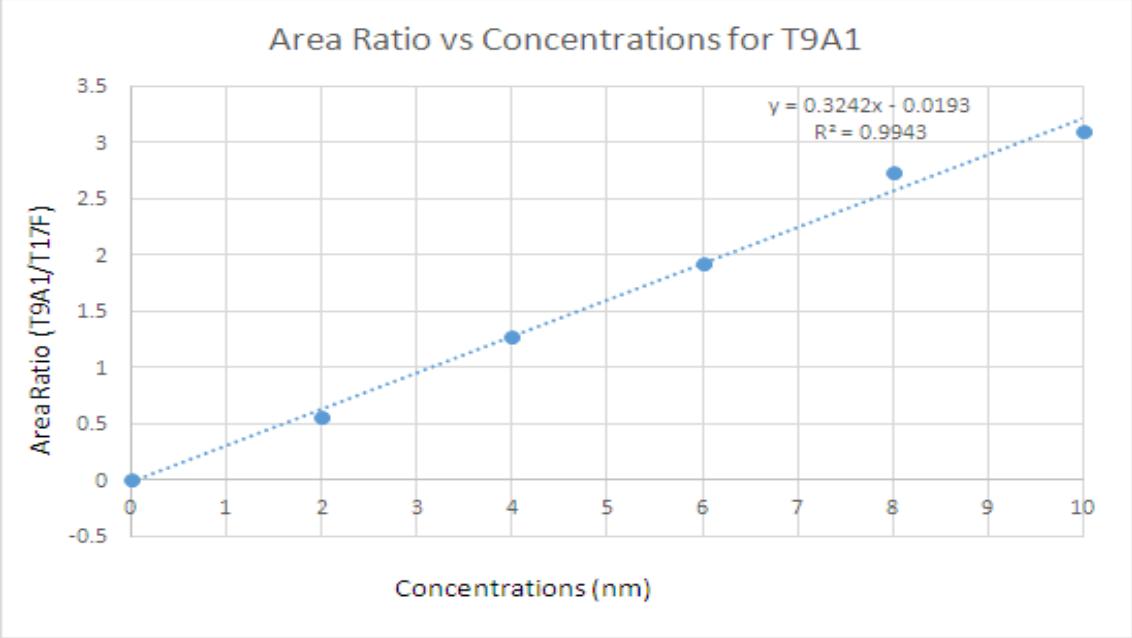

Figure 3.7 Calibration curve for calibrant B- T9A1

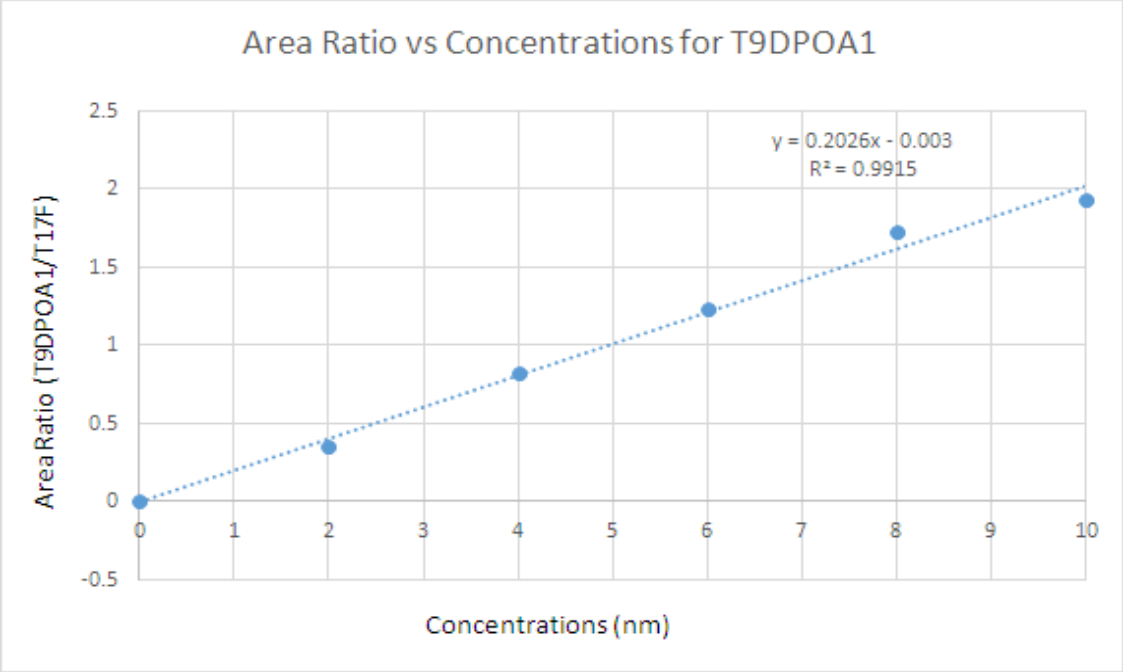

Figure 3.8 Calibration curve for calibrant B- T9DPOA1

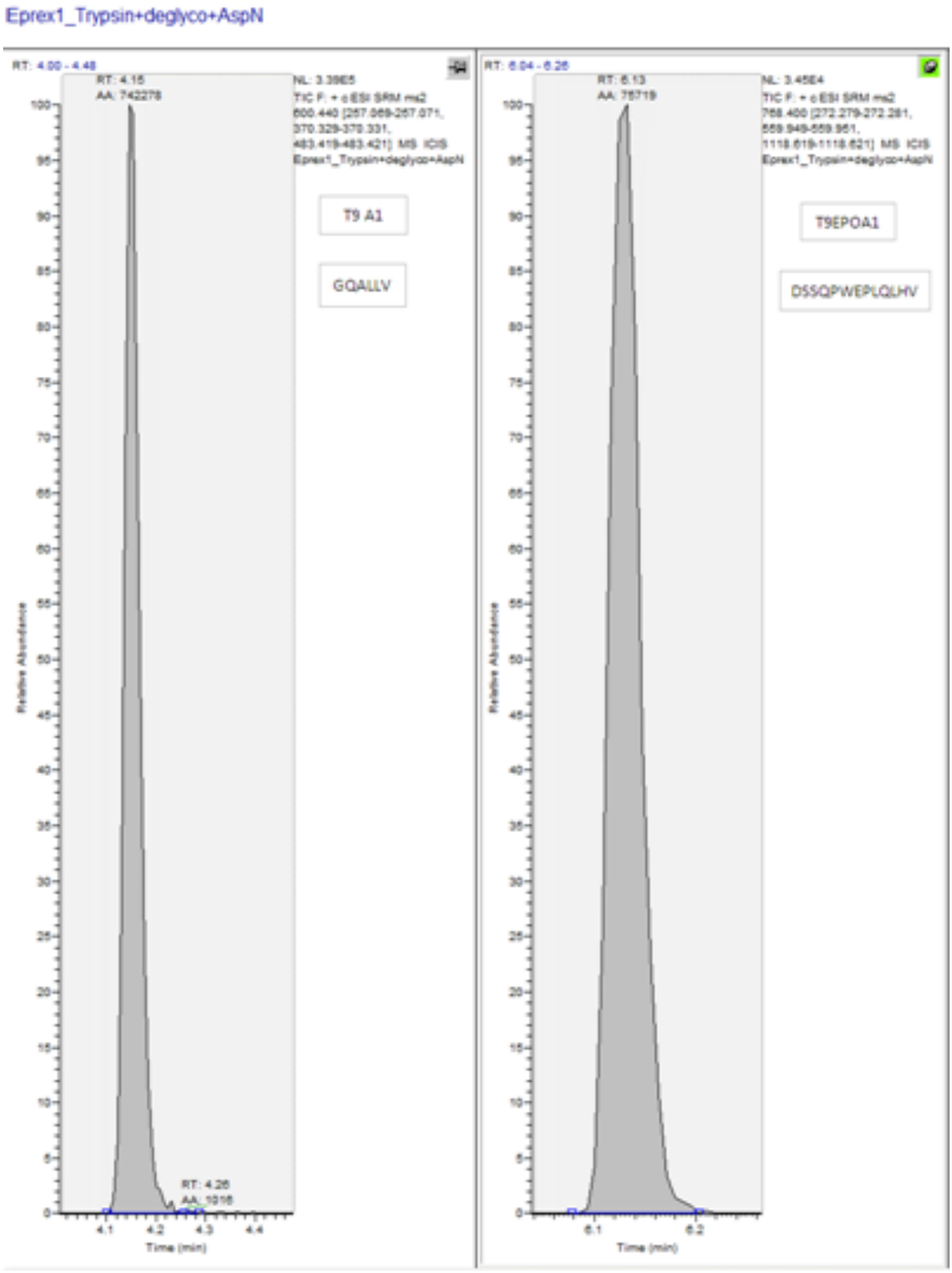

Figure 3.9 EPO peptides after Asp-N digestion

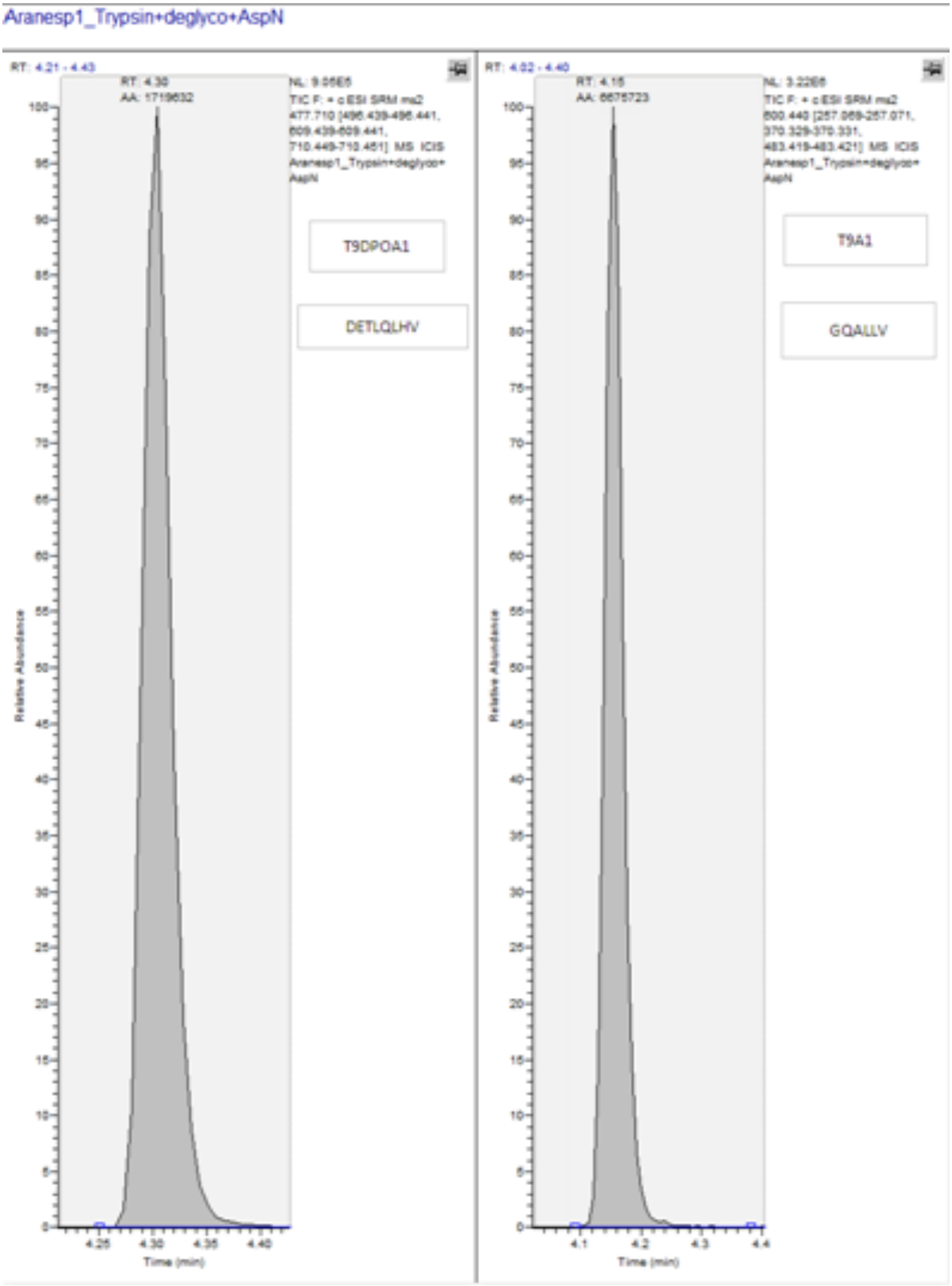

Figure 3.10 DPO peptides after Asp-N digestion

Figure 3.11 EPO peptides after tryptic digestion and deglycosylation

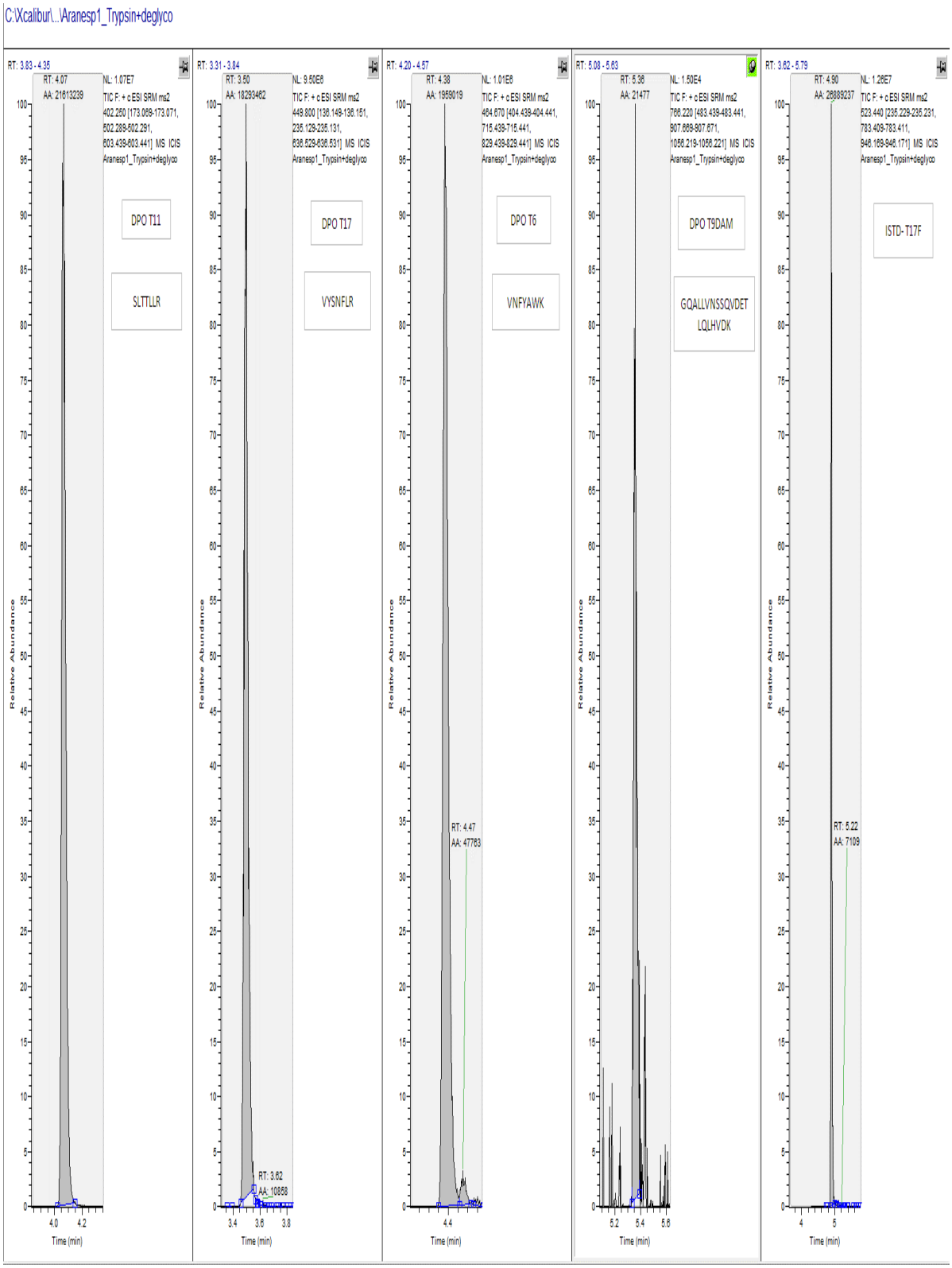

Figure 3.12 DPO peptides after tryptic digestion and deglycosylation

3.4 Conclusion

The MAIIA EPO purification kit is able to fulfil the requirements for use as a Pre-MS step for human and equine EPO doping analysis for plasma samples. The recovery of the rhEPO spiked in plasma is comparable or better than the post-spiked recoveries for non-glycosylated and glycosylated peptides respectively. The glycosylated peptides sensitivity could be achieved by the Asp-N digestion converting most of the EPO T9DAM or DPO T9DAM to the smaller peptide T9A1 and T9EPOA1 or T9DPOA1, which resulting in a higher intensity. We consider this pre-analytical purification step efficient, as it is able to achieve comparable or better intensity than the post-spiked result. The addition of Asp-N digestion helped to enrich the deaminated peptide T9, which gives a higher intensity for the Asp peptides, which could help to differentiate and identify the rhEPO and DPO in EPO doping.

Chapter 4: Immobilisation of trypsin enzyme onto porous glass beads and comparing of an on-line immobilised trypsin enzyme reactor and off-line in-solution trypsin digestion for rhEPO/ DPO

4.1 Introduction

The most important step in the sample preparation for proteomics is the conversion of proteins to peptides. This bottom-up approach for fragment peptides from enzymatic digestion of proteins, followed by LCMS was chosen in the study for screening and confirming of rhEPO and DPO (Figure 4.1). Trypsin is a protease that specifically cleaves the C-terminal proteins at the arginine, R and lysine, K position (Figure 4.2), creating peptides in the preferred mass range for MS sequencing and with a basic residue at the carboxyl terminus of the peptide, producing information-rich, easily interpretable peptide fragmentation mass spectra.

Digestion of proteins with a highly specific enzyme that produce fragments of the amino acid sequence which are characteristic of the intact material, and are also compatible with detection/identification using liquid chromatography-mass spectrometry, is an important step in contemporary proteomics. In-solution based protein digestion is the traditional way of achieving this, but this procedure has several drawbacks. Firstly it is a time consuming step, which requires up to 18 hours of incubation in order to produce a reasonable amount of the peptides [74-75, 180]. Secondly the by-products generated by the auto-digestion of the enzyme add chemical noise and, in some cases, the similarity between the autolysis fragments and the peptides from the protein can even complicate the interpretation of the results. These issues can be minimised by immobilisation of the protease onto a solid support [76], since the digestion time is dramatically reduced because the enzyme-to-substrate ratio is significantly enhanced. By doing this immobilisation the opportunity for enzyme autolysis by-products to be formed is significantly reduced. This approach enables a high-localized concentration of the enzyme and a

significant acceleration of the digestion without any auto digestion due to the site isolation effect [77-79]. Furthermore, attaching an enzyme to a solid support provides increased stability towards any chemical denaturants and organic solvents that may be present as a consequence of the preparation steps conducted prior to the digestion [80]. When used in an on-line configuration, this method can also reduce the amount of sample handling required [76] and offers a more efficient way to process samples where the amount of material available is limited.

Enzymes can be entrapped in polyacrylamide gels [75&76] or covalently attached onto the surface of micro-beads [81-82], monolithic columns [83-87] and the inner walls of open capillaries or microchannels in microfluidics devices [88-89]. Of all of these available options, the use of monolithic supports has attracted the most attention because they are easy to fabricate and the polymeric support generally provides fast mass transfer and low backpressure [90-91]. Monoliths composed of porous solid with small-sized skeletons and relatively large through-pores, could offer fast mass transfer and high enzyme binding capacity, making them superior supports for enzyme immobilisation [71]. Their large accessible surface area combined with a limited diffusion path length facilitates the rapid conversion of substrates [72, 180-182] resulting in the limited generation of autolysis products due to the site isolation effect [3, 183-184]. The fused silica capillary format for containing the immobilised enzyme reactors provides a convenient way to combine this step directly with hyphenated liquid chromatography-mass spectrometry [98, 128, 136].
Covalent attachment has several advantages over entrapment methods [177, 185] such as prevention of leaching, reduced diffusional constraints and no substrate mass limitations. Covalent immobilisation of trypsin onto controlled pore glass (CPG)

particles is a classical method that is highly effective for rapid production of micro-scale immobilised enzyme reactor systems, which can easily be fabricated. Rigid glass particles can withstand high pressure in fluidic systems better than agarose beads, but better thermal stability than crosslinked polymer beads and have a good solvent compatibility. The high surface-to-volume ratio of CPG particles allows high enzyme loading when packed as a bed compared to membranes and they provide almost as good mass transfer as monolithic IMERs.

Diisosthiocyanate (DITC), which was employed in this work, acts as a useful spacer (as it increases the accessibility) between the enzyme and the aminopropylated CPG particle. It was evaluated that activity was slightly higher when immobilisation was carried out in the presence of Ca^{2+} whereas more enzyme could be immobilised in its absence [186].

In this chapter, I had reported a study on immobilisation of trypsin with high apparent specific activity onto covalently immobilised *via* the 1, 4-diisothiocyanatobenzene (DITC) linker onto aminopropylated controlled pore glass (CPG), DITC-CPG particles and on the influence of calcium ions added during the immobilisation procedure. The immobilisation of trypsin on porous glass beads was also compared with the immobilisation of trypsin on microreactors.

An on-line digestion (trypsin reactor) was compared with the off-line (in-solution) digestion, and two different types of tryptic microreactors were fabricated and immobilised. An evaluation of the relative efficiency of the digestion technique was carried out by comparing the results obtained from the off-line (in-solution trypsin

digestion) method versus the on-line approach with either trypsin immobilised inside an open tubular dextran-modified capillary or a monolithic column where the trypsin was covalently bound to the surface.

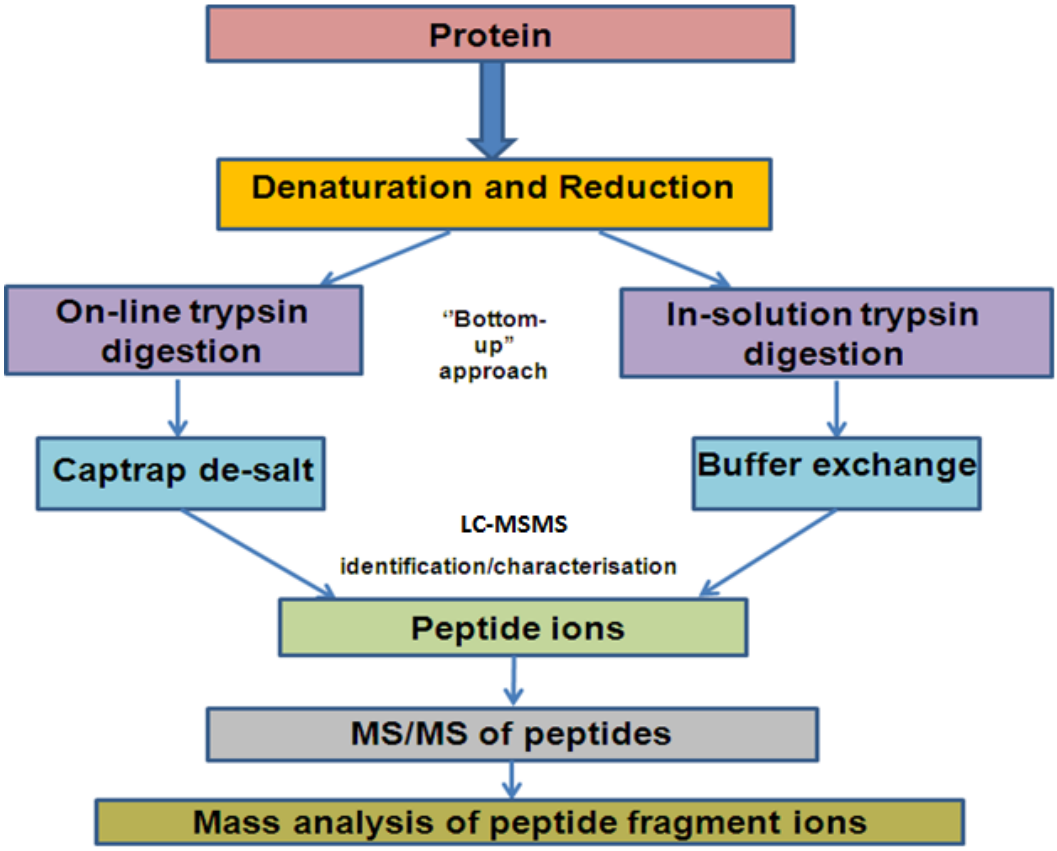

Figure 4.1 Workflow of bottom-up approach for protein sample preparation

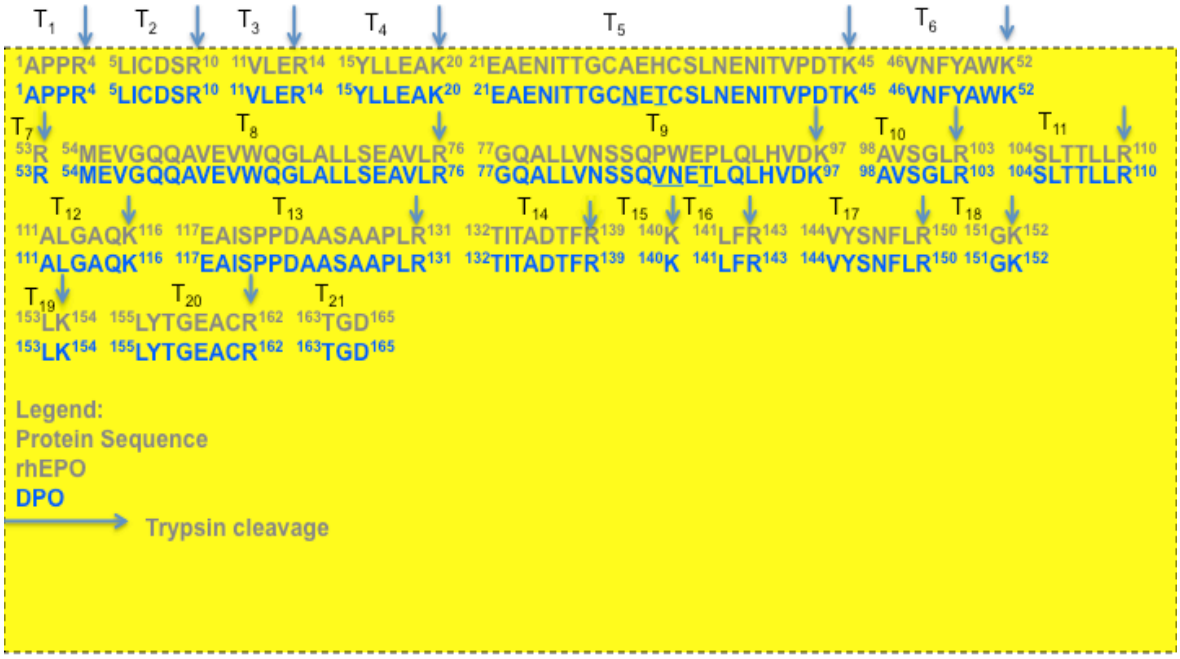

Figure 4.2 Tryptic digest for rhEPO and DPO

4.2 Materials and Instrumentation

4.2.1 Materials.

Diisothiocyanato-CPG (80-120 mesh, 700 Å average pore size, 54 µmol diisothiocyanato-CPG per g of glass), tetrahydrofuran (THF) with molecular sieve, Aminopropyl triethoxysilane (APTES) and N-(3-dimethylaminopropyl) - N'ethylcarbodiimide hydrochloride (EDC) and N-hydroxysuccinimide (NHS) were purchased from Sigma/ Aldrich Singapore. Carbonyl diimidazole (CDI) was purchased from Alfa Aesar Chemical Company (Singapore) while carboxyl-modified dextran 10 (CMD) was purchased from pK Chemicals A/S (Denmark). Amino-modified dextran (AMD) 3000 MW was from Invitrogen, Eugene, Oregon, USA. Sodium carbonate, calcium chloride, sodium hydroxide, polyethylene glycol 10,000 (PEG), sodium bicarbonate, sodium chloride, dimethoxysulfoxide (DMSO), ammonium persulfate (APS), dimethyl sulfoxide (DMSO), ammonium persulfate

(APS) were all from Merck (Singapore). Methacryloxypropyltrimethoxysilane (Bind-silane), acrylamide, *N.N'*-methylenebisacrylamide, *N,N,N',N'* Tetramethylethylenediamine (TEMED), N-acryloxysuccinimide (NAS) and benzamidine were purchased from Acros Singapore. Methanol and Toluene were from Fisher (Singapore). Trypsin lyophilised from Bovine pancreas was purchased from Thermo Scientific Singapore. The fused silica capillary 50 µm i.d. was supplied by Polymicro U.S.A. The water used throughout all experiments was Milli-Q Gradient A10 from Millipore (Singapore). Epoetin alfa, Eprex® the recombinant human erythropoietin, 10,000 IU/ ml was purchased from Jassen-Cilag AG, (Schaffhausen, Switzerland). Darbepoetin alfa, Aranesp® 40 µg/ 0.4ml were obtained from Amgen Manufacturing Limited a subsidiary of Amgen Inc. (Thousand Oaks, CA, USA).

4.2.2 Instrumentation.

Experiments were undertaken using a Tempo™ nano MDLC by Eksigent, with an Eksigent AS1 Autosampler coupled to the nano-electrospray III source (experiment for comparison of immobilisation of trypsin on CPG beads with on-line trypsin enzyme reactor) or TIS source (experiment for comparison of on-line enzyme reactor and off-line enzyme digestion) of an AB Sciex 4000 Qtrap LC-MSMS operated by Analyst 1.5 software. The autosampler has a 6-port injection valve with a 20 µl injection loop. For the nano-electrospray set-up, a 50 µm fused silica capillary was fitted from the injection port and coupled to the trypsin enzyme reactor (on-line enzyme digestion) or coupled to the HALO™ C18 0.3 x 150 mm, 2.7 µm analytical column (off-line digestion on CPG beads), another 50 µm fused silica capillary was coupled from the analytical column to the nano-electrospray head which holds a new

objective 50 µm tapered metal tip. For the TIS source set-up, a 50 µm fused silica capillary was fitted from the injection port and coupled to the trypsin enzyme reactor (for on-line enzyme digestion) with a microtight union, where the trypsin enzyme reactor is placed in the oven at 37 °C or coupled directly to the HALO™ C18 0.3 x 150 mm, 2.7 µm analytical column (for off-line in-solution digestion) and joint by another union with another 50 µm fused silica capillary connected to the 6-port switching valve, passing through a CAPTRAP™, PEPTIDE (Michrom Bioresources, Inc.). When this switching valve is switched, the pump running an organic solvent gradient, delivers the sample from the CAPTRAP to the analytical column and then to the TIS source (Figure 4.3).

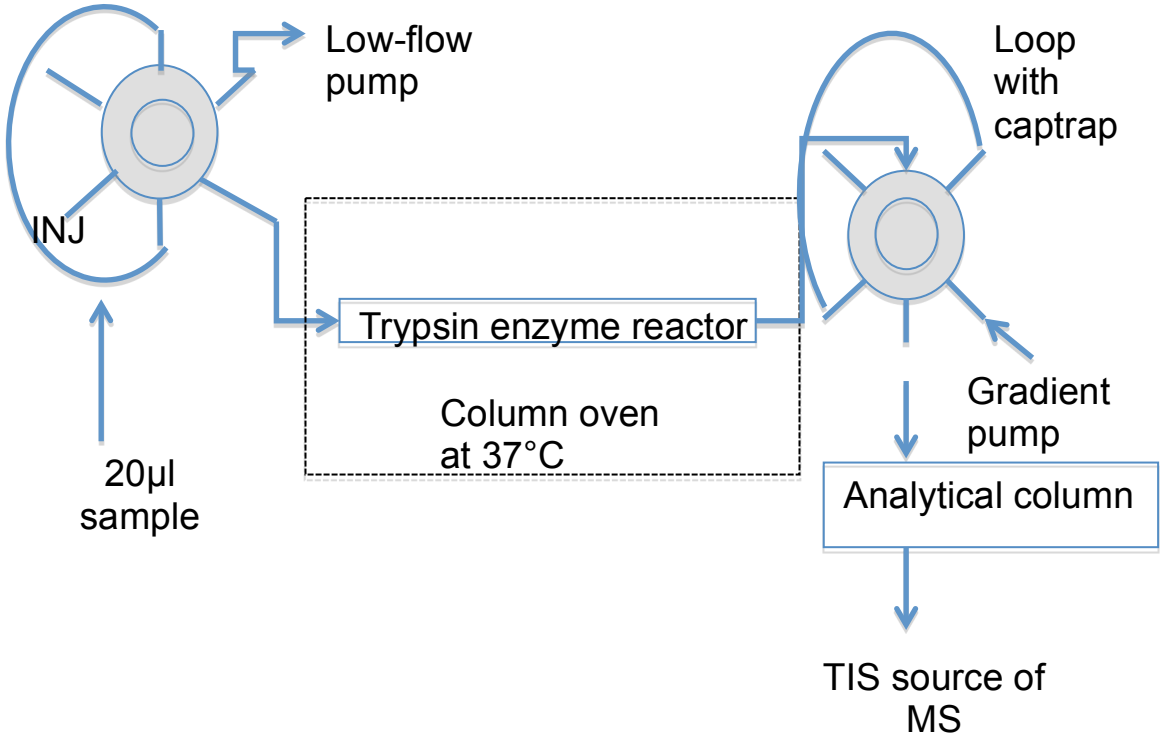

Figure 4.3 Schematic diagram of an on-line set-up of trypsin enzyme reactor

4.2.3 LC Conditions

4.2.3.1 The mobile phase used for both loading and gradient pumps were (A) 0.15 % FA in water and (B) ACN.

4.2.3.2 Nanospray set-up the gradient pump initial conditions were 95 % A and 5 % B followed by a 20 min gradient to 5 % A and 95 % B, holding at 95 % B for 10 min, and returning to its initial condition at 26 min and re-equilibrating in preparation for the next injection between 26 and 35 min, at a flow rate 4 µl/ min.

4.2.3.3 TIS set-up the loading pump was set at 1 µl/ min isocratic for 95 % A and 5 % B. The gradient pump initial conditions were 95 % A and 5 % B followed by a linear gradient 10 min gradient to 5 % A and 95 % B, holding at 95 % B for 5 min, and returning to initial conditions at 16 min and re-equilibrating in preparation for the next injection between 16 and 25 min.

4.2.4 MS Conditions

4.2.4.1 The nano-electrospray source voltage was set at 2800 V, Nebuliser gas GS1 at 20 psi, curtain gas, CUR at 30 psi, Heater gas GS2 at 0 psi and TEMP was set at 0℃.

4.2.4.2 The positive ion source voltage was set at 4500 V, GS 1 at 15 psi, GS 2 at 10 psi, CUR at 30 psi and TEMP at 350 °C.

4.2.5 Preparation of DITC-CPG beads

THF was dried with molecular sieves. 5 ml of dried THF was dispensed into a dried conical flask; 50 mg of weighed DITC was added into the conical flask. 1 g of CPG beads was added. The mixture in the conical flask was stirred with a magnetic stirrer, with the nitrogen gas blowing at room temperature for 2 hr. The mixture was then filtered and washed with 100 ml of toluene. (The filtrate and toluene washes can be concentrated to recover DITC, which is repurified by crystallisation). The beads was then washed with 150 ml of anhydrous MeOH and dried under vacuum. The beads were stored at 4 °C under N_2.

4.2.6 Trypsin immobilisation on DITC-CPG beads

TPCK-treated trypsin was covalently coupled to the support (DITC-CPG) as follows: 10 mg of washed DITC-CPG beads were reacted with 5 mg of trypsin solution (10^{-4} M) in 100 mM sodium carbonate at pH 9.5 (~ 1 ml) in either the presence or absence of 11.5 mM calcium chloride. The mixture was allowed to react with gentle shaking at 25 °C. The reacted support was decanted and washed with 3 volumes of 100 mM sodium carbonate at pH 9.5, containing 0.5 M sodium chloride and then with 3 volumes of the same solution without sodium chloride. The reaction supernatant and all wash solutions were recovered for determination of unbound trypsin. The trypsin-DITC-CPG (Figure 4.4) particles were dried on a filter paper in 37 °C oven for 30 min; it was then poured into the amber vial and blow dried with N_2.

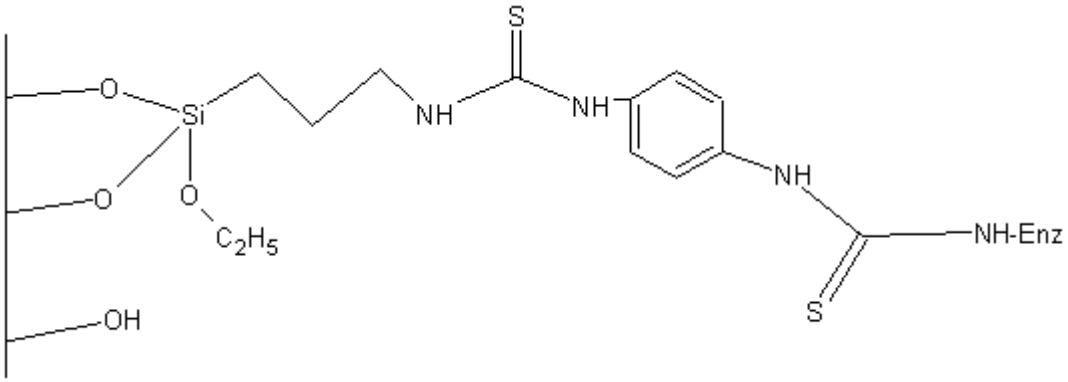

Figure 4.4 Structure of trypsin-DITC-CPG

4.2.7 Tryptic digest with trypsin-DITC-CPG beads

2.5 mg or 5 mg of trypsin-DITC-CPG beads was weighed and added into the prepared 300 µl of spiked Eprex with a concentration of 2 or 20 ng on-column injections. It was then placed in the oven at 37 °C for oven digest. The same amount was repeated for the trypsin-DITC-CPG beads with calcium chloride. The same concentrations were also prepared for the on-line digestion.

4.2.8 Preparation of dextran-coated fused silica capillaries

Firstly, the 160 cm x 50 µm fused silica capillaries were cleaned at a flow rate of 5 µl/min with 2 M NaOH for 30 min, 0.1 M HCl for 30 min, H_2O for 5 min and finally with EtOH for 5 min. The dextran-coated capillaries were prepared as follows: the clean capillaries were incubated for 60 min with a 10 % APTES solution in EtOH. After this step, the capillaries were flushed at a flow rate of 5µl/min with EtOH for 5 min and then dried overnight at 50 ºC. To modify the surface with dextran, the capillaries were incubated for 30 min with a solution of 5 % CMD in H_2O also containing 200 mM EDC and 50 mM NHS. After 30 min they were flushed for 5 min

at 5 µl/min with H_2O, then filled with a solution of 10 % AMD in H_2O and incubated once more overnight. The resulting dextran-modified capillaries were washed at a flow rate of 5 µl/min with both H_2O and MeOH for 5 min, after which 100 mM CDI in acetone was injected for 30 min. After this activation step, they were flushed with EtOH and H_2O for 5 min. A solution containing 2.5 mg/ml trypsin in 50 mM ammonium bicarbonate was injected at a flow rate of 2 µl/min and the enzyme coupling was allowed to couple for 8 hr. The reaction was stopped by injection of 1 M glycin pH 3. Finally the resulting trypsin micro-reactors were flushed with H_2O and stored in a closed box at 4 ºC or used immediately. All reactions were conducted at room temperature except for the drying step following APTES incubation. The chemistry of the surface modification and enzyme immobilisation in fused-silica capillaries has previously been described in ref. [4].

4.2.9 Preparation of the co-polymerised monolith column

27 cm x 250 µm i.d. fused silica capillaries were pre-treated with 1 M NaOH for 30 min, then flushed with 3 ml of 0.1 M HCl, and finally, rinsed with 3 ml water. Thereafter, a 50 % (v/v) Bind-Silane (bifunctional reagent) in acetone was introduced and left inside the column for 40 min at room temp. Finally, the capillary was rinsed with water and acetone, and then dried with N_2 gas. The monolith was prepared by dissolving 20 mg of acrylamide, 30 mg of *N, N'*-methylenebisacrylamide, and 30 mg of PEG per ml of 0.2 M sodium bicarbonate/ 0.5M sodium chloride (pH~8) buffer. The mixture was vortexed for a few seconds and heated at 55 – 60 ºC for 15 min to completely dissolve the monomers. To 0.5 ml of this solution, 2 µl of 20 % (v/v) TEMED were added. The mixture was then degassed for 15 min using N_2 gas

delivered through fused silica tubing. Next 5 µl of *N*-acryloxysuccinimide (NAS) (140 mg/ml, 828 mM) dissolved in DMSO was added. Since DMSO is of a higher density than the buffer, the NAS was added on top of the solution, while degassing was used to ensure a thorough mixing of the NAS with the solution buffer. After 1 min, 2 µl of 20 % (w/v) ammonium persulfate (APS) was added in order to initiate polymerisation. The APS was dispensed into the middle part of the solution while degassing, to ensure an efficient and rapid mixing. After 30 s, a 19 µl aliquot of this solution was removed and quickly mixed (so as to avoid contact with oxygen) with 1 µl of freshly prepared trypsin (20 mg/ml in a buffer containing 0.5 M benzamidine). This mixing step was performed without N_2 degassing. An activated (Bind-Silane) capillary was then inserted into the trypsin-monomer vial, whereby the solution filled the tubing by capillary action. Immobilisation/ polymerisation was allowed to proceed for 30 min at room temperature with the capillary ends covered with parafilm.

4.2.10 Preparation of samples

10 µl of 84 ng/µl Eprex® was spiked into 100 µl of 50 mM ammonium bicarbonate buffer in an auto sampler vial. This vial was placed on the auto sampler for direct injection into the on-line trypsin reactor coupled to the analytical column and to the TIS source for detection or add 1 µl of (2.5 mg/ml trypsin prepared in 50 mM ammonium bicarbonate buffer) into the spiked sample for an off-line digestion in the 37 °C oven for 3 hr digestion.

4.3 Results and Discussion

The covalently immobilisation of 1,4- diisothiocyanatobenzene (DITC) linker onto aminopropylated controlled pore glass (CPG) particles which reaction conditions involving enzyme, solid support and linker are important parameters since they determine the biochemical, mechanical and kinetic properties of the immobilised enzyme. It is recognised that trypsin autolysis is inhibited by addition of calcium ions to the enzyme reaction solution [186].

Hence, in this experiment, I had made a comparison of immobilising trypsin onto the DITC-CPG beads with and without calcium chloride. Figure 4.5 showing the Eprex digested in the DITC-CPG beads with $CaCl_2$ and Figure 4.6 showing the Eprex digested in the DITC-CPG beads without $CaCl_2$, both are digesting at the same concentration and injected 20 ng onto the column. Most of the peptides had an increased in intensity, except one of the peptides, EPO peptide T4 remained the same intensity. A few of the peptides achieved twice in the intensity for the digestion in the DITC-CPG beads with $CaCl_2$. This had shown that the addition of calcium chloride does help in improving the digestion, since there is an improvement in the sensitivity.

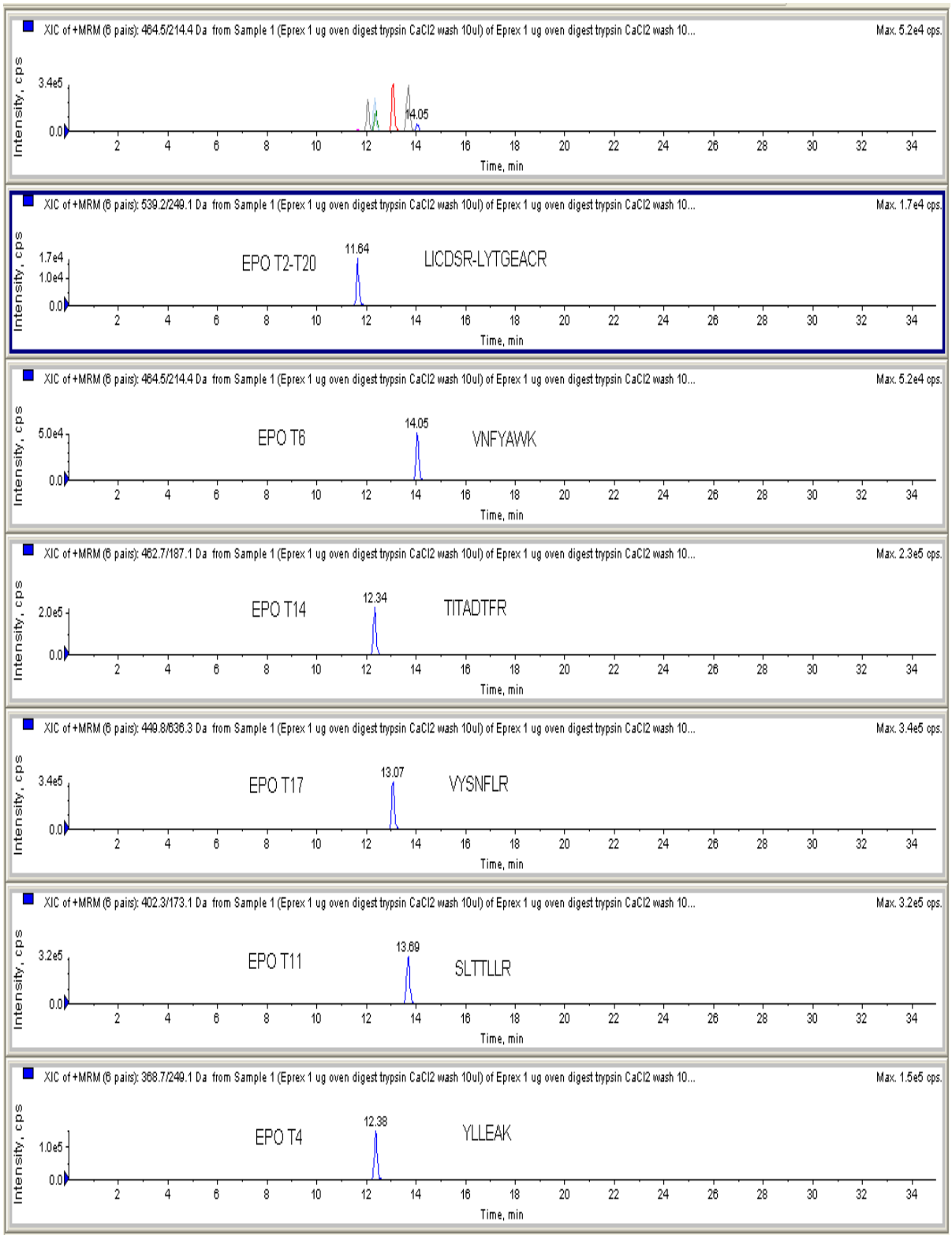

Figure 4.5 Eprex digested in trypsin immobilised onto DITC-CPG beads with $CaCl_2$

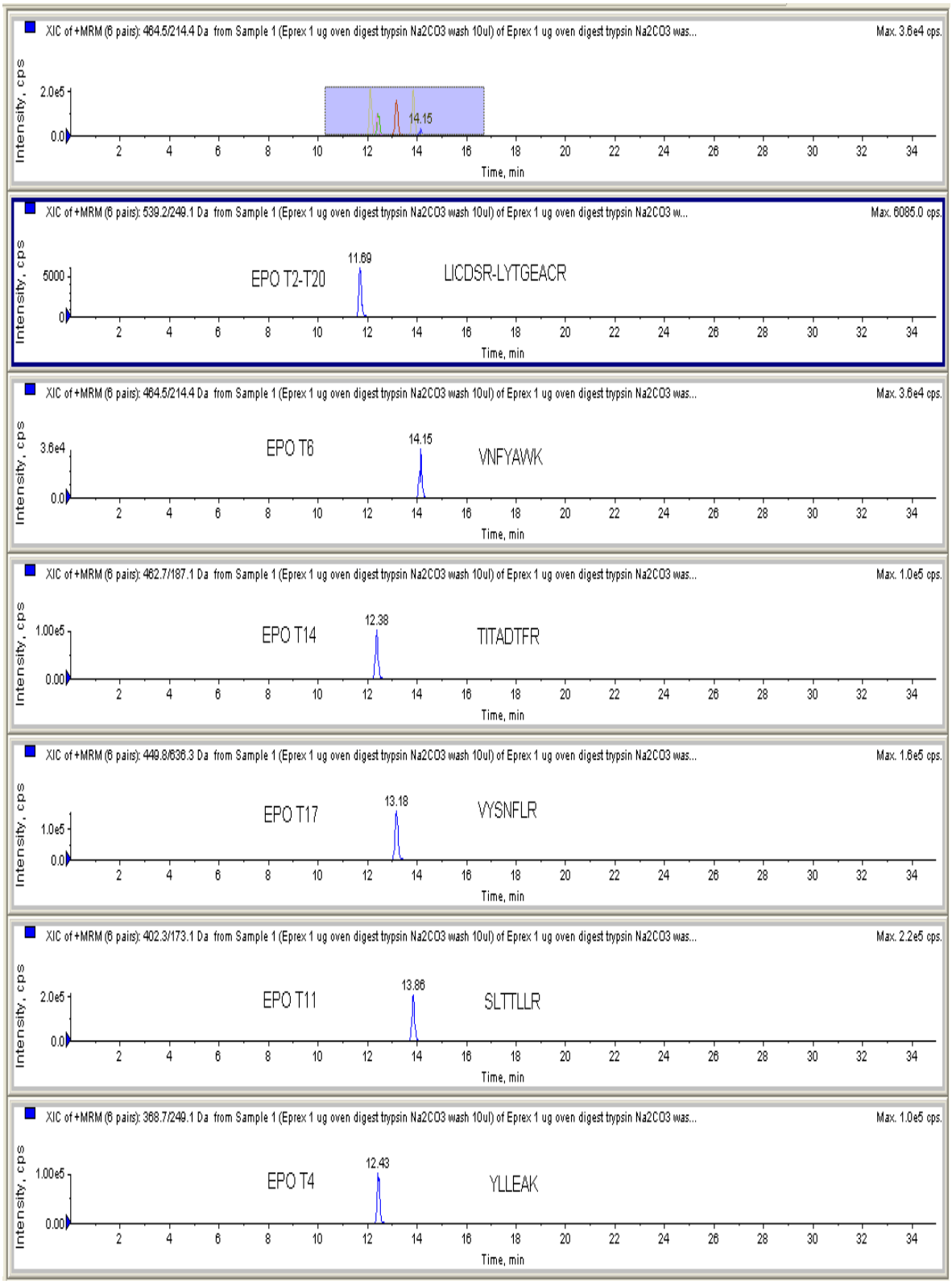

Figure 4.6 Eprex digested in trypsin immobilised onto DITC-CPG beads without $CaCl_2$

I had also compared the trypsin immobilised onto DITC-CPG beads with the on-line enzyme reactor. I had injected both digestions at 2 ng (Figure 4.7 and 4.8) and 20 ng (Figure 4.9 and 4.10) on-column. From both the concentrations, it can be seen that the Eprex digested on the on-line enzyme reactor which trypsin was immobilised onto the dextran-modified capillary showed a higher in intensity compared to the Eprex digested in the 5 mg of trypsin-DITC-CPG beads.

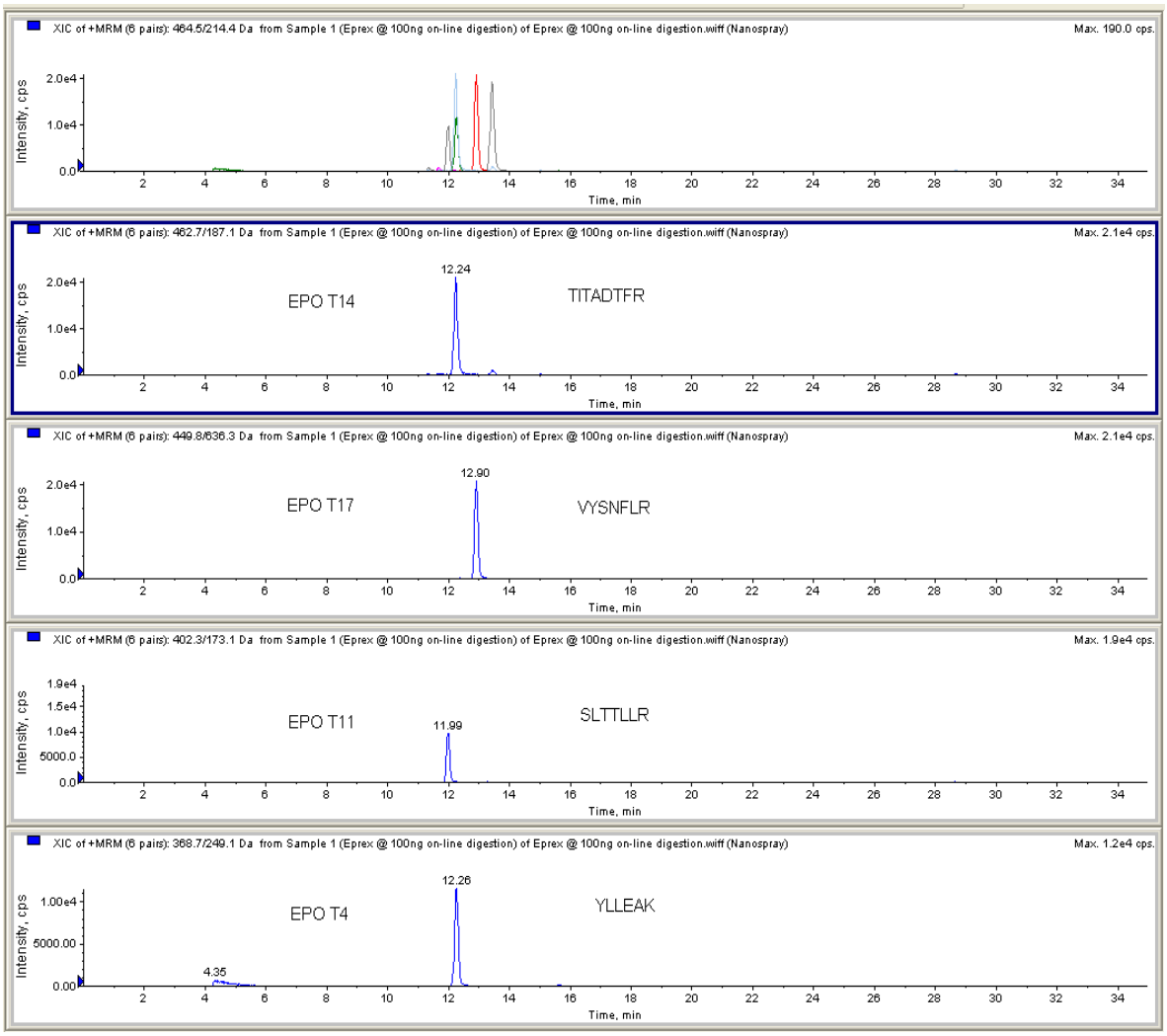

Figure 4.7 On-line enzyme reactor digestion for 2 ng Eprex injected on-column

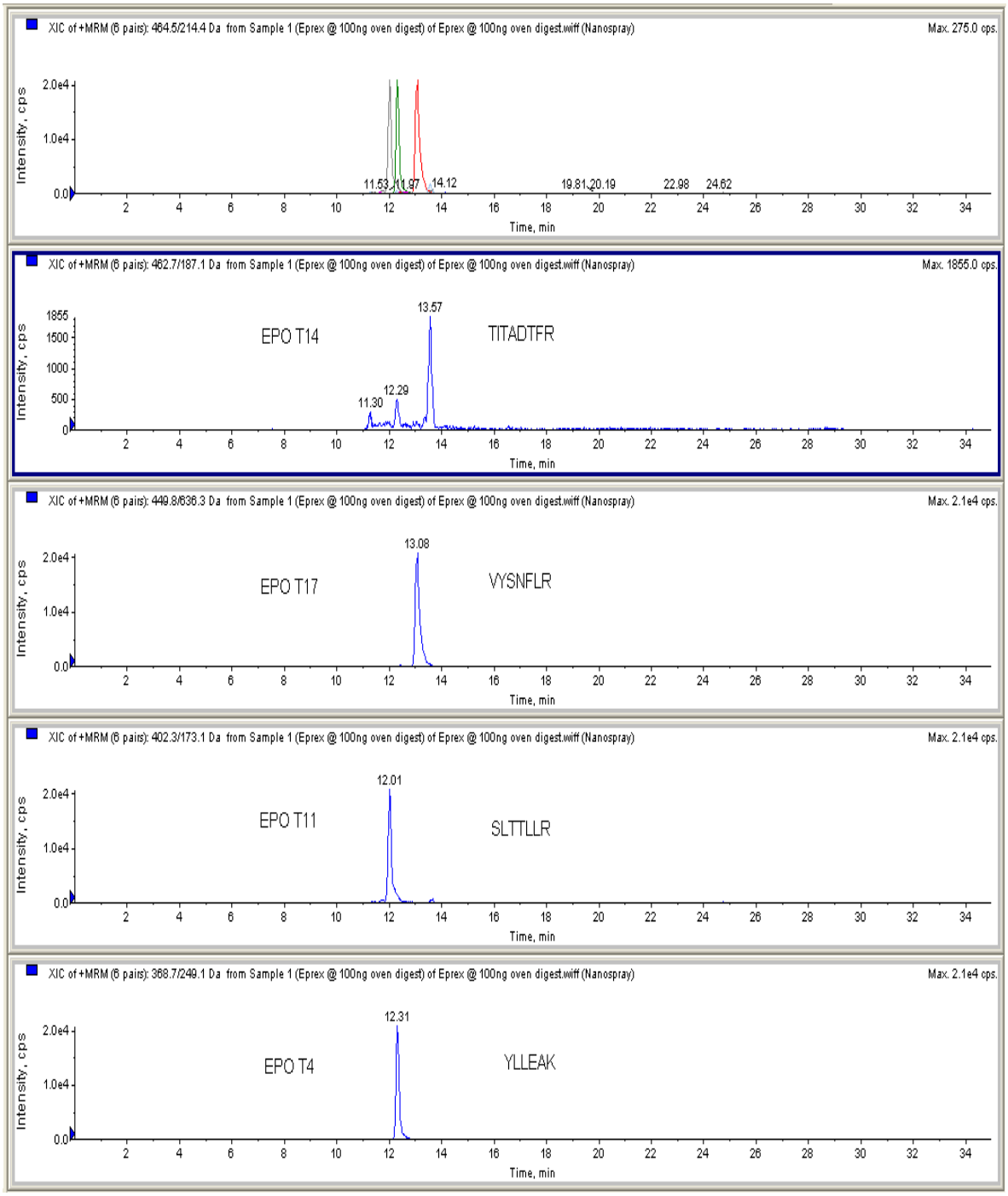

Figure 4.8 Off-line trypsin digestion in 5 mg DITC-CPG beads for 2 ng Eprex injected on-column

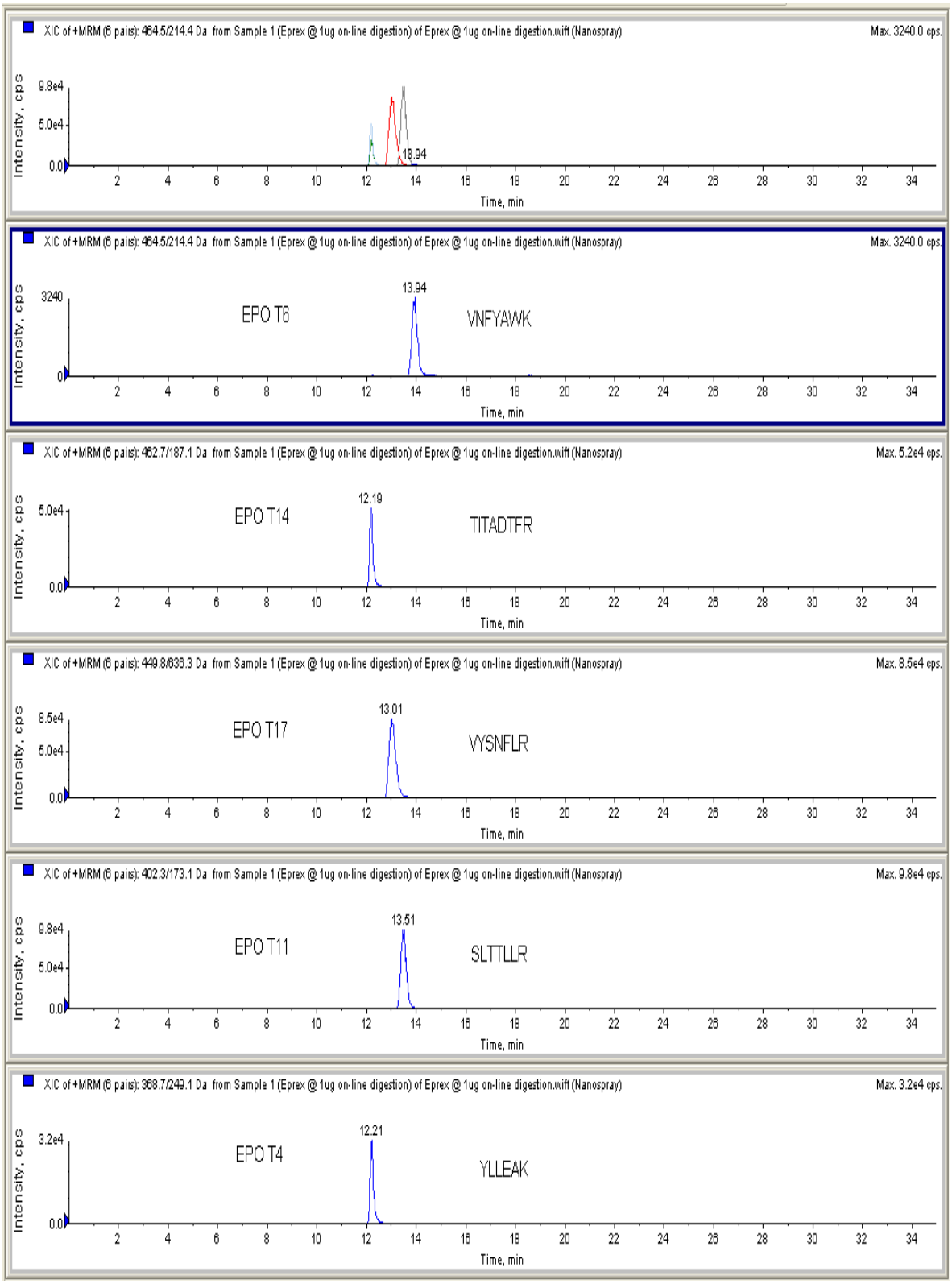

Figure 4.9 On-line enzyme reactor digestion for 20 ng Eprex injected on-column

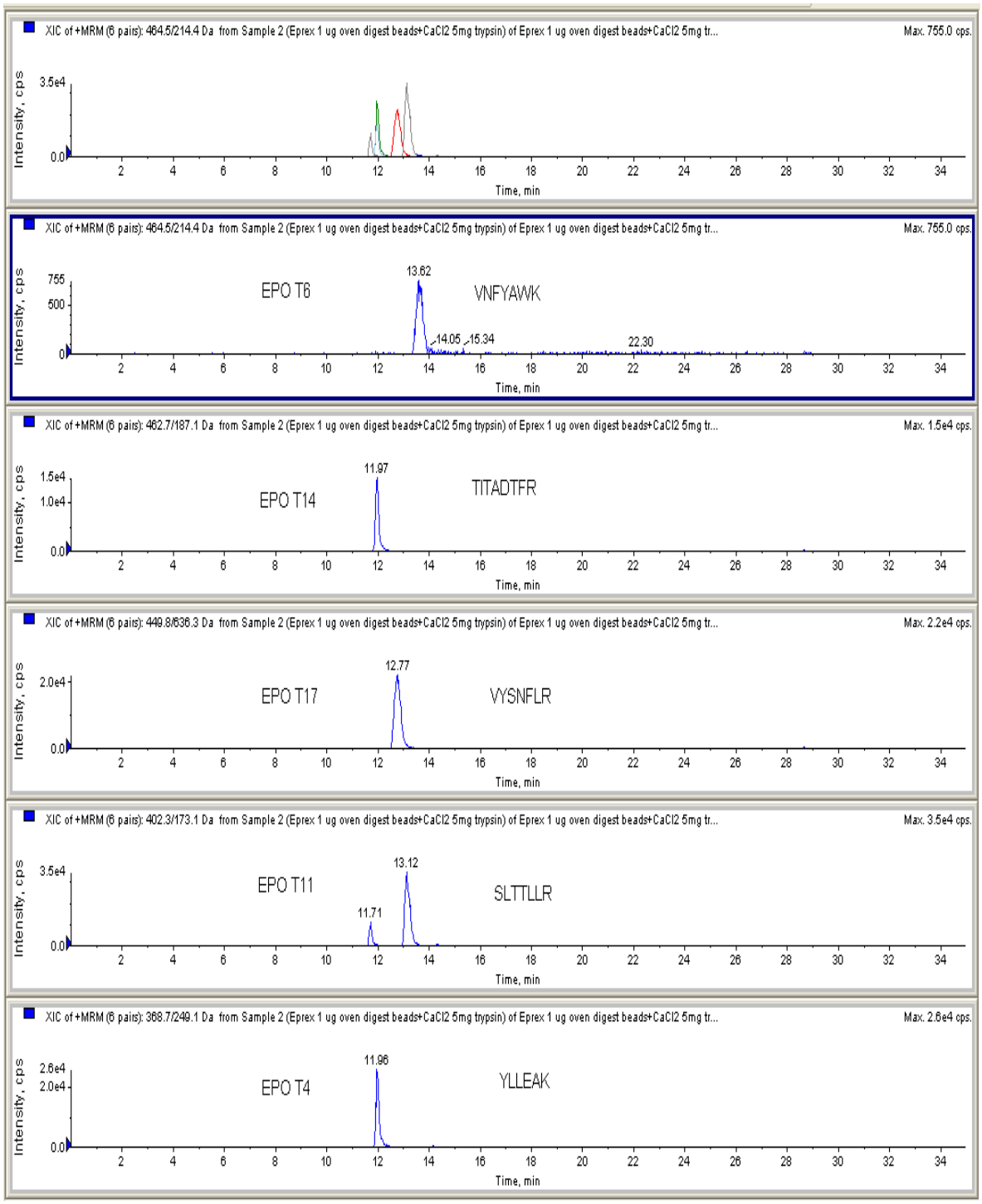

Figure 4.10 Off-line trypsin digestion in 5 mg of DITC-CPG beads for 20 ng Eprex injected on-column

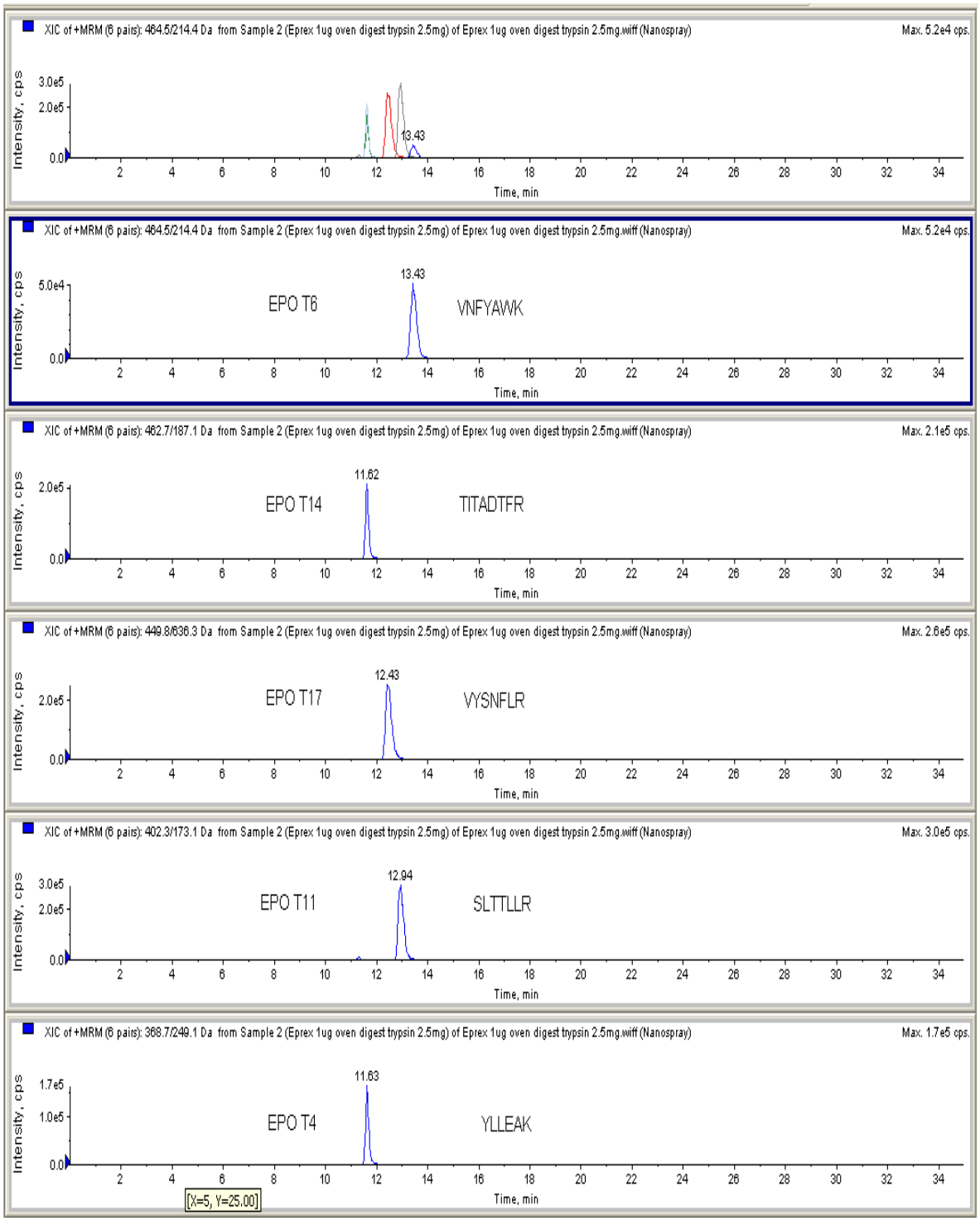

Figure 4.11 Off-line trypsin digestion in 2.5 mg of DITC-CPG beads for 20 ng Eprex injected on-column

However, when the Eprex was digested in 2.5 mg of DITC-CPG beads with $CaCl_2$ (Figure 4.11), this showed a much better (~10 x) intensity compared to the digestion in 5 mg of DITC-CPG beads with $CaCl_2$ and on-line enzyme digestion. It could be seen that when twice the trypsin-DITC-CPG beads was added, it caused a decrease in intensity by ~ 10 x. Hence, this could most likely be an autolysis which causes a decrease in the intensity. Thus, the amount of trypsin digestion can cause a variable in the sensitivity.

From this experiment, I observed that the digestion in 2.5 mg of immobilised trypsin-DITC-CPG beads could achieve a much better sensitivity. However, there is a lot of off-line preparation work required to wash and trypsin immobilised on the beads and off-line digestion.

I elected to use silica capillaries derivatised with a dextran hydrogel to passivate the silica surface as these should provide less non-specific adsorption of proteins and also offer a means to immobilise a larger amount of enzyme when compared to an unmodified surface [84 & 187]. As an alternative strategy, I coupled the enzyme to a monolithic polymer that had been fabricated inside a fused silica capillary. The digestion efficiencies of the two trypsin reactors fabricated in this manner were compared with the results from an in-solution digestion. Figures 4.12 and 4.13 show the EICCs obtained from a diluted Eprex™ standard using an on-line digestion with the dextran-modified reactor and the monolithic reactor respectively. The off-line (*i.e.* in-solution) enzyme digestion is shown in Figure 4.14. This data is summarised in Figure 4.15, which shows that the highest overall

abundance for the peptides was obtained when using the trypsin immobilised on dextran-modified fused silica reactor. For example, the EPO peptide T17 (VYSNFLR) has shown a response that was approximately 4 times higher than that from the in-solution digest and almost twice as high as that obtained when the monolithic reactor was used. It was also interesting to note that the EPO peptide T6 (VNFYAWK), which was below the detection limit in the in-solution digestion, was readily identified in the EICCs from both of the enzyme reactors. Some of the other peptides in these digests showed a similar result for both of the immobilised enzyme reactors and also the in-solution digestion. Triplicate injections onto the dextran-modified enzyme reactor were shown (Figure 4.16) to have a maximum CV of approximately 5 % for all digested peptides and therefore this reactor also offers better reproducibility when compared to using trypsin bound to the monolith, where the variation between injections was found to be much higher, ranging from 5 to 37 % CV. Thus, both of the on-line enzyme digestion reactors were more robust, achieved better sensitivity and reduced the digestion time when compared to the off-line in-solution enzyme digestion method. Another advantage is that I could use these reactors for more than 50 injections without an obvious loss of activity and this is a cost benefit in comparison to limitation of a one-time use of the enzyme during in-solution digestion.

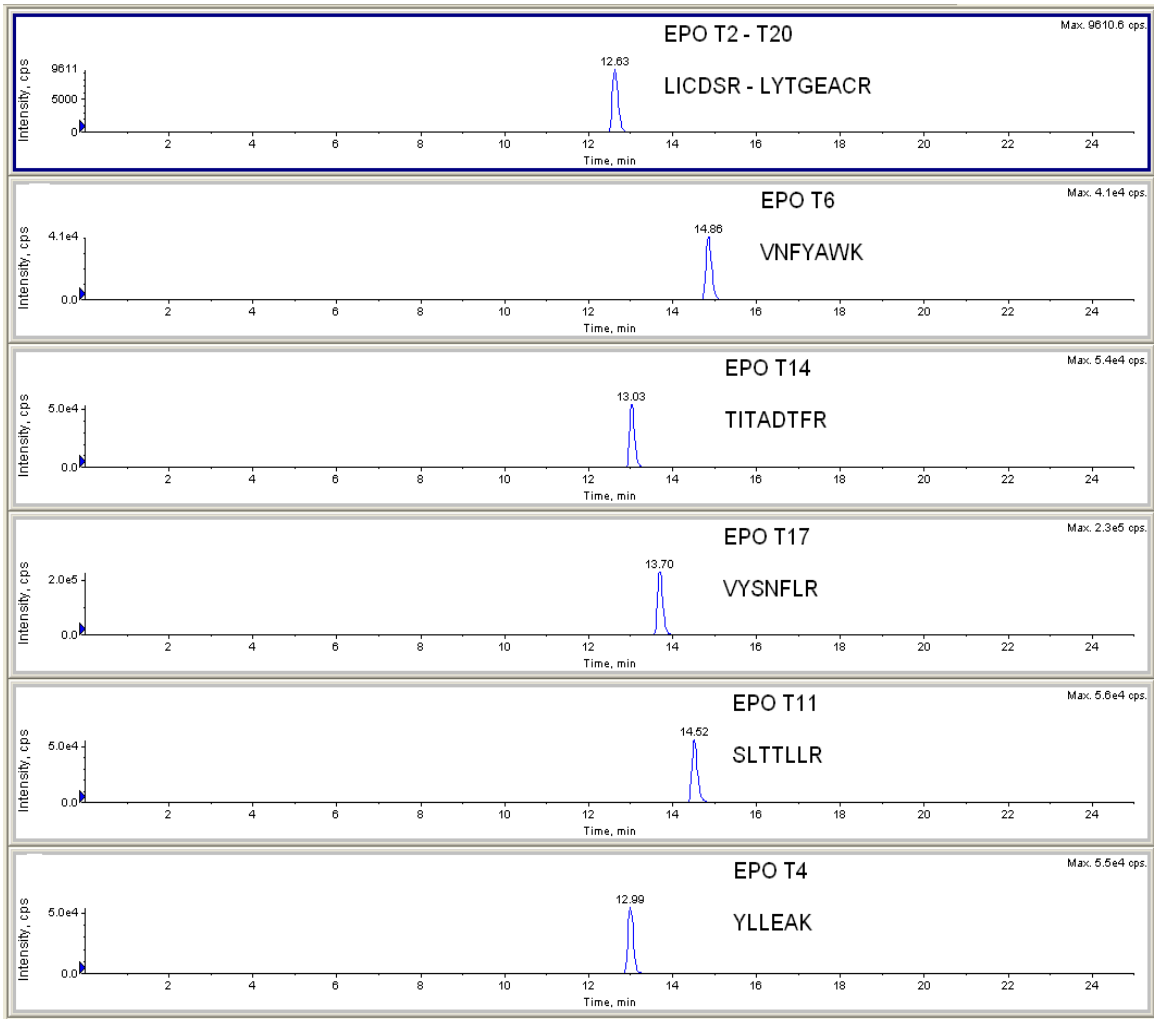

Figure 4.12 Extracted ion chromatogram showing EPO peptides digested on-line on a trypsin immobilised dextran-coated open tubular fused silica capillary.

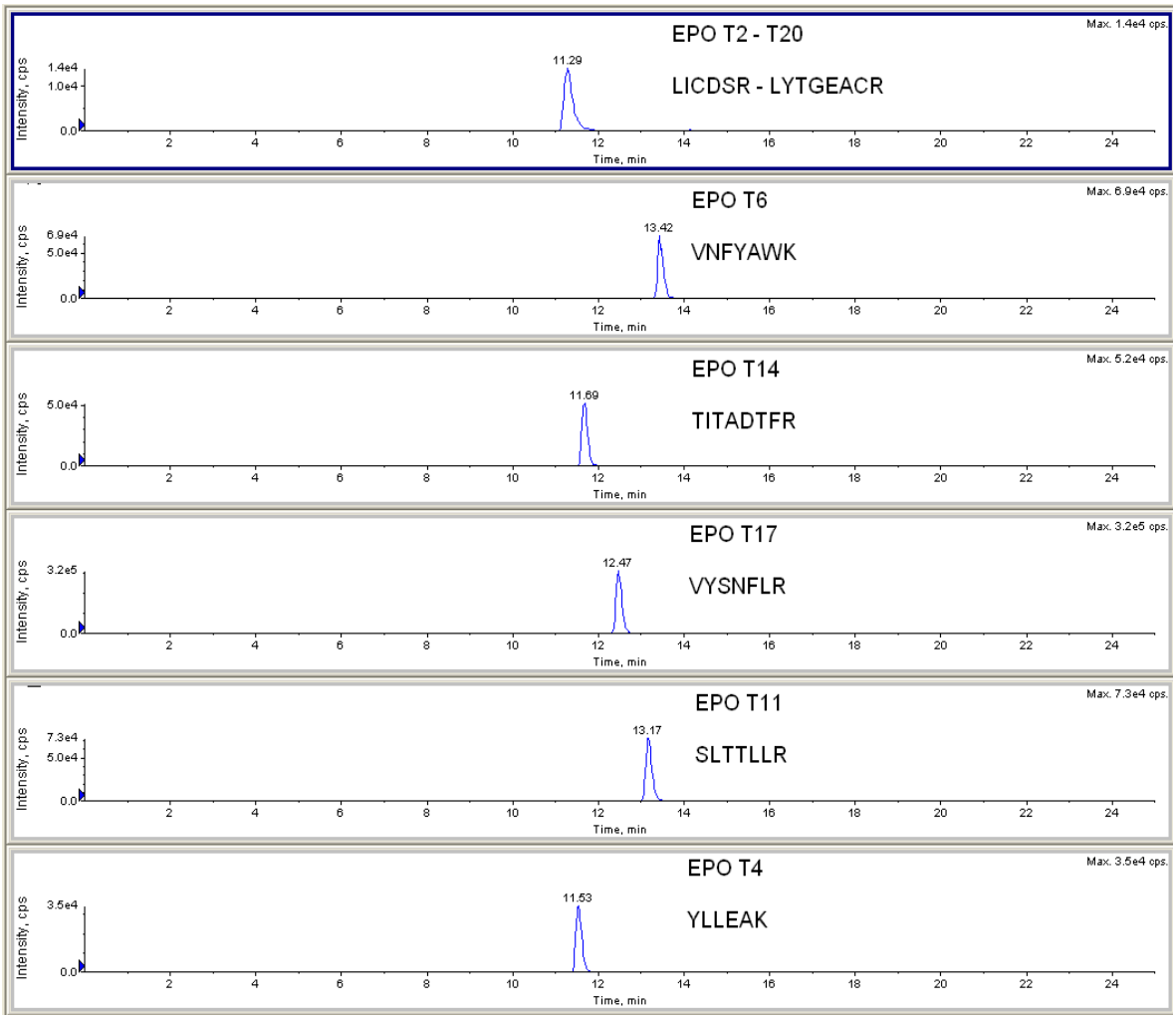

Figure 4.13 Extracted ion chromatogram showing EPO peptides digested on-line on a trypsin immobilised co-polymerisation monolith.

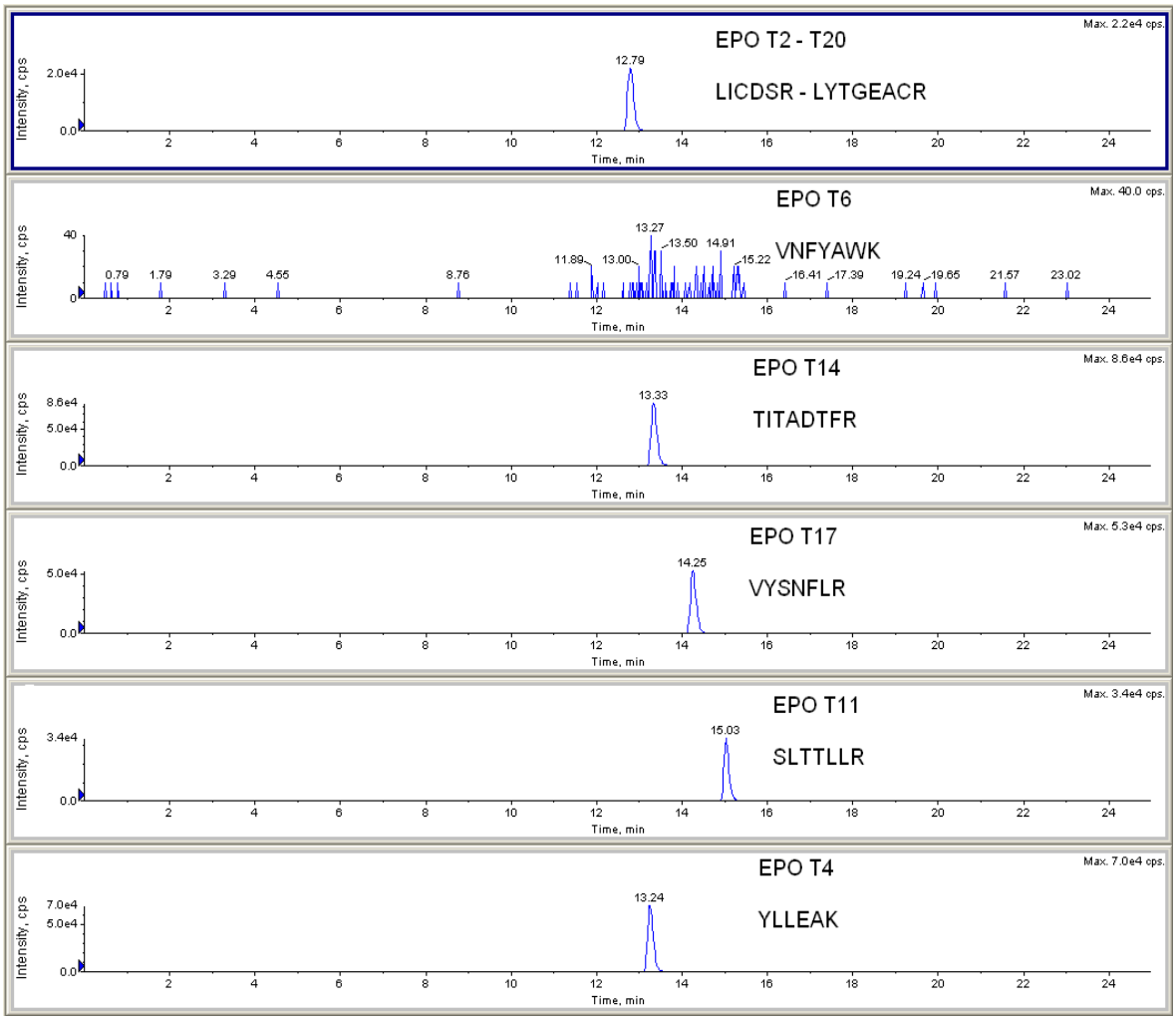

Figure 4.14 Extracted ion chromatogram showing EPO peptides digested off-line in-solution digestion.

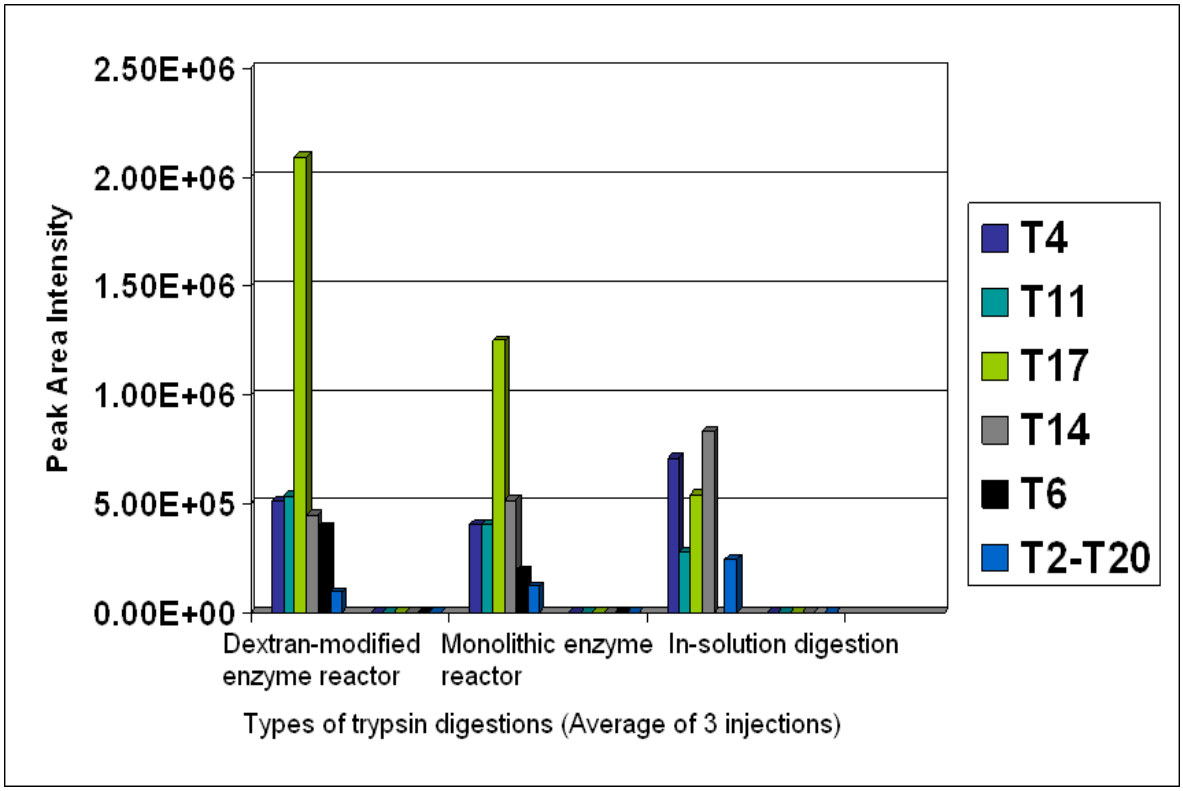

Figure 4.15 Graph summarising the peak area intensity of the two different types of enzyme reactors and in-solution enzyme digestion

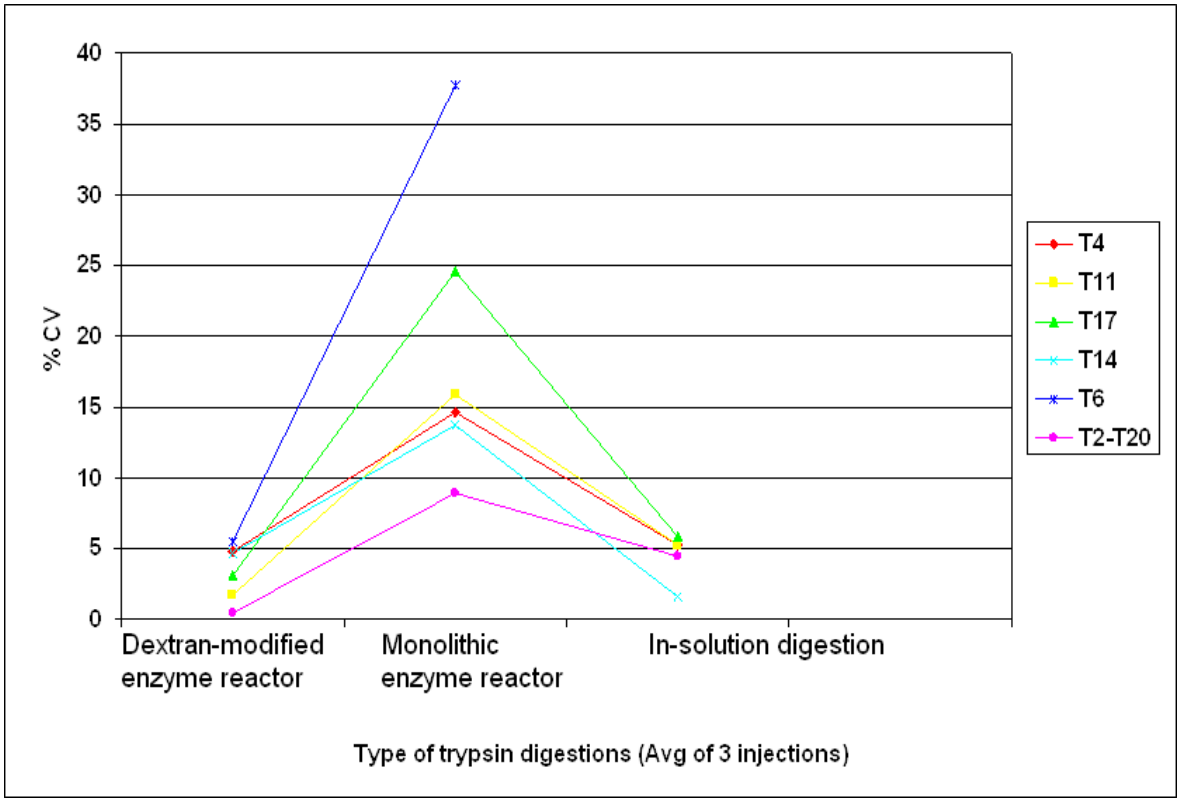

Figure 4.16 Graph summarising the reproducibility of the two different types of enzyme reactors and in-solution enzyme digestion.

4.4 Conclusion

The goal to replace an off-line (in solution) enzyme digestion with a fast and efficient on-line method that could be applied to detect rhEPO in equine plasma extracts has been achieved. I have demonstrated that immobilising trypsin on a dextran-coated capillary offers better sensitivity in addition to efficiency and repeatability performance enhancements when compared to the use of a monolithic capillary for this purpose. Future work will look at optimising the loading flow rate during the digestion/deglycosylation/trapping stage in order to reduce the cycle time between

injections and/or multiplexing the analysis to improve the overall throughput of the method.

Chapter 5: Discussion on the results obtained for different orientations of on-line immobilised PNGase F reactors

5.1 Introduction

EPO is a regulator of erythropoiesis, the process that controls the production of red blood cells in mammals and, therefore it is likely to be performance enhancing when given to racehorses [3]. Although the intact rhEPO can be detected by mass spectrometry [3], the most common way of screening for its presence is to digest an affinity extracted sample with trypsin and then conduct a target analysis for the characteristic peptides using LC-MSMS [184]. It is also possible to use this method to differentiate rhEPO from the synthetic epogen analogue Darbepoetin Alpha (DPO) since in addition to the presence of several peptides that are characteristic to both proteins, the peptides T5 (21-45) and T9 (77-97) have unique amino acid sequences that are specific to each protein (Figure 5.1). Unfortunately, this is not a straightforward process as the T5 and T9 product from both rhEPO and DPO are a population of glycopeptides with highly variable sialic acid containing glycan motifs that severely hinder detection under ESI-MS conditions.

Glycopeptides consist of a peptide and a glycan part covalently bound to asparagine residues (N-linked) or to serine or threonine residue (O-linked). The EPO tryptic digest shows three groups of glycopeptides. N-linked glycans, mainly di-, tri- and tetra-antennary structures of the complex type, are shown to attach to N24 and N38 in the T5 fragment of tryptic peptide ^{21}EAE**N**ITTGCAEHCSLNE**N**ITVPDTK^{45} and N83 in T9 fragment of tryptic peptide, ^{77}GQALLV**N**SSQPWEPLQLHVDK^{97}. The O-glycans are linked to the T13 fragment, peptide ^{117}EAISPPDAA**S**AAPLR^{131} with glycosylation at S126. Darbepoetin alfa (DPO) has a similar polypeptide backbone as rhEPO but with five amino acids differences (highlighted in red in peptide sequence below) and contains 5 N-linked carbohydrate at the T5 and T9 fragments.

The DPO tryptic digest shows the N-linked glycans at N24, N30 and N38 in the T5 fragment of tryptic peptide ^{21}EAE**N**ITTGC**N**ET**T**CSLNE**N**ITVPDTK^{45} and N83 and N88 in the T9 fragment of tryptic peptide ^{77}GQALLV**N**SSQV**N**ET**T**LQLHVDK^{97}. Thus, these are the only two unique tryptic digest peptide fragments, which can differentiate and identify the rhEPO from DPO.

Glycosylation of proteins is one of the most common posttranslational modifications (PTM) in the modulation of their structure and and functions. There are various pathways for protein modification with sugars (glycans), one of the most common ways is the addition of glycans to an asparagine (N-linked) or to serine or threonine (O-linked).

Consequently, an efficient process to remove the sugar moieties from the peptides is a key requirement for a successful analysis and Peptide-N-glycosidase F (PNGase F), which selectively releases N-linked glycans by hydrolysing the amide bond at the asparagine side chain [98], is frequently used for this purpose. This reaction is usually performed in solution using PNGase F mixed with the substrate in a small volume of buffer and, to keep cost under control, only a small quantity of the enzyme is typically used to catalyse the cleavage. As a result, the ratio of the glycolytic enzyme to substrate is usually lower than optimal. However, by efficiently immobilising the same amount of enzyme onto a solid support, this catalysis could be improved because only a small percentage of the sample is ever in contact with the enzyme at any time during the passage of the liquid through the reactor. Furthermore, only a small aliquot from the extract requires deglycosylation before

each LC/MS/MS analysis, and this further enhances the overall enzyme to substrate ratio.

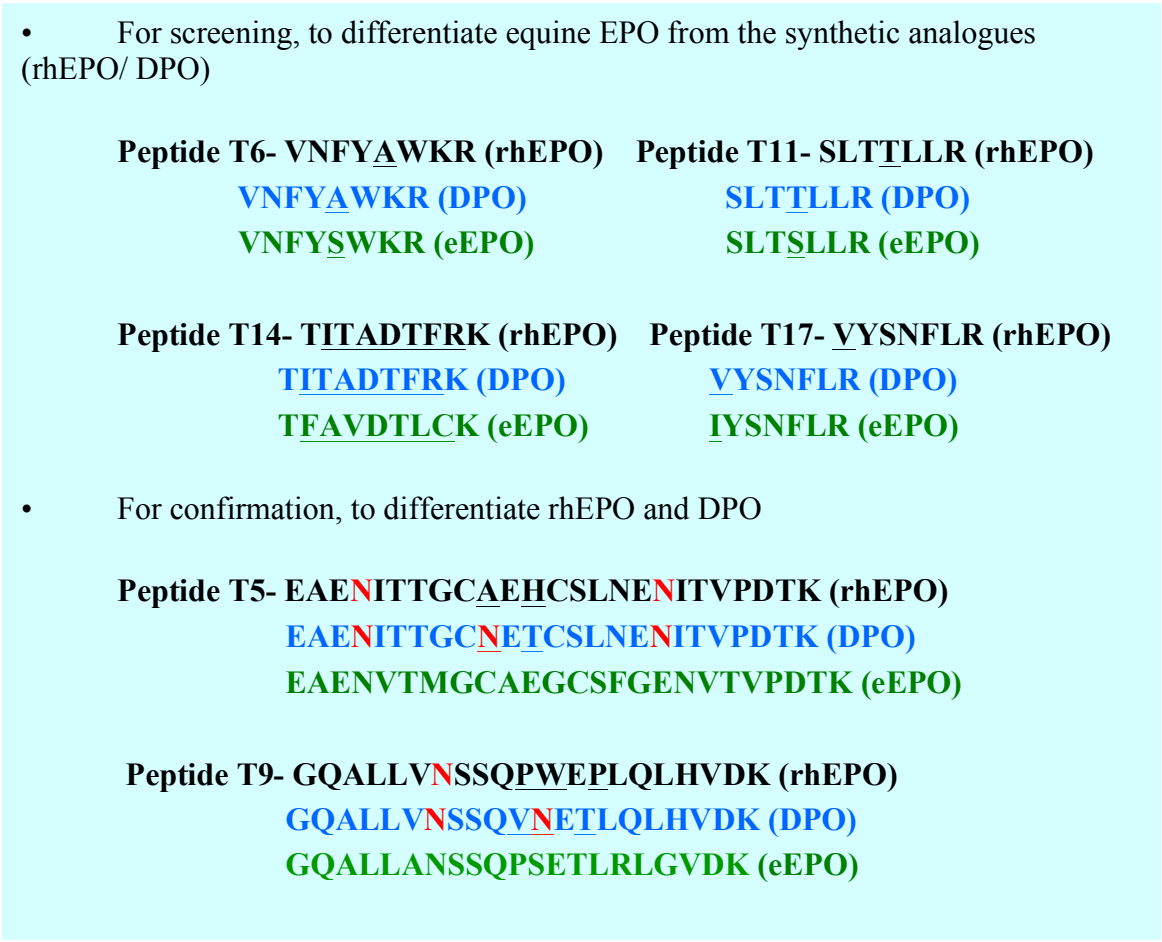

Figure 5.1 The unique tryptic fragment for differentiation of rhEPO and DPO

In this chapter I report on the results obtained using serially connected trypsin and PNGase F reactors that were coupled in an on-line configuration with LC-ESI/MSMS. A monolithic PNGase F enzyme reactor was made. Coupling of the on-line trypsin digestion reactor and PNGase F deglycosylation reactor in series considerably reduced the preparation time and by linking these directly to the mass spectrometer, the sample losses and/or overall potential for contamination with plasticisers and

other chemical noise could be minimised. It was demonstrated in this chapter that both the non-glycosylated peptides and the glycosylated tryptic peptides could be detected within a single analytical run.

5.2 Materials and Instrumentation

5.2.1 Materials.

Sodium hydroxide, polyethylene glycol 10,000 (PEG), sodium bicarbonate, sodium chloride, dimethoxysulfoxide (DMSO), ammonium persulfate (APS), dimethyl sulfoxide (DMSO), ammonium persulfate (APS) were all from Merck (Singapore). Methacryloxypropyltrimethoxysilane (Bind-silane), acrylamide, *N.N'*-methylenebisacrylamide, *N,N,N',N'* tetramethylethylenediamine (TEMED), N-acryloxysuccinimide (NAS) and benzamidine were purchased from Acros Singapore. Peptide-N-glycosidase (PNGase F) 500,000 U/ml was purchased from New England Biolabs and the fused silica capillary 100 µm i.d. were supplied by Polymicro U.S.A. The water used throughout all experiments was Milli-Q Gradient A10 from Millipore (Singapore). Epoetin alfa, Eprex® the recombinant human erythropoietin, 10,000 IU/ ml was purchased from Jassen-Cilag AG, (Schaffhausen, Switzerland). Darbepoetin alfa, Aranesp® 40 µg/ 0.4ml were obtained from Amgen Manufacturing Limited a subsidiary of Amgen Inc. (Thousand Oaks, CA, USA).

5.2.2 Instrumentation. Experiments were undertaken using a Tempo™ nano MDLC by Eksigent, with an Eksigent AS1 Autosampler coupled to the TIS source of an AB Sciex 4000 Qtrap LC-MSMS operated by Analyst 1.5 software. The autosampler has

a 6-port injection valve with a 20 µl injection loop. A 50 µm fused silica capillary was fitted from the injection port and coupled to the trypsin enzyme reactor with a microtight union, where the trypsin enzyme reactor and PNGase F reactor are coupled with a microtight union and placed in the oven at 37 ºC and joined with another union with another 50 µm fused silica capillary connected to the 6-port switching valve, passing through a CAPTRAP™, PEPTIDE (Michrom Bioresources, Inc.). When this switching valve is switched, the pump running an organic solvent gradient, delivers the sample from the CAPTRAP to the 2.7 µm HALO™ C18 0.3 mm i.d. x 150 mm, analytical column and then to the TIS source (Figure 5.2).

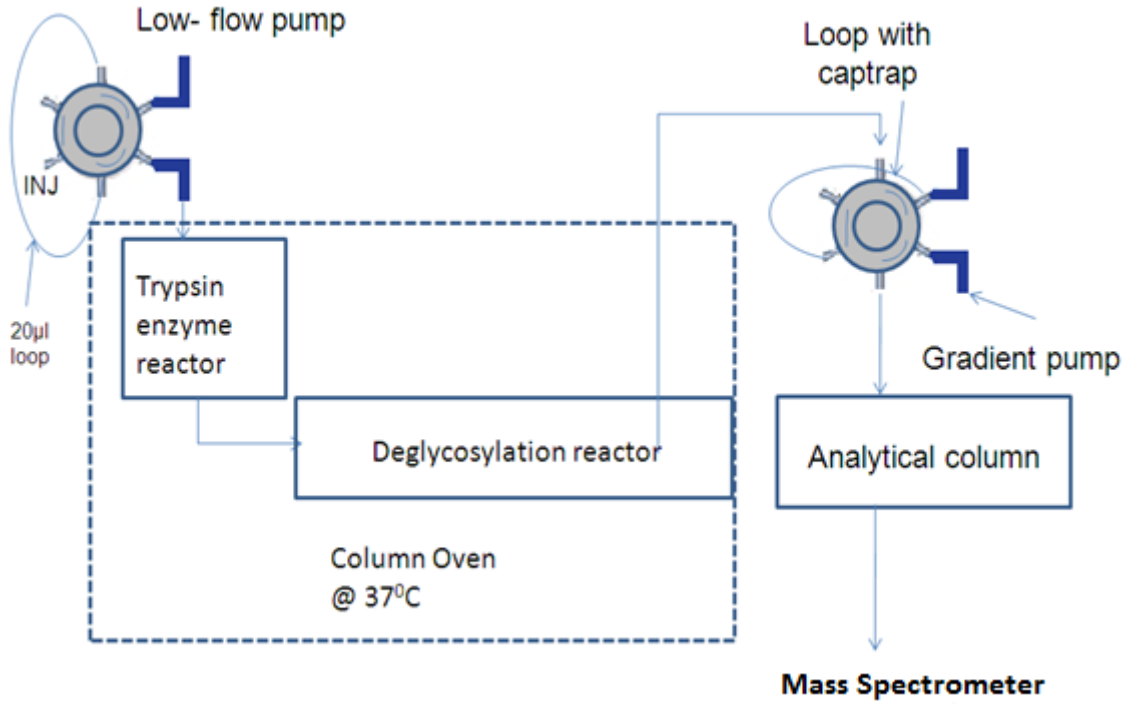

Figure 5.2 Schematic diagram of an on-line set-up with enzyme reactors coupled to LC-MSMS

5.2.3 LC Conditions

5.2.3.1 The column used was a 2.6 µm 100 Å fused core Kinetex C_{18} 50 mm x 2.1 mm i.d.

5.2.3.2 The mobile phase used was (A) 0.15 % FA in water and (B) ACN at a flow rate 4 µl/ min;

5.3.3.3 The initial conditions were 95 % A and 5 % B followed by a linear gradient from 5 % A to 95 % B in 10 min, holding at 95 % B for 5 min, and returning to initial conditions at 16 min and re-equilibrating in preparation for the next injection between 16 and 25 min.

5.2.4 MS Conditions

5.2.4.1 The positive TIS ion source voltage was set at 4500 V, GS 1 at 15 psi, GS 2 at 10 psi, CUR at 30 psi and TEMP at 350 °C.

5.2.5 Preparation of the co-polymerised monolith column

27 cm x 100 µm i.d. fused silica capillaries were pre-treated with 1 M NaOH for 30 min, then flushed with 3 ml of 0.1 M HCl, and finally rinsed with 3 ml water. Thereafter, a 50 % (v/v) Bind-Silane (bifunctional reagent) in acetone was introduced and left inside the column for 40 min at room temp. Finally, the capillary was rinsed with water and acetone, and then dried with N_2 gas. The monolith was prepared by dissolving 20 mg of acrylamide, 30 mg of *N, N'*-methylenebisacrylamide, and 30 mg of PEG per ml of 0.2 M sodium bicarbonate/ 0.5 M sodium chloride (pH~8) buffer.

The mixture was vortexed for a few seconds and heated at 55 – 60 ºC for 15 min to completely dissolve the monomers. To 0.5 ml of this solution, 2 µl of 20 % (v/v) TEMED were added. The mixture was then degassed for 15 min using N_2 gas delivered through fused silica tubing. Next 5 µl of *N*-acryloxysuccinimide (NAS) (140 mg/ml, 828 mM) dissolved in DMSO was added. Since DMSO is of a higher density than the buffer, the NAS was added on top of the solution, while degassing was used to ensure a thorough mixing of the NAS with the solution buffer. After 1 min, 2 µl of 20 % (w/v) ammonium persulfate (APS) was added in order to initiate polymerisation. The APS was dispensed into the middle part of the solution while degassing, to ensure an efficient and rapid mixing. After 30 s, a 2 µl aliquot of this solution was removed and quickly mixed (so as to avoid contact with oxygen) with 1 µl of PNGase F. This mixing step was performed without N_2 degassing. An activated (Bind-Silane) capillary was then inserted into the PNGase F-monomer vial, whereby the solution filled the tubing by capillary action. Immobilisation/ polymerisation were allowed to proceed for 30 min at room temperature with the capillary ends covered with parafilm.

5.2.6 Preparation of samples

10 µl of 84 ng/µl Eprex® was spiked into 100 µl of 50 mM ammonium bicarbonate buffer in an auto sampler vial. This vial was placed on the auto sampler for direct injection into the on-line enzyme microreactors coupled to the analytical column and to the TIS source for detection.

5.3 Results and Discussion

In order to detect the tryptic glycopeptides, a deglycosylation step using the enzyme PNGase F to cleave the N-glycan is necessary to make these protein fragments compatible with LC-MSMS detection. However, the PNGase F enzyme offered by vendors in relatively small quantities at a comparatively high cost and so the high-wastage procedure for coating the dextran modified capillary was too costly to attempt. Thus the monolithic enzyme reactor was the only type prepared for this study and this provided good performance in comparison to the results that were achieved when it was carried out in an in-solution deglycosylation (Figure 5.3), as the peak abundances for deglycosylated peptides obtained in-solution were lower than for the on-line deglycosylation reactors. EPO perfused through the PNGase F reactor were shown to be effectively deglycosylated on a time scale of seconds using low nanogram to microgram per microliter concentration (corresponding to a total sample consumption of 0.1 μg of a glycoprotein).

The trypsin and deglycosylation reactors (held inside an oven at 37 ºC) were coupled to the autosampler and a trap column as shown in Figure 5.2. The first factor that I evaluated was whether positioning the trypsin reactor either before or after the deglycosylation reactor in the flow path, produced any noticeable effect on the detection of the target peptides. Thereafter I tried sandwiching the trypsin reactor between two PNGase F reactors, but rather unexpectedly this orientation produced a 50 % drop in the intensities for both T5DAM and T9DAM (Figure 5.4) when compared to the TRYPSIN➔PNGase F orientation. Lastly I doubled the length of the deglycosylation reactor that was connected after the trypsin reactor and this brought

about a favourable increase in the EICCs intensity for T5DAM and T9DAM (Figure 5.5). Overall these results showed that there was a major difference in the abundance of the glycosylated peptides when using different on-line configurations. For example, T9 DAM shows an EICCs with 10 times lower abundance than when the PNGase F reactor followed the trypsin reactor (Figure 5.6). When two PNGase F reactors are placed after the trypsin reactor, the intensity of T5DAM is doubled to that of when only one PNGase F reactor is used. From this approach, by increasing the length of PNGase F reactor, we could enhance the sensitivity of the deglycosylated peptides. However, this approach can cause a slight decrease in the non-glycosylated peptides. This is still acceptable as the drop is insignificant and importantly, the glycopeptides have much higher sensitivity (almost 10 x) than the traditional in-solution digestion, which greatly helped to identify the rhEPO and DPO in doping.

The reactor enzyme activity was shown to be reproducible (except for EPO T6) and all non-glycosylated and glycosylated peptides have less than 20 % coefficient variation (Figure 5.7). The glycosylated peptides showed a good repeatability of less than 10 % for the orientation when two PNGase F reactors are placed after the trypsin reactor.

These results were promising, as even though it takes an hour (at 1 µl/min flow rate) to pass the sample through the reactors, this is considerably shorter than the two days that it normally takes to complete the off-line sample preparation and it was

also able to get an improvement in the sensitivity for both the non-glycosylated and glycosylated tryptic peptides in the Eprex™ digest.

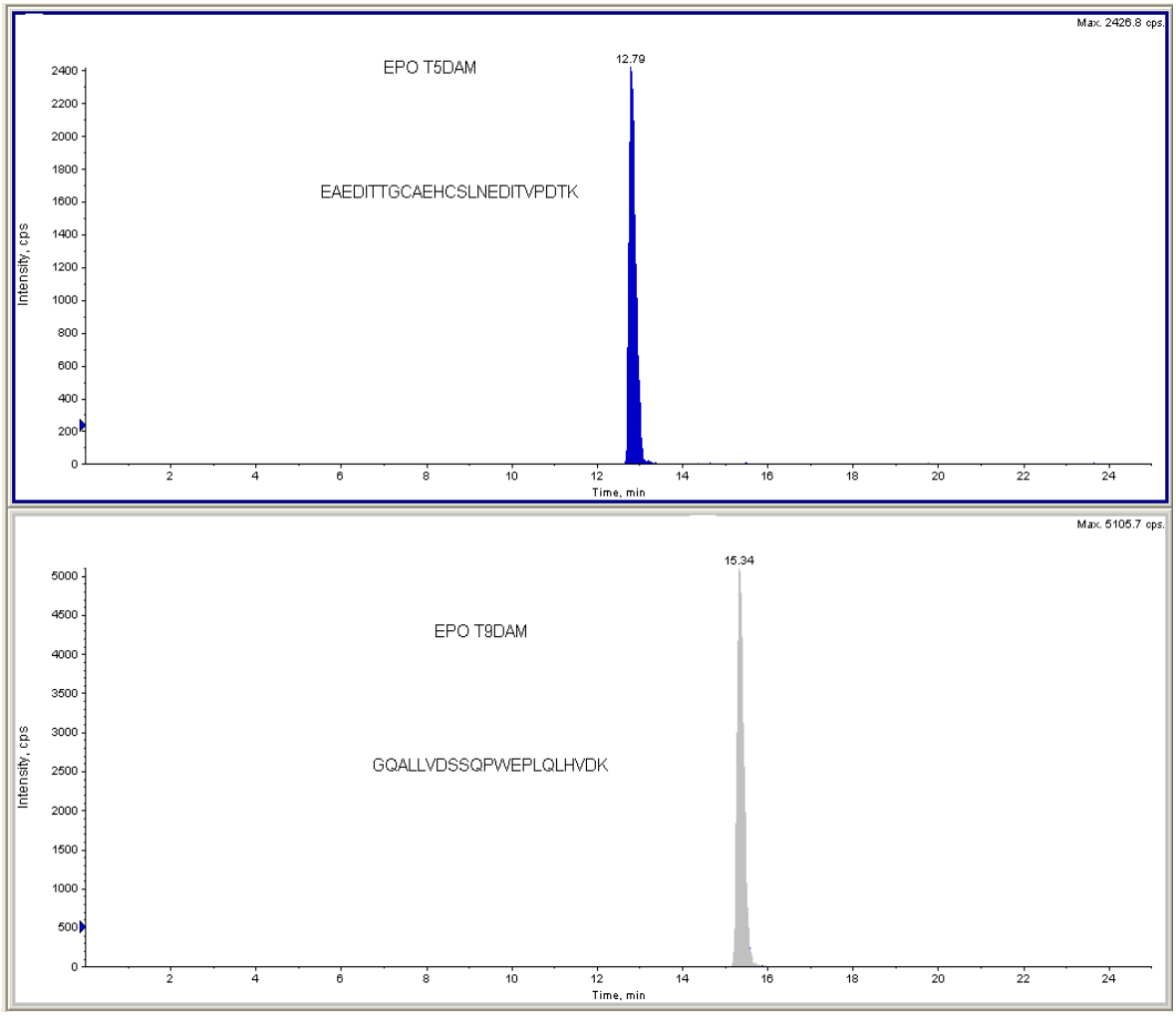

Figure 5.3 Extracted ion chromatogram showing the EPO peptides deglycosylated off-line in-solution digestion

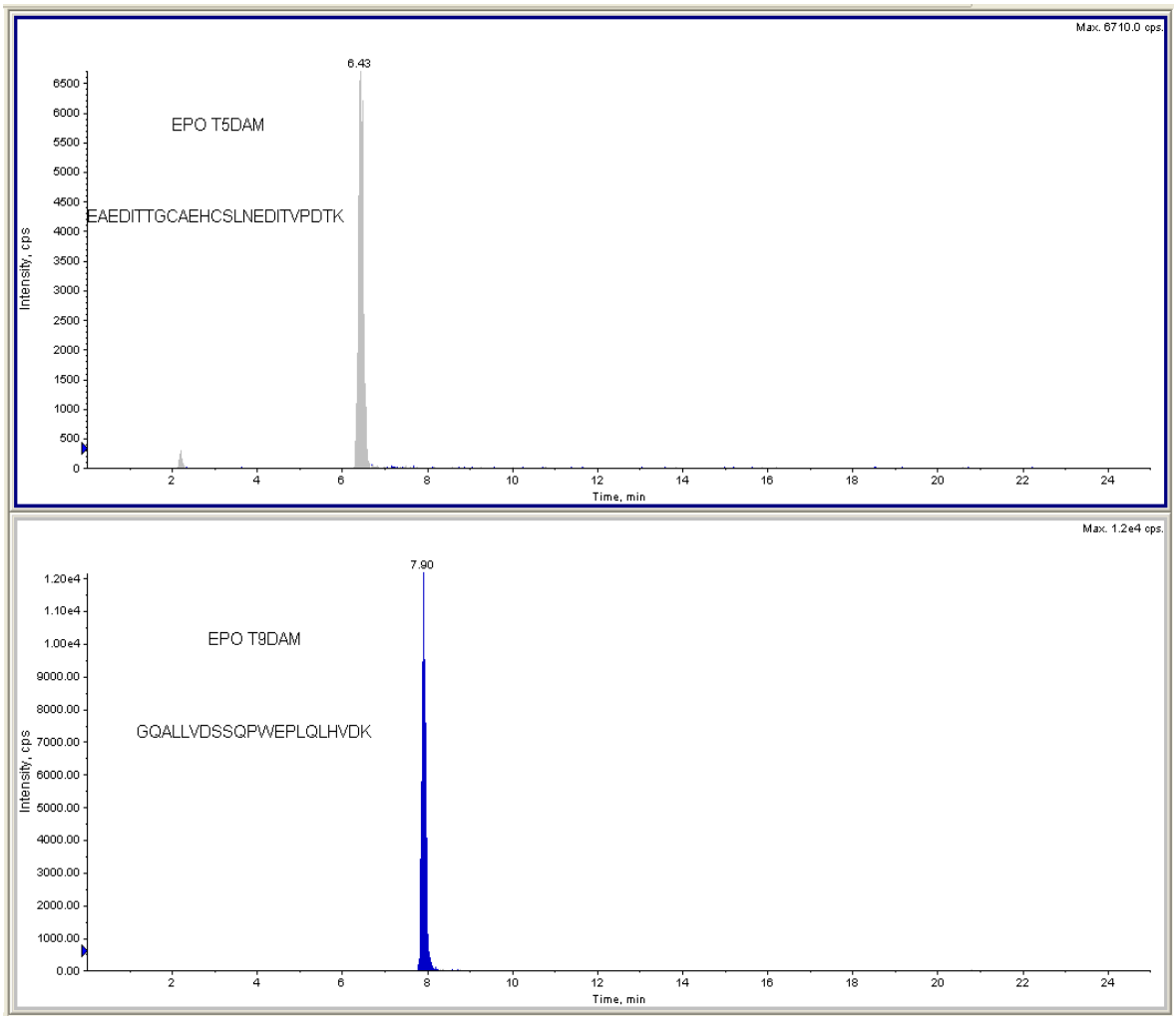

Figure 5.4 Extracted ion chromatogram showing the EPO peptides digested on-line by the orientation of deglycosylation-trypsin-deglycosylation reactors

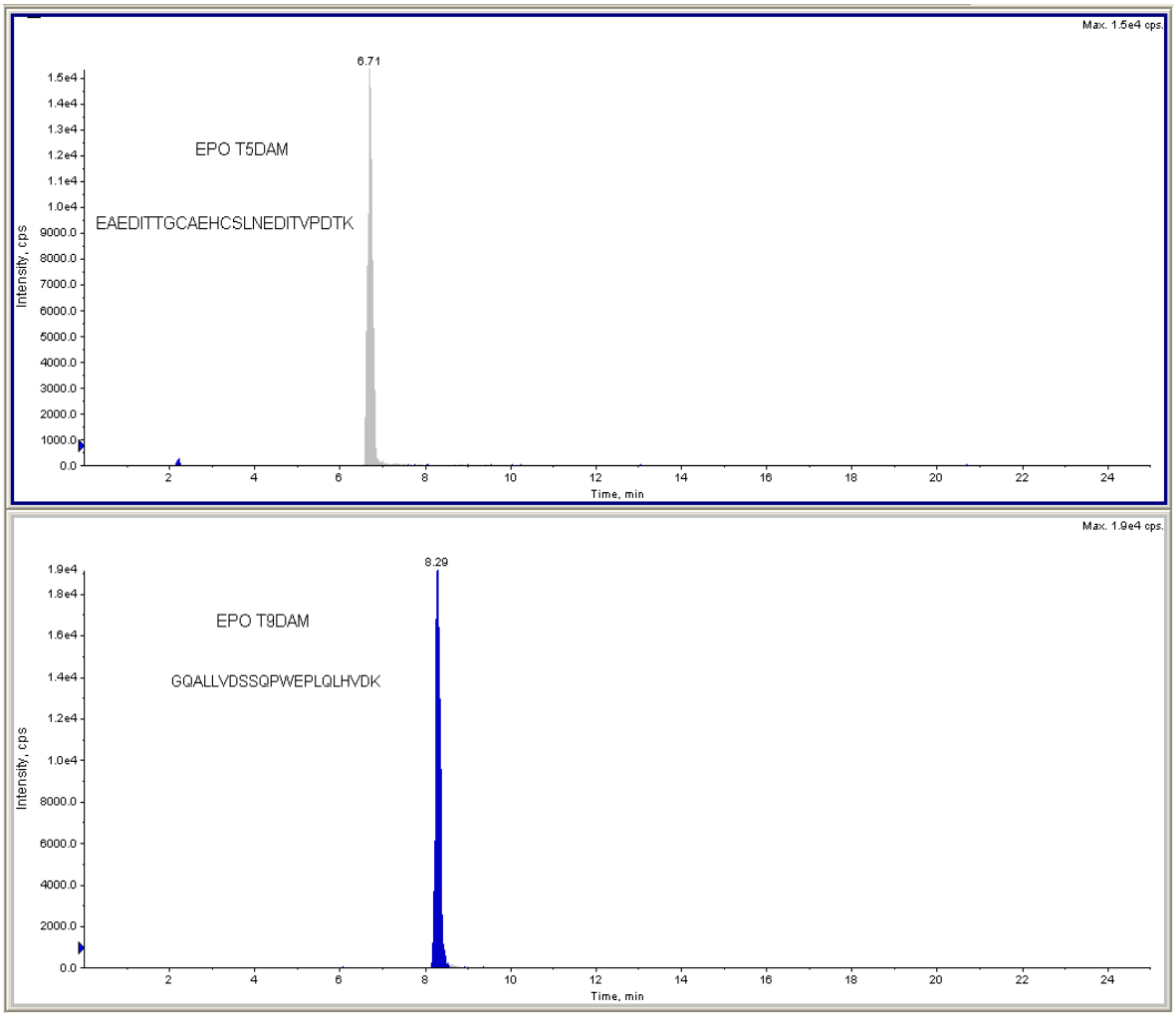

Figure 5.5 Extracted ion chromatogram showing the EPO peptides digested on-line by the orientation of trypsin-deglycosylation-deglycosylation reactors

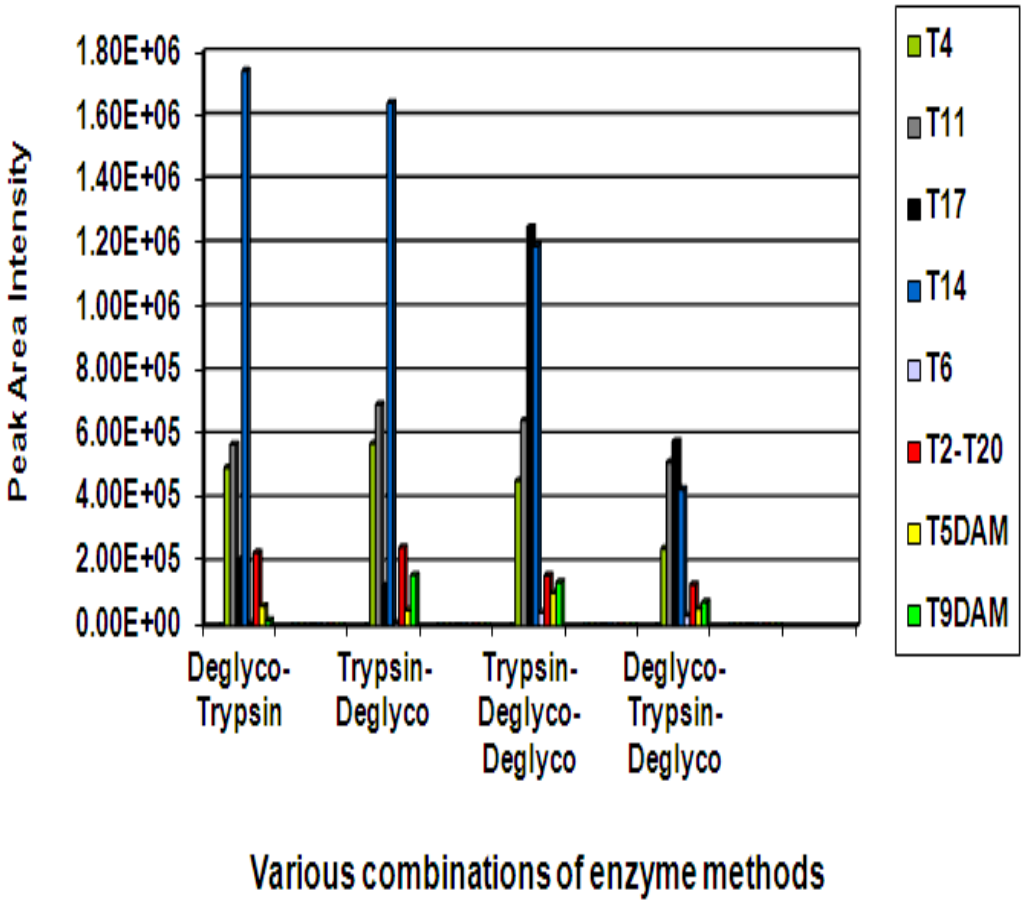

Figure 5.6 Graph summarising the peak area intensity for various orientations of the enzyme reactors

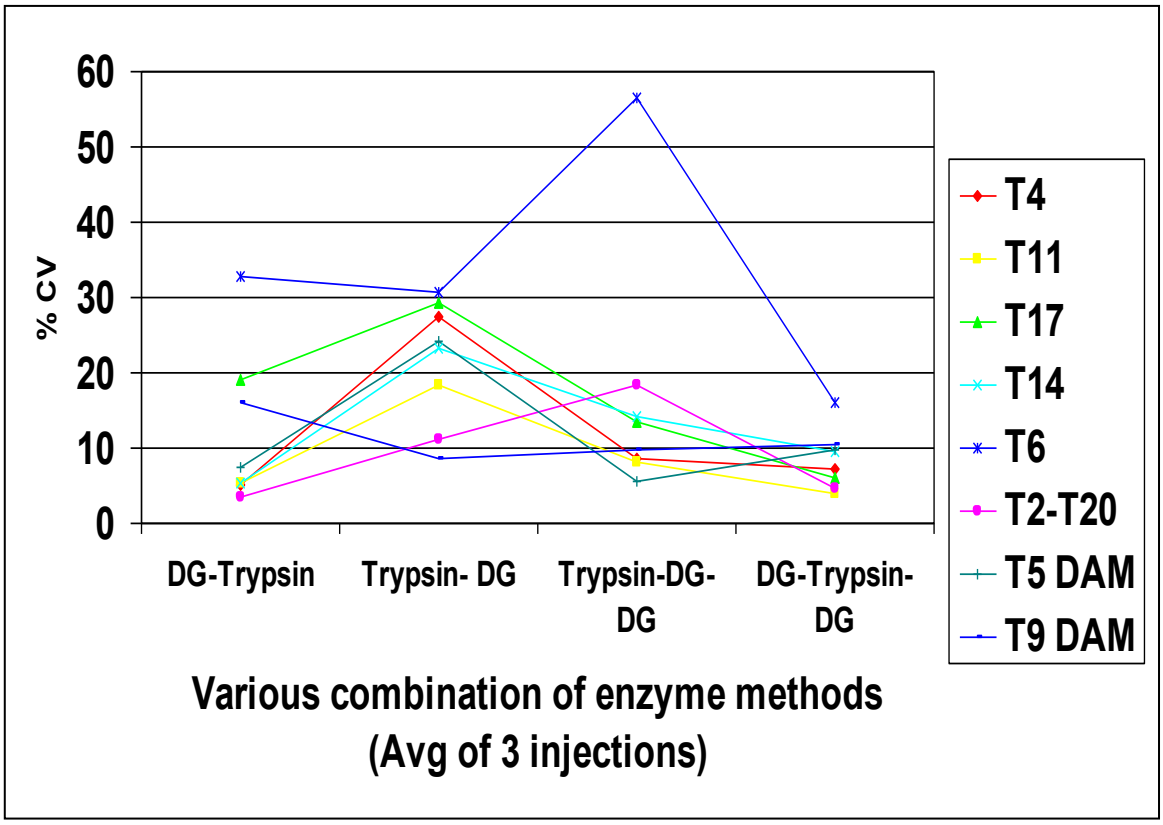

Figure 5.7 Graph showing the reproducibility of the various orientations of enzyme reactors

5.4 Conclusion

I have also demonstrated that the PNGase F enzyme can be successfully coupled to a monolithic column in order to fabricate a deglycosylation reactor and, in combination with the trypsin reactor, was used to detect both the digested non-glycosylated and glycosylated peptides in an on-line digestion/LC-MSMS configuration with good sensitivity and acceptable repeatability. This time saving technique minimises the extent of manual sample handling, which reduces the potential sources of contamination. Future work will look at optimising the loading flow rate during the digestion/deglycosylation/trapping stage in order to reduce the

cycle time between injections and/or multiplexing the analysis to improve the overall throughput of the method.

Chapter 6: Novel monolithic HILIC stationary phase

6.1 Introduction

Peptide screening following a selective enzymatic (*e.g.* trypsin) digestion of susceptible amide bonds in the protein is an important technique for testing for the presence of bio-therapeutics. Reversed-phase (RP) chromatography is frequently used to separate peptides derived in this manner, but hydrophilic peptides are poorly retained under these conditions and consequently valuable information can be lost because early elution renders them highly susceptible to ion-suppression effects in ESI-MS. Ion suppression results from the presence of less volatile compounds that can change the efficiency of droplet formation or droplet evaporation, which in turn affects the amount of charged ion in the gas phase that ultimately reaches the detector. Thus, in this work, I demonstrate the suitability of using HILIC chromatography as a complementary approach to RP by analyzing peptides produced by tryptic digestion of the glycoproteins rhEPO and DPO. HILIC is an orthogonal approach to RP [128, 136, 141, 188] and this work demonstrates the benefits gained by using a low aqueous content mobile phase to increase sensitivity in ESI-MS [134,143]. This separation mode has also been used for the enrichment of PTMs such as glycosylation [135], N-acetylation [137] and phosphorylation [138] in proteomics applications.

Hydrophilic interaction chromatographic (HILIC) has become increasingly popular in separation science due to its complementary selectivity to reversed-phase liquid chromatography (RPLC), and the fact that it also has good compatibility with LC-MS and 2D LC [128].

HILIC is characterized by the use of a hydrophilic stationary phase and a relatively hydrophobic mobile phase containing a high percentage of a water miscible organic solvent [189]. The order of elution is usually reversed relative to RP chromatography, with hydrophilic compounds being retained on the packing material for a longer period than hydrophobic compounds. This occurs because the HILIC stationary phase becomes enriched with water and thus polar analytes partition preferentially into this thin hydrophilic layer from the more hydrophobic mobile phase environment [128]. It makes use of polar stationary phases in combination with apolar aqueous, typically acetonitrile-rich eluents, and allows retention of hydrophilic solutes through interactions with polar functionalities and/ or partitioning into an absorbed water layer.

When using gradient HILIC [128, 134, 141 and 143] the analytes retained on the stationary phase are eluted by lowering the hydrophobicity of the mobile phase and this is accomplished by simply increasing the water content. In most cases elution occurs before the mobile phase contains 30 % water [128]. The conditions required for elution of a specific compound are dependent on the type of stationary phase used as well as the mobile phase composition, including the percentage and type of organic solvent, the type and concentration of salts and also the pH [143].

The polar zwitterionic monolith provides an environment that is not only capable of hydrophilic interaction with polar and charged analytes but also offers the opportunity for weak electrostatic interaction with analytes carrying either positive or negative charges to occur [190]. Whilst increasing the hydrophilicity of the monolith would enhance HILIC interactions, this type of polymers can be affected by shrinkage in

water and swelling in organic solvents and this is related to the lack of or the inhomogeneity of the crosslinking [191]. The resulting instability of the chromatographic support as the eluent composition changes leads to reduced column efficiency and a loss of resolution [192-193]. Therefore, to counteract this problem, a highly crosslinked polymer with good homogeneity is preferred.

A previous study [194-196] described the use of the monomer BVPE, which has a spacer between aromatic rings that allows both vinyl groups to retain the same reactivity to free radical polymerisation, that yields a homogeneous highly crosslinked polymer in a short polymerisation time. The resulting monoliths also had significant proportions of both mesopores and macropores and this allowed for the rapid and high resolution separation of low molecular weight compounds, as well as larger biomolecules, on the same monolithic support. Furthermore, the high fraction of flow-channels provided enhanced column permeability and lower backpressure.

According to Van Deemter *et al*. [197], column efficiency (height equivalent to a theoretical plate HETP) is directly proportional to the particle diameter of the stationary phase. Therefore, a good monolith should exhibit a good (bimodal) pore-size-distribution of macropores (>75 μm) and mesopores (2-50 nm). By employing an approach introduced by Trojer *et al*. [198], which uses polymerisation time as a polymerisation parameter for tailoring the porous properties of organic monoliths [196], I used different polymerisation times to evaluate the effect that this would have on the efficiency of HILIC monolith column prepared by thermal-initiated co-polymerisation of SPE-*co*-BVPE inside a 200-μm-i.d. fused silica capillary. The

composition of the polymerisation mixture was optimised in order to obtain satisfactory performance for column permeability, efficiency, and separation. The optimised monolithic column was evaluated for the separation of neutral, acid and basic analytes in a HILIC mode. The variations of organic solvent content on separation have been investigated. To date, only a few papers have reported on the fabrication of HILIC monoliths and this is the first to report the formation of such a product by the co-polymerisation of SPE and BVPE.

In this chapter, I have also reported on the synthesis of a monolithic co-polymer using DMBVBS, which is a novel organosilane cross-linker [191] synthesized using the Grignard Reaction. BVPE, the cross-linker used in our previous publication [199], is a solid that only dissolves in the porogen monomer mixture at elevated temperature and so pre-heating of the equipment prior to polymerisation is vital to avoid precipitation. However, it is difficult to distribute the heat uniformly and so the temperature fluctuations that inevitably occur when filling the capillary can lead to the production of inconsistent monolithic columns. Whereas DMBVBS is readily soluble in the SPE/porogen mixture at room temperature and this makes it much easier to handle [194, 200-201]. The DMBVBS/SPE combination was co-polymerised within the confines of 200 μm ID fused silica capillaries to produce a monolithic column with better resolution than was achieved with (BVPE cross-linked) formulation. The column yielded good peak shapes with narrow peak width at half height and satisfactory resolution of the rhEPO and DPO derived tryptic peptides that were targeted using ESI-MSMS in the selected reaction monitoring mode.

6.2 Materials and Instrumentation

6.2.1 Materials.

The monomer SPE was a kind gift of Raschig GmBH (Ludwigshafen, Germany). Magnesium ribbon, tetrahydrofuran (THF) inhibitor-free, azobisisobutyronitrile (AIBN), toluene, thiourea, acrylamide, acenapthalene, thymine, adenine, cytosine, uridine, cytidine were all purchased from Aldrich Chemical (Poole, UK). 3-(trimethoxysilyl)-propyl methacrylate (γ-MAPS), ammonium acetate were obtained from BDH Laboratory Supplies (Poole, UK). *p*-vinylbenzyl chloride, uracil and ammonium formate were purchased from Fluka (UK). HPLC-grade methanol and acetonitrile (ACN) were obtained from Fisher Scientific (Leicestershire, UK). The water used throughout all experiments was from Millipore synergy UV (UK). The fused silica capillary with a dimension of 200 μm i.d. (350 μm o.d.) was purchased from Composite Metal Services Ltd. (Hallow, Worcestershire, UK).

The monomer *N*, *N'*-dimethyl-*N*-methacryloxyethyl-*N*-(3-sulfopropyl) ammonium betaine (SPE), 3-(trimethoxysilyl)-propyl methacrylate (γ-MAPS), sodium chloride (brine solution), sodium bicarbonate ($NaHCO_3$), anhydrous sodium sulfate (Na_2SO_4), diethyl ether, petroleum ether and ammonium acetate were purchased from Merck (Singapore). Magnesium ribbon, tetrahydrofuran (THF) inhibitor-free, azobisisobutyronitrile (AIBN), *p*-vinylbenzyl chloride, dichlorodimethylsilane (DCDMS), DL-dithiothreitol (DTT) and ammonium formate were all purchased from Sigma Aldrich (Singapore). HPLC-grade methanol, toluene and acetonitrile (ACN) were obtained from Fisher Scientific (Singapore). Sequencing grade modified Trypsin (P/N No. V5111) and protein deglycosylation mix kit were purchased from

Promega (Singapore). The water used throughout all experiments was Milli-Q Gradient A10 from Millipore (Singapore). The fused silica capillary with a dimension of 200 µm i.d. (350 µm o.d.) was purchased from Polymicro (USA). Epoetin alfa, Eprex® the recombinant human erythropoietin, 10,000 IU/ ml with a concentration of 84 µg/ ml was purchased from Jassen-Cilag AG, (Schaffhausen, Switzerland). Darbepoetin alfa, Aranesp® 40 µg/ 0.4ml was obtained from Amgen Manufacturing Limited a subsidiary of Amgen Inc. (Thousand Oaks, CA, USA). Human EPO 1 mg/ ml protein was purchased from Genway Biotech, Inc. (San Diego, CA, USA). Peptide SLTTLLR (human EPO peptide T11), peptide TITADTFR (human EPO peptide T14) and peptide VYSNFLR (human EPO peptide T17) were synthesised by Auspep Pty. Ltd. (Tullamarine, Victoria, Australia). C18 Zip-Tip® was obtained from Millipore Corporation (Billerica, MA, USA). Nanosep 30 KDa OMEGA was obtained from PALL Corporation (USA).

6.2.2 Instrumentation.

Experiments for *poly* (SPE-*co*-BVPE) were undertaken with a laboratory-built HPLC system that comprised an Applied Biosystems 783A programmable absorbance detector (Ramsey), a four-port injection valve with a 100 nl internal loop from Valco (Houston, TA), and a DINA binary pump with software version 1.29 (KYA Technologies Corporation) was used to run both isocratic and gradient conditions. Detection wavelength was set at 214 nm for the standard test mix 1 and 254 nm was set for test mix 2. A Data Apex chromatographic Clarity data station (Aston Scientific Ltd., Bucks, UK) was used for data acquisition and data handling. Chromatograms were converted to an ASCII file and exported as notepad and redrawn using Microsoft excel.

Experiments for both HILIC monoliths were undertaken using a Tempo^{TM} nano MDLC by Eksigent, with an Eksigent AS1 Autosampler coupled to a TIS of AB Sciex 4000 Qtrap LC-MSMS operated by Analyst 1.5 software. The autosampler has a 6-port injection valve with a 20 µl injection loop. The 200 µm x 30 cm capillary filled with the monolith was coupled directly between the injection port and the TIS using a short length of 50 µm deactivated silica capillary.

6.2.3 LC conditions for SPE-co-BVPE

6.2.3.1 The mobile phase used for the standard test mix and base test mix was (A) 5mM Ammonium formate pH 3 and (B) ACN at a flow rate 4000 nl/min. It was run at isocratic condition 5 % A and 95 % B.

6.2.3.2 The mobile phase used for the separation of pyrimidines and purines was (A) a pre-mix buffer of 95 % ACN and 5 % of 10 mM ammonium acetate at pH 8.6 and (B) a pre-mix buffer of 50 % ACN, 45 % water and 5 % of 10 mM ammonium acetate at pH 8.6, which run with a flow rate 4000 nl/min. The initial condition at 100 % A was held for 6 min, this was modified on a linear gradient to 100 % B at 9 min and hold for 3 min. At 13 min, it was returned to 100 % A and re-equilibrated till the run ends at 20 min.

6.2.3.3 The mobile phase used for the separation of EPO peptides was (A) 10 mM ammonium acetate at pH 8.6 and (B) ACN at a flow rate 5 µl/min. The initial condition was 5 % A and 95 % B, it was changed on a linear gradient to 95 % A and 5 % B at 15 min. After holding at 5:95 for 5 min., the composition was returned to initial conditions over 60 seconds. The column was re-equilibrated in preparation for the next injection between 21 and 30 min.

6.2.4 Reversed- Phase LC Conditions

6.2.4.1 The column used was a HALO^{TM} C18 0.3 x 150 mm packed with 2.7 µm Fused Core particles;

6.2.4.2 The mobile phase used was (A) 0.1 % formic acid in water and (B) ACN at a flow rate 4 µl/min.;

6.2.4.3 The initial conditions were 95 % A and 5 % B and this was modified on a linear gradient to 5 % A and 95 % B at 10 min. After holding at 5:95 for 5 min. the composition was returned to initial conditions over 60 seconds. The column was re-equilibrated in preparation for the next injection between 11 and 20 min.

6.2.5 Five minute HILIC gradient LC

6.2.5.1 The mobile phase used was (A) 0.1 % formic acid in water and (B) ACN at a combined flow rate of 4 µl/min.;

6.2.5.2 The composition at the start was 5 % A and 95 % B and was changed on a linear gradient to 95 % A and 5 % B at 5 min. These conditions were held for 5 minutes before returning to initial conditions over 60 seconds. The column was re-equilibrated in preparation for the next injection between 11 and 20 min.

6.2.6 Ten minute HILIC gradient LC

6.2.6.1 The mobile phase used was (A) 0.1% formic acid in water and (B) ACN at a combined flow rate of 4 µl/min.;

6.2.6.2 The composition at the start was 5 % A and 95 % B and was changed on a linear gradient to 95 % A and 5 % B at 10 min. These conditions were held for 5 min. before returning to initial conditions over 60 seconds. The column was re-equilibrated in preparation for the next injection between 16 and 25 min.

6.2.7 Preparation of 1, 2-bis (*p*-vinylphenyl) ethane (BVPE).

BVPE synthesis was accomplished by a Grignard dimerisation of *p*-vinylbenzyl chloride (Figure 6.1). A detailed protocol of the preparation of BVPE is described in [134, 150, 184]. BVPE was re-crystallised from methanol to further increase the purity of the product. The purity of the product was checked and confirmed by GC-MS.

6.2.8 Preparation of *poly* (SPE-*co*-BVPE) monoliths.

In order to provide anchoring sites for the polymer, each capillary was treated with γ -MAPS, a bifunctional reagent, prior to polymerisation using a method described elsewhere [145]. 50 mg of SPE and 50 mg of BVPE were weighed into a 1.5 ml screw-cap vial, and then 220 µl of methanol and 180 µl of toluene were added and mixed in an ultrasonic bath at 40 ºC for 15-20 min. When completely dissolved 5 mg of AIBN was then added and completely dissolved. Nitrogen was bubbled into the mixture for 5 min to remove the dissolved gases. The polymerisation mixture was introduced into a pre-heated silanised fused silica capillary which was immersed in the ultrasonic bath operating at 40 ºC. Both the polymerisation mixture and capillary have to be kept warm at all times, as the polymerisation mixture quickly precipitates if it is not warm when filling the mixture, which could result in it precipitating in the capillary. After the capillary was completely filled with the polymerisation mixture, both ends of the capillary were sealed with GC septa, and the capillary was kept in a water bath at 75 ºC for 2 hr. (reaction as in Figure 6.2). The capillary column was then rinsed with methanol to remove the porogenic solvents and any other unreacted soluble compounds. A 2-3 mm detection window was created at a distance of 5 cm

from the end of the column using a thermal wire stripper. Monolithic material at this point was pyrolysed and then flushed out with methanol. The resulting capillary column has an effective length of 27.5 cm. A 0.5 cm length of the capillary containing monolith inside was cut for scanning electron microscopy (SEM) analysis (JEOL JSM-5600 LV, Tokyo, Japan).

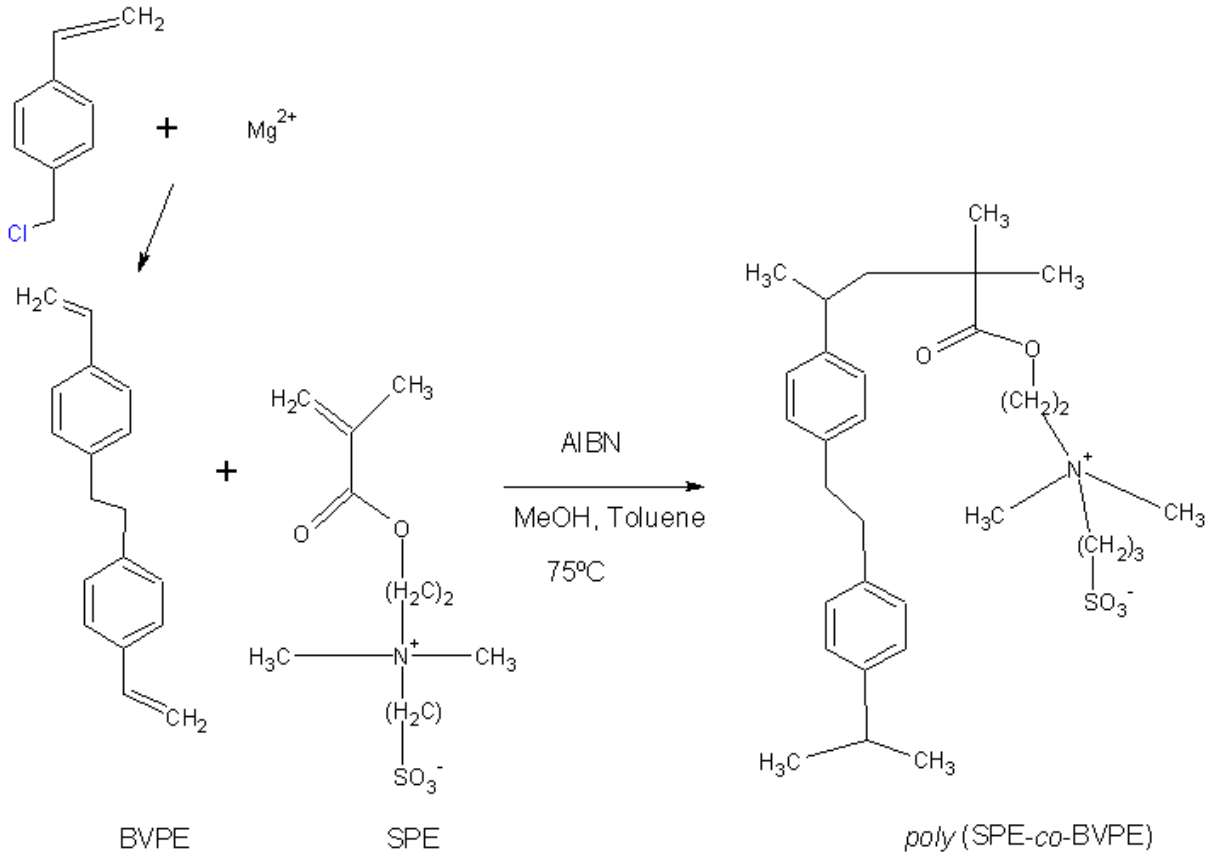

Figure 6.1 Schematic drawing for the synthesis of cross-linker BVPE by Grignard reaction of p-vinylbenzyl chloride, and the subsequent copolymerisation with SPE

6.2.9 Preparation of dimethyl bis (*p*-vinylbenzyl)silane (DMBVBS).

DMBVBS was synthesised by the Grignard Reaction of *p*-vinylbenzyl chloride and dichlorodimethylsilane (Figure 6.2). Magnesium ribbon (7.3 g, 0.12 mol) and 200 ml

THF were placed in a schlenck tube under argon. After addition of dichlorodimethylsilane (12 ml; 0.04 mol) and p-vinylbenzyl chloride (28.2 ml; 0.08 mol) the mixture was carefully stirred with a magnetic stirrer to initiate the Grignard reaction. Thereafter, the solution was sonicated for 2 h, and then washed consecutively with brine, saturated $NaHCO_3$, brine and finally dried over anhydrous Na_2SO_4. After evaporation of the organic solvent, the resulting crude product was purified by flash column chromatography (petroleum ether/ diethyl ether 95: 5) to yield DMBVBS as a viscous colorless product. This synthesis followed exactly the method as published in ref. [187]. The purity of the product was checked and confirmed by proton and carbon NMR spectroscopy [187].

6.2.10 Preparation of *poly* (SPE-*co*-DMBVBS) monoliths.

In order to provide anchoring sites for the polymer, prior to polymerisation each capillary was treated with γ-MAPS, a bifunctional reagent, using a method described elsewhere [202]. 50 mg of SPE and 50 mg of DMBVBS were weighed into a 1.5 ml screw-cap vial, and then 220 µl of methanol and 160 µl of toluene were added and mixed by vortexing. When the mixtures are completely dissolved, 5 mg of AIBN was added, then vortexed to completely dissolve the mixture. Nitrogen was bubbled into the mixture for 5 min to remove the dissolved gases. Next, the polymerisation mixture was introduced into the silanised fused silica capillary. After the capillary was completely filled, both ends were sealed with GC septa, and the capillary placed in a water bath at 75 ºC for 2 hr (reaction as in Figure 6.2). The capillary column was then rinsed with methanol to remove the porogenic solvents and any other unreacted soluble compounds. The resulting capillary column has an effective length of 30 cm.

A 0.5 cm length of capillary containing monolith inside was cut for SEM analysis (JEOL JSM-5600 LV, Tokyo, Japan).

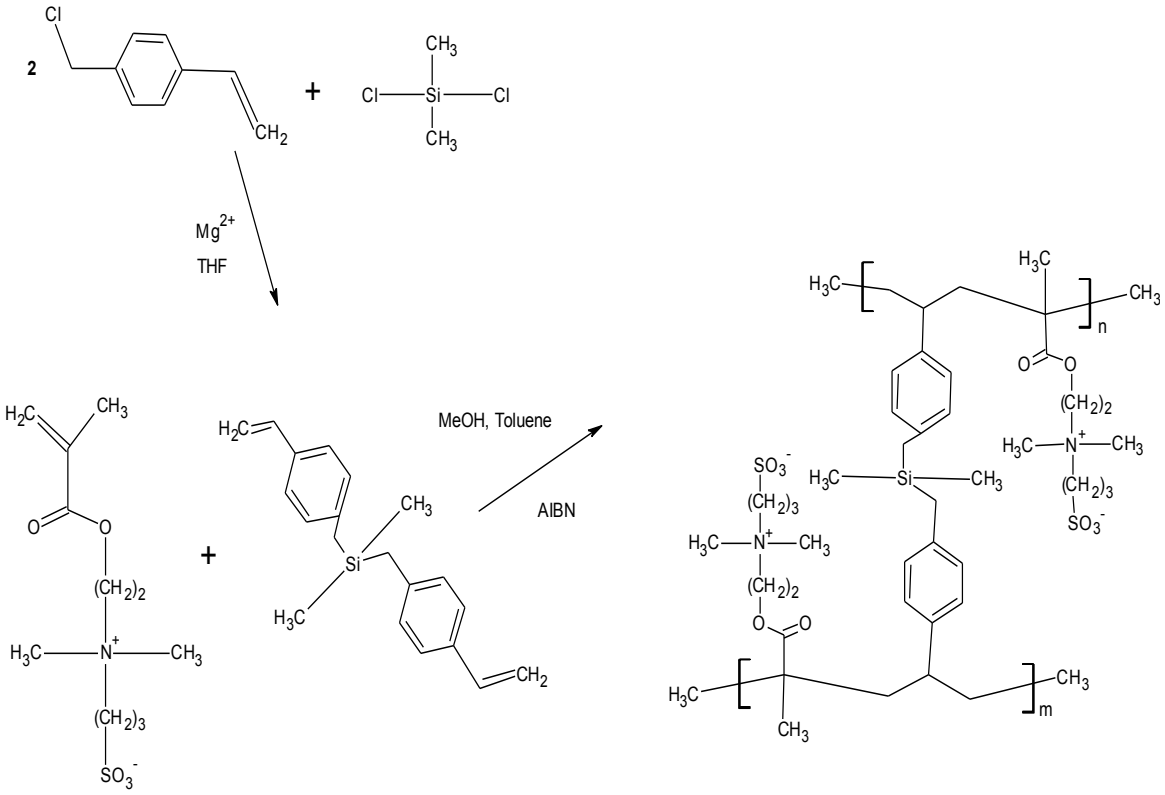

Figure 6.2 Schematic drawing for the synthesis of cross-linker DMBVBS by Grignard reaction of p-vinylbenzyl chloride and dichlorodimethylsilane, and the subsequent copolymerisation with SPE

6.2.11 Preparation of test mix and base mix samples.

The standard test mix of toluene, thiourea and acrylamide were prepared in 1 mg/ml in 100 % ACN. The base mix of uracil, adenine and cytosine were prepared in 1 mg/ml in 70 % H_2O and 30 % ACN. The pyrimidines and purines were prepared in 2 mg/ml in a separate mix, for mix 1 consisting of acenapthalene, uridine, cytidine, cytosine and thymine were prepared in 70 % ACN and 30 % H_2O, whereas the mix 2

consisting of uracil and adenine were prepared in 70 % H_2O and 30 % ACN. Then prepare 1 mg/ml of the two mixes by taking 1 ml from each mix.

6.2.12 Preparation of peptide samples.

EPO peptide standard mix, VWQGLALLSE (EPO peptide E9), AISPPDAASAAPLRTITAD (EPO peptide E12), APPRLTCDSRVLERYLLEAKEAE (EPO peptide E10) and AEDITTGCAEHCSLNE (EPO peptide E5DAM) were prepared at a concentration of 100 ng, except for EPO E5DAM at a concentration of 1000 ng each in their initial buffer condition (95 % ACN and 5 % 10 mM ammonium acetate). EPO peptide standard mix, SLTTLLR (EPO peptide T11), TITADTFR (EPO peptide T14) and VYSNFLR (EPO peptide T17) were prepared at a concentration of 10 ng each in their initial running buffer conditions (HILIC - 95 % ACN, 5 % 0.1 % FA in water and for the C18 reversed-phase- 5 % ACN, 95 % 0.1 % FA in water). The deglycosylated and trypsin digested Epoetin alfa (Eprex®) and darbepoetin alfa (Aranesp®) were prepared as follows: 10 ng of Eprex® and 40 ng of Aranesp® were each spiked into 50 mM ammonium bicarbonate pH 7.8 buffer. The respective spiked samples were processed by taking 50 µl of each sample and placing them in eppendoff tubes, then adding 5 µl of 100 mM DTT in 50 mM ammonium bicarbonate as reducing agent. They were then left at room temperature for 10 min. After 10 min, deglycosylation steps were carried out for all samples. Deglycosylation was carried out by adding 5 µl of 10 x deglycosylation reaction buffers and 5 µl of Protein Deglycosylation Mix from the Promega protein deglycosylation kit. Samples were then gently vortexed and centrifuged at 3000 rpm to allow the sample to collect at the bottom of the tube. Samples were then incubated in the oven at 37 ºC for 16 hr. After the deglycosylation step, the samples were each transferred onto the 30 KDa

nanosep filter, then centrifuged at 3000 rpm for 10 min. 100 µl of 50 mM ammonium bicarbonate was added onto the 30 KDa nanosep filter and centrifuged at 3000 rpm for 20 min and then this step was repeated. After repeating the buffer exchange, it was followed by the trypsin digestion step. 5 µl of (20 µg per 100 µl) of trypsin enzyme was added and incubated in the oven at 37 ºC for 3 hrs. After the trypsin enzyme digestion step, the sample was desalted using a C18 Zip-Tip™ following the manufacturer's protocol. The tip was first conditioned with 0.15 % FA in water, then ACN, followed by loading of the sample. After loading, the sample was washed with the aqueous buffer and the sample eluted with the 95 % ACN and 5 % aqueous buffer. 20 µl of this eluent was injected onto the synthesised monolithic HILIC column.

6.3 Results and Discussion

According to Greiderer *et al.* [191], shorter polymerisation times for BVPE crosslinked co-polymers leads to more space within the polymer clusters (lower polymer density) with the flow channels that are larger and, consequently, the total porosity is enhanced. For this reason, a study was undertaken at different polymerisation times (1, 2, 4, 8 and 12 h) to determine the optimal time for producing this monolithic support. The results I obtained have supported Greiderer's observation and, for example, the SEM photographs show that the polymer clusters that are formed become bigger as the polymerisation time increases. After 1, 2 and 4 h polymerisation time, it can be seen (Figures 6.3a, b and c respectively) that the polymer cluster consists of smaller polymer microglobules compared to that from the 8 and 12 h polymerisation times (Figure 6.3d and e). Since mesoporosity can be regarded as a function of the microglobule size, the smaller they are the higher the

fraction of mesopores is expected. It can be observed from the SEM images that the fraction of mesopores and thus specific surface area is optimised when the polymerisation time is reduced.

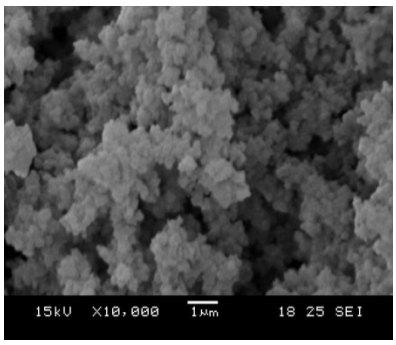

a.

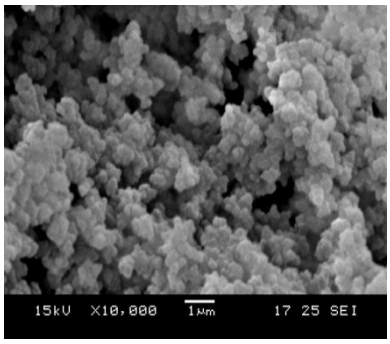

b.

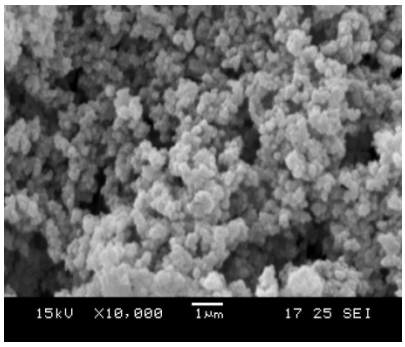

c.

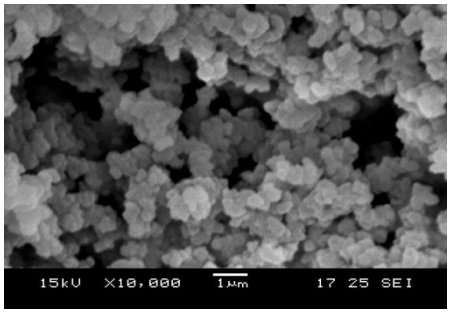

d.

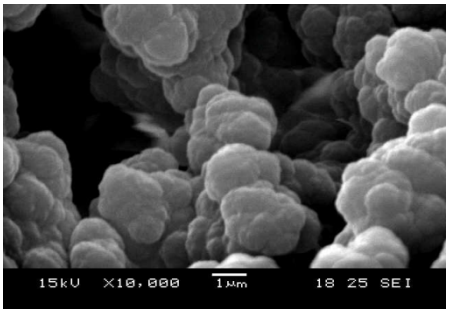

e.

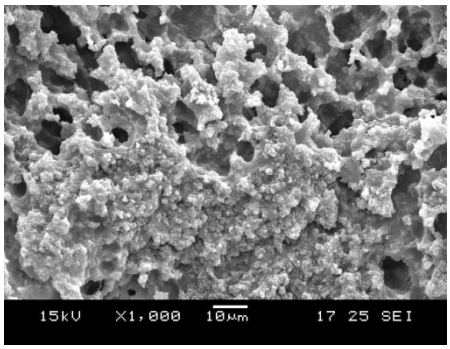

f.

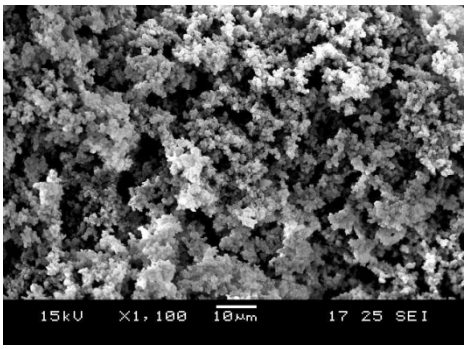

g.

Figure 6.3 SEM images of monolithic columns prepared at different polymerisation times (a- 1 h, b- 2 h, c- 4 h, d- 8 h, e- 12 h) and different AIBN (f- 1 mg, g- 5 mg)

The five capillary columns obtained from the different polymerisation times were installed on the HPLC system and the pressure of each column was recorded (Table 6.1) with the mobile phase (95 % ACN: 5 mM ammonium formate pH 3) at a flow rate of 5000 nl/min and it is evident from this data that the backpressure due to the capillary column increases with increasing polymerisation time.

Polymerisation time	Sample	Retention time (min.)	Efficiency (theoretical plates)	Backpressure (psi)
1 h	Acrylamide	1.250	1610	580
	Toluene	1.340	1065	
	Thiourea	2.733	1231	
	Uracil	1.820	1206	
	Adenine	2.160	931	
	Cytosine	2.787	976	
2 h	Acrylamide	1.740	7702	1885
	Toluene	1.827	7394	
	Thiourea	3.943	9889	
	Uracil	2.540	4759	
	Adenine	3.037	3184	
	Cytosine	3.843	3983	

Polymerisation time	Sample	Retention time	Efficiency (theoretical plates)	Backpressure (psi)
4 h	Acrylamide	1.727	929	2074
	Toluene			
	Thiourea	3.837	734	
	Uracil	2.407	889	
	Adenine	2.80	630	
	Cytosine	3.617	627	
8 h	Acrylamide	1.900	500	2784
	Toluene			
	Thiourea	4.053	989	
	Uracil	2.633	1186	
	Adenine	3.093	784	
	Cytosine	3.930	1940	
12 h	Acrylamide	1.533	1241	3074
	Toluene			
	Thiourea	3.543	1280	
	Uracil	2.220	875	
	Adenine	2.703	421	
	Cytosine	3.507	589	

Table 6.1 Comparison of the column efficiencies and back pressures for the different polymerisation time of the columns

The column efficiencies of the five capillary columns at different polymerisation times were measured using test mix 1 consisting of toluene, acrylamide and thiourea (Table 6.1). It can be seen that a 2 h polymerisation time has the best column efficiencies. Triplicate injections were undertaken using test mix 1 (toluene, acrylamide and thiourea) followed by a second test mix containing the basic compounds (uracil, adenine and cytosine). The columns produced by polymerisation times above 4 h generated poor peak shapes, decreased resolution and lower peak intensity. For example, toluene and acrylamide in the first test mix were merged into a single peak and the base test mix showed poor peak shape for the 3 bases with a low intensity and a resolution of < 1.5.

The best results were obtained with the column produced with a 2 h polymerisation step. For example, the resolution between uracil and adenine and acrylamide and toluene is twice that for column produced with the 1 h polymerisation time (see Figures 6.4 and 6.5) and the efficiency, measured by theoretical plates per meter, was also found to be between 3.1 and 7.3 greater. The theoretical plates per meter obtained on testing under isocratic elution conditions (95 % ACN + 5 % 5 mM ammonium formate pH 3) was 35,930, 26,888 and 28,007 for thiourea, toluene and acrylamide respectively. Whilst a base mixture containing uracil (18,034), adenine (11,935) and cytosine (14,496) yielded slightly lower results. Therefore, the 2 h polymerisation capillary was selected as the optimal polymerisation time.

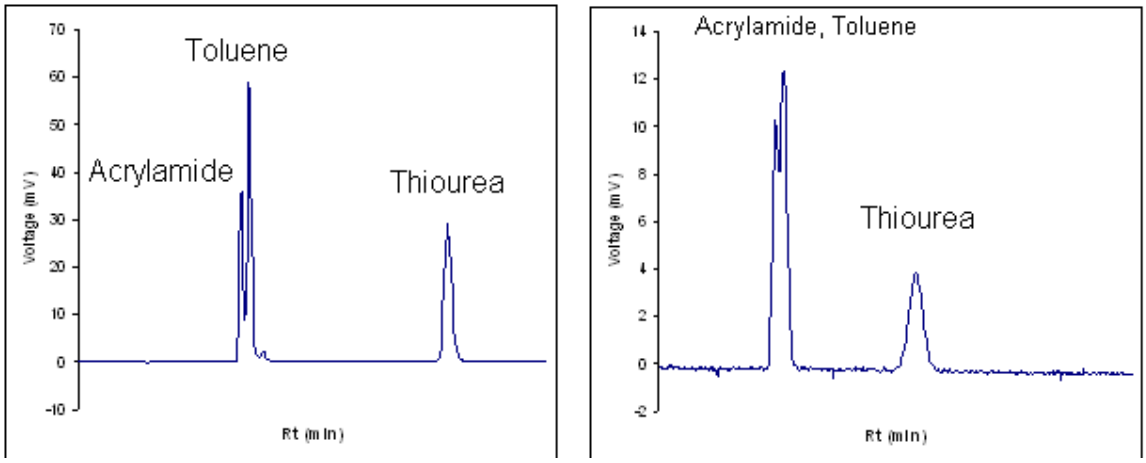

a b

Figure 6.4 Separation of the standard test mix for a) 2 h polymerisation, b) 1h polymerisation

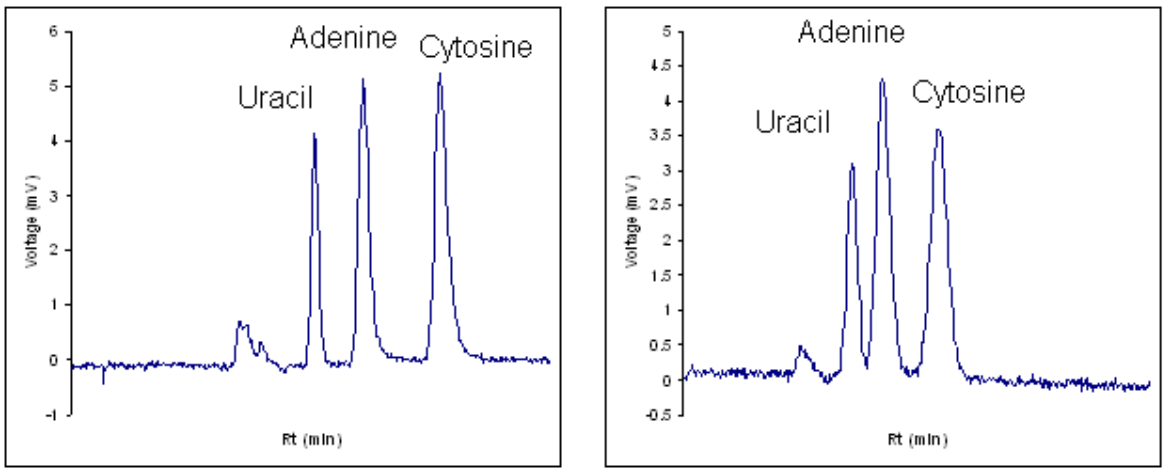

a **b**

Figure 6.5 Separation of base test mix for a) 2 h polymerisation, b) 1h polymerisation

The initiator was added at a constant concentration (1 % w/w with respect to the monomer) for producing monolithic columns for the experiment to evaluate the effect of the polymerisation time. After selecting the optimal time I compared the effect of adding 1 % and 5 % w/w. with respect to the monomer with a 2 h polymerisation time. The increase in initiator improved the results and the resolution obtained for 5 % w/w was twice that obtained when using the 1 %. For example, the column efficiency was between 3.7 to 4.6 times higher than for 1 mg AIBN. This column was able to resolve the toluene and acrylamide peaks in the test mixes and produced narrower peaks with a better shape (see Figures 6.6 and 6.7). Thus, the 2 h polymerisation time with 5 mg AIBN for every 100 mg of monomers in the porogen has been shown to be the optimised condition for producing *poly* (SPE-*co*- BVPE) monolith columns.

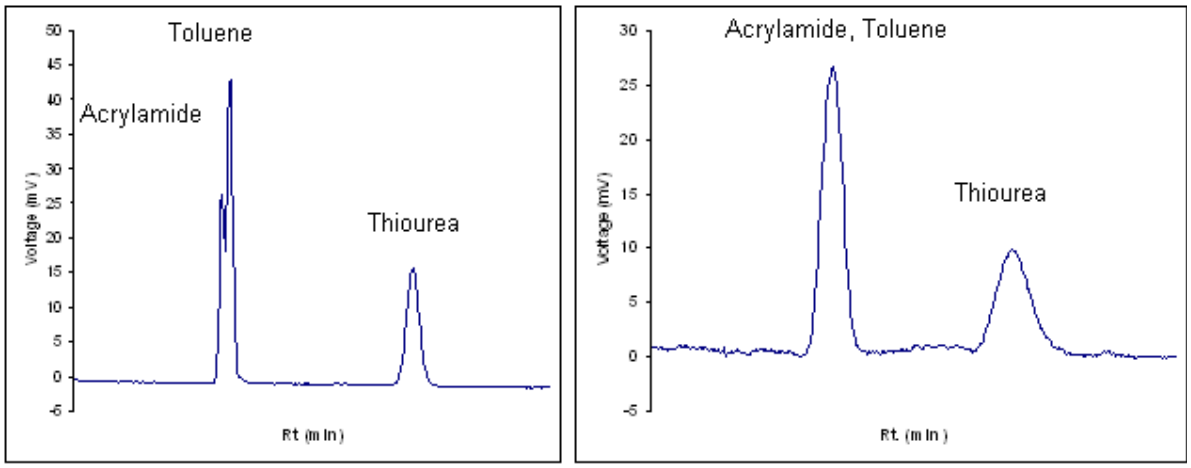

a **b**

Figure 6.6 Separation of standard test mix for a) 5 mg AIBN, b) 1 mg AIBN

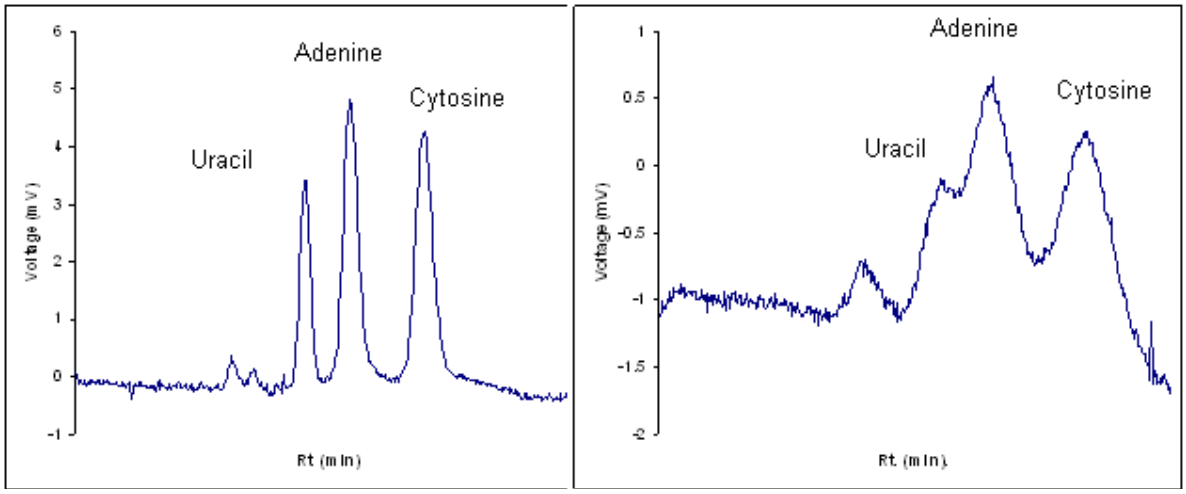

a **b**

Figure 6.7 Separation of base test mix for a) 5 mg AIBN, b) 1 mg AIBN

Applications. Separation of bases and neutral compounds.

The polar zwitterionic *poly* (SPE-*co*-BVPE) surface can provide a hydrophilic environment. A mixture of bases, neutral and acidic compounds were run using a mobile phase gradient starting from 95 % ACN to 50 % ACN, with 5 % buffer in both solvents. Pyrimidines and purines are often used for the evaluation of HILIC columns and a mixture of thymine, uracil, adenine, cytosine, uridine and cytidine was used for the evaluation of *poly* (SPE-*co*-BVPE) monolithic columns in this work. Figure 6.8 shows good separation within 10 minutes for the 6 components of the mixture of pyrimidines and purines (acenaphthalene as t_0 marker) and the peaks were sharp and symmetrical peaks.

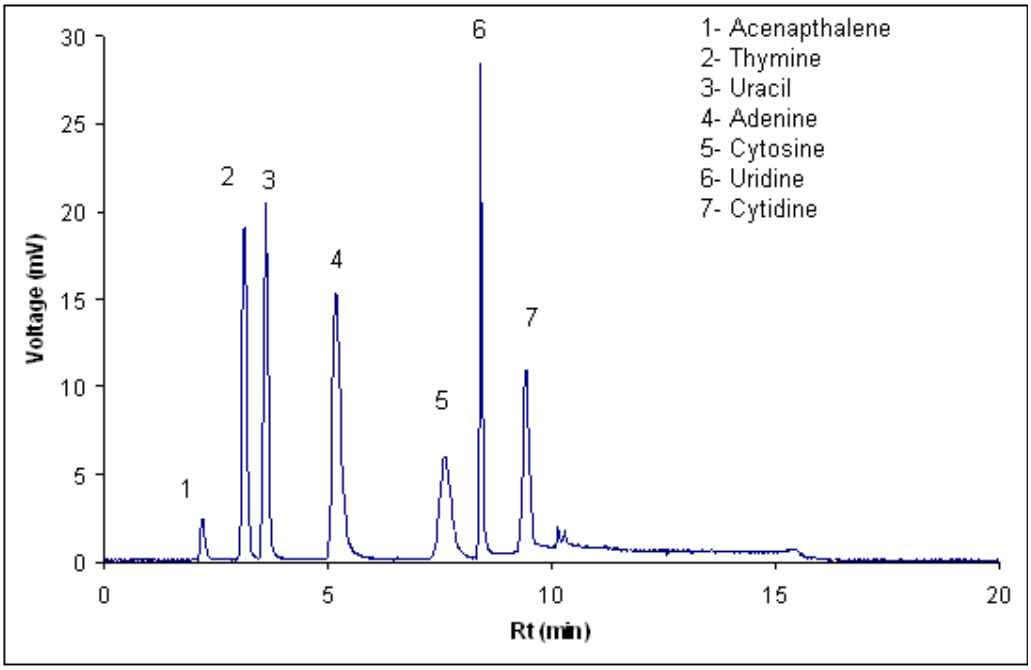

Figure 6.8 Separation of pyrimidines and purines

Application. Separations of EPO peptides compounds.

A mixture of erythropoietin (EPO) peptides, that are synthetic analogues of those generated by tryptic digestion of the intact protein, were separated using the 2 h (5 % w/w AIBN) column and MS/MS detection. The total ion current chromatograms showed sharper peaks with higher intensities than that obtained compared to a commercial C18 column. However, the resolution of peptides was not as good when compared to the separation obtained for small molecule (see Figure 6.9).

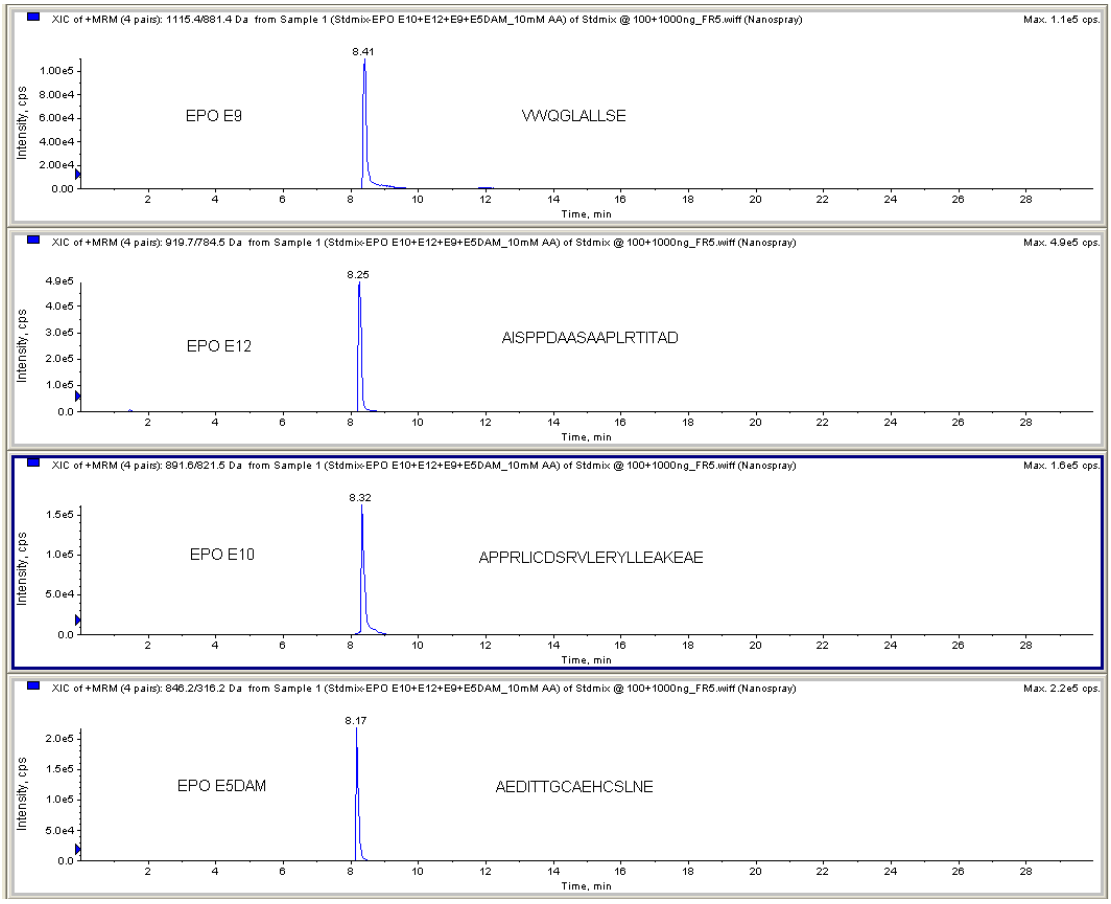

Figure 6.9 Separation of Gluc digested EPO peptides on poly (SPE-co-BVPE)

The synthesis of a HILIC monolithic column, consisting of SPE-*co*-BVPE, that provided good separation of small basic and neutral compounds. However, I was unable to find a set of chromatographic conditions that could satisfactorily resolve a mixture of synthetic EPO Gluc and tryptic digested (Figure 6.9 and 6.12) peptide standards using this column and I concluded that I was not going to be able achieve our goal without reformulating the monomer composition. I opted to substitute the BVPE with DMBVBS, as the latter cross-linker is less difficult to handle than BVPE because it can be used without warming either the monomer/porogen mixture or the filling equipment prior to polymerisation. In addition to this benefit, a co-polymeric

monolithic column made with this cross-linker had been shown [187] to be effective in separating peptides.

According to Greiderer *et al.* [191], reducing the polymerisation time for the SPE-*co*-BVPE cross-linked co-polymer leads to more space within the polymer clusters (lower polymer density) with the formation of larger flow channels and enhanced porosity. My study, which used this monomer formulation with polymerisation times between 1 and 12 hours, confirmed that the polymer clusters become bigger as the polymerisation time increases. Furthermore, when I used a five times higher concentration of the initiator, the performance of the monolithic columns produced was approximately double that obtained with only 1 % AIBN. Therefore, based on this outcome, I elected to initiate the polymerisation of the modified monomer formulation using 5 % (w/w) AIBN and I selected a polymerisation time of two hours because this had given the best results with the previous monomer mixture. A SEI (Figure 6.10) of the new HILIC monolith showed that the material produced had relatively small microglobules, which is considered a sign of good mesoporosity, combined with an acceptable proportion of the macropores required for the rapid and high resolution separation of both low molecular weight compounds and biomolecules. The typical backpressure of the 200 µm x 30 cm monolithic column at 4 µl/min. with the HILIC mobile phase was observed to be very low (around 435 psi) and the high permeability of the co-polymer is consistent with the abundance of macropores seen in the SEI results.

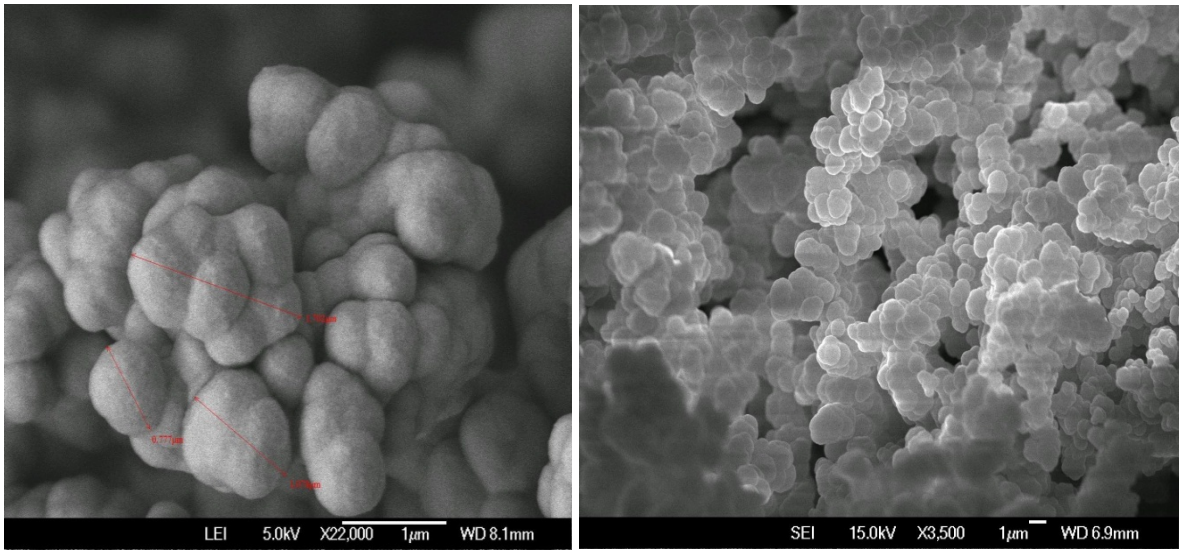

Figure 6.10 Scanning electron image (SEI) and lower electron image (LEI) of poly SPE-co-DMBVBS monolithic column.

Therefore, since SEI showed that the material looked to be suitable for this purposes, it was decided that there was probably little benefit to be obtained by undertaking a study to optimise the fabrication conditions and I proceeded to evaluate whether the novel monolithic column was capable of resolving a mixture of the synthetic rhEPO and DPO tryptic peptides T11 (SLTTLLR), T14 (TITADTFR) and T17 (VYSNFLR). The EICC of the standard mix of EPO peptides (Figure 6.11) shows relatively symmetrical peak shapes and it is evident from these results that this column was able resolve these peptides, unlike the poor results obtained on the SPE-*co*-BVPE (Figure 6.12) material. Furthermore, the elution order for the peptides on the SPE-co-DMBVBS monolith was reversed in comparison to the results I obtained on a C18 RP packed column (data not shown) and this confirms that the mode of separation is primarily HILIC. As anticipated, the calculated peak area for the analytes separated on this monolith was higher than the results obtained using the C18 RP column and

this is because the higher organic content of the HILIC mobile phase favours the ESI desolvation process which in turn enhances sensitivity.

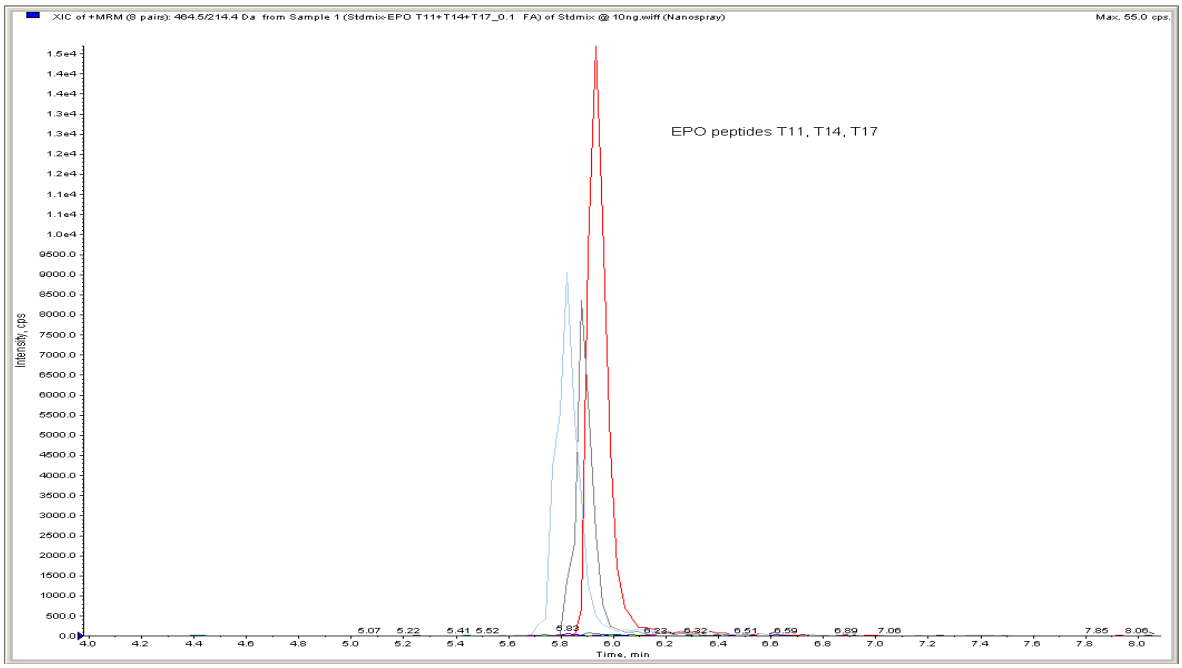

Figure 6.11 Separation of EPO peptide standard mix on poly SPE-co-DMBVBS HILIC monolith

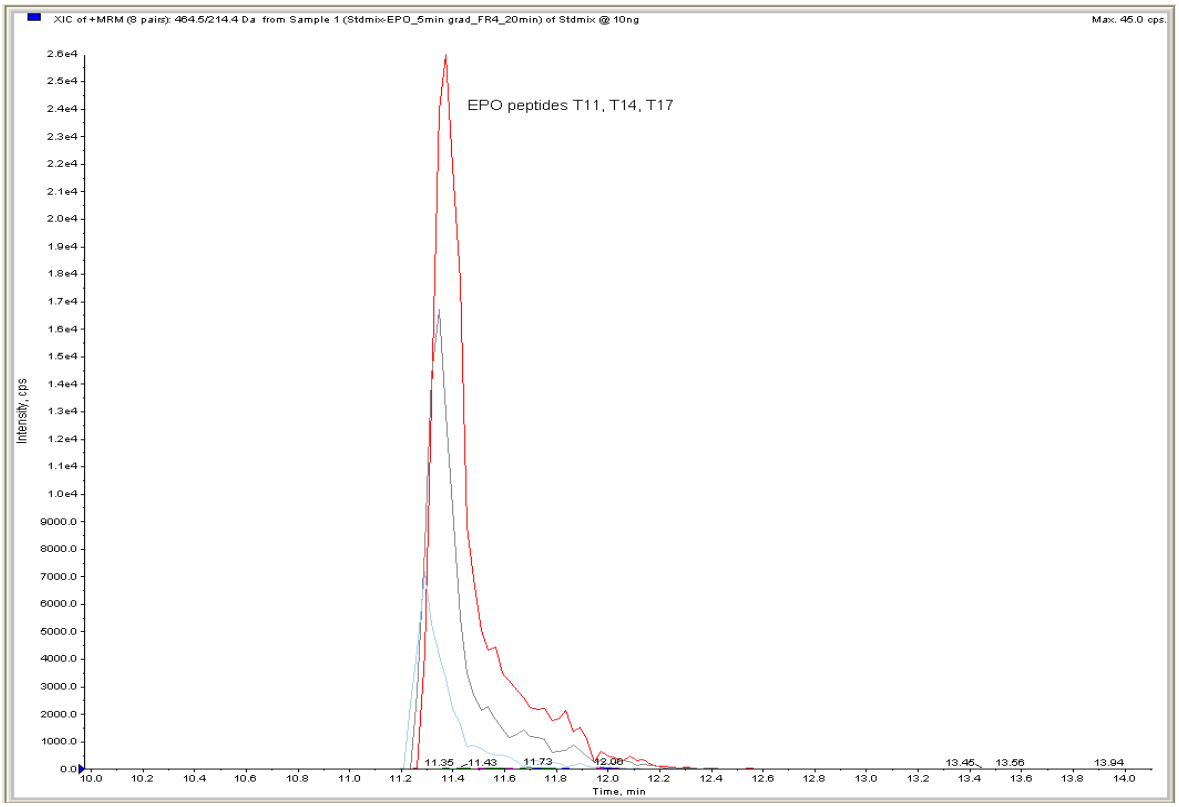

Figure 6.12 Separation of EPO peptide standard mix on poly SPE-co-BVPE HILIC monolith

The primary reason for synthesising the SPE-*co*-DMBVBS monolith was to produce a monolithic column that could be used to enhance the sensitivity of the analytical method employ to identify the characteristic tryptic digestion peptides that are unique to either rhEPO (Eprex®) or DPO (Aranesp®). The doping control samples that were collected from racehorses are extracted and screened for the presence of the tryptic peptides common to these two epogens. However, when a positive result is obtained, it is necessary to differentiate rhEPO from DPO by targeting the analysis towards the peptides fragment T5 (21-45) and T9 (77-97), as the amino acid sequence from this region is specific to each protein. Unfortunately, rhEPO and/or DPO T5 and T9 are glycopeptides with highly variable sialic acid containing glycan motifs and this

severely hinders detection under ESI/MS conditions. This necessitates the inclusion of a deglycosylation step and for this study the glycosidase mixture (PNGase F, O-Glycosidase and Neuraminidase) that was used previously [3] was replaced by the Promega Deglycosylation Mix™ that also contains the β1-4-galactosidase and β-N-acetylglucosaminidase enzymes.

I had tested the performance of this column using a reduced/deglycosylated rhEPO sample which had been digested before being desalted using a C_{18} Zip-Tip™. The eluate (ACN) was injected onto the HILIC monolith column without the inclusion of an evaporation and reconstitution step. Since removal of the N-linked glycosyl moieties from T5 and T9 causes deamination of asparagine (N) to aspartic acid (D), the SRM method used to monitor MSMS transitions for the deaminated T5 and T9 peptide fragments EPO T5DAM (EAE**D**ITTGCAEHCSLNE**D**ITVPDTK) and EPO T9DAM (GQALLV**D**SSQPWEPLQLHVDK) peptides. The XIC (Figure 6.13) from the SRM experiment showed well separated peaks consistent with the presence non-glycosylated tryptic peptides (*e.g.* T6, T14 and T17) as well as (deglycosylated) EPO T5DAM and EPO T9DAM peptides. These results were well correlated with the data observed when analysing the synthetic peptide reference materials (data not shown) under the same conditions. When an equivalent Zip-Tip™ purified digest (2X conc. reconstituted in 95 % of 0.1 %FA water plus 5 % ACN) was analysed using the C18 RP column (Figure 6.14) the elution order was reversed and the more polar EPO T5DAM was not as well retained as the separation undertaken using HILIC conditions. Hence, for the reasons that I have already elaborated, this peptide exhibited a better response in the HILIC separation mode and an injection from the 5 ng digest of Eprex® produces approximately the same response on HILIC as a 10 ng

digest in C18 RP mode. Thus, it can be seen that there was a real improvement in sensitivity on the HILIC monolith compared to use of the C18 RP conditions.

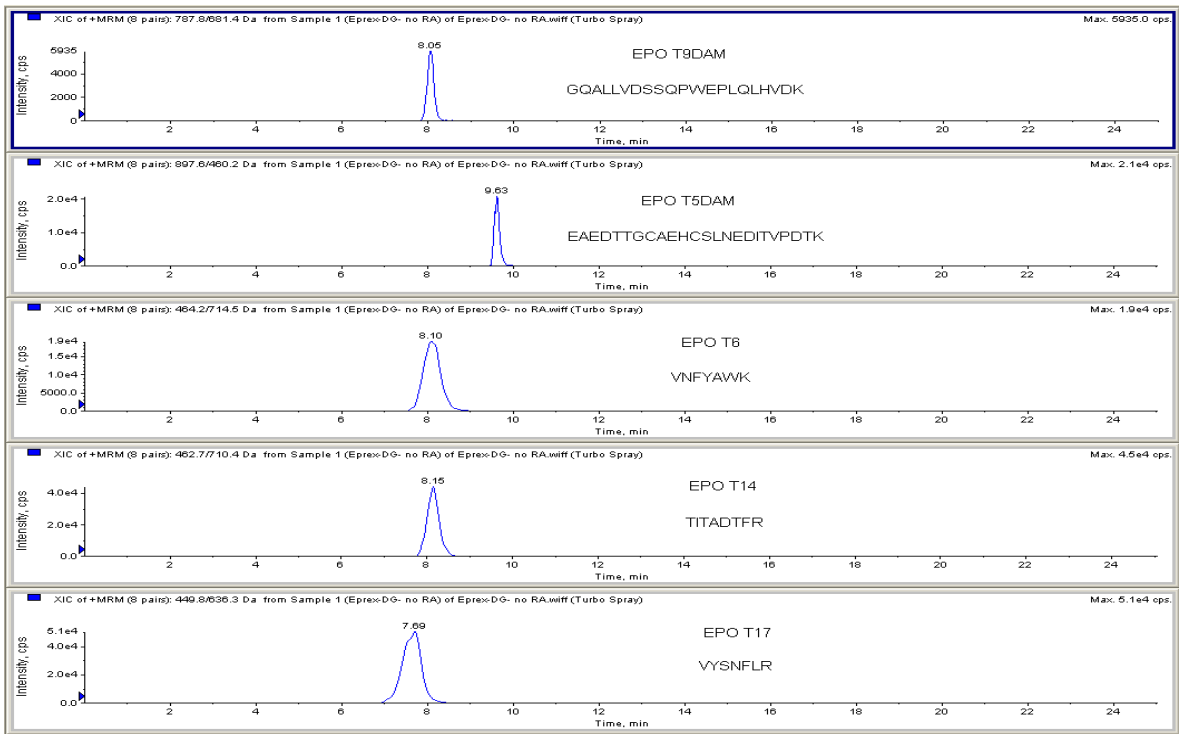

Figure 6.13 Extracted ion chromatogram of the separated deglycosylated and tryptic digested Eprex on poly SPE-co-DMBVBS HILIC monolith

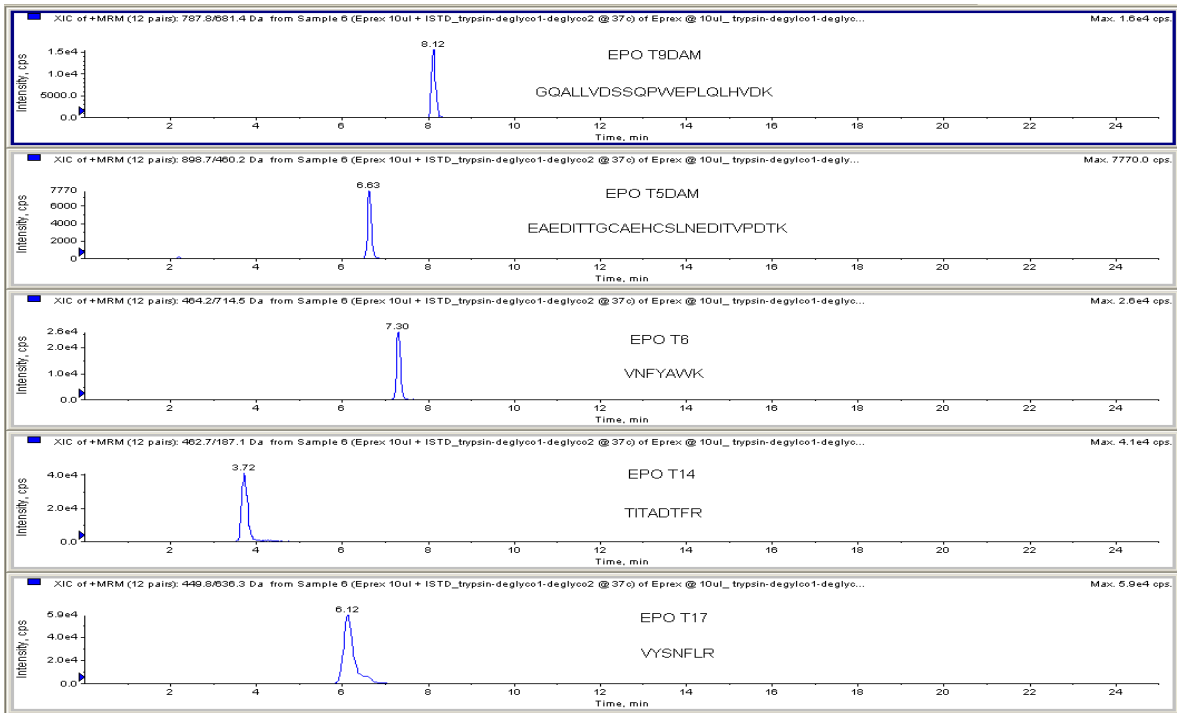

Figure 6.14 Extracted ion chromatogram of the separated deglycosylated and tryptic digested Eprex on RP column

Guan *et al.* [43] have proposed that the detection of EPO T5DAM would be a suitable way of differentiating rhEPO from the structurally similar darbepoetin alfa (*i.e.* DPO) and the presence of DPO T9DAM (GQALLV**D**SSQV**D**ETLQLHVDK) would be conclusive proof that DPO was present in the sample. However, it was found that using DPO T5DAM (EAE**D**ITTGC**D**ETCSLNE**D**ITVPDTK) is a better way to achieve this goal, as under HILIC conditions the SRM peak intensity (Fig. 6.15) from this peptide was almost an order of magnitude better than the result from the DPO T9DAM in the same digest. This is a somewhat contradictory result, as Guan and co-workers were unable to detect even a trace of the DPO T5DAM in their digests. However, one explanation could be that they did not reduce the protein and this resulted in a missed cleavage due to the intact 29-33 disulphide bridge and/or they

created conditions whereby cys-cys polymerisation could have led to depletion of this cysteine containing peptide from the digest solution. Alternatively, it is also possible that the RP conditions that they employed were not as well suited to the sensitive detection of this peptide as the HILIC analysis has been shown to be.

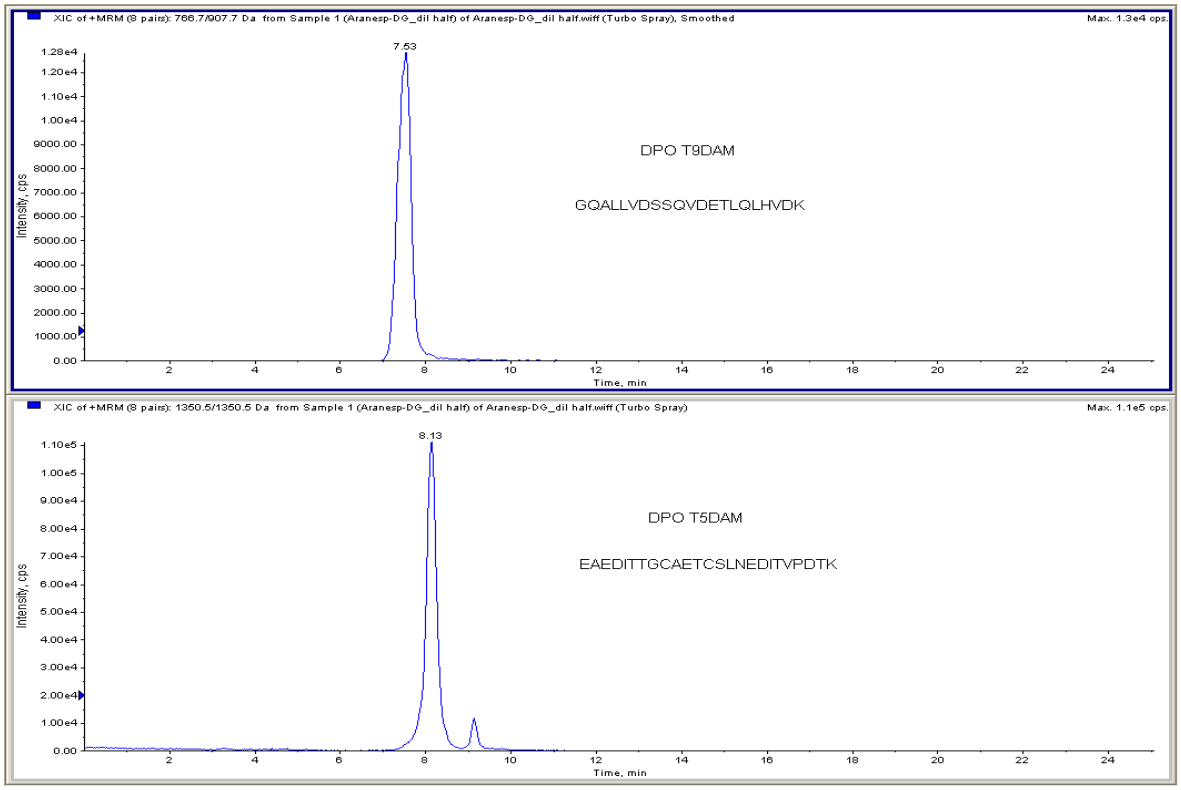

Figure 6.15 Extracted ion chromatogram of the separated deglycosylated and trypsin digested Aranesp on poly SPE-co-DMBVBS HILIC monolith.

6.4 Conclusion

A highly hydrophilic porous monolith, *poly* (SPE-*co*-BVPE) formed within capillary columns of 200 µm i.d. was successfully applied for the rapid and high resolution separation of low molecular weight compounds, such as (pyrimidines and purines)

and produce symmetrical peaks for high molecular weight compounds such as peptides, albeit with less selectivity for the EPO tryptic peptides. Variation of the polymerisation time has a considerable impact on the porous properties of organic monoliths prepared by thermally initiated free radical polymerisation. The reduction of polymerisation time resulted in HPLC stationary phases that are characterised by the presence of a sufficiently high amount of mesopores to efficiently separate low-molecular weight compounds. At the same time, the total porosity is enhanced due to decreased monomer to polymer conversion. This, in turn leads to the enlargement of the flow channel size and thus to increase column permeability. Their exceptional chromatographic performance towards a range of representative low-molecular weight compounds, confirms the incorporation of accessible mesopores onto the polymeric network surface. Further investigations are underway in order to extend the applicability of HILIC monoliths to include their use during the analysis of peptides generated by enzymatic digestion of proteins.

A hydrophilic porous polymer based monolith stationary phase, poly (SPE-co-DMBVBS) has been shown to be able to provide satisfactory resolution of peptides with relatively symmetrical peak shapes and the detection of the targeted peptides using ESI/MS was improved in comparison to the results obtained using a commercial RP column. As noted in the previous work [195], a 2 hour polymerisation step was optimal to produce a monolithic column with enhanced total porosity due to decreased monomer conversion and the enlargement of the flow channels which yields a corresponding increase in column permeability. Due to the good stability and low pressure drop experienced on this monolithic support, rapid separation of the 3 deglycosylated tryptic digested peptides was accomplished using a 5 minute HILIC

gradient (*e.g.* see Figure 6.11). The monolithic columns were easier to fabricate than those made using BVPE cross-linker and offered far superior resolution for peptides. Furthermore, due to the low backpressure, if required, the 30 cm columns can probably be used at significantly higher flow rates or the improved separation between 2 compounds could be achieved by producing longer columns.

Chapter 7: An orthogonal WCX-HILIC set-up with on-line mass spectrometry to screen and confirm the rhEPO and DPO

7.1 Introduction

Reversed-phase (RP) liquid chromatography is the most frequently employed method for sample separation prior to mass spectrometric (MS) based proteomics analyses [203-207]. However, complex proteomics samples are often comprised of species of vastly differing hydrophobicities, including relatively polar analytes such as glycopeptides and phosphopeptides. These polar analytes tend to absorb weakly on the RP stationary phase and often elute directly with the dead volume. The poor retention of these compounds leads to decreased effective sensitivity in electrospray MS due to ion suppression and, as a consequence, potential loss of valuable biological information.

In recent years, the use of HILIC has become more popular due to the growing need for the analysis of polar compounds that are not well retained under RP conditions and also the need to achieve better separation of these analytes in order to address the complexity of the samples to be analyzed [208]. Another advantage of this mode of chromatography is that the mobile phase conditions that are used for HILIC are highly compatible with MS, as the high organic content that is commonly used can potentially increase sensitivity in ESI-MS [134,143]. Despite its capability for separating relatively polar compounds, HILIC tends to be less useful for separating hydrophobic peptides. To overcome this obstacle, two separate injections of the samples on a RP and HILIC column could be performed; however, such analyses would require double the amount of sample.

Ideally, the combination of RP and HILIC in tandem would combine their complementary selectivity and allow for the separation of both hydrophobic and hydrophilic compounds in a single analytical method [209-212]. RP-HILIC is an attractive prospect as a hyphenated system for proteomics because both RP and HILIC employ the electrospray ionisation compatible aqueous buffers and water miscible organic solvents, such as acetonitrile. In theory, off-line coupling of RP-HILIC can be performed by simply collecting the effluent from the RP separation and re-injecting this onto the HILIC phase. However, there is a disadvantage as offline collection is labour intensive and often results in significant sample loss. Consequently online coupling is the preferred option, but the primary technical challenge of implementing a serial RP-HILIC system is overcoming the solvent strength incompatibility between RP and HILIC. RP requires a low-organic solvent for separation, whereas HILIC separation is performed using a high-organic medium, therefore, the predominantly aqueous RP flow must be converted to a high-organic concentration prior to its diversion onto the HILIC column [213] for separation in the second dimension. Failure to address this problem would lead to peak broadening occurring on the HILIC dimension.

RP cannot resolve many of the post-translationally modified isoforms (*e.g.* methylated, acetylated and phosphorylated variants) from the unmodified proteins and from each other [150]. Weak cation exchange-hydrophilic interaction LC (WCX-HILIC) has proven to be an excellent complementary orthogonal mode to RP and has been successfully used to separate acetylated isoforms of histone H4 [151], methylated isoforms of histone H4 [152], phosphorylated isoforms of histone H1 [153], as well as sequence variants of histone H1 [154]. WCX-HILIC, is a mixed-

mode form of chromatography introduced by Alpert in 1990 [128]. It features the simultaneous presence of dominant hydrophilic interaction, (the mechanism for separation of differentially methylated isoforms) and electrostatic interaction between the stationary phase and the analyte due to an ionic WCX stationary phase, (the mechanism for separation of differentially acetylated isoforms) [155].

‘’Top-down’’ and ‘’bottom-up’’ approaches are the two main analytical strategies for proteome separation and identification. Using the ‘’top-down’’ approach the intact proteins are directly separated by HPLC and identified by MS. The alternative ‘’bottom-up’’ approach firstly digests the proteins into peptides, then separates them using liquid chromatography and detects them using tandem mass spectrometry [214]. Two-dimensional (2D) and multidimensional chromatographic techniques coupled to mass spectrometric detection have been applied recently to improve the sensitivity and reproducibility for peptide analyses. Multidimensional chromatographic techniques can potentially improve selectivity and reduce matrix effects. To increase the resolution and peak capacity for ‘’entire-component’’ analysis of complex samples, the hyphenation of different chromatographic separation modes has proven to be a successful strategy [215]. When doing so, the selection of orthogonal separation conditions is of primary importance in order to achieve a maximum difference in selectivity between two separations. The separation principle of reversed-phase is based on the partitioning of the analytes between a hydrophobic stationary phase and a polar hydrophilic mobile phase. Peptides are loaded onto a RP column under low-organic-solvent conditions, which cause the peptides to partition onto the RP packing material. Salts and the majority of components used in digestion protocols tend to remain in the low organic solvent

and thus RP is often used to ‘desalt’ and concentrate the sample. Separation (or elution of the peptide) is then achieved by increasing the organic modifier content in the mobile phase and once the mobile phase is of sufficient hydrophobicity the peptide will start to partition between the two phases as it moves along the column [216]. However, peptides are not strongly retained under RP conditions and typically elution from the packing material can be achieved with less than 40 % of the organic modifier, which means that there is too much aqueous content in the mobile phase to provide retention under the HILIC mechanism and this makes online hyphenation of these stationary phases difficult. Therefore, in this experiment, RP was employed as a trap column to desalt the tryptic digest aqueous sample and thereafter the sample is released at high organic concentration from the RP trap column onto a WCX trap column. WCX and HILIC are complementary modes as both the WCX and HILIC mechanisms function in the presence of a high organic solvent concentration. Thus, a neutral or slightly basic pH 95 % ACN aqueous mobile phase can be employed to trap the peptides onto the WCX column and a lower pH 95 % ACN aqueous mobile phase can then be used to release them with onto the HILIC analytical column for separation. This method of online coupling of RP-HILIC using the WCX as an intermediate trap has the potential to resolve the incompatibility of mobile phase between RP and HILIC and it also provides a way of simultaneously analysing both the hydrophilic and hydrophobic peptides in the sample. Online hyphenation also possesses other advantages, such as minimal loss of sample, no vial contamination, and no sample dilution [148-149].

7.2 Materials and Instrumentation

7.2.1 Materials.

DL-dithiothreitol (DTT) and ammonium formate were all purchased from Sigma Aldrich (Singapore). HPLC-grade methanol and acetonitrile (ACN) were obtained from Fisher Scientific (Singapore). Ammonium bicarbonate and ammonium acetate were purchased from Merck (Singapore). Sequencing grade modified Trypsin (P/N No. V5111) and protein deglycosylation mix kit were purchased from Promega (Singapore). The water used throughout all experiments was obtained from a Milli-Q Gradient A10 from Millipore (Singapore). Epoetin alfa, Eprex® the recombinant human erythropoietin, 10,000 IU/ ml was purchased from Jassen-Cilag AG, (Schaffhausen, Switzerland). Darbepoetin alfa, Aranesp® 40 µg/ 0.4 ml was obtained from Amgen Manufacturing Limited a subsidiary of Amgen Inc. (Thousand Oaks, CA, USA). Human EPO 1 mg/ ml protein was purchased from Genway Biotech, Inc. (San Diego, CA, USA). Peptide SLTTLLR (human EPO peptide T11), peptide TITADTFR (human EPO peptide T14) and peptide VYSNFLR (human EPO peptide T17) were synthesised by Auspep Pty. Ltd. (Tullamarine, Victoria, Australia). Nanosep 30 KDa OMEGA was obtained from PALL Corporation (USA).

7.2.2 Instrumentation.

Experiments were undertaken using a Tempo™ nano MDLC by Eksigent, with an Eksigent AS1 Autosampler coupled to a Turbo Ionspray (TIS) of AB Sciex 4000 Qtrap LC-MSMS operated by Analyst 1.5 software. The autosampler has a 6-port injection valve with a 20 µl injection loop. An in-house fabricated 3 µm particle size

WCX trap packed into a 250 µm x 20 cm capillary, was coupled to an additional 6-port valve. When switched to the inject position, it becomes in-line with the 200 µm x 30 cm capillary filled with the fabricated HILIC monolith mentioned in the previous Chapter (Figure 7.1). A CAPTRAP™ from Michrom Bioresources, Inc. was installed after the injection valve, connecting the loading buffer line to the external 6-port valve (Figs. 7.6 a & b).

7.2.3 LC Conditions

Solvent A for the loading pump was 10 mM ammonium acetate pH 5.5, while solvent B was ACN at a flow rate of 1 µl/min. Solvent A for the gradient pump was 0.1 % Formic acid in water, and for B 100 % ACN. For Figure 7.1 the samples were loaded at a flow rate of 1 µl/min using 95 % A and 5 % B for 50 min. The gradient pump flow rate was 4 µl/min. The initial conditions of 95 % B and 5 % A were held for 10 min, and then a gradient was run from 95 % B to 5 % B for 20 min. The gradient was then held for 5 min and then returned to the initial conditions at 36 min, followed by re-equilibration for 4 min. The mobile phase used for Figures 7.6 a & b are the same as in Figure 7.1, and the loading and gradient pump profile is presented in Table 7.1.

Time (min)	CH1		CH2		Valve	
	% A (10 mM AA)	% B (ACN)	% A (0.15% FA)	% B (ACN)		
0	5	95	95	5		
30	5	95	95	5	INJ	
35	5	95	5	95		Captrap™ release peptides to WCX at high organic
64	5	95	5	95		
65	5	95	5	95	LOAD	Valve switch release peptides from WCX at low pH to HILIC
75	5	95	95	5	INJ	Return to initial condition to re-equilibrate Captrap™
95	5	95	95	5		Start gradient on HILIC from high organic to low organic to separate peptides.
115	95	5	95	5		
125	95	5	95	5		
130	5	95	95	5	LOAD	Return to initial condition to re-equilibrate both trap columns and HILIC
135	5	95	95	5		
150	5	95	95	5		

Table 7.1 Gradient profile of loading and eluting pump

7.2.4 MS Conditions

The source temperature was maintained at 350 °C with nebuliser, desolvation gas and curtain gas settings at 15, 10 and 30 psi respectively. Ion source voltage was maintained at 4500 V. Analytes were detected using multiple reaction monitoring (MRM) at a dwell time of 100 ms per transaction. Each peptide was optimised for Q1 selection, fragmentation, and Q3 selection using declustering potential (DP) and collision energy (CE) as shown in Table 7.2.

rhEPO/ DPO peptides	Q1 (m/z)	Q3 (m/z)	Time (msec)	DP	CE
T6	464.2	714.5	200	68	22
T17	449.8	636.3	200	73	22
T14	462.7	710.4	200	127	20
EPO T9DAM	787.8	939.4	200	57	29
EPO T5DAM	897.6	460.2	200	85	20
EPO T5DAM (Reduction/ Alkylation)	1345.1	1345.1	200	85	20
DPO T9DAM	766.7	907.7	200	89	27
DPO T5DAM	1350.5	1350.5	200	89	27

Table 7.2 rhEPO/DPO peptides MRM, DP and CE setting

7.2.5 Preparation of samples.

Human EPO was spiked using 5 µl of (10 µg/µl), Aranesp® was spiked using 40 µl of (0.1 µg/µl), Eprex® was spiked using 10 µl of (84 µg/ml). Thirty five microliters of 50 mM ammonium bicarbonate buffer pH 7.8 was added to each of the spiked samples, vortex mixed, followed by the addition of 5 µl of 100 mM DTT in 50 mM ammonium bicarbonate (reducing agent). They were then left at room temperature for 10 min. After 10 min, deglycosylation steps were undertaken for all samples. Deglycosylation was undertaken by adding 5 µl of 10 x deglycosylation reaction buffers and 5 µl of protein deglycosylation mix from a Promega protein deglycosylation kit. Samples were then gently vortexed and centrifuged at 3000 rpm to allow the sample to collect at the bottom of the tube. Samples were then incubated in the oven at 37 ºC overnight. After the deglycosylation step, the samples were each transferred to a 30 KDa nanosep filter then centrifuged at 3000 rpm for 10 min. Buffer exchange was carried out by adding 200 µl of 50 mM ammonium bicarbonate buffer pH 7.8 onto the 30 KDa nanosep filter and then centrifuging at 3000 rpm for 20 min. This step was then repeated. 100 µl of 50 mM ammonium bicarbonate pH 7.8 was added to the filter and transferred to a vial. 10 µl (20 µg/100 µl) of trypsin enzyme was then added and the mixture was incubated in the oven at 37 ºC for 3 hr. After the enzyme digestion, 4 µl of 10 % FA in ACN was added into the digested solution to stop enzyme digestion. The digested samples were then transferred into auto-sampler injection vials ready for injection.

7.3 Results and Discussion

To use HILIC as a separation column in an on-line experiment, the issues relating to the incompatibility of the sample preparation buffer need to be resolved, as this could not be injected onto the HILIC column without significantly limiting the injection volume or perhaps reducing the aqueous content to less than 10 % by diluting the sample with ACN. In the previous Chapter the analytes, which are in an aqueous solution, required a Zip-tip™ treatment to desalt and reconstitute the peptides in a high organic mobile phase before injecting the sample onto the HILIC column. As explained in the theory section, online 2D separation possesses advantages, such as minimal loss of sample, no vial contamination, and no sample dilution. Hence, I wanted to omit the above preparation step and use on-line hyphenation to achieve the desired outcome.

In the first part of the experiment I analysed spiked samples, prepared as described in section 7.2.5, followed by analysing using the WCX-HILIC configuration. Samples were loaded onto the auto-sampler for direct injection via the WCX trap column by loading the sample using a high aqueous content 10 mM ammonium acetate at pH 5.5 with a flow rate of 1 µl/min to load the WCX trap (hold for 50 min) followed by a gradient elution with an acidic aqueous buffer (0.1 % FA) mixed with ACN. This was programmed over 20 min from high organic to high aqueous buffer to elute the peptides. Under the acidic conditions used for the HILIC gradient separation, the WCX does not retain the peptides and so these are released from the trap when the valve switches into the 1➔6 position.

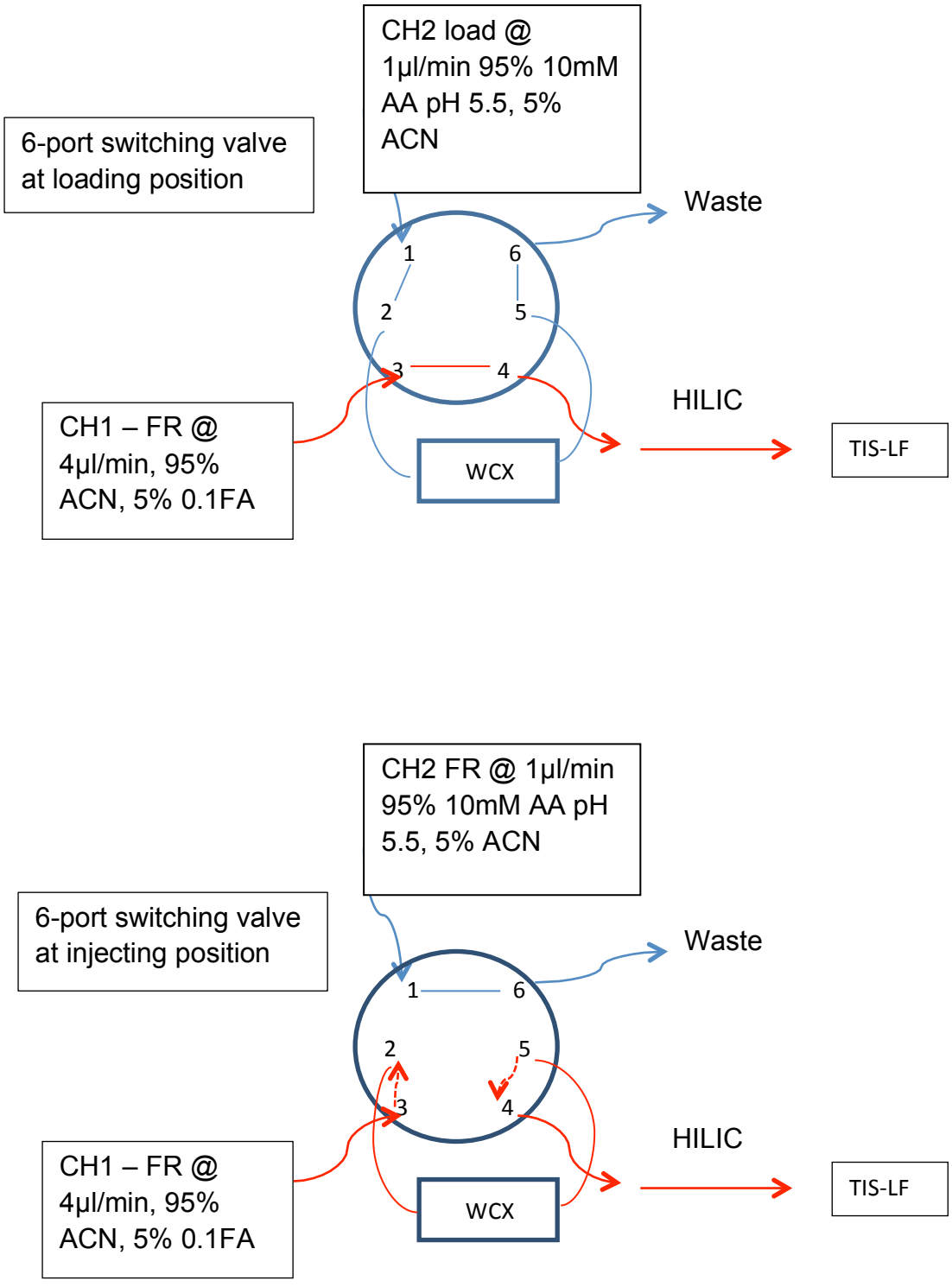

Figure 7.1 Schematic drawing of 6-port switching valves showing the loading of sample and injecting of sample into the WCX and HILIC column.

Though this required a longer elution time than the off-line approach, both the non-glycosylated and glycosylated peptides from the Eprex® sample were separated (as shown in Figure 7.2) and it was able to achieve a better peak shape. However the intensity of extracted ion chromatograms were similar compared to that achieved using the off-line preparation coupled with injection onto the HILIC column (Figure 7.3). The Darbepoetin (Aranesp®) results obtained showed that it could also distinguish both the non-glycosylated and glycosylated peptides (Figure 7.4) *via* this separation and detection approach. In this regard a better peak shape and the intensity were observed for some peptides, but some were slightly lower when compared to the off-line preparation and injection onto the same HILIC column.

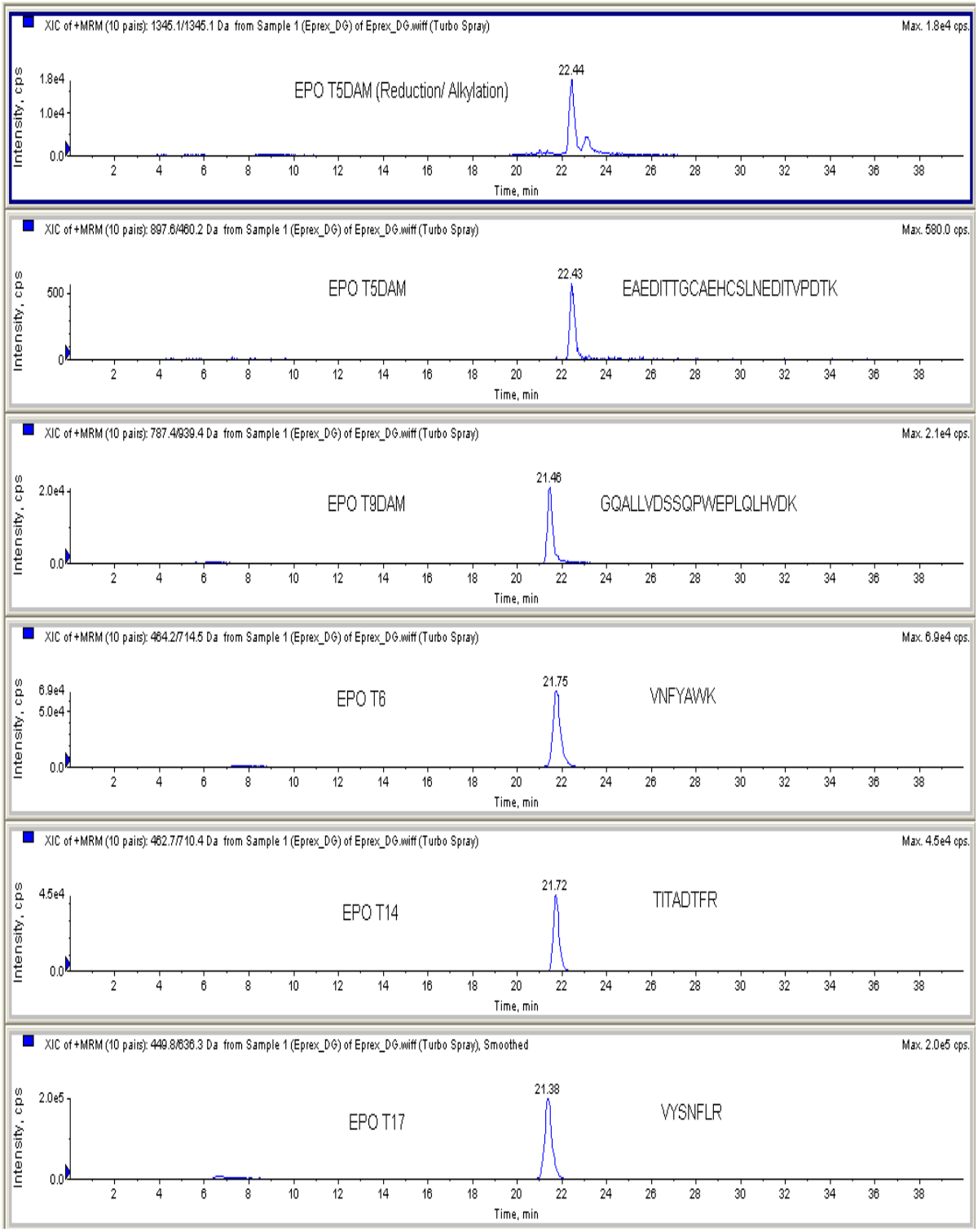

Figure 7.2 Extracted ion chromatogram showing deglycosylated and tryptic digested Eprex via WCX-HILIC.

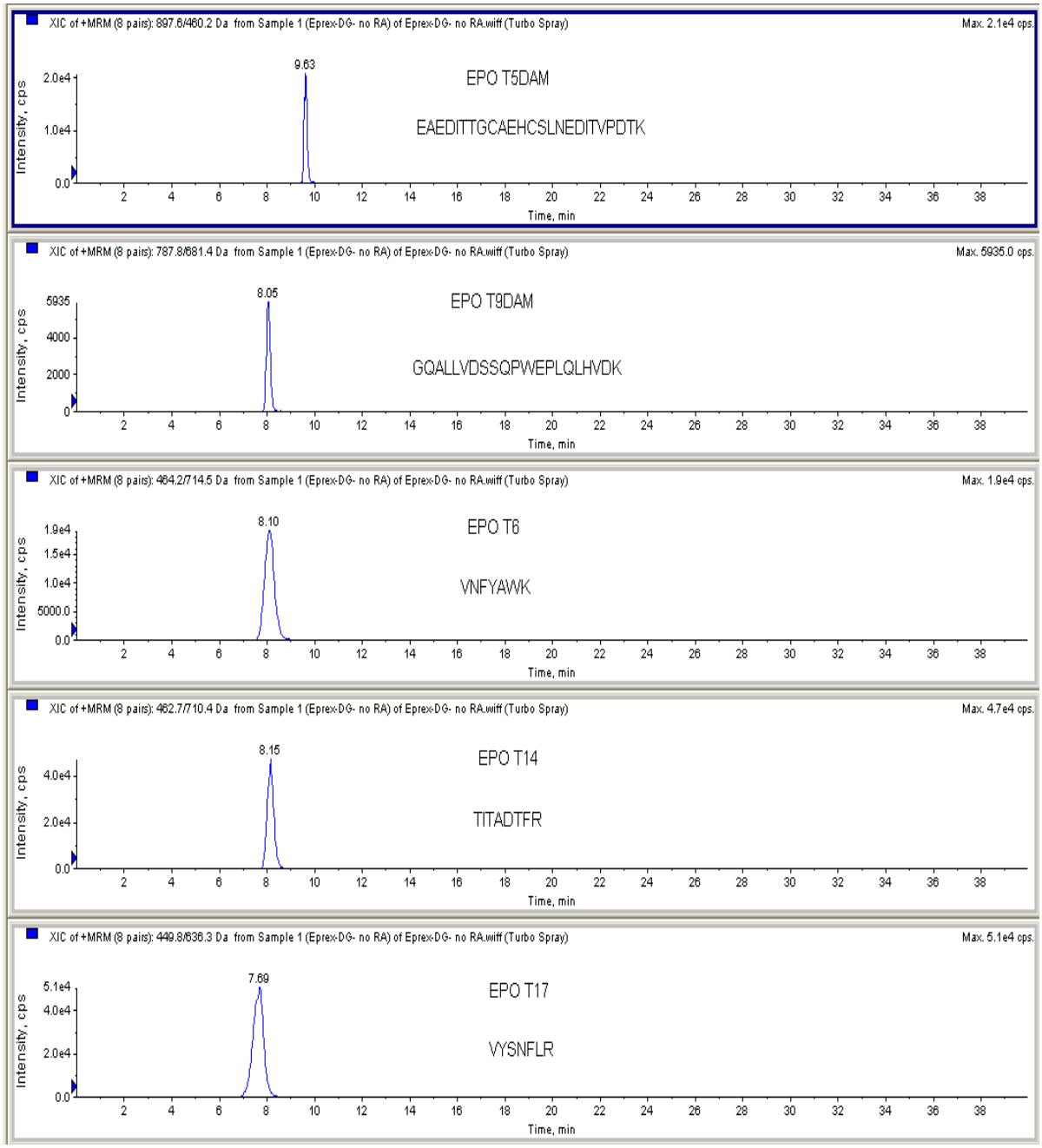

Figure 7.3 Extracted ion chromatogram showing deglycosylated and tryptic digested Eprex prepared off-line and injected directly onto HILIC.

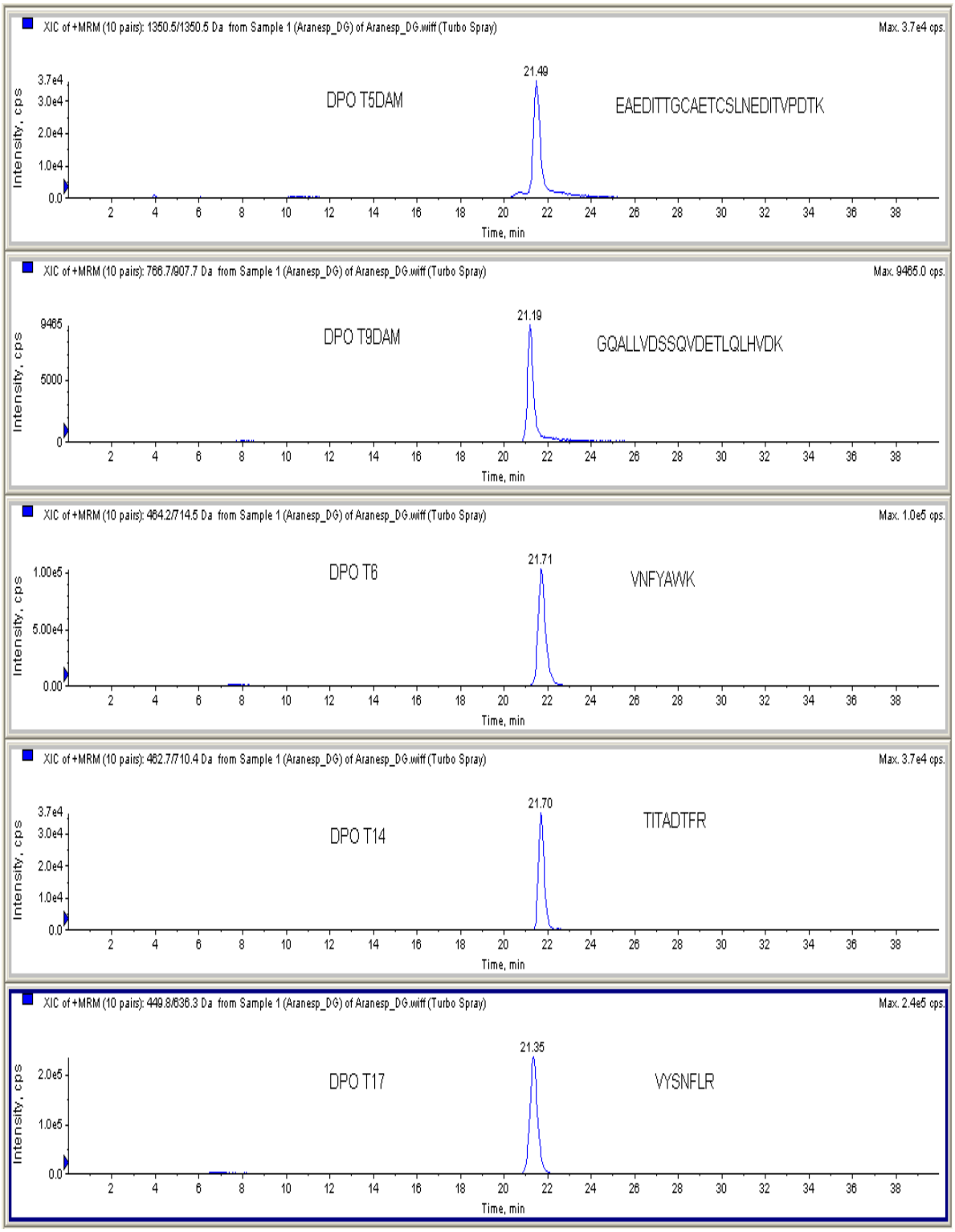

Figure 7.4 Extracted ion chromatogram showing deglycosylated and tryptic digested Aranesp via WCX-HILIC.

After evaluating WCX-HILIC, a reverse phase Captrap™ was then included into the flow path to desalt the sample. After the Captrap™ was added, the gradient programme was modified to compensate for the additional time required during the loading steps. The sample was loaded onto the Captrap™ at a flow rate 1 µl/min with 95 % 10 mM ammonium acetate at pH 5.5 and 5 % ACN. During this step any residual material from the previous injection was flushed off of the WCX trap and the HILIC column was equilibrated with 95 % ACN and 5 % 0.1 FA in water using second LC pump at flow rate 4 µl/min. When the 6-port switching valves was switched to the inject position a gradient from 95 % aqueous to 5 % aqueous was used to elute the peptides from the Captrap™ to WCX trap column (Figure 7.5). The use of a gradient elution step allows for equilibration of the WCX packing material using the higher pH aqueous buffer and creates an environment that is suitable for the retention of the peptides under high organic mobile phase condition conditions. This is an advantage because when the 6-port switching valve is switched back to the loading position the high percentage of ACN in the mobile phase enhances refocusing of the peptides onto the stationary phase of the monolithic HILIC column. The WCX releases the peptides at the acidic pH and the eluting peptides were then resolved on the HILIC column (Figure 7.6). Whilst the HILIC gradient is running the WCX is re-equilibrated in order to be ready for the next injection. The chromatogram from the EPO standard mix, that was run using on the Captrap™-WCX-HILIC online system in Figure 7.6 a & b, is shown in Figure 7.7. The run time of 150 min was much longer than using the off-line sample preparation approach, as very conservative programme timing was used to be certain that the entire sample injection volume was able to pass through the Captrap™ and to ensure that all of the peptides were firstly transferred from Captrap™ to WCX and subsequently from the

WCX to the HILIC column. The cycle time can be reduced by optimization of the flow rates and utilizing trap columns that have a lower dead volume than the items that were used in this experiment. However, even taking into account the length of time taken to complete the online preparation, this is offset by the advantages of minimizing the sample handling, as well as reducing sample loss and contamination. The automation can be run unattended and therefore it can be run 24 hours/day and seven days a week without the need for constant operator input or monitoring.

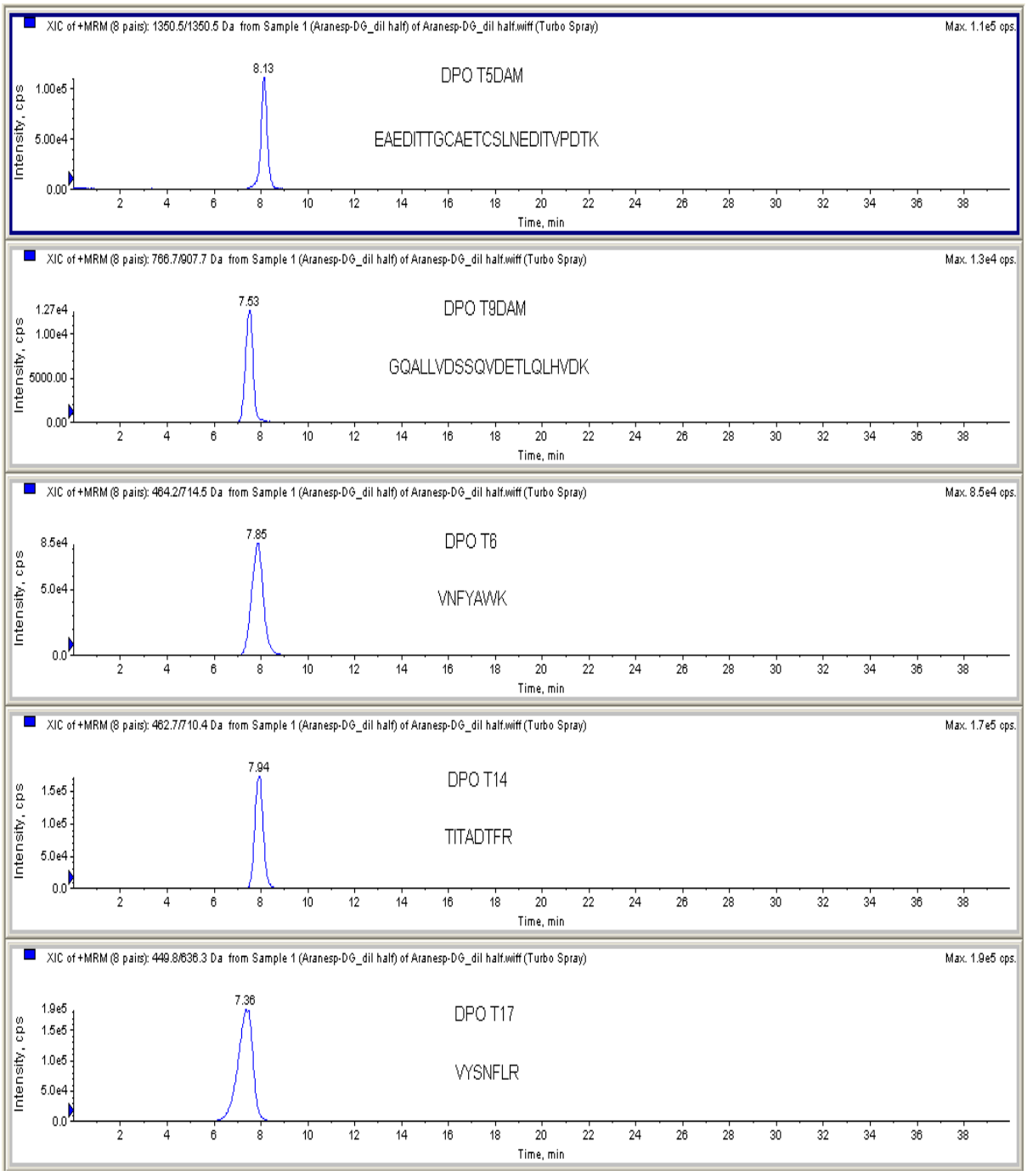

Figure 7.5 Extracted ion chromatogram showing deglycosylated and tryptic digested Aranesp prepared off-line and injected directly onto HILIC.

a)

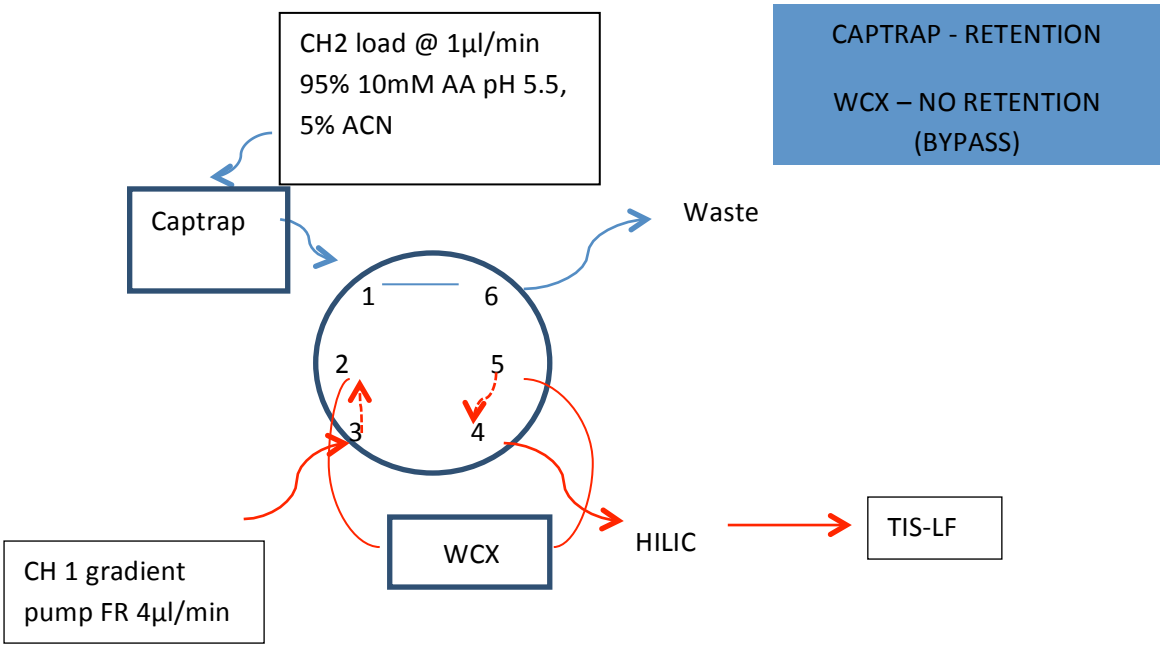

b)

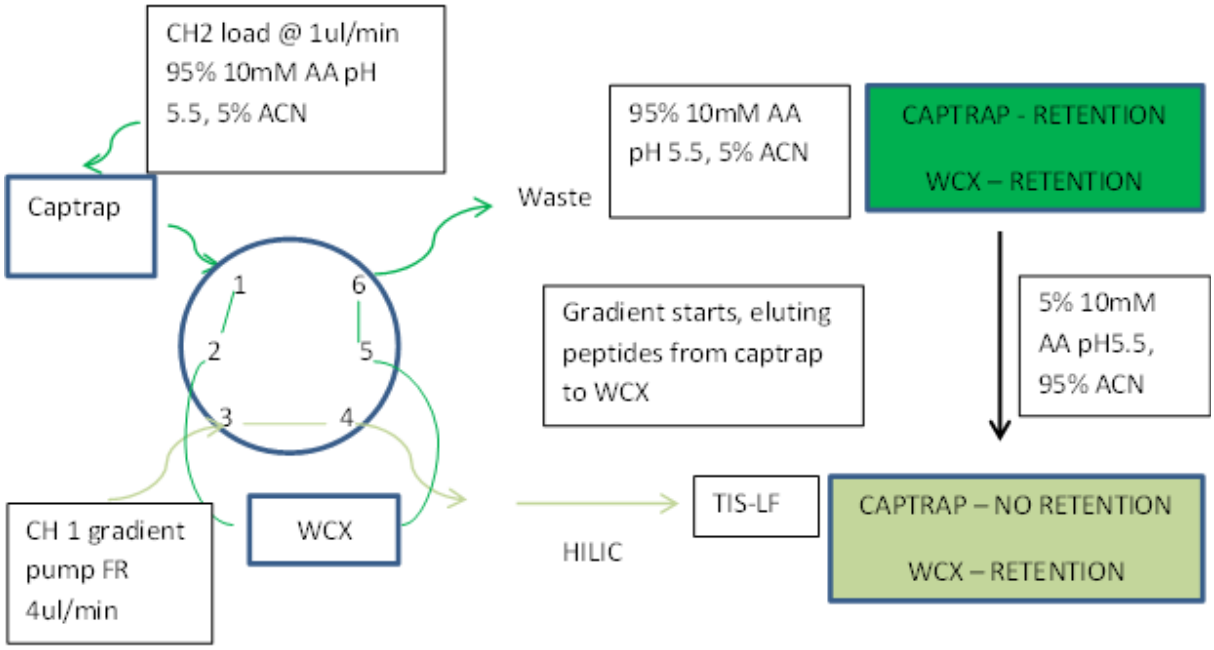

Figure 7.6 a) Schematic drawing of 6-port switching valves showing the loading of sample on the Captrap™, and transferring the sample from Captrap™ to WCX. B) 6-port switching valves showing the releasing of peptides from the WCX to HILIC and separation of peptides on HILIC.

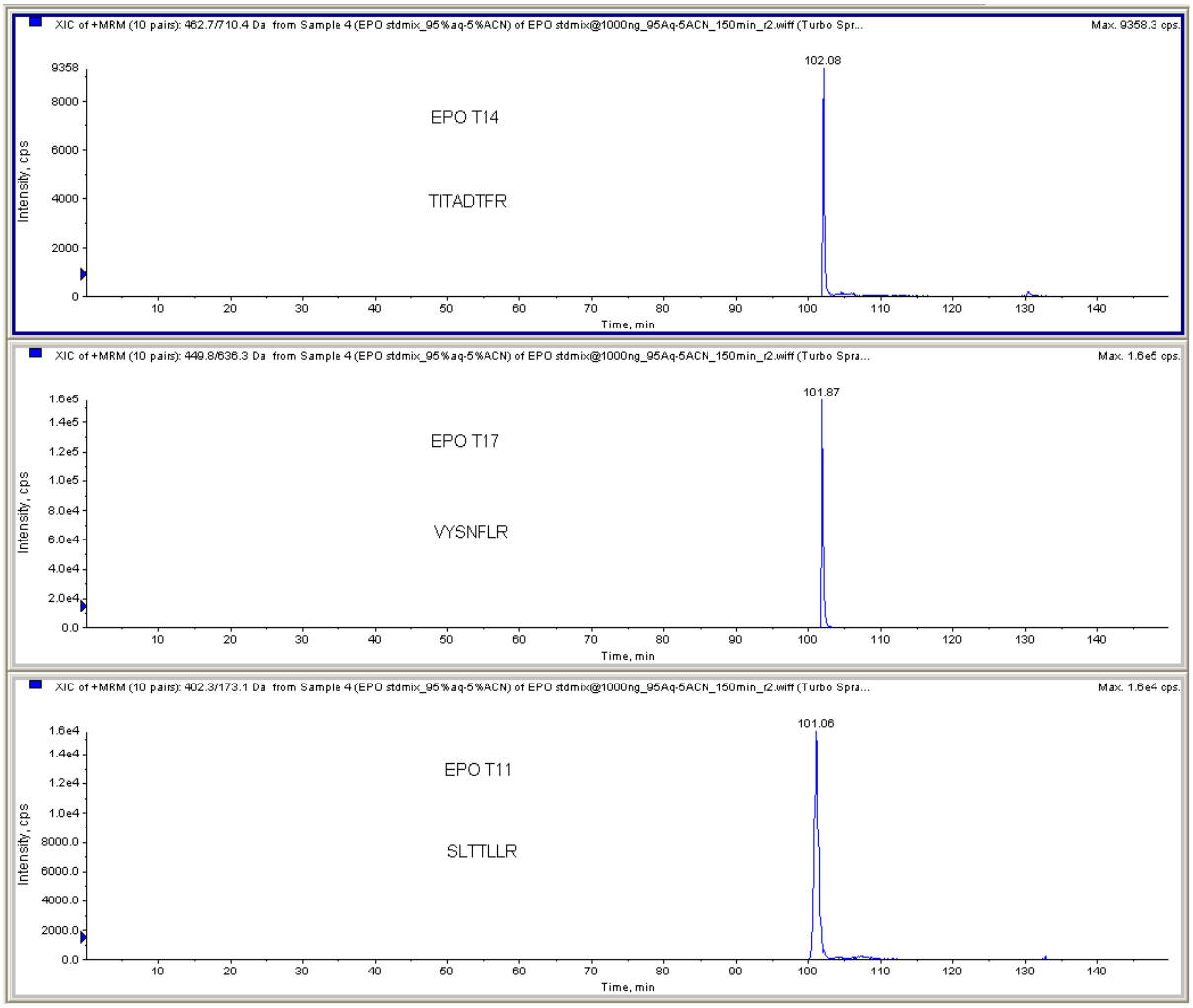

Figure 7.7 Extracted ion chromatogram showing the separation of EPO peptides standard mix on-line on the Captrap™-WCX-HILIC multi-dimensional set-up.

7.4 Conclusion

The on-line coupling of RP➔ WCX ➔ HILIC can resolve the lack of HILIC refocusing that can occur when peptides are eluted from a RP column using a high aqueous content mobile phase. On-line hyphenation possesses some advantages, such as minimal loss of sample, little or no contamination from the laboratory ware used to undertake the off-line processing and allows for highly efficient use of samples as only the quality required for the actual analytical run is consumed. It can be left to run 24 hours a day and seven days a week without constant input from laboratory staff. The configuration set-up is not very complicated as a single 6-port switching valve and two pumps, one for loading at neutral or mildly basic conditions and a gradient pump for the HILIC separation, will suffice. The loading pump loads the aqueous sample onto Captrap™ under neutral or mildly basic pH condition and elutes the retained peptides from the Captrap™ to WCX where they are re-trapped on the WCX under conditions that are compatible with HILIC. The high organic content of the mobile phase helps to ensure that when the peptides are released from the WCX under acidic conditions they can be refocused on the HILIC column. This helps to maintain good peak shape for the analytes under the HILIC mode. Thus, this on-line configuration has solved the issue whereby the high water content encountered under RP elution conditions would also act as a strong eluent under HILIC conditions and would lead to broader peaks. The results show that this configuration enables on-line concentration and desalting, which minimized the preparation steps and good sensitivity was achieved.

Chapter 8 Overall Conclusions & Recommendations for Future Work

8.1 Overall Conclusions

The main aim of this research project was to explore methods for the fast and sensitive detection of rhEPO/ DPO in equine doping. Unfortunately, EPO is a complex glycoprotein and plasma is a complicated biological matrix, which requires various sample preparation steps from immunoaffinity extraction of sample through to the enzyme digestion of the protein to peptides, followed by deglycosylation of the glycopeptides to allow for sensitive detection as low as 0.1 - 0.2 ng of Epoetin present in the equine plasma sample.

In Chapter 2, I have shown that with capillary flow LC of 4 µl/min, detection of rhEPO showed a better sensitivity than when using the high flow LC of 100 µl/min. This method was capable of detecting 0.2 ng of immunoaffinity extracted Eprex from equine plasma sample, compared to the high flow LC where the limit of detection is 10 ng of immunoaffinity extraction from equine plasma. In this chapter, a novel internal tapered capillary tip was fabricated and packed with commercial C_{18} silica material, which was subsequently coupled to a nano-electrospray source and run at a flow rate of 500 nl/min. The nanoflow LC showed a much better sensitivity than both the capillary and high flow LC, however, it is a great challenge to fabricate the internal taper tip and also to optimise the nanospray in order to achieve good sensitivity. It is not easy to attain a reproducible result.

In Chapter 3, another immunoaffinity method was investigated using the MAIIA EPO purification kit, which is much faster with shorter steps (prepared within 3-4 hours)

compared to using the magnetic beads which required linkage of anti-rhEPO antibody to the magnetic beads followed by overnight incubation of the anti-rhEPO with rhEPO spiked plasma, rinsing of the magnetic beads and elution of rhEPO from the anti-rhEPO (takes 2 days). A post-spike experiment was carried out to compare with the spike Eprex in plasma samples going through the MAIIA IAC extraction; the recovery achieved was comparable or better than the post-spiked method for both the non-glycosylated and glycosylated peptides. In this chapter, I also explored the possibility of adding the Asp-N enzyme digestion in order to aid the enrichment of the deaminated peptide T9, which gives a higher intensity for the T9A1 and T9DPOA1 peptides fragment, which could help to differentiate and identify the rhEPO and DPO in EPO doping.

In Chapter 4, the immobilisation of trypsin on various supports (controlled pore glass beads and a micro-scale reactor (μIMER)) was compared with the in-solution digestion. Both immobilisations showed better results than the in-solution digestion. However, immobilising on the CPG required a lot of off-line effort whereas, the on-line enzyme reactor can be re-used for about 1 month and up to about 30 – 40 injections. Therefore, this is a fast and efficient on-line method that could be applied to detect rhEPO in equine plasma extract.

In Chapter 5, I have also successfully demonstrated the PNGase F deglycosylation on-line reactor. A trypsin reactor followed by a deglycosylation reactor was coupled on-line in a column oven and coupled to the MS, where the sample was directly injected and digested on-line. This on-line set-up could detect both the digested non-

glycosylated and glycosylated peptides with good sensitivity and acceptable repeatability. This time saving technique minimises the extent of manual sample handling, which reduces the potential sources of contamination.

In Chapter 6, a novel HILIC monolith was fabricated in order to separate the EPO peptides. A study of different polymerisation times and an increase of initiator concentration were carried out. The increase in initiator concentration helps to reduce the polymerisation time, achieving sufficiently high amounts of the mesopores necessary to efficiently separate the compounds. This column was able to provide satisfactory resolution of peptides with relatively symmetrical peak shapes and sensitive detection of the peptides was improved compared to the results obtained using a commercial reversed-phase column.

In Chapter 7, an on-line coupling of RP➔ WCX ➔ HILIC was configured to accommodate an on-line digestion sample with high aqueous content, which is incompatible with the loading buffer (high organic) required for HILIC separations. The loading pump loads the aqueous sample onto the Captrap™ (RP) under neutral or mildly basic pH conditions and elutes the retained peptides from the Captrap™ (RP) onto the WCX phase where they are re-trapped under conditions that are compatible with HILIC chromatography. The high organic content of the mobile phase helps to ensure that when the peptides are released from the WCX trap column under acidic conditions they can be re-focused on the HILIC column. The results show that this configuration enables on-line concentration and desalting, with good sensitivity and minimised preparation steps.

In summary, this work has shown that on-line set-up for the detection of rhEPO/ DPO in equine doping is achievable with fast detection and good sensitivity. It is also capable of confirming either rhEPO or DPO being doped. However, there is a potential to further develop this work to a complete on-line detection with an on-line immunoaffinity extraction column and further improving the sensitivity by enriching the glycopeptides.

8.2 Recommendations for future work

According to the results discussed in the respective chapters, the following areas are recommended for further development.

1. As can be seen from Chapter 2, using the fabricated internal tapered capillary tip filled with C_{18} silica, gave a much better sensitivity than the high flow and capillary flow LC. This is the area where it can be expanded on the skill of setting up nanospray with a more reproducible and durable method. The internal tapered capillary can be packed with the HILIC monolith, however this requires skill and technique to polymerise the monolith in the internal tapered capillary. The tip needs to be properly sealed whilst not breaking it during and after polymerisation when removing the seal.

2. In Chapter 3, it can be seen that using a MAIIA purification kit can achieve a good recovery for the immunoaffinity extraction. This area can be explored to make it an on-line immunoaffinity extraction column by immobilising

the antibodies on the monolith. This requires the incorporation of an on-line buffer exchange. This could greatly help in a total elimination of the off-line sample handling. As for using the Asp-N enzyme for the identification of the N-terminal of aspartic residue, this Asp-N enzyme could also be immobilised on a micro-reactor and coupled directly after the deglycosylation reactor, in the following manner, trypsin-→ deglycosylation→ Asp N enzyme reactors on-line.

3. Both the trypsin and PNGase F reactors described in Chapters 4 and 5, could be explored by making a longer immobilising column, and this could help in enhancing the sensitivity of the digest. Future work could also look at optimising the loading flow rate during the digestion/deglycosylation/trapping stage in order to reduce the cycle time between injections and/or multiplexing the analysis to improve the overall throughput of the method.

4. The HILIC monolith has potential of further development as it has a low backpressure, so if required, the 30 cm columns can probably be used at significantly higher flow rates or the improved separation between 2 compounds could be achieved by producing longer columns. As mentioned above, this could be fabricated in an internal tapered capillary tip for nanospray, and this might be able to further enhance the sensitivity.

5. The orthogonal set-up could be improved by changing the loading pump to a micro pump, where the loading flow can be set higher at 4-5 µl/min, instead of the nano flow pump, where the maximum flow could only be set at 1

µl/min. This could shorten the time for re-equilibrating all the trap columns and the analytical column.

References

[1] W. Jelkmann, Erythropoietin: structure, control of production, and function, Physiol. Rev. 72 (2) (1992) 449-489.

[2] W. Jelkmann, Molecular biology of erythropoietin, Intern. Med. 43 (8) (2004) 649-659.

[3] S.M.R. Stanley, A. Poljak, J. Chromatogr. B 785 (2003) 205-218.

[4] R.M.A. Bento, L.M.P. Damasceno, F.R. Aquino Neto, Rev. Bras. Med. Esporte 9(3): (2003) 181-190, (English Version) - May/Jun.

[5] http://glycam.org/old/

[6] http://enfo.agt.bme.hu/drupal/en/node/9728

[7] C.G. Winearls, Nephrol. Dial Transplant. 13 Suppl. 2, (1998) 3-8.

[8] N.H. Yu, E.N.M. Ho, T.S.M. Wan, A.S.Y. Wong, Anal. Bioanal. Chem. 396 (2010) 2513-2521.

[9] J.C. Egrie, J.K. Browne, Br. J. Cancer 84 Suppl. 1, (2001) 3-10.

[10] J.C. Egrie, E. Dwyer, J.K. Browne, A. Hitz, M.A. Lykos, Exp. Hematol 31 (2003) 290-299.

[11] I. C. Macdougall, K. U. Eckardt, The Lancet 368 (2006) 947.

[12] W. Jelkmann, Br. J. Haematol 141 (2008) 287.

[13] S. Fishbane, A. Pannier, X. Liogier, J. Clin. Pharmacol. 47 (2007) 1390-1397.

[14] J.W. Fisher Exp. Biol. Med. 228 (2003) 1-14.

[15] J. Mi, S. Wang, X. Ding, Z. Guo, M. Zhao, W. Chang, J. Chromatogr. B 843 (2006) 125-130.

[16] P. Connes, S. Perrey, A. Varray, C. Prefaut, C. Caillaud, *Pflugers Arch.* Eur. J. Physiol. 447 (2003) 231-238.

[17] B. T. Ekblom, Best Pract. Res. Clin. Endocrinol. Metab. 14 (2000) 89-98.

[18] W. Jelkmann, Curr. Pharm. Biotechnol. 1 (2000) 11-31.

[19] P. Mossuz, F. Girodon, S. Hermouet, I. Dobo, E. Lippert, M. Donnard, V. Latger-Cannard, N. Boiret, V. Praloran, J. C. Lecron, Clin. Chem. 51 (2005) 1018-1021.

[20] E. R. Eichner, Med. Sci. Sports Exercise 24 (1992) S315-S318.

[21] Association of Racing Commissioners Internationa, Inc. (ARCI) (2009) Uniform classification guidelines for foreign substances and recommended penalties and model rule. http://www.arci.com/modelrules.html. Accessed 20th April 2011.

[22] Federation Equestre Internationale (FEI) (2010) Prohibited substances list. http://www.feicleansport.org/ProhibitedSubstancesList_Jan2010.pdf. Accessed 20th April 2011.

[23] World Anti-Doping Agency (WADA) Questions and answers on EPO detection. http://www.wada-ama.org/en/Resources/Q-and-A/Q-A-EPO-Detection/. Accessed 19th April 2011.

[24] The 2011 Prohibited List International Standard (the World Anti-Doping Code) 2011 World Anti-Doping Agency, Clause S2 (2010) http://www.wada-ama.org/Documents/World_Anti-Doping_Program/WADP-Prohibited-list/To_be_effective/WADA_Prohibited_List_2011_EN.pdf. Accessed 1st June 2011

[25] T. R. J. Lapping, A. P. Maxwell, Equine Vet. J. 29 (1997) 12.

[26] C. Schwarzwald, K. W. Hinchcliff, Proceedings of the 50th Annual Convention American Association Equine Practitioners, Denver, CO, (2004), S. E. Palmer, American Association of Equine Practitioners, Lexington, KY (2004) 270-271.

[27] J. Mi, S. Wang, X. Ding, Z. Guo, M. Zhao, W. Chang, J. Chromatogr. B, 843 (2006) 125-130.

[28] L. Wide, B. Wikström, K. Kriksson, Upsala, J. Med. Sci. 108 (2003) 229-238.

[29] F. Lasne, M-A. Popot, E. Varlet-Marie, L. Martin, J-A. Martin, Y. Bonnaire, M. Audran, J. de Ceaurriz, J. Anal. Toxico. 29 (2005) 835-837.

[30] J. Roberts, P. Brown, S. Cade, J. Faustino-Kemp, F. Lasne, RB. Williams and E. Houghton, Proceedings of the 14th International Conference of Racing Analysts and Veterinarians, Florida, USA, (2003) 2002. R&W, Newmarket, 231-242.

[31] J. Roberts, N. Basgallop, P. Brown and J. Faustino-Kemp, Proceedings of the 15th International Conference of Racing Analysts and Veterinarians, Dubai, United Arab Emirates, (2005) 2004. R&W Communications, 188-195.

[32] D.H. Catlin, A. Breidbach, S. Elliott, J. Glaspy, Clin. Chem. 48 (2002) 2057-2059.

[33] A.W. Wognum, V. Lam, R. Goudsmit, G. Krystal, Blood 76 (7) (1990) 1323-1329.

[34] J. Yan, J.B. Mi, W.B Chang, Chin. Chem. Lett. 15 (8) (2004) 939-942.

[35] E.N.M. Ho, T.S.M. Wan, A.S.Y. Wong, K.K.H. Lam, B.D. Stewart, J. Chromatogr. A 1201 (2008) 183-190.

[36] K. Hirayama, R. Yuji, N. Yamada, K. Kato, Y. Arata, I. Shimada, Anal. Chem. 70 (1998) 2718-2725.

[37] N. Kawasaki, M. Ohta, S. Hyuga, M. Hyuga, T. Hayakawa, Anal. Biochem. 285 (2000) 82-91.

[38] F. Guan, C.E. Uboh, L.R. Soma, E. Birks, J. Chen, J. Mitchell, Y. You, J. Rudy, F. Xu, X. Li, G. Mbuy, Anal. Chem. 79 (2007) 4627-4635.

[39] G. Stubiger, M. Marchetti, M. Nagano, R. Grimm, G. Gmeiner, C. Reichel, G. Allmaier, J. of Sep. Sci. 28 (2005) 1764-1778.

[40] G.H. Zhou, G.A. Luo, Y. Zhou, K.Y. Zhou, X.D. Zhang, L.Q. Huang, Electrophoresis 19 (1998) 2348-2355.

[41] S. Gupta, A. Sage, A.K. Singh, Anal. Chim. Acta. 525 (2005) 96-109.

[42] M. Ohta, N. Kawasaki, S. Hyuga, M. Hyuga, T. Hayakawa, J Chromatogr. A 910 (2001) 1-11.

[43] F. Guan, C.E. Uboh, L.R. Soma, E. Birks, J. Chen, Y. You, J. Rudy, X. Li, Anal. Chem. 80 (2008) 3811-3817.

[44] R. Abellan, R. Ventura, S. Pichini, A.F. Remacha, J.A. Pascual, R. Pacifici, R. Di Giovannandrea, P. Zuccaro, J. Segura, J. Pharm. Biomed. Anal. 35 (2004) 116-1177.

[45] M. Beullens, J.R. Delanghe, M. Bollen, Blood 107 (2006) 4711-4713.

[46] M. Lönnberg, Y. Dehnes, M. Drevin, M. Garle, S. Lamon, N. Leuenberger, T. Quach, J. Carlsson, J. Chromatogr. A 1217 (2010) 7031-7037.

[47] M. Azarkan, J. Huet, D. Baeyens-Volant, Y. Looze, G. Vandenbussche, J. Chromatogr. B 849 (2007) 81.

[48] F. Lasne, L. Martin, J. A. Martin, J. de Ceaurriz, Int. J. Biol. Macromol. 41 (2007) 354-357.

[49] M.C. Hennion, V. Pichon, Immuno-based sample preparation for trace analysis, J. Chromatogr. A 1000 (2003) 29-52.

[50] C. Hagman, D. Ricke, S. Ewert, S. Bek, R. Falchetto, F. Bitsch, Anal. Chem. 80 (2008) 1290-1296.

[51] L.J. Dekker, J. Bosman, P.C. Burgers, A. van Rijswijk, R. Freije, T. Luider, R. Bischoff, J. Chromatogr. B 847 (2007) 65-69.

[52] L. Huang, G. Harvie, J.S. Feitelson, K. Gramatikoff, D.A. Herold, D.L. Allen, R. Amunngama, R.A. Hagler, M.R. Pisano, W.W. Zhang, X. Fang, Proteomics 5 (2005) 3314-3328.

[53] A.N. Hoofnagle, J.O. Becker, M.H. Wener, J.W. Heinecke, Clin. Chem. 54 (2008) 1796-1804.

[54] Y.C. Lee, G. Block, H. Chen, E. Folch-Puy, R. Foronjy, R. Jalili, C.B. Jendresen, M. Kimura, E. Kraft, S. Lindemose, J. Lu, T. McLain, L. Nutt, S. Ramon-Garcia, J. Smith, A. Spivak, M.L. Wang, M. Zanic, S.H. Lin, Protein Expression Purif. 62 (2008) 223-229.

[55] M. Dubois, F. Becher, A. Herbet, E. Ezan, Rapid Commun. Mass Spectrom. 21 (2007) 352-358.

[56] M.J. Berna, Y. Zhen, D.E. Watson, J.E. Hale, B.L. Ackermann, Anal. Chem. 79 (2007) 4199-4205.

[57] L. Franco Fraguas, J. Carlsson, M. Lönnberg, J. Chromatogr. A 1212 (2008) 82-88.

[58] M. Takeuchi, S. Takasaki, H. Miyazaki, T. Kato, S. Hoshi, N. Kochibe, A. Kobata, J. Biol. Chem. 263 (1988) 3657-3663.

[59] M. Lönnberg, J. Carlsson, J. Chromatogr. A 1127 (2006) 175-182.

[60] M. Lönnberg, M. Drevin, J. Carlsson, J. Immunol. Meth. 339 (2008) 236-244

[61]http://www/wadaama.org/Documents/Science_Medicine/Funded_Research_Projects/Completed_Projects/2005/05A1JC-Carlsson.pdf. Assessed 9 Jan 2011.

[62]MAIIADiagnostics(2010),http://www.maiiadiagnostics.com/research/epo_doping_test.pdf. Accessed 9 Jan 2011.

[63] M. Lönnberg, J. Carlsson, J. Immunol. Methods 246 (2000) 25-36.

[64] F. Lasne, L. Martin, N. Crepin, J. de Ceaurriz, Anal. Biochem. 311 (2002) 119-126.

[65] M. Lönnberg, J. Carlsson, J. Chromatogr. B 763 (2001) 107-120.

[66] M. Lönnberg, J. Carlsson, Anal. Biochem. 293 (2001) 224-231.

[67] M. Lönnberg, M. Drevin, J. Carlsson, J. Immunol. Methods 339 (2008) 236-244.

[68] M. Lönnberg, M. Andrén, G. Birgegård, M. Drevin, M. Garle, J. Carlsson, Anal. Biochem. 420 (2012) 101-114.

[69] B. Küster, A. Shevchenko, M. Mann. In Proteolytic Enzymes (A Practical Approach), Oxford University Press: Oxford, UK, (2001) 149-185.

[70] D. Lopez-Ferrer, B. Canas, J. Vazquez, C. Lodeiro, R. Rial-Otero, I. Moura, J. L. Capelo, Trends Anal. Chem. 25 (2006) 996.

[71] J. Krênková, F. Foret, Electrophoresis 25 (2004) 3550-3563.

[72] G. Massolini, E. Calleri, J. Sep. Sci. 28 (2005) 7-21.

[73] J. Ma, L. Zhang, Z. Liang, W. Zhang, Y. Zhang, Anal. Chim. Acta 632 (2009) 1.

[74] G. T. Hermanson, A.K. Mallia, P. K. Smith (Eds.), Immobilized Affinity Ligand Techniques (Chinese Translation Edition), Science Press, Beijing, (1996) 29-34, 125-128.

[75] N.A. Plate, L.I. Valuev, N.S. Egorov, M.A. Al-Nuri, Prikladnaia biokhimiia I mikrobiologiia 13 (1977) 673-676.

[76] A.K. Palm, M.V. Novotny, Rapid Commun. Mass Spectrom. 18 (2004) 1374-1382.

[77] J.R. Freije, P.P.M.F.A. Mulder, W. Werkman, L. Rieux, H.A.G. Niederlander, E. Verpoorte, R. Bischoff, J. Proteome Res. 4 (2005) 1805-1813.

[78] T.N. Krogh, T. Berg, P. Hojrup, Anal. Biochem. 274 (1999) 153-162.

[79] Y. Li, B. Yan, C. Deng, W. Yu, X. Xu, P. Yang, X. Zhang, Proteomics 7 (2007) 2330.

[80] S. Ota, S. Miyazaki, H. Matsuoka, K. Morisato, Y. Shintani, K. Nakanishi, J. Biochem. Biophys. Methods 70 (2007) 57-62.

[81] D. Goradia, J. Cooney, B.K. Hodnett, E. Magner, Biotechnol. Prog. 22 (2006) 1125-1131.

[82] K. Bencina, A. Podgornik, A. Štrancar, M. Benčina, J. Sep. Sci. 27 (2004) 811-818.

[83] J. Krenkova, Z. Bilkova, F. Foret, J. Sep. Sci. 28 (2005) 1675-1684.

[84] E.C.A. Stigter, G.J. de Jong, W.P. van Bennekom, Anal. Bioanal. Chem. 389 (2007) 1967-1977.

[85] L.J. Lin, J. Ferrance, J.C. Sanders, J.P. Landers, Lab Chip 3 (2003) 11-18.

[86] J. Ma, L. Zhang, Z. Liang, W. Zhang, Y. Zhang, J. Sep. Sci. 30 (2007) 3050-3059.

[87] J. Krênková, F. Svec, J. Sep. Sci. 32 (2009) 706-718.

[88] F. Svec, C.G. Huber, Anal. Chem. 78 (2006) 2101-2017.

[89] F. Svec, J.M.J. Fréchet, Science 273 (1996) 205-211.

[90] D. Josic, A. Buchacher, A. Jungbauer, J. Chromatogr. B 752 (2001) 191-205.

[91] M. Ye, S. Hu, R. M. Schoenherr, N. J. Dovichi, Electrophoresis 25 (2004) 1319-1326.

[92] A.K. Palm, M.V. Novotny, Rapid Comm. Mass Spectrom, 19 (2005) 1730-1738.

[93] M. E. Taylor, K. Drickamer, Introduction to Glycobiology Oxford University Press: Oxford, 2003.

[94] Y. Yoshida, J. Biochem. 134 (2003) 183.

[95] J. B. Lowe, J. D. Marth., Annu. Rev. Biochem. 72 (2003) 643.

[96] B. Küster, T.J.P. Naven, D.J. Harvey, J. Mass Spectrom. 31 (1996) 1131.

[97] Y. Mechref, M.V. Novotny, Anal. Chem. 70 (1998) 455.

[98] K.J. Mussar, G.J. Murray, B.M. Martin, T. Viswanatha, J. Biochem. Biophys. Methods 20 (1989) 53-68.

[99] J. Krenkova, N.A. Lacher, F. Svec, J. Chromatogr. A, 1216 (2009) 3252-3259.

[100]http://www.sigmaaldrich.com/technicaldocuments/articles/biology/glycobiology/n-linked-glycan-strategies.html.

[101] J. Rivers, L. McDonald, I.J. Edwards, R.J. Beynon, J. Proteome Res. 7 (2008) 921-927.

[102] M.A. Bynum, H.F. Yin, K. Felts, Y.M. Lee, C.R. Monell, K. Killeen, Anal. Chem. 81 (2009) 8818-8825.

[103] M.A. Prozio, A.M. Pearson, Biochim. Biophys. Acta 384 (1975) 235-241.

[104] J. Noreau, G.R. Drapeau, J. Bacteriol. 140 (1979) 911-916.

[105] G.R. Drapeau, J. Bio. Chem. 255 (1980) 839-840.

[106] W. Ni, S. Dai, B. L. Karger, Z, S. Zhou, Anal. Chem. 82 (2010) 7485-7491.

[107] S.M. Fields, Anal. Chem. 68 (1996) 2709-2712.

[108] F. Svec, J.M.J. Fréchet, Anal. Chem. 64 (1992) 820-822.

[109] H. Minakuchi, K. Nakanishi, N. Soga, N. Ishizuka, N. Tanaka, Anal. Chem. 68 (1996) 3498-3501.

[110] S. Hjertén, J.L. Liao, R. Zhang, J. Chromatogr. 473 (1989) 273-275.

[111] M.Q. Huang, Y. Mao, M. Jemal, M. Arnold, Rapid Commun. Mass Spectrom. 20 (2006) 1709-1714.

[112] S. Zhou, H. Zhou, M. Larson, D.L. Miller, D. Mao, X. Jiang, W. Naidong, Rapid Commun. Mass Spectrom. 19 (2005) 2144-2150.

[113] R.S. Plumb, G. Dear, D. Mallett, J. Ayrton, Rapid Commun. Mass Spectrom. 15 (2001) 986-993.

[114] H. Ken, H. Natsuki, Y. Katsuya, N. Masaru, T. Nobuo, Anal. Chem. 78 (2006) 5729-5735.

[115] N.W. Smith, Z. Jiang, J. Chromatogr. A, 1184 (2008) 416-440.

[116] S. Garbis, G. Lubec, M. Fountoulakis, J. Chromatogr. A 1077 (2005) 1-18.

[117] I. Gusev, X. Huang, C. Horváth, J. Chromatogr. A 855 (1999) 273.

[118] M. Motokawa, H. Kobayashi, N. Ishizuka, H. Minakuchi, K. Nakanishi, H. Jinnai, K. Hosoya, T. Ikegami, N. Tanaka, J. Chromatogr. A 961 (2002) 53.

[119] S. Hjertén, J. L. Liao, R. Zhang, J. Chromatogr. 473 (1989) 273.

[120] F. Svec, J. Sep. Sci. 27 (2004) 747.

[121] H. Zou, X. Huang, M. Ye, Q. Luo, J. Chromatogr. A 954 (2002) 5.

[122] C. Viklund, F. Svec, J. M. J. Fréchet, Chem. Mater. 8 (1996) 744-750.

[123] W. Walcher, H. Oberacher, S. Troiani, G. Hölzl, P. Oefner, L. Zolla, C. G. Huber, J. Chromatogr. B 782 (2002) 111.

[124] de Gennes, P.G. Scaling Concepts in Polymer Physics; Cornell University Press: Ithaca, NY, (1979) 115.

[125] T.S. Reid, R. A. Henry, Am. Lab. 31 (1999) 24.

[126] R.D. Voyksner, in: R.B. Cole (Ed.), Electrospray Ionization Mass Spectrometry, John Wiley & Sons, Hoboken, NJ, 1997, 323.

[127] Z. Jiang, N. Smith, Z. Liu, J. Chromatogr. A 1218 (2011) 2350-2361.

[128] A. J. Alpert, J. Chromatogr. 499 (1990) 177-196.

[129] S. D. Brown, C.A. White, M. G. Bartlett, Rapid Commun. Mass Spectrom. 16 (2002) 1871.

[130] R. Oertel, U. Renner, W. Kirch, J. Pharm. Biomed. Anal. 35 (2004) 633.

[131] R. Oertel, V. Neumeister, W. Kirch, J. Chromatogr. A 1058 (2004) 197.

[132] V. V. Tolstikov, O. Fiehn, Anal. Biochem. 301 (2002) 298.

[133] M. Gilar, P. Olivova, A.E. Daly, J.C. Gebler, Anal. Chem. 77 (2005) 6426-6434.

[134] W. Naidong, Anal. Technol. Biomed. Life Sci. 796 (2003) 209-224.

[135] P. Hagglund, J. Bunkenborg, F. Elortza, O.N. Jensen, P. Roepstorff, J. Proteome Res. 3 (2004) 556-566.

[136] P. Hemstrom, K. Irgum, J. Sep. Sci. 29 (2006) 1784-1821.

[137] P.J. Boersema, N. Divecha, A.J.R. Heck, S. Mohammed, J. Proteome Res. 6 (2007) 937-946.

[138] D.E. McNulty, R.S. Annan, In: 55th ASMS Conference Mass Spectrometry, Indianapolis, IN, 3-7 June 2007.

[139] http://www.pubmedcentral.nih.gov/articlerender.fcgi?artid=2324128.

[140] P.J. Boersema, S. Mohammed, A.J.R. Heck, Anal. Bioanal. Chem. 391 (1) (2008) 151-159.

[141] B.Y. Zhu, C.T. Mant, R.S. Hodges, J. Chromatogr. A 548 (1991) 13-21.

[142]http://www.inertsil.com/general/Inertsil_HILIC_Hydrophilic_Interaction_Chromatography_HPLC_Column_General_Information.html.

[143] Y. Guo, S. Gaiki. J. Chromatogr. A 1074 (2005) 71-80.

[144] http://www.sielc.com/Technology_HILIC.html.

[145] E.S. Grumbach, D.M. Diehl, U.D. Neue, J. Sep. Sci. 31 (2008) 1511-1518.

[146] M.P. Washburn, D. Wolters, J.R. Yates, 3rd, Nat. Biotechnol. 19 (2001) 242-247.

[147] Y. Shen, J.M. Jacobs, D.G. II Camp, R. Fang, Anal. Chem. 76 (2004) 1134-1144.

[148] J.M. Peng, J.E. Elias, C.C. Thoreen, L.J. Licklider, S.P. Gygi, J. Proteome Res. 2 (2003) 43-50.

[149] K. Wagner, T. Miliotis, G. Marko-Varga, R. Bischoff, K.K. Unger Anal. Chem. 74 (2002) 809-820.

[150] H. Lindner, J. Wesierska-Gadek, W. Helliger, B. Puschendorf, G. Sauermann, J. Chromatogr. 472 (1989) 243-249.

[151] H. Lindner, B. Sarg, C. Meraner, W. Helliger, J. Chromatogr. A. 743 (1996) 137-144.

[152] B. Sarg, E. Koutzamani, W. Helliger, I. Rundquist, H.H. Lindner, J. Biol. Chem. 277 (2002) 39195-39201.

[153] H. Lindner, B. Sarg, W. Helliger, J. Chromatogr. A, 782 (1997) 55-62.

[154] H. Lindner, B. Sarg B, B. Hoertnagl, W. Helliger, J. Biol. Chem. 273 (1998) 13324-13330.

[155] C.T. Mant, R.S. Hodges, J. Sep. Sci. 31 (2008) 2754-2773.

[156] M. Tswett, Physical chemical studies on chlorophyll adsorption. Ber. Dtsch. Chem. Ges. 24 (1906) 316.

[157]http://www.chromatographyonline.com/lcgc/data/articlestandard/lcgceurope/382003/69718/article.pdf.

[158] C.G. Horváth, B.A. Preiss, S.R. Lipsky, Anal. Chem. 39(12) (1967) 1422-1428.

[159] C.G. Horváth, S.R. Lipsky, Anal. Chem. 41 (10) (1969) 1227-1234.

[160] M.E. Swartz, J. of Liquid Chromatogr. & Related Technologies, 28 (7-8) (2005) 1253-1263.

[161] R. Willoughby, E. Sheehan, S. Mitrovich, What are your LC/MS alteranatives? In a global view of LC/MS; How to solve your most challenging analytical problems, Global View Publishing, Pittsburg, PA, USA, 51.

[162] F.A. Mellon, Liquid Chromatography/Mass Spectrometry, In: VG Monographs in Mass Spectrometry, Volume 2, No. 1.

[163] http://www.monzir-pal.net/Instrumental%20Analysis/Contents/Chapter26.htm.

[164] R. Ventura, D. Fraisse, M. Becchi, O. Paisse, J. Segura, J. Chromatogr. 562 (1991) 723.

[165] Finnigan, LCQ-Deca manual, Getting Started, Revision A: 1-4. 3.

[166] J.V. Iribarne, B.A. Thomson, J. of Chemical Physics 64(6) (1976) 2287-2294.

[167] S. Nguyen, J.B. Fenn, Proc. Natl. Acad. Sci. U.S.A 104(4) (2007) 1111-7.

[168] M. Dole, L.L. Mack, R.L. Hines, R.C. Mobley, L.D. Ferguson, M.B. Alice, J. of Chemical Physics 49(5) (1968) 2240-2249.

[169] http://download.springer.com/static/pdf/18/chp%253A10.1007%252F978-1-60327-2339_6.pdf?auth66=1411724446_c313fd628b33df734d8dc75ae7e1c17b&ext=.pdf.

[170] Edmond de Hoffmann, Vincent Stroobant (2003). Mass Spectrometry: Principles and Applications (Second ed.). Toronto: John Wiley & Sons, Ltd. P. 65.

[171] S. Peterman, C. Uboh, F. Guan, L.Soma, E. Birks, J. Chen, ThermoScientific Application Note: 408.

[172] M. Thevis, W. Schaenzer, Mass Spectrom. Rev. *26* (2007) 79-107.

[173] G. Stubiger, M. Marchetti, M. Nagano, C. Reichel, G. Gmeiner, G. Allmaier, Rapid Commun. Mass Spectrom. 19 (2005) 728-742.

[174] J. Zheng, D. Norton, S.A. Shamsi, Anal. Chem. 78 (2006) 1323-1330.

[175]http://www.maelabs.ucsd.edu/mae156/mae156a_f03/sponsored_projects_files/MSsetup.gif

[176] M. Lönnberg, Membrane-Assisted Isoform Immunoassay: Separation and Determination of Protein Isoforms (Comprehensive Summaries of Uppsala Dissertations from the Faculty of Science and Technology, No. 691, Acta Universitatis Upsaliensis, 2002.

[177] G. Roman-Gusetu, K.C. Waldron, D. Rochefort, J. Chromatogr. A. 1216 (2009) 8270-8276.

[178] F. Lasne, J. de Ceaurriz, Nature 405 (2000) 635.

[179] F. Lasne, J. Immunol. Methods 276 (2003) 223-226.

[180] F. Svec, Electrophoresis. 27 (2006) 947-961.

[181] E. Calleri, C. Temporini, E. Perani, C. Stella, S. Rudaz, D. Lubda, G. Mellerio, J.L. Veuthey, G. Caccialanza, G. Massolini, J. Chromatogr. A, 1045 (2004) 99-109.

[182] C. Temporini, E. Perani, F. Mancini, M. Bartolini, E. Calleri, D. Lubda, G. Felix, V. Andrisano, G. Massolini, J. Chromatogr. A, 1120 (2006) 121-131.

[183] L. Geiser, S. Eeltink, F. Svec, J.M.J Fréchet, J. Chromatogr. A, 1188 (2008) 88-96.

[184] S.M.R. Stanley, D. Chua, Advances in Bioscience and Biotechnology, 5 (2014) 651-660.

[185] A.L. Tarentino, Flavastacin (2004) In Handbook of Proteolytic Enzymes, 2nd Ed., 631-632, Elsevier, London.

[186] C. Dartiguenave, H. Hamad, K.C. Waldron, Anal. Chim. Acta 663 (2010) 198-205.

[187] E.C.A. Stigter, G.J. de Jong, W.P. van Bennekom, Biosens. Bioelectron. 21 (2005) 474-482.

[188] T. Yoshida, Anal. Chem. 69 (1997) 3038-3043.

[189] A.J. Alpert, P.C. Andrews, J. Chromatogr. 443 (1988) 85-96.

[190] Z.J. Jiang, N.W. Smith, P.D. Ferguson, M.R.Taylor, Anal. Chem. 79 (2007) 1243-1250.

[191] S.H. Lubbad, Acta. Chim. Solv. 57 (2010) 880-887.

[192] F. Nevejans, M. Verzele, J. Chromatogr, 350 (1985) 145-150.

[193] W.H. Li, H.D. Stöver, A.E. Hamielec, J. Polym. Sci. A, 32 (1994) 2029-2038.

[194] L. Trojer, S.H. Lubbad, C.P. Bisjak, G.K. Bonn, J. Chromatogr. A, 1117 (2006) 56-66.

[195] A. Greiderer, L. Trojer, C.W. Huck, G.K. Bonn, J. Chromatogr. A, 1216 (2009) 7747-7754.

[196] A. Greiderer, Jr. S.C. Ligon, C.W. Huck, G.K. Bonn, J. Sep. Sci, 32 (2009) 2510-2520.

[197] J.J. Van Deemter, F.J. Zuiderweg, A. Klinkenberg, Chem. Eng. Sci, 5 (1956) 271-289.

[198] L. Trojer, C.P. Bisjak, W. Wieder, G.K. Bonn, J. Chromatogr. A, 1216 (2009) 6303-6309.

[199] H.C. Foo, J. Heaton, N.W. Smith, S. Stanley, Talanta, 100 (2012) 344-348.

[200] W. Wieder, S.H. Lubbad, L. Trojer, C.P. Bisjak, G.K. Bonn, J. Chromatogr. A, 1191 (2008) 253-262.

[201] S.H. Lubbad, M.R. Buchmeiser, J. Sep. Sci. 32 (2009) 2521-2529.

[202] Z.J. Jiang, N.W. Smith, P.D. Ferguson, M.R. Taylor, J. Biochem. Biophys. Methods, 70 (2007) 39-45.

[203] K. Sandra, M. Moshir, F. D'Hondt, K. Verleysen, K. Kas, P. Sandra, J. Chromatogr. B, 866 (2008) 48-63.

[204] J.M. Saz, M.L. Marina, J. Sep. Sci., 31 (2008) 446-458.

[205] M.C. Garcia, J. Chromatogr. B, 825 (2005) 111-123.

[206] M.C. Garcia, A.C. Hogenboom, H. Zappey, H. Irth, J. Chromatogr. A. 957 (2002) 187-199.

[207] D. Ren, G. Pipes, G. Xiao, G.R. Kleernann, P.V. Bondarenko, M.J. Treuheit, H.S. Gadgil, J. Chromatogr. A, 1179 (2008) 198-204.

[208] R.N. Xu, L. Fan, M.J. Rieser, T.A. El-Shourbagy, J. Pharm. Biomed. Anal. 44 (2007) 342-355.

[209] P. Dugo, O. Favoino, R. Luppino, G. Dugo, L. Mondello, Anal. Chem. 76 (2004) 2525-2530.

[210] P. Dugo, V. Skerikova, T. Kumm, A. Trozzi, P. Jandera, L. Mondello, Anal. Chem. 78 (2006) 7743-7750.

[211] I. François, A. de Villiers, P. Sandra, J. Sep. Sci. 29 (2006) 492-498.

[212] M.A. Hawryl, E. Soczewinski, E, Chromatographia, 52 (2000) 175-178.

[213] M.P.Y Lam, S.O. Siu, E. Lau, X.L. Mao, H.Z. Sun, P.C.N. Chiu, W.S.B. Yeung, D.M. Cox, I.K. Chu, Anal. Bioanal. Chem. 398 (2010) 791-804.

[214] Q. Wu, H.M. Yuan, L.H. Zhang, Y.K. Zhang, Anal. Chim. Acta, 731 (2012) 1-10.

[215] G. Greco, T. Letzel, LCGC ChromatographyOnline.com The Hyphenation of HILIC, Reversed-Phase HPLC, and Atmospheric-Pressure-Ionization MS, May 1, 2012 Special Issues.

[216] S.D. Palma, M.L. Hennrich, A.J.R. Heck, S. Mohammed, J. Proteomics, 75 (2012) 3791-3813.